INTERNATIONAL HYDROLOGICAL PROGRAMME

Catchment hydrological and biochemical processes in the changing environment

Seventh Conference of the European Network of Experimental and Representative Basins (ERB) Liblice (Czech Republic), 22 – 24 September 1998

IHP/UNESCO - ERB

PROCEEDINGS

Edited by

V. Elias
and
I.G. Littlewood

IHP-V | Technical Documents in Hydrology | No. 37
UNESCO, Paris, 2000

SC-2000/WS/38

Acknowledgement

Grant Agency of the Czech Academy of Sciences (Grant research project A306071), Grant Agency of the Czech Republic (Grant research project 526/98/0805) and Project COST 615.10 and Ministry of the Environment of the Czech Republic for supporting this work. Miloslav Šír, Miroslav Tesař and Josef Bucek for editorial cooperation.

Introduction

These Proceedings comprise 34 contributions focusing on the main subject of the Seventh ERB Conference, namely the hydrological and biochemical processes in the changing environment. Input data for their preparation were collected from experimental and representative basins located across Europe. These data, concerning their spatial density, monitoring frequency and types of derived parameters are, in most cases, much more detailed than otherwise possible with the common monitoring networks. Through this, one of the aims of ERB is being fulfilled - to study in detail processes and their interaction in the soil, vegetation, atmosphere and hydrosphere system.

The principle of sustainable development set by the UN Conference on the Environment and Development in Rio de Janeiro in 1992 is a categorical imperative of the necessary behaviour of mankind in coming years. Its implementation into practice requires the following five steps: (1) determination of the capacity of the available water resources in each region, (2) estimation of their degree of man-induced impacts, (3) identification of limits, the crossing of which could lead to a collapse, (4) improved capabilities of modelling hydrological and related processes, (5) assessment of whether the actions requested in the social-economic sector would not lead to crossing of the limits identified. From this viewpoint, a number of contributions to the Seventh ERB Conference, focusing on the monitoring, modelling, man-induced changes of water regime, knowledge of the runoff process in various time-space scales, etc., have undoubtedly their point in the problems discussed.

A range of contributions deal with a problem of a higher degree of the hydrological balance. It involves a complex approach combining the inseparable balance of energy, substance and nutrient fluxes with amount of water. Thus, it supports development of the temporal balance that should be the basic information tool for reasonable water use in regions with scarcity of water or regions under water crisis. Other contributions concern new techniques of hydrological modelling, measurements and also of assessment of water regime, etc.

In concluding, it is possible to say, that the contributions, even when prepared by representatives of 11 countries, give a useful overview of the current stage of experimental hydrology in Europe. In their wide spectrum of subjects they bring a number of useful stimuli for formulation of new phases of international key programmes such as IHP of UNESCO, OHP of WMO and scientific plans of IAHS for the beginning of the next century. Warm and cordial acknowledgements are extended to the authors and organisers of the Seventh ERB Conference.

Dr. Josef Hladný
Chairman of National Committee for Hydrology (IHP) of the Czech Republic

Note from the Editors

Manuscripts were referred for their technical and scientific suitability for publication by the Chairperson of the Session which the Paper or Poster was presented orally at Conference and by the members of the Scientific Committee. The Editors are indebted to the following Session Chairmen for undertaking the review procedure:

- Andreas Herrmann (Institut für Geographie und Geoökologie, TU Braunschweig, Germany)
- Pavol Miklánek (Ústav hydrólogie SAV, Bratislava, Slovakia)
- Ian Littlewood (Institute of Hydrology, Wallingford, United Kingdom)
- Pertti Seuna (Suomen Ympäristökeskus, Helsinki, Finland)

Readers of the Proceedings are requested to bear in mind that many of the papers are by authors whose first language is not English. Editing was undertaken without returning the manuscripts to authors for final proof-reading, spending about the same amount of time on each Paper. The editorial result may be a little uneven in places. If, for example, non-standard phrases are encountered in the Proceedings, readers are requested to bear in mind the practical limits on resources that could be made available for such aspects of preparing the Papers for publications.

Václav Eliáš
Institute of Hydrodynamics, Prague, Czech Republic

Ian G. Littlewood
Institute of Hydrology, Centre for Ecology and Hydrology, Wallingford, UK

Contents

Seasonal simulation of the soil water regime - a sensitivity analysis

T. Bayer[1], O. Syrovátka[2], M. Šír[1], M. Tesař[1]

[1]Institute of Hydrodynamics, Academy of Sciences of the Czech Republic, Experimental Basis Nový Dvůr 31, CZ 38473 Stachy. [2]Institute of Entomology, Academy of Sciences of the Czech Republic, Branišovská 5, CZ 37005 České Budějovice, Czech Republic.

1 Introduction

"In spite of the importance of the soil hydraulic characteristics for the computation and for the modelling in the soil hydrology, irrigation and drainage, runoff hydrology etc., the methods of their determination up to recently developed are restrictive for the routine use. If characteristics are measured on undisturbed core samples, the representativeness is questionable and the data thus obtained are not applicable directly to the solution of the flow problems in the field or in the catchment." (Šír et al., 1988).

In the article cited, the method of field estimation of soil hydraulic characteristics is described. The aim of this paper is to demonstrate the applicability of this method for the simulation of the soil water regime. The question addressed is: How does the retention curve variability influence modelled water regime? A source of retention curve variability is the natural soil heterogeneity inside one genetic soil horizon. Retention curves are measured on undisturbed soil samples of volume 100 cm^3.

2 Theory

2.1 Soil water balance components

In the vegetation season, the water balance of the soil cover is characterised by the time series of following components:

- rain precipitation P,
- infiltration into soil profile,
- ponding height or surface runoff,
- removal of water for plant transpiration T,
- evaporation from the soil surface E,
- water storage in the soil profile W,
- outflow from the soil to the bedrock or groundwater level (L - leakage),
- inflow to the soil from the bedrock or groundwater level caused by the capillary rise (S - seepage).

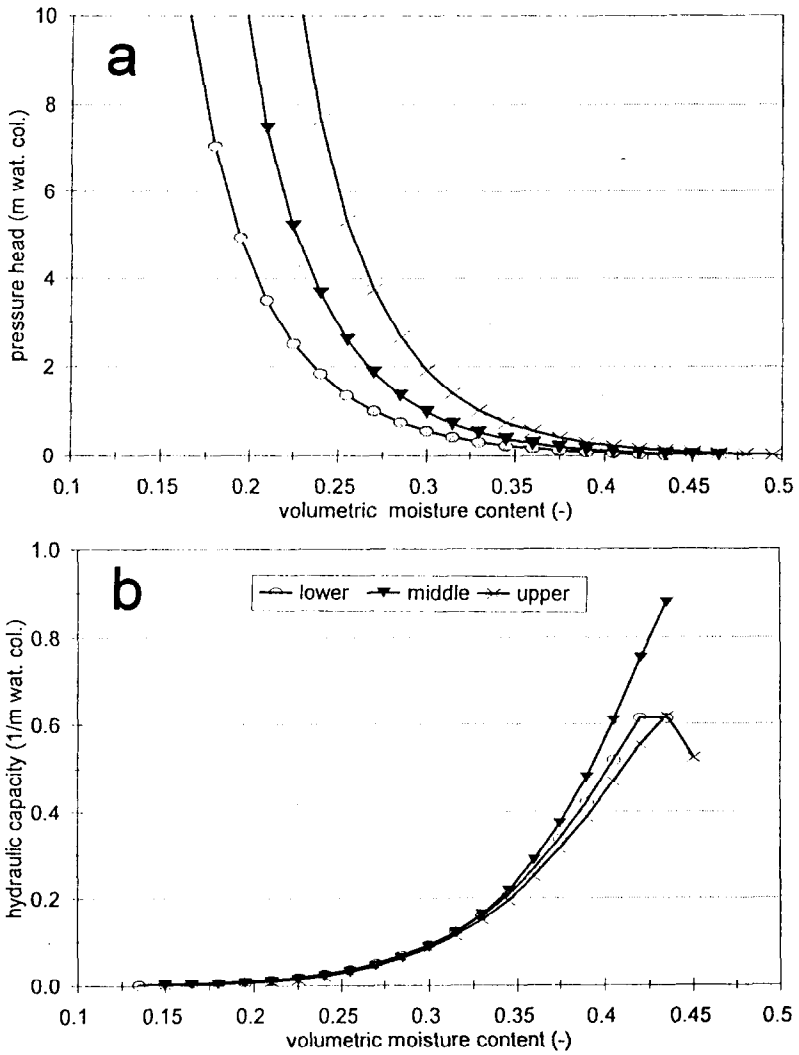

Figure 1: Lower, middle and upper (a) retention curve, (b) hydraulic capacity, Hnojnice, second place, depth 30 cm.

Over a whole day, usually all of the precipitation infiltrates. Therefore, we can consider the daily precipitation sum as the amount of infiltrated water entering the soil. On the sites covered by vegetation, the surface runoff is a rare phenomenon. Evaporation directly from the soil surface in localities overgrown with dense vegetation cover is negligibly small. For the study sites considered here, the water balance of the soil is sufficiently described by the equation:

$$W_{i+1} - W_i = P + S - T - L, \tag{1}$$

where P, S, T, and L are daily totals (mm). W_i and W_{i+1} are water storage in the soil profile in two successive days. The balance components W, S and L are determined by the one-dimensional simulation of the soil water movement. P is measured and T is determined as a potential transpiration PT. Actual transpiration T can be in some cases smaller then potential one. The rules governing this restriction are dependent on the characteristics of a vegetative cover. Potential transpiration is determined by the energy balance method from meteorological data (Pražák et al., 1994).

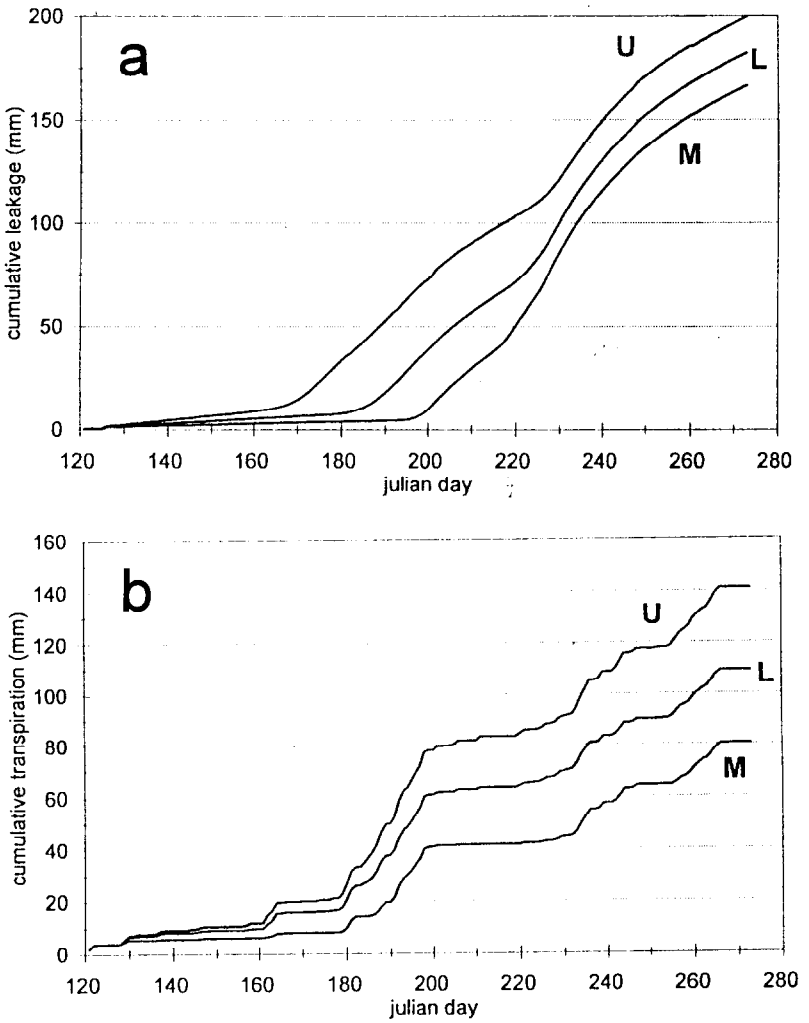

Figure 2: Time series of simulated (a) leakage, (b) transpiration in the form of summation curves. Hnojnice, second place, season 1987. U/M/L - simulation results for upper/middle/lower retention curve.

2.2 Soil moisture dynamics

For the simulation of the one-dimensional soil water movement, Richards' equation is applied. In this equation, the soil water retention curve and unsaturated hydraulic function together with the saturated hydraulic conductivity are soil hydraulic characteristics. The soil water retention curve is expressed by the modified equation of Van Genuchten, the unsaturated hydraulic function is determined by Mualem's capillary model (Šír et al., 1988). The soil water uptake for plant transpiration is modelled by the sink term in Richards' equation (Feddes et al., 1987).

2.3 The SWAP Model

The SWAP model based on the solution of Richards' equation (Feddes, Kowalik, Zaradny, 1987) is used for water movement simulation. The model requires following input data:

- number and thickness of soil genetic horizons,
- retention curve and the saturated hydraulic conductivity for each horizon,
- initial condition, i.e. depth profile of the hydraulic head or soil moisture,
- daily totals of rain precipitation,
- daily totals of potential transpiration,
- depth of root zone, characteristics of sink term for given vegetation cover,
- lower boundary condition (e.g. free drainage at the soil bottom, depth of groundwater level etc.).

The model produces time series of balance components S, T, L and W in daily totals (mm) as a response to the given precipitation and potential transpiration.

2.4 Retention curves processing

The output of retention curve measurement is a serie of values for volumetric moisture and pressure head. These points are fitted by van Genuchten's function. Retention curves measured on several samples taken from one genetic horizon lead to a family of curves. The greatest pressure head values form the upper boundary and the smallest value forms the lower boundary. Each of these boundaries is then fitted by van Genuchten's function. In this way, upper and lower retention curves are constructed. Finally, the middle retention curve is plotted. An example is shown in Fig. 1a. Fig. 1b shows hydraulic capacities derived from the retention curves in Fig. 1a.

3 Experimental work

3.1 Experimental sites

Three locations for sampling and measurements were selected.

The first location includes the medieval agricultural terraces of Hnojnice Hill in the Bavorov Highlands. Three sites differing in the soil cover thickness were selected. Undisturbed soil samples from each soil horizon were taken, generally three samples from each horizon. The first site was the upper part of the hill with a convex slope shape (535 m a. s. l., slope 11.3° and aspect 46°). The samples were taken from depths of 7 cm (Ap horizon) and 34 and 40 cm (cambic horizon). This site is considered to be an infiltration zone. The second site is the upper edge of an agricultural terrace (497 m a. s. l., slope 26° and aspect 7°) where the soil profile has maximal thickness. The samples were taken at depths of 7 and 30 cm. The soil profile is very homogenous, and genetic horizons are minimally distinctive. This site is considered to be an accumulation zone where the infiltrated water is absorbed and stored. The third site lies below this terrace where the soil profile was thinned by the terrace building. It is located at an altitude of 496 m a. s. l., its slope is 14.9° and the aspect is 8°. Soil samples were taken at depths of 5 and 17 cm (Ap, horizon of cultivation) and 24 cm (cambic horizon).

The second location is a spring area Senotín (610–690 m a. s. l.) in the landscape protected area 'Czech Canada'. Three experimental sites differing in the soil water regime were selected in this region: original wet-meadow ecosystem (not drained); cultivated meadow (drained by systematic pipe drainage); and restored meadow (pipe drainage was destroyed).

On the first experimental site, original wet meadow with stagnogleyic soils, the samples were taken from two places. The first is situated at an altitude of 662 m a. s. l., with slope value 3.27° and aspect 220°. The second is situated at an altitude of 665 m a. s. l. where soil hydromorphic conditions are not uniform and the water level fluctuates more. Soil samples were taken at depths of 12 cm (histic horizon) and 45 cm (stagnogleyic horizon).

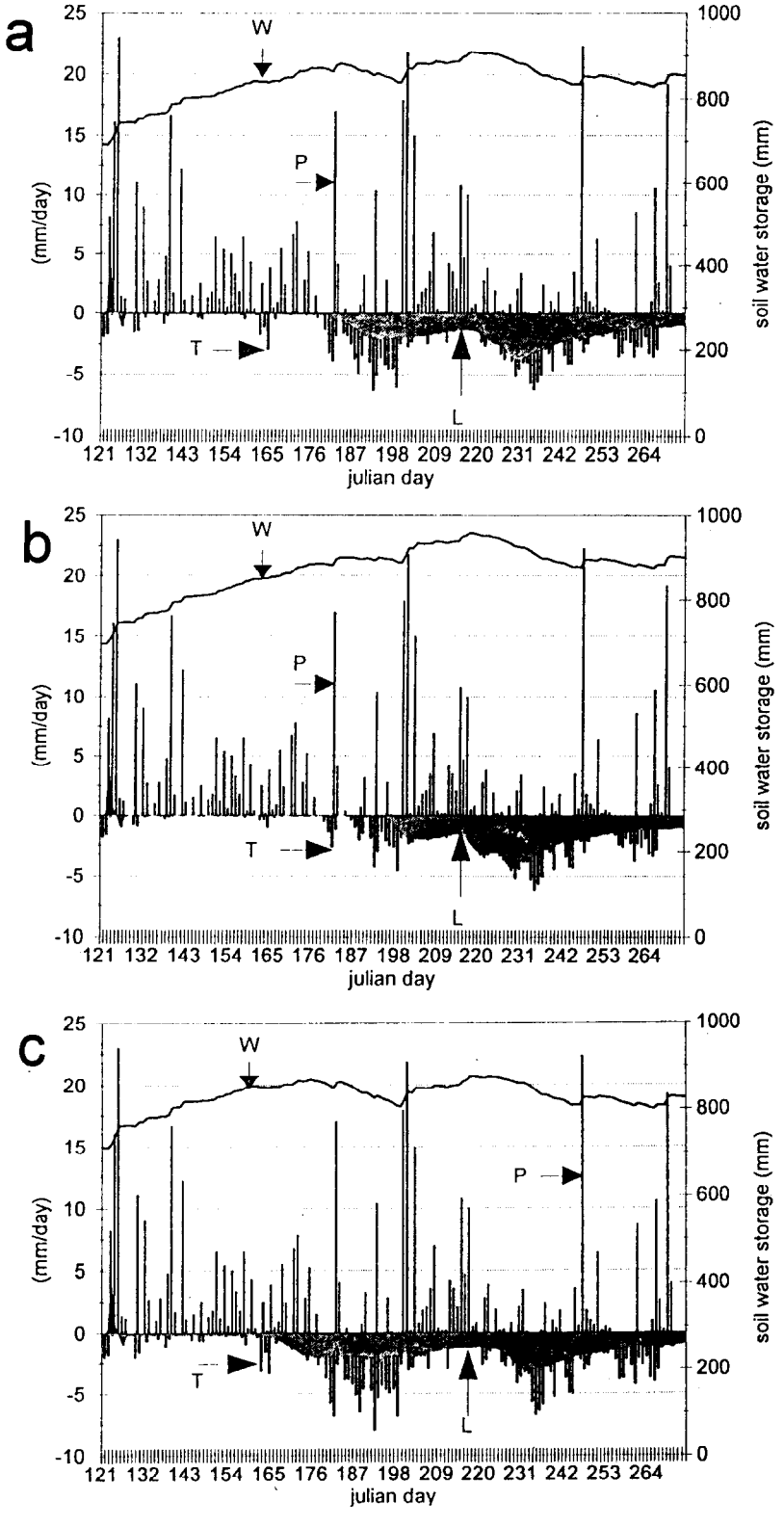

Figure 3: Simulation of the soil water regime. Hnojnice, second place, soil depth 250 cm, cold season, (a) lower, (b) middle, and (c) upper retention curve. W (mm) - soil water storage, P, T and L (mm/day) - daily sum of precipitation, transpiration and leakage.

On the second experimental site (drained and cultivated meadow), soil samples were taken from three places. The first place is situated at an altitude of 671 m a. s. l. with slope 3.2° and aspect 326°. Soil samples were taken at depths of 9 cm (histic horizon) and 50 cm (stagnogleyic horizon). The second place lies in the middle of the experimental site, at an altitude of 659 m a. s. l. Its slope is 13.2° and the aspect is 326°. The soil samples were taken at depths of 15 cm (histic horizon) and 45 cm. The third place lies in the lower part of this site; its altitude is 656 m a. s. l., slope is 3,2° and aspect is 347°. Soil conditions are between stagnogley and gleyic cambisol. Soil samples were taken at depths of 8 and 27 cm.

On the third experimental site (restored), the soil samples were taken from three places. On this site, dominant soil type is gleyic cambisol. The first place lies at the altitude 681 m a. s. l., its slope value is 3.2° and aspect is 120°. Samples were taken at depths 8 cm (Ap) and 47 cm (cambic horizon). The second place lies at an altitude of 676 m a. s. l., with the slope 4.5° and aspect 118°. Soil samples were taken at depths of 9 and 53 cm. The third place is at 674 m a. s. l., with slope 5.7° and aspect 115°. Samples were taken at depths of 13 and 47 cm.

The third locality is a runoff area Zábrod situated in the Šumava Mts. (Bohemian Forest). Its soil cover is formed by acid brown soil developed on paragneiss. The soil profile has a 30 cm thick A horizon covered by permanent grass. The mean elevation is 790 m a. s. l., the average annual air temperature is 6.1°C, and the average annual precipitation is 840.6 mm.

3.2 Measurement of soil hydraulic characteristics

In the field, undisturbed soil samples were taken from within 100 cm^3 rings. Retention curves were measured using the pressure plate apparatus. Saturated hydraulic conductivity of each soil horizon was estimated with the help of the method described in Šír et al. (1988).

4 Simulation

A sensitivity analysis of the SWAP model is done for the cold (1987), intermediate (1986) and warm seasons (1983). The soil water regime in each season is modelled for three retention curves - upper, middle and lower - on the agricultural terraces Hnojnice (3 places) (Fig. 2, 3) and spring area Senotín (one site, two places and two sites, three places). The soil water regime in the 1987 season was modelled in the locality Zábrod (Fig. 4).

5 Results and discussion

Generally, retention curve variability does not influence simulation results in hydromorphic soil stands. In the spring area Senotín, no difference was observed in the simulations for upper and lower retention curves. This conclusion was proved not only on hydromorphic stands but also on secondary terrestrial soils on drained, cultivated meadows. In these localities, the plant transpiration was not restricted. The soil moisture in the root zone was sufficient during the whole season.

On the agricultural terraces Hnojnice, some differences were observed in the simulations for upper and lower retention curves (Fig. 2, 3). Generally, in the warm season the model demonstrates higher intensity of percolation, therefore, considering this option, the water is stored for a shorter time. While in the case of the upper curves is higher

tensiometric pressure along with the same value of soil moisture, the model considers shift in the sink term which is interpreted as a limiting factor of transpiration.

In the cold season, we have obtained some differences for the second place, on the terrace edge. For the upper curves, the soil profile is drained more continuously and there is lower outflow.

Modelled and measured courses of tensiometric pressure in the locality Zábrod show good accordance - see Fig. 4a and 4b.

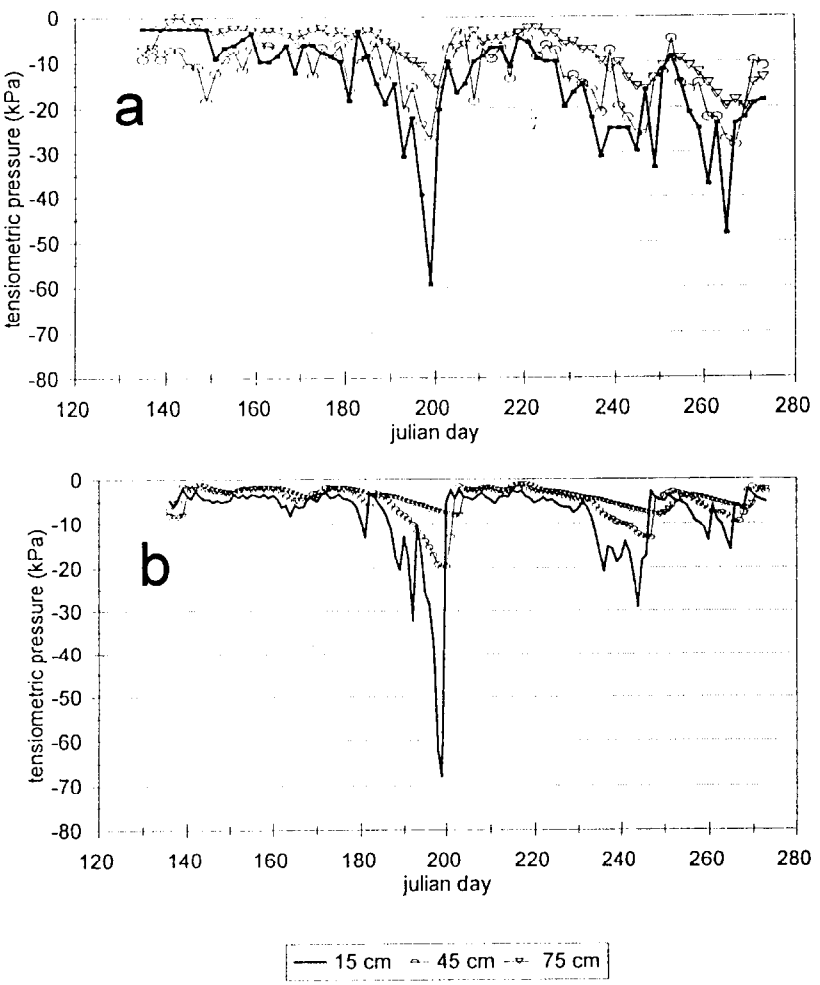

Figure 4: (a) Measured tensiometric pressures, Zábrod 1987. (b) Simulated tensiometric pressures, Zábrod 1987.

6 Conclusion

In most studied cases, retention curve variability does not influence modelled soil water balance. Retention curves variability could approve as (i) earlier or later starting of outflow from the soil profile, (ii) higher or lower intensity of outflow. Natural soil heterogeneity inside one genetic soil horizon does not depreciate simulation results. The significant artefact is adding or deleting of retention curve inflexion point on the approximated middle retention curve. It approve as a shift to hydraulic capacity with or without local maximum

(in the considered interval) and vice versa. Therefore, the similar retention curves (upper, middle and lower) must be similar in the capacity expression. In this case, the method of field estimation of the soil hydraulics characteristics (Šír et al., 1988) can be used for simulation of the soil water regime.

Acknowledgements

We would like to express thanks to Work Group SWAP (DLO - Winand Staring Centre and Wageningen Agricultural University, Wageningen, The Netherlands) for kindly supplying us with the computer programme SWAP. Grant Agency of the Czech Academy of Sciences (Project No A306071) and Grand Agency of the Czech Republic (Project No 526/98/0805) supported this work.

References

[1] Belmans, C. - Wesselink, J. G. - Feddes, R. A. (1983): Simulation Model of the Water Balance of a Cropped Soil SWATRE. J. Hydrol. 63: 271–286.

[2] Feddes, R. A. - Kowalik, P. J. - Zaradny, H. (1987): Simulation of Field Water Use and crop Yield. Simulation monograph. Pudoc, Wageningen.

[3] Pražák, J. - Šír, M. - Tesař, M. (1994): Estimation of plant transpiration from meteorological data under conditions of sufficient soil moisture. J. Hydrol. 162: 409–427.

[4] Šír, M. - Kutílek, M. - Kuráž, V. - Krejča, M. - Kubík, F. (1988): Field estimation of the soil hydralic characteristics. Soil Technology 1: 63–75.

Discharge capacity analysis of a river channel:

application to the Strážnice gauging station on the River Morava after a historical flood

K. Brych, F. Dittrt, V. Eliáš

Institute of Hydrodynamics, Academy of Sciences of the Czech Republic,
Pod Paťankou 5, CZ 16612 Praha 6, Czech Republic.

1 Introduction

Determination of river discharge at stream-gauging stations is routine practice for an experienced hydrological service which regularly carries out hydrometric measurements to define stage-discharge rating curves. Nevertheless, at high flood discharges the regular rating curve may be less valid or its range insufficient. This was the case for many of the official gauging stations in the basins of the upper Elbe, Odra and Morava rivers during the extremely devastating high floods which afflicted part of Central Europe in July 1997.

Consequently, many peak discharges and rating curves had to be determined after the passage of the flood by indirect methods which make use of the energy equation for computing streamflow. This methods involve physical characteristics of the channel, water-surface elevations at the time of peak stage and hydraulic factors based on physical characteristics (roughness coefficients). The case study presented here forms part of the Ministry of Environment Project entitled: "Evaluation of the floods of July 1997" (Hladný, 1998).

2 Generation and course of the flood

Two periods of heavy precipitation determined the generation of the flood which affected Central Europe from the 4^{th} to the 9^{th} and from the 17^{th} to the 21^{st} of July 1999. Both situations were caused by an undulating cold front. In the first case, which was more significant for the flood generation, the movement of the front from the southwest Alpine area was slowed down and cold air came through the valley of the river Rhone into the northwest Mediterranean region. A deepening low pressure was formed which, as it moved northeast, was the origin of high precipitation mainly in the eastern Czech Republic and southern Poland. The propagation of this low pressure was blocked by a high pressure over southern Scandinavia and for a long time it remained stationary over southern Poland. Precipitation amounts were enhanced by the orographic effect of the mountain chains. In the first period (4^{th} to 9^{th}) 234 mm was registered at the raingauge station Lysá Hora. For

the development of the runoff situation the five days precipitation amounts were decisive. In this period 586 mm of precipitation fell at Lysá Hora. The total precipitation volume was estimated in the basin of the river Morava to be 1.5 billion m^3 and in the basin of the river Odra to be 1 billion m^3. In some tributary rivers the discharge exceeded the values corresponding to floods of 100-year recurrence interval (Q_{100}). In the lowland reach of the river Morava the floodwave was transformed by the effect of inundation of the adjacent regions, but the discharge was still high due to the inflow from the tributaries. A peak discharge 1200 m^3s^{-1} was estimated at the Morava-Kroměříž gauging station but an area of 20 km^2 of inundated floodplain downstream took a large volume and lowered the discharge to 1034 m^3s^{-1}. The overflow of the riverbanks appeared at the discharge of 600–700 m^3s^{-1}.

3 Hydrological conditions at the Strážnice gauging station

The Middle Morava river reach lies at the river km 134.3. The gauging station Strážnice (catchment area 9146 km^2, in operation since 1939) represents the most important gauging station for estimating the behaviour of the river Morava to the estuary of river Dyje. The mean discharge is about 60 m^3s^{-1} (from the time series 1931–1980). Stream bed slope ranges from 0.0003 to 0.0002 at the Dyje estuary (km 70). The river channel is regulated and lies in clayey and sand-and-clay alluvial deposits. For the computation of discharge a survey of the cross sections of the channel reach was carried out.

4 Discharge capacity of the river Morava at Strážnice

4.1 Estimates of the discharge in the cross section by the slope-area method

By means of a geodetic survey of the river bed geometry (cross section of the gauging station and cross section of the cableway) the discharge was calculated by the formula (ČSN ISO 1070)

$$Q = KS^{1/2} \tag{1}$$

where Q is discharge (m^3s^{-1}), S is the friction slope. K is the conveyance which in the Manning equation equals

$$K = \frac{1}{n} AR^{2/3} \tag{2}$$

where A is the cross sectional area, R is the hydraulic radius, n is the Manning roughness coefficient. For both cross sections the conveyances K_i were calculated from cross section geometry corresponding to the gradually growing stage. The Manning roughness coefficient n was gained by evaluation of the field measurements carried out by the Brno branch of the Czech Hydrometeorological Service CHMI (see Table 1 and Fig. 1).

In the discharge computations the value of $n = 0.0325$ was used. This value is in a good conformity with the values recommended for natural channels in textbooks. The friction slope S between two considered cross sections is defined as

$$S = \Delta h + \frac{1}{L}\left(\frac{\alpha_1 v_{1h}^2}{2g} - \frac{\alpha_2 v_{2h}^2}{2g}\right) \tag{3}$$

where Δh is the difference in water surface elevation at two sections, α_1, α_2 are the velocity coefficients, v_1, v_2 are the average velocities in the cross sections, L is the lengths of the reach. The difference in water surface elevation Δh was measured by the Brno branch of the CHMI in the critical days of the flood, and are given in Table 2.

Table 1: Record of discharge measurements.

Day	Water stage h (cm)	Discharge Q (m^3/s)	Hydraulic radius R (m)	Mean profile velocity V (m/s)
4.3.1997	314	143.2	2.63	0.91
22.4.1997	212.5	79.8	1.81	0.82
27.5.1997	147.5	44.8	1.23	0.73
11.7.1997	699.7	532.9	4.85	1.25
14.7.1997	749	687.3	5.23	1.44
21.7.1997	687	530.4	4.78	1.26
29.7.1997	477.5	232.8	3.61	0.94
8.9.1997	284	101.4	2.31	0.78
9.10.1997	135.5	26.7	0.98	0.55
18.11.1997	218	67.3	1.82	0.70
12.12.1997	279.5	107.8	2.24	0.85
15.1.1998	200.5	61.6	1.63	0.73
20.2.1998	196.5	58.8	1.57	0.72
9.4.1998	198.7	62.8	1.57	0.74

Table 2: Water surface elevation measurement.

Day	Water stage h (cm)	Difference Δh (cm)	Length of the reach L (m)	Water slope $S = \Delta h/L$
10.7.1997	696.0	3	38	0.00078947
10.7.1997	696.0	2	40	0.0005
10.7.1997	696.0	5	78	0.00064202
15.5.1997	123.0	4	118.13	0.0003386

The value of the water level slope taken into the consideration for the discharge computations equals to: $\Delta h/L = 0.0003386$ at the stage $h = 123.0$ and $\Delta h/L = 0.0006410$ at the stage $h = 696.0$. A linear interpolation was applied between these two values, and is shown as the dashed line of Fig. 2. The full line in Fig. 2 was determined under the condition that the friction slope S used in the first step was corrected in such a manner that in the hydrometrically measured points its value was set up with the aim of approaching the result to the measured discharge.

The computation of the discharge corresponding to any stage was carried out by iteration. The first approximation was made under the assumption that the friction slope is equal to the water level slope. In the following step the average velocities ν_1 and ν_2 as Q/ν and consequently all remaining values needed in the Eq. 3 for the friction slope S were determined.

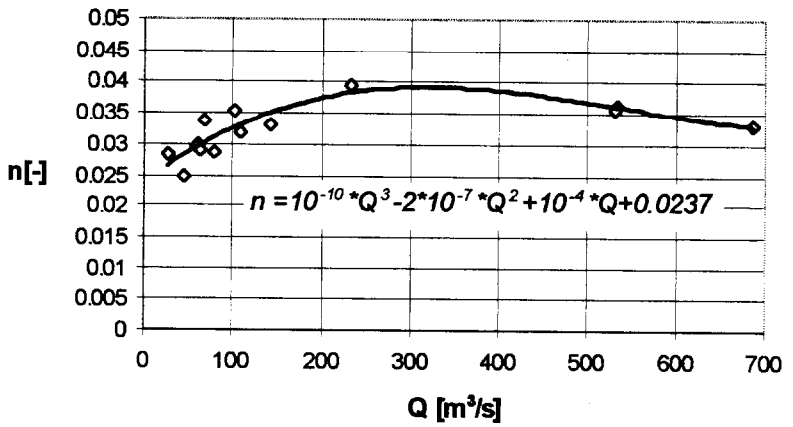

Figure 1: Manning roughness coefficient n evaluated from the CHMI discharge measurements (Eq. 1).

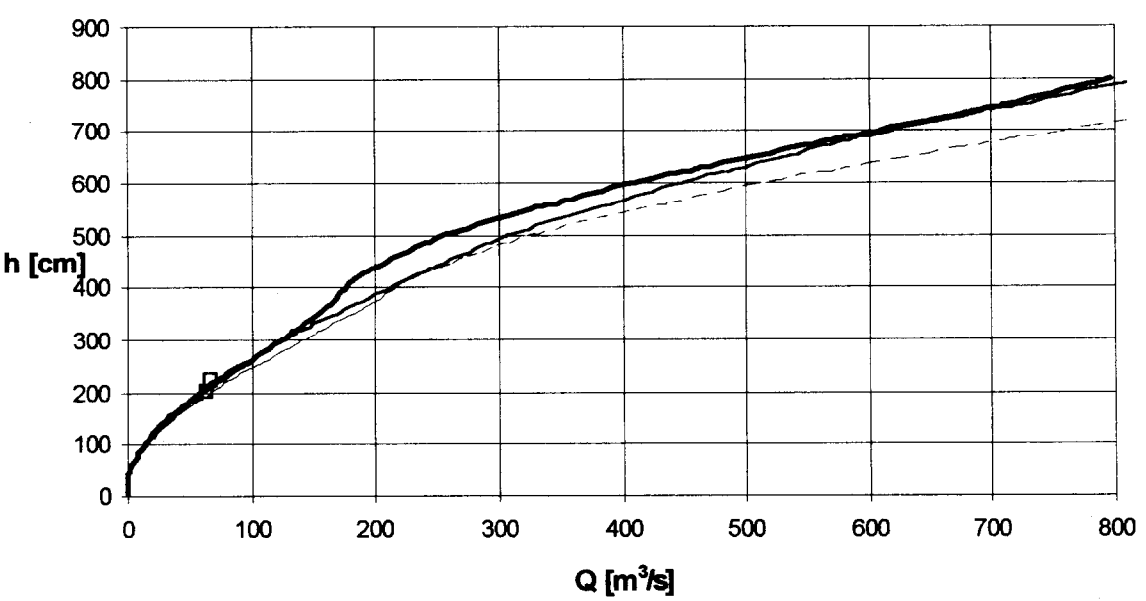

Figure 2: Rating curve of Morava-Strážnice gauging station estimated by area-slope method. Dashed line - interpolation between two values of the water level slope. Full line - friction slope corrected according to the measured discharge. Fine line - estimated Q with $n = 0.0325$, $S = 0.0003$.

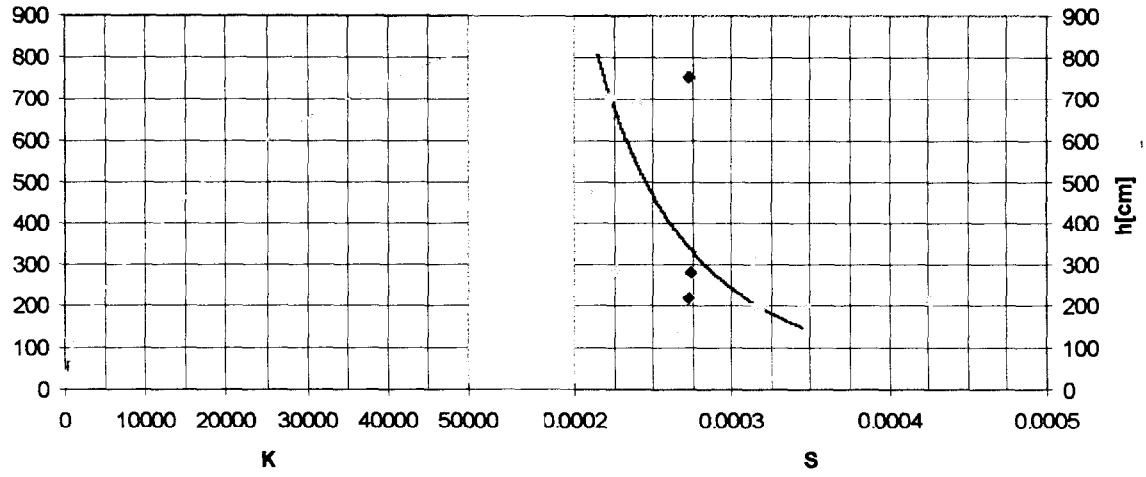

Figure 3: Conveyance K and friction slope S at Morava-Strážnice cross section.

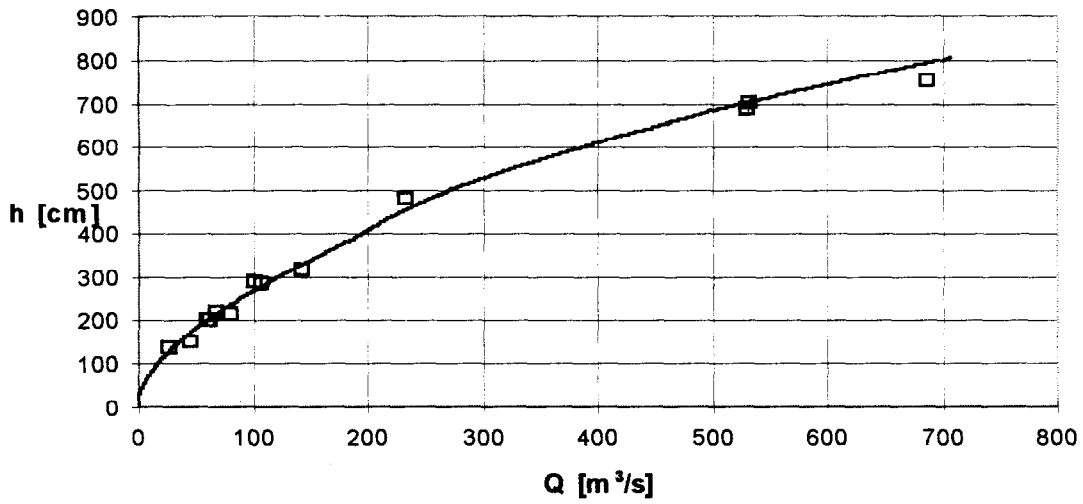

Figure 4: Rating curve of Morava-Strážnice gauging station estimated by means of the conveyance slope method.

4.2 Estimates of the discharge in the cross section by the conveyance slope method

The values of the friction slope S are usually not known even for measured discharges but it is possible to determine $S^{1/2}$ by dividing each measured discharge by its corresponding K value computed from the geometry of the measured cross section (WMO, 1980). Values of gauge height versus S for the measured discharges at the Strážnice gauging station are plotted as a curve of best fit in Fig. 3.

The extrapolation facilitates the knowledge that this curve tends to be constant at the higher stages and that constant slope is the slope of the river bed. The discharge Q is obtained by multiplying the value of the K from the K curve by the value of $S^{1/2}$ from the S curve for the same gauge hight. By means of this procedure the rating curve of Strážnice station was extrapolated for ungauged points (Fig. 4).

4.3 Discharge estimates by means of the HEC-RAS program

Based on a geodetic survey of several river cross sections a geometric model of the studied river reach was developed. After calibration of the model with data measured at the cross section of the gauging station a short time after the flood the new rating curve was computed. An example of a typical output using the HEC-RAS software is presented in Fig. 5.

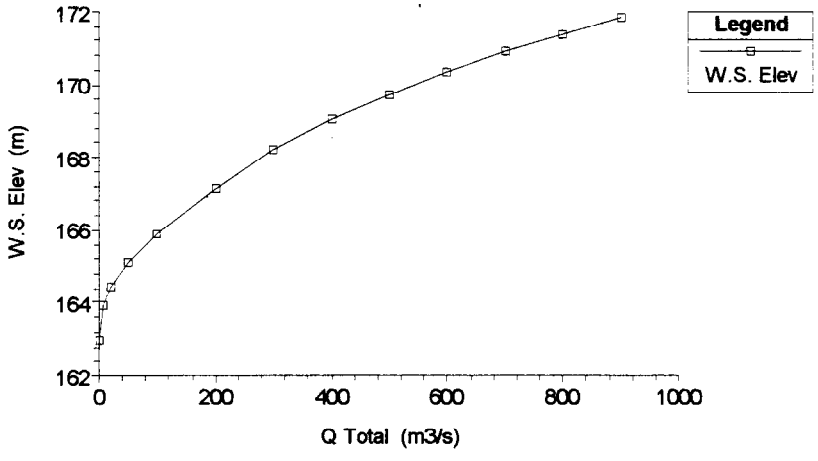

Figure 5: Rating curve Morava-Strážnice gauging station calculated by the HEC-RAS program.

5 Conclusions

Three methods of discharge capacity estimation based on a river bed geometry survey were applied. There are deviations from the officially used rating curves in all cases. The conveyance slope method is less laborious, does not depend so much on subjective decisions and could be more reliable than the area-slope method. It should be realised that errors may result from the use of equations (which were designed for steady flows) in unsteady conditions especially at flood peaks. The use of an available software, e.g. HEC RAS, and computer processing enables the calibration of an adequate model and computation of several variants of spatially distributed roughness coefficient.

References

[1] ČSN ISO 1070 Liquid flow measurement in open channels. Slope-area method. Prague 1994

[2] WMO, 1980, World Meteorological Organisation Manual on Stream Gauging Operational Hydrology, Report No. 13, WMO No. 519, Geneva, Switzerland 1980

[3] Hladný, J. et al. (1998). Vyhodnocení povodňové situace v červenci 1997 (Evaluation of the flood situation in July 1997), Ministry of Environment of the Czech Republic. Research Report of the Czech Hydometeorological Institute, Ed. CHMI Prague

Rainfall-runoff processes modelling using the Sacramento and Brook models

in the Cal Rodó catchment (Pyrenees, Spain)

J. Buchtele[1], M. Buchtelová[1], F. Gallart[2], J. Latron[2], P. Llorens[2], C. Salvany[2], C. & A. Herrmann[3]

[1]Institute of Hydrodynamics, Academy of Sciences of the Czech Republic, Pod Paťankou 5, CZ 166 12 Praha 6, Czech Republic. [2]Consejo Superior de Investigaciones Científicas, Institut de Ciències de la Terra "Jaume Almera" (CSIC), Lluís Sole i Sabarís, s/n. 08028 - Barcelona, Spain. [3]Institute of Geography and Geoecology, University of Braunschweig, Langer Kamp 19c, Braunschweig, Germany.

1 Introduction

Within the VAHMPIRE project, a full exercise of calibration-validation has been done with several hydrological models (SHETRAN, TOPMODEL, TOPKAPI, BROOK and SACRAMENTO). The modelling teams have been provided with a 34-month series of input data (rainfall and weather), but only a 17-month series of discharge data for calibration of models (the calibration period). The validation of the models has been performed externally by the managers of the catchments, through comparison of simulated versus observed variables.

This paper presents a part of this exercise and analyses, namely the performances, of two lumped models: the conceptual SACRAMENTO model (Burnash, 1995); and the physically based BROOK model (Federer, 1993).

The daily discharges simulated by these two models are compared with the observed discharges for the whole 34-month period. The behaviour of simulated sub-surface water storages and runoff component simulation are also analysed but without comparison with observed values.

2 The study area

The Cal Rodó catchment (4.17 km^2) is located within the Vallcebre catchment in the southern margin of the Pyrenees at altitudes between 1100 m and 1700 m. Fig. 1 provides an overview of the configuration of the catchment. Bedrock is formed by an alternation of massive limestone beds outcropping in the southern half of the catchment and red smectite-rich mudstones over which well structured loamy soils have developed. The original hillslope topography has been affected by the construction of terraces over more than a third of the catchment surface area. These terraces used for cultivation have undergone an abandonment process in the last 60 years and have been progressively naturally reforested by *Pinus sylvestris* that nowadays cover 60 % of the catchment.

Climate is defined as mountain Mediterranean with a mean annual temperature of 9°C, an annual reference evapotranspiration of 850 mm and a mean annual rainfall of 900 mm. In the catchment, water deficit is frequent in summer, enhanced or reduced following the high inter and intra-annual variability of the pluviometric regime.

The instrumentation of the Cal Rodó catchment that started in 1991, for the study of sediment dynamics (Balasch et al., 1992), has been highly improved since 1994 for the study of runoff generation mechanisms (Latron et al., 1996) and interception losses (Llorens et al., 1997, Llorens, 1997). The present instrumention (Latron et al., 1998) allows the continuous measurement of incoming and outgoing fluxes in a set of 4 nested catchments as well as the assessment of their internal hydrological dynamics.

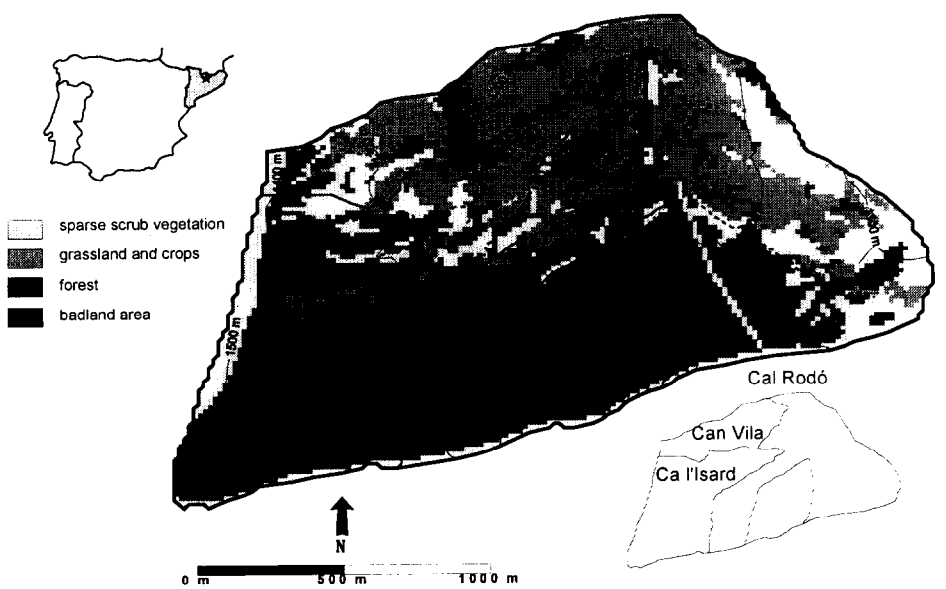

Figure 1: Map of the Vallcebre catchment.

3 The models

3.1 The Sacramento model

The Sacramento soil moisture accounting model SAC-SMA, coupled with the Anderson (1973) snow model, allows continuous simulations over several years. It is a conceptual water balance model with lumped inputs and parameters. It takes into account vertical gradients of air-temperature and its consequences for snow deposits. The model provides an overview of several components of the water balance i.e. runoff, sub-surface water storages etc. The following features of this tool should be mentioned as specific in connection with the analysed processes:

- Percolated water is computed as an amount proportional to the deficits of water in five zones ('reservoirs') of the model. The corresponding five water storage variables are:
  - Upper and Lower Zone Tension Water Maximum UZTWM, LZTWM.
  - Upper Zone Free Water Maximum UZFWM.
  - Lower Zone Free Primary and Supplementary Maximum LZFPM, LZFSM.

- Actual evapotranspiration is evaluated separately for the five mentioned zones of the model, also proportionally to deficits in these zones.
- Six runoff components are generated by the model:
    - Direct runoff, from the parts of the catchment that becomes impervious after saturation DIR.
    - Runoff from the permanently impervious parts of the basin IMP.
    - Surface runoff SUR.
    - Interflow INT.
    - Supplementary baseflow (i.e. essentially the seasonal component of outflows from groundwater storages) SUP.
    - Primary baseflow (i.e. its long term part) PRM.

3.2 The Brook 90 model

This model simulates the land phase of the precipitation - evaporation - streamflow part of the hydrologic cycle for small, uniform (lumped parameter) catchment. For evaluation of potential transpiration it uses the Penman-Monteith (Monteith, 1965) equation and the Shuttleworth and Wallace (1985) procedure for separation of soil evaporation and transpiration from sparse canopies. Water is stored in the model as intercepted rain or snow, as snow on the ground, as soil water in several layers and as groundwater.

Evaporation has five components:

- Evaporation of intercepted rain IRVP.
- Evaporation of intercepted snow ISVP.
- Evaporation from snow cover SNVP.
- Soil evaporation, from the top soil layer SLVP.
- Transpiration from each soil layer that contains roots TRAN.

Net precipitation may go:

- Immediately to streamflow via a variable saturated source area SRFL.
- To streamflow via vertical macropore flow followed by downslope pipe flow BYFL.
- To create downslope component of flows DSFL.
- The groundwater component of streamflow GWFL, is simulated as a fixed fraction of groundwater. A fixed fraction of groundwater outflow may be deep seepage.

4 Results

In initial experiments the SAC-SMA model has been applied for the three sub-basins, i.e. for Cal Rodó, Cal 'Isard and Can Vila as this model does not need so much information about basins as the BROOK model. These preliminary calibrations showed some difficulties in the data sets, like the representativeness of the air temperatures because of the altitude differences within the catchments. Although winter is usually the season with less precipitation in the area, some snowfalls occurred during the analysed period, snowmelt process being therefore not negligible.

Three phenomena have been evaluated in the experiments carried out till now: runoff, sub-surface water storages and evapotranspiration. Attention has been paid to accuracy of runoff simulation as it integrates all the processes into one closing point.

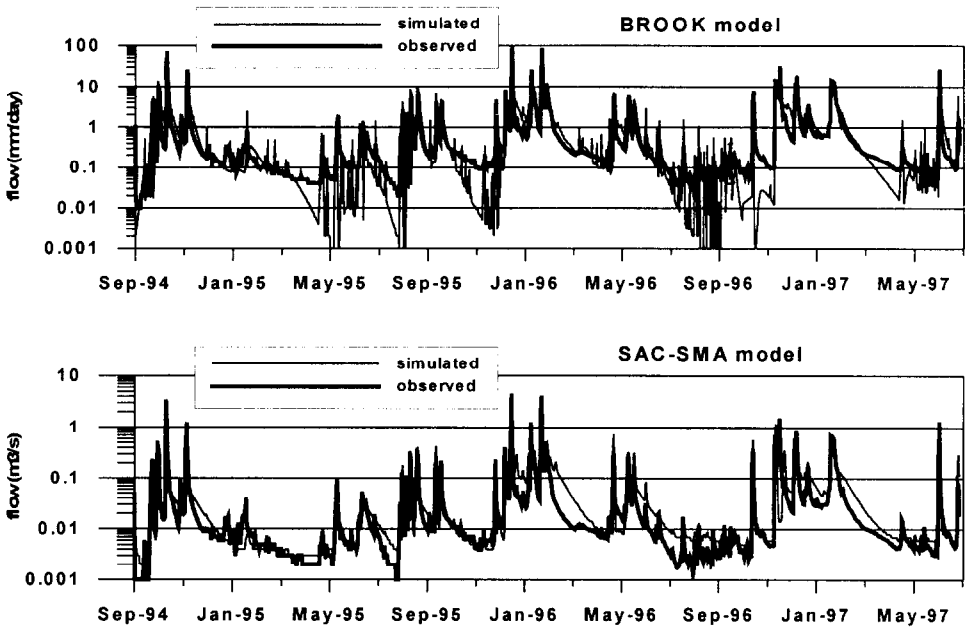

Figure 2: Runoff simulation for Cal Rodó, years 1994–97.

4.1 Observed and simulated discharges

Simulations using the SAC-SMA model are more smooth than the outputs of the BROOK model and in all three sub-basins the results of the SAC-SMA model are evidently more accurate during low flow periods. This is apparent in semilogarithmic hydrographs, whereas hydrographs simulated by the BROOK model show a clear underestimation of low flows and depletion parts of simulated hydrographs are quicker than observed ones, see Fig. 2.

However, the overall accuracy as evaluated by means of the Nash and Sutcliffe (1970) criterion is better with the BROOK model, as shown on Table 1.

Table 1: Values of the Nash & Sutcliffe criterion for different catchments and models (calibration period).

Catchment	Model	
	SAC-SMA	BROOK
Cal Rodó	0.598	0.832
Cal 'Isard	0.615	0.804
Can Vila	0.555	0.874

There are probably two reasons. During the process of manual calibration attention has been paid mainly to the simulation of long-lasting low flow periods, the obtained parameters not allowing the models to behave correctly when simulating the high peaks of such Mediterranean catchments. On the other hand the Nash and Sutcliffe (1970) criterion overestimates the significance of high flows as squared values are used as inputs for its computation.

The first reason means that the improvement of SAC-SMA simulations is still possible, although simulation of low flows will presumably be worsened, and it is unclear that the reliability of the overall water balance computation would be significantly changed.

Previous simulations using the BROOK model showed high sensitivity of simulated flows to types of vegetation cover (Buchtele et al., 1998) and some recent experiments seem to indicate that the accuracy of baseflow simulations using the BROOK model could be improved probably with longer time series, but quick decreases of simulated low flows as shown of Fig. 2 seem difficult to be avoided.

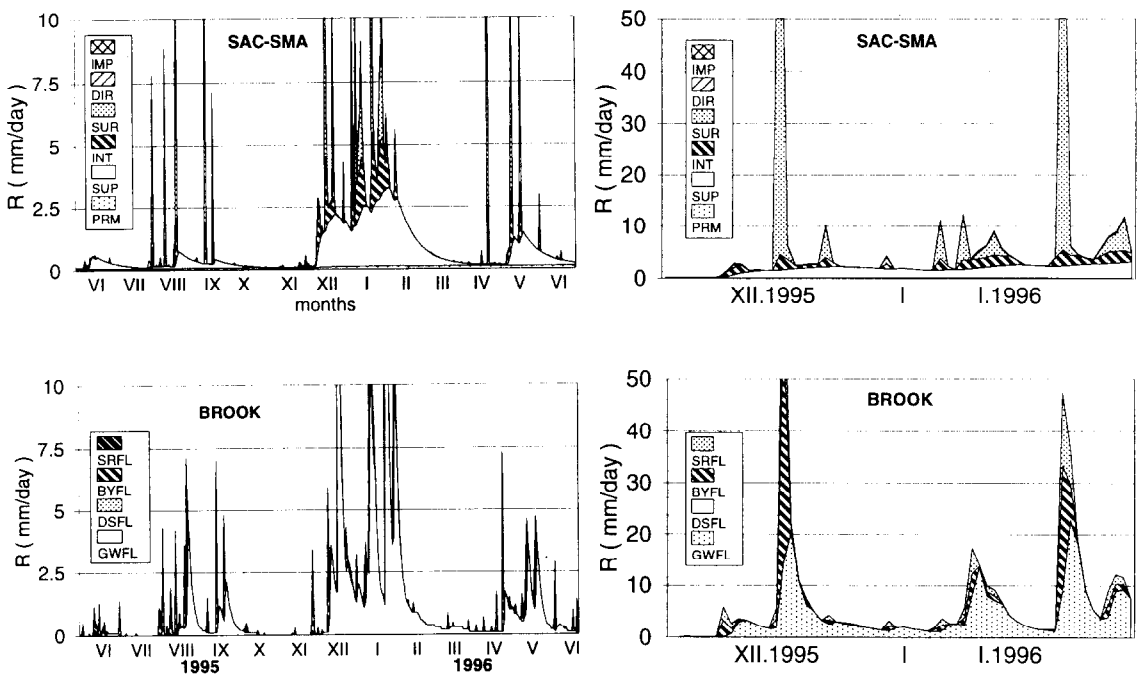

Figure 3: Simulated runoff components in the Cal Rodó basin for period two years and for one part two months long. The acronyms of components are given in text.

4.2 Runoff components

The proportions of simulated runoff components using both models are presented in Table 2. Even in this preliminary work, it becomes evident that the flow components obtained by simulation show specific characteristics that must be analysed taking into account the climatic conditions. In humid catchments, both the SAC-SMA and the BROOK models show that baseflow is the main component of runoff for different lithology and basin size (Buchtele et al., 1996). Nevertheless, runoff components simulated for the Cal Rodó catchment by the BROOK model (Fig. 3) show that there are two kinds of runoff events: high and wide peaks with a baseflow contribution of more than 25 %; and narrow and usually smaller peaks with insignificant baseflow contribution. This simulation result is consistent with observations that show the seasonality of hydrological behaviour for this catchment (Latron et al., 1996; Gallart et al., 1997) and deserves further work.

4.3 Sub-surface water storages

Due to the different structure of the models used it is not possible to compare absolute values of outputs from both models. For example, it is desirable to take into account that the SAC-SMA model distinguishes tension water and two free water zones, while the BROOK model provides only one output of this kind, but it has a more complex structure of interception processes. Therefore it is reasonable to compare only the range of variability of water storages in both models. Although the absolute volumes are rather different, similarity is well evident in the given period (Fig. 4). Discrepancies between the two models seem more important during dry periods, when the BROOK model simulates lower water storage, consistent with the lower baseflow predicted by this model (Fig. 2).

Table 2: Simulated runoff components of the Cal Rodó basin (in percents).

SAC-SMA	IMP+DIR	SUR	INT	SUP	PRM	Sum
(%)	4.2	49.0	9.8	30.0	7.0	100
BROOK		SRFL	DSFL	BYFL	GWFL	
(%)		16.0	0.5	20.7	62.8	100

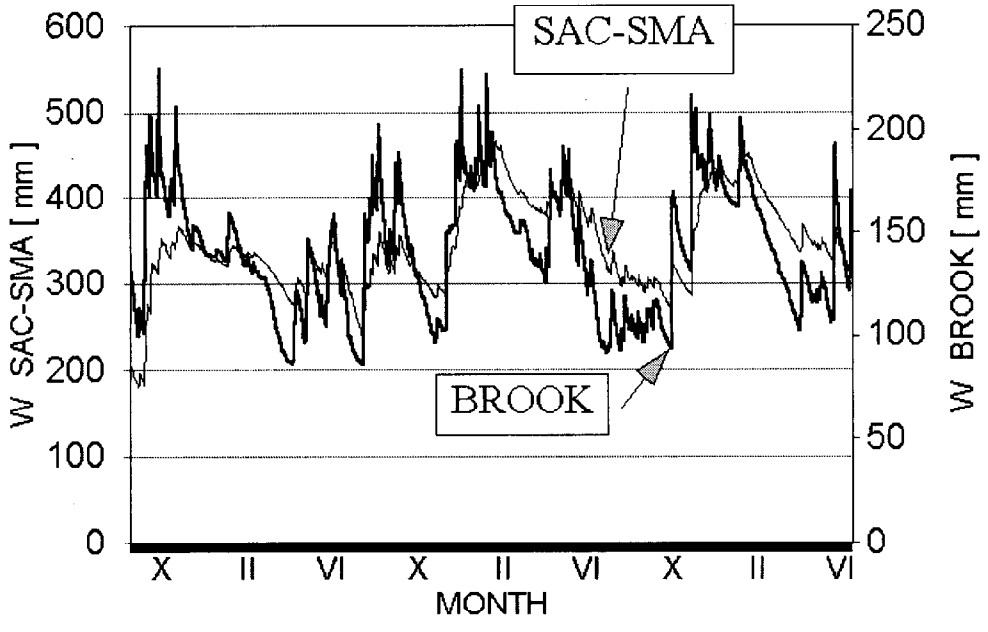

Figure 4: Simulated sub-surface water storages in years 1994–97.

5 Conclusion

Simulations of rainfall-runoff processes for Cal Rodó basin provide results which confirm the dominant role of vegetation cover for the water balance of a small basin in season-

ally dry climate conditions. Adequate evaluation of the evapotranspiration process is, therefore, a very important task for prediction of basin behaviour.

Simulations of runoff components using two different models do not provide directly comparable results. Baseflows represent the main part of runoff in both cases but during late summer rainstorms the contribution of baseflow is insignificant.

Similarity of simulated variation in sub-surface water storages suggests that such information could be useful for evaluation of tendencies in the catchment behaviour.

Acknowledgements

This work forms part of the project VAHMPIRE, contract ENV4-CT95-0134, funded by the European Community, Climate and Environment Programme. The authors from the Czech Republic acknowledge the support of GA of the Academy of Sciences of the Czech Republic (grant A 3060605) and of GA of the Czech Republic (grant 205/99/1561).

References

[1] Anderson, E. A. (1973): NWSRFS - Snow accumulation and ablation model; NOAA Technical Memorandum NWS HYDRO-17, U.S. Dept. Of Commerce, Silver Spring, Md.

[2] Balasch, J. C., Castelltort, X., Llorens, P., Gallart, F. (1992): Hydrological and sediment dynamics network design in a Mediterranean mountainous area subject to gully erosion. In: J. Bogen, D. E. Walling and T. Day (Eds.), Erosion and transport monitoring programmes in river basins. IAHS Pub. no. 210: 433–442.

[3] Buchtele, J., Eliáš, V., Tesař, M., Herrmann, A. (1996): Runoff components simulated by rainfall - runoff models, Hydrol. Sci. J. 41: 49–60.

[4] Buchtele, J., Herrmann, A., Maraga, F., Bajracharya, O. R.: (1998) Simulation of Effects of Land-use Changes on Runoff and Evapotranspiration In: K. Kovář, U. Tappeiner, A. E. Peters, R. G. Graig (Eds.) Hydrology, Water Resources and Ecology in Headwaters, Proc. Head Water '98 Conf., 20.–23. April 1998, Merano. IAHS Publ. no. 248: 99–106.

[5] Burnash, J. C. R. (1995): The NWS River Forecast System - Catchment Modeling. In: V.P. Singh (Ed.), Computer Models of Watershed Hydrology. Water Resources Publications. 311–366.

[6] Federer, C. A. (1993): BROOK 90 - A Simulation Model for Evapotranspiration, Soil Water and Streamflow. USDA Forest Service, Durham, NH, USA.

[7] Gallart, F., Latron, J., Llorens, P., Rabadà, D. (1997): Hydrological functioning of Mediterranean mountain basins in Vallcebre, Catalonia: some challenges for hydrological modelling. Hydrological Processes 11: 1263–1272.

[8] Latron, J., Gallart, F., Salvany, C. (1998): Analysing the role of phreatic level dynamics on the streamflow response in a Mediterranean mountainous experimental catchment (Vallcebre, Catalonia). In: J. Bucek, M. Šír, M. Tesař (Eds.), Catchment Hydrological and Biochemical Processes in Changing Environment. Publ. of Abstract of the VIIth ERB Conference, Liblice, September 1998. 63–66.

[9] Latron, J., Llorens, P., Gallart, F. (1996): Spatial and temporal patterns of runoff generation processes in mountainous Mediterranean basins (Vallcebre, Catalonia). In: D. Viville, I. G. Littlewood (Eds.), Ecohydrological processes in small basins. UNESCO, IHP-V Technical Documents in Hydrology 14: 93–98.

[10] Llorens, P. (1997): Rainfall interception by a Pinus Sylvestris forest patch overgrown in a Mediterranean mountainous abandoned area. II. Assessment of the applicability of Gash's analytical model. Journal of Hydrology 199: 346–359.

[11] Llorens, P., Poch, R., Latron J., Gallart, F. (1997): Rainfall interception by a Pinus Sylvestris forest patch overgrown in a Mediterranean mountainous abandoned area. I. Monitoring design and results down to the event scale. Journal of Hydrology 199: 331–345.

[12] Monteith, J. L. (1965). Evaporation and environment. In: G. Fogg (Ed.), The State and Movement of Water in Living Organisms. Symp. Soc. Exper. Biol. 19: 205–234.

[13] Nash, J. E., Sutcliffe, J. V. (1970): River flow forecasting through Conceptual Models. I. A discussion on principles. Journal of Hydrology 65: 125–137.

[14] Shuttleworth, W. J., Wallace, J. S. (1985): Evaporation from sparse crops - an energy combination theory. Quart J. Royal Meteorol. Soc. 111: 839–855.

The importance of throughfall measurement in evaluating hydrological and biogeochemical fluxes:

Example of coniferous catchment (Mont-Lozère, France)

J. F. Didon-Lescot

UMR 5651 du CNRS "Espace", University of Nice, Domaine Carlone,
98 boulevard E. Herriot, F-06204 Nice, France.

1 Introduction

At the catchment scale, hydrological and biogeochemical fluxes are often calculated in terms of input/output budgets: precipitation input minus streamflow output (Hornung et al., 1990). Measuring the precipitation is sufficient for catchments with low-lying vegetative cover. However, in the case of tree-covered catchments, depending on elevation and the species in question, forests can favour both cloud deposition and atmospheric deposition (Cape et al., 1991; Harding et al., 1992, Lindberg and Owens, 1993). This can have a significant effect on the functioning of mountain and forest ecosystems, be it beneficial (additional supply of water that reduces water stress, or of minerals that improve poor soil) or detrimental (acid deposition). Here we treat the example of a coniferous catchment in the Mont-Lozère area (southern region of the Massif Central in France), under study since 1981 (Lelong et al., 1990; Didon-Lescot, 1996), as well as the uncertainties associated with evaluation of inputs.

2 Methods

The Mont-Lozère catchments (ERB FR 110) are located in the Cevennes area, in southern France, 80 km from the Mediterranean Sea (Fig. 1). The catchments are small (0.2–0.8 km^2), all on the same parent rock (granite) and with the same south-facing exposure (Lelong et al., 1990). They differ only in the type of vegetation (Norway spruce, beech, grassland). The spruce catchment, at 1350–1500 m altitude, was planted in 1930 and cut over in 1987–89, the plantation appeared relatively sparse (390 trees per hectare) with declining stands. There are also small stands of beech of similar age at the base of the catchment. Three plots under spruce and beech at 1400 m in elevation were used for studying throughfall, first under continuous spruce canopy (1987–88), then in isolated patches of spruce or beech (1989–92) surrounded by a low-lying vegetation when the forest was cut down. Another catchment, covered with beech, at approximately 1150 m elevation, was used as a reference. Mean rainfall for the period 1981–97 was 2000 mm, varying between 1146 mm (1985) and 3392 mm (1996). Snowfall varied from 10 to 40 % of the total annual precipitation.

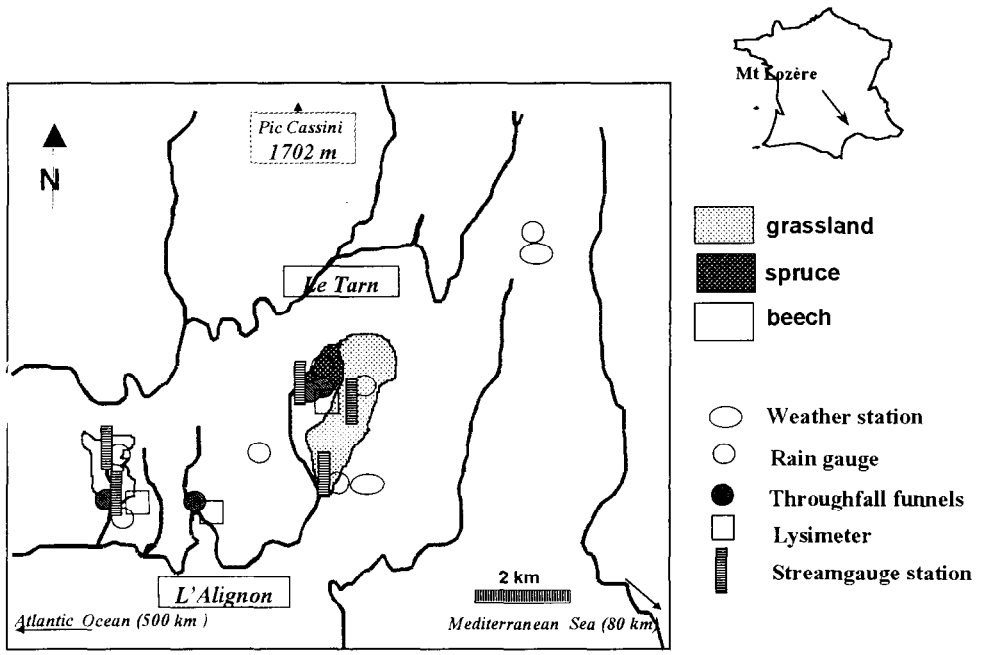

Figure 1: Location map.

Each catchment is equipped with a rain gauge, a stream gauge station, and water collectors (rain collector, streamwater sampler) for measuring hydrological and hydrochemical fluxes (Didon-Lescot, 1996). For estimating atmospheric deposition to forests, the set-up included: a network of ten 350 cm^2 PVC throughfall funnels connected to 10-litre collecting drums (overflow at 328 mm), each 2 m apart; five collectors per rubber stemflow collar at 1.3 m above the ground and 30-litre drum for beech, on trees chosen for their representative trunk diameter (9.5 to 22 cm); a single stemflow collector for spruce (coeval population, median for Ø 130: 27.5 cm). An equivalent set-up was established during the same period on the beech-forested catchment.

The water was usually collected for analysis after each rainfall event (20–40 per year). Fluxes in clearings and under the canopy were calculated by multiplying concentrations by the amount of water.

3 Results

3.1 Throughfall volumes (Table 1)

For the period 1987–88, foliage drip under continuous canopy represents 78 % of rainfall amount, varying from 70 % in the summer to 81 % in winter. For 1989–1992, the results vary considerably for the isolated patches, depending on the vegetation species. Under spruce, throughfall represents 90 % of annual precipitation and stemflow is less than 1 %. Under beech, foliage drip varies from 62 to 70 % and stemflow from 25 to 30 %. Annual interception $Int = R-(TH+ST)$ (R - rainfal, TH - throughfall, ST - stemflow), expressed as a percentage of annual precipitation, varies from -2 to 9 % under spruce and from 2 to 12 % under beech.

Table 1: Yearly and seasonal volumes (mm) of throughfall TH, stemflow ST, and interception Int, compared to rainfall R, under spruce and beech, for the 1400 m site at Mont-Lozère, from 1987 to 1992.

	1987	1988	1989	1990	1991	1992	1987	1988	1989	1990	1991	1992	1987	1988	1989	1990	1991	1992
Spruce	Year						Winter: 1/10-30/4						Summer: 1/5-30/9					
R	1681	2685	1391	1398	1347	2014	1527	2114	1186	1011	851	945	154	571	205	388	496	1069
TH	1328	2112	1253	1326	1337	2047	1242	1711	1109	1056	913	1086	86	400	144	270	424	961
ST			10	10	10	15			9	7	6	7			2	3	4	8
Int	353	574	128	63	1	-47	285	403	68	-53	-68	-148	68	171	60	115	69	101
% R	0.21	0.21	0.09	0.04	0.00	-0.02	0.19	0.19	0.06	-0.05	-0.08	-0.16	0.44	0.30	0.29	0.30	0.14	0.09
Beech	Year						Winter: 1/10-30/4						Summer: 1/5-30/9					
R			1391	1398	1347	2014			1186	1011	851	945			205	388	496	1069
TH			856	977	897	1257			727	737	591	553			129	240	306	704
ST			421	390	369	512			377	319	264	291			44	71	105	221
Int			114	32	81	245			82	-45	-4	101			33	78	85	144
% R			0.08	0.02	0.06	0.12			0.07	-0.04	0.00	0.11			0.16	0.20	0.17	0.13

During summer (for beech, the growing season is from May 1 to September 30) interception for the species varies from 13 to 20 % and during winter (the dormant period from October 1 to April 30) from 11 to - 4 %. For spruce, interception varies from 9 to 30 % in summer, and is often predominantly negative during winter. The negative values for interception suggest that total precipitation has been under-estimated. We interpret this to be due to a 'hidden' deposition by cloud condensation, particularly under spruce, that is observed over 1400 m in altitude. The phenomenon occurred 33 times from 1989 to 1992, mostly during the winter months. The intensity recorded under coniferous canopy was sometimes considerable: up to 7 $mm.h^{-1}$ (Fig. 2).

At the 1150 m beech site, mean seasonal or annual interception is always positive, varying between 10 and 25 % with the season, indicating the almost certain absence of cloud deposition at this altitude (Hanchi, 1994).

3.2 Atmospheric inputs (Table 2)

The rainfall at Mont-Lozère is moderately acid (pH 4.7), with predominance of Ca and Na, Cl and SO_4-S (Durand et al., 1992). After passing through the foliage, throughfall contains the same major ions as rainfall, with more or less comparable quantities under beech and considerably higher ones under spruce. Under beech, net throughfall flux $TH + ST - R$ (R - rainfal, TH - throughfall, ST - stemflow) is significant only for K (due to foliage leaching), moderate for Ca, Mg and SO_4-S, and negative for H (cationic exchange) and N (absorption). Under spruce, there is an overall enrichment for all elements. Foliage leaching is important for K and Mg, moderate for Ca and accounts for 95 % of the enrichment for K, 50 % for Mg, and 20 % for Ca according to other French studies with similar coniferous stands (Dambrine et al., 1995). Otherwise, the increase in throughfall flux values is due mainly to other inputs: marine aerosols (Cl, Na); trapped dust particles brought in from the Sahara, which are abundant during dry years and rich in Ca and SO_4-S; and dry acid deposition (H, N).

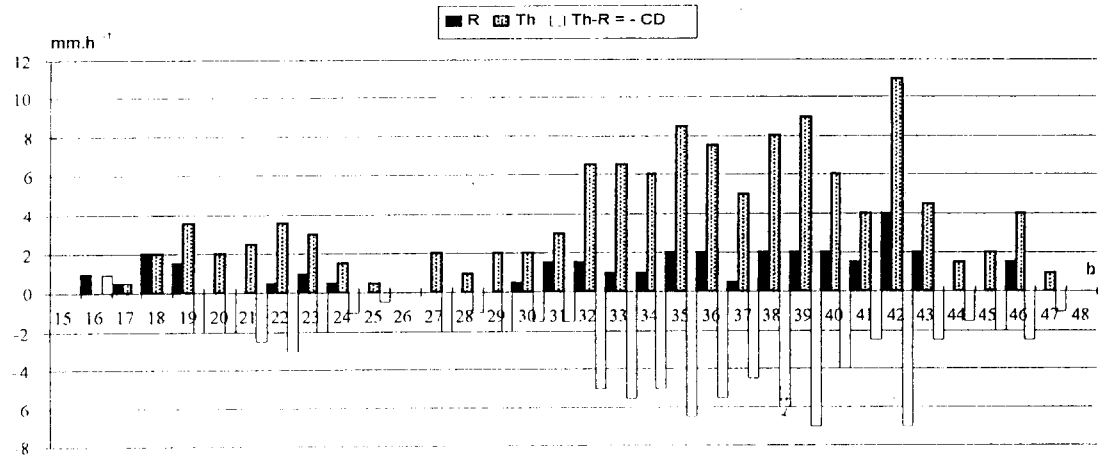

Figure 2: Example of a cloud deposition event (15 and 16/5/1995). Hourly intensity ($mm.h^{-1}$) for rainfall R, throughfall TH and cloud deposition CD under the 1400 m spruce site. Starting at 15 hours.

4 Discussion

Total precipitation is under-estimated in the hydrologic fluxes, because cloudwater is not taken into account. However, under continuous canopy cover the latter input is insignificant, particularly in 1987–88 before the forest was cut over (Table 1). It is possible to evaluate the impact of cloud deposition for the isolated patches which remain. If we assume that interception for spruce is constant with the same magnitude all year round, the values for summer (an almost entirely cloud-free period) can be transposed to the winter period. Based on mean summer interception for 1989–92, we could have to increase winter precipitation by 20 % to obtain the same interception rate, resulting in a 13 % increase in annual rainfall. It would not be realistic to extrapolate site results to the entire catchment, because the excess of cloud deposition over the isolated patches of spruce is linked to an edge effect, as is often the case in sparse high-elevation forests (Linberg and Owens, 1993). In the absence of more precise measurements, if we refer to studies on other mountain sites (Cape et al., 1991; Harding et al., 1992), we can still assume that: i) there is cloud deposition at 1400 m and higher in this area; and ii) there is a 5–10 % under-estimation of total precipitation. Given the lack of precision in rainfall figures, this has relatively little influence on the hydrological balances here; Table 3 shows realistic actual evapotranspiration AET in the three catchments and similar values in the two forested catchments (Lelong et al., 1990).

As for hydrological fluxes in the spruce catchment, under the canopy it is always significantly higher than the input measured in clearings (Tables 2 and 4). Once again, it is difficult to transpose the hydrochemical fluxes measured at the plot scale to the catchment scale. For example, the rainfall input/output budgets $R - O$ for chloride during the period 1987–88 before clearing is just about balanced. If we take into account total deposition estimated in the catchment [TD= wet deposition R + fraction of dry deposition $DD * x$), in order to allow for incomplete forest cover], the budgets become clearly cumulative (Table 4), although chloride is reputed to be a conservative element.

We note that a 30 % decrease in chloride deposition would be necessary to balance the budget, which is high but compatible with the results of similar studies on deposition

Table 2: Atmospheric inputs and throughfall fluxes (kg.ha^{-1}.yr^{-1}, H in eq. ha^{-1}.yr^{-1}) under spruce and beech for the 1400 m site at Mont-Lozère, from 1989 to 1991. R rainfall, TH throughfall, ST stemflow, net throughfall $NT = TH + ST - R$, DD dry deposition, FL foliage leaching.

		H	Ca	Mg	K	Na	NH_4-N	SO_4-S	Cl	NO_3-N
Norvay	R	0.52	17.6	2.3	2.6	12.9	5.8	17.5	22.9	7.4
spruce	TH	1.13	38.2	7.2	23.2	30.5	9.9	44.7	59.2	19.5
	NT	0.61	20.6	4.9	20.6	17.6	4.1	27.2	36.3	12.1
	DD	0.61	16.5	2.5	1.0	15.8	4.1	24.5	32.7	12.1
	FL	0.00	4.1	2.5	19.6	1.8	0.0	2.7	3.6	0.0
Beech	TH	0.16	14.0	2.1	10.9	8.3	3.4	13.2	17.3	4.6
	ST	0.10	4.3	0.8	3.8	2.8	0.6	5.0	5.7	1.6
	$TH + ST$	0.26	18.3	2.9	14.7	11.1	4.0	18.2	23.0	6.2
	NT	-0.26	0.7	0.6	12.1	-1.8	-1.8	0.7	0.1	-1.2
	DD		0.6	0.3	0.6			0.7		
	FL	0.00	0.1	0.3	11.5	-0.2	0.0	0.1	0.0	0.0

Table 3: Hydrological balances in the three catchments for the period 1981-87. Actual evapotranspiration AET calculated as $R - S$, R - rainfall, S - streamflow.

	Rainfall R (mm)	Streamflow S (mm)	AET (mm)
Grassland	1859	1472	387
Spruce	1865	1253	612
Beech	1769	1173	596

patterns as a function of distance to the forest edge (Beier, 1991; Harding et al., 1992). Other reasons could explain the imbalance in the chloride budget. Looking at the 1989–91 period, during the clearfelling of the spruce, which reduces drastically the possibility of occult deposition, the budget remains unbalanced. The measurement of hydochemical fluxes at the forest-floor and in the organic-mineral soil indicates the possibility of chloride storage in these compartments (Didon-Lescot, 1996).

Dry deposition estimated by throughfall at the spruce site is high: equal to values for wet deposition of Ca and Mg but lower for K, and higher for S and Cl (Table 2). Supposing the same over-estimation for the cations as for chloride at the catchment scale, deposition would be 4.7 kg.ha^{-1}.y^{-1} for Ca, 0.8 for Mg and 0.5 for K (Table 5). In spruce mediterranean mountain ecosystems, these inputs could limit the weathering of bedrock calculated as the balance between the output for biomass removal and hydrochemical fluxes (Didon-Lescot, 1996). Calculated deposition (wet + dry) is sufficient for Ca but not for Mg and K. For Mg, particularly, the level of the output is high and appears as a possible hazard for the sustainable development of spruce forestry in this low Mg-soil context.

Table 4: Input/output budget ($kg.ha^{-1}.y^{-1}$) for chloride including dry deposition for 1987–88 and 1989–91 in the Spruce catchment at Mont-Lozère. TD total deposition (see text), O output by streamflow.

	1987–88	1989–91
Rainfall R	32.8	22.9
Throughfall TH	55.5	59.2
Net throughfall $TH - R$	22.7	36.3
Dry deposition DD	20.4	0.0
Total deposition $TD = (R + x * DD)$	43.1	22.9
Output O	34.2	17.0
$I - O = TD - O$	8.8	5.9

Table 5: Cation catchment budget CB for spruce at Mont-Lozère for 1982–86. Fluxes in $kg.ha^{-1}.y^{-1}$. DD dry deposition (data from 1987–88).

	Ca	Mg	K
Rainfall R	15.2	2.5	2.7
Dry deposition DD	4.7	0.8	0.5
Biomass removal BR	3.4	0.7	1.7
Stream output O	17.3	6.7	3.8
$CB = (R + DD) - (BR + O)$	-0.8	-4.1	-2.3

5 Conclusion

Observations at the spruce site at Mont-Lozère provide indirect evidence of cloud deposition, which can account for more than 10 % of incidental rainfall at the forest edge. This excess of water can be explained by a higher altitude of the site and by the efficiency of spruce foliage to trap droplets. However, it is difficult to extrapolate these figures to the catchment itself. Because the forest is cloud-prone only in winter, the supplemental cloudwater has no compensating effect on the water stress affecting the forest in summer. The values for throughfall content (the combined result of wet deposition, dry deposition and biological exchange with the canopy) are high compared to those for wet deposition alone. If one takes into account a probable 30 % over-estimation due to the irregular pattern of deposition within the forest, it becomes possible to extrapolate values for dry deposition over the entire wooded catchment. Such deposition would appear to be essential for the development of forests on soils that are poor in exchangeable cations, especially for calcium and magnesium.

Acknowledgements

This research has been supported by the DEFORPA project (1985–89) from French Ministry of Environment, and by the ENCORE project (1990–94) from ECC-DG XII. The author would like to thank particularly F. Lelong and B. Guillet, from URA 724/CNRS (University of Orleans) the managers of the ERB Mont-Lozère, P. Durand and A. Hanchi who provided throughfall data from the beech catchment, and G. Drouet and S. Cassault for the chemical analysis.

References

[1] Beier C. (1991). Separation of gaseous and particulate dry deposition of sulfur at a forest edge in Denmark. J. Environ. Qual. 20, 460–466.

[2] Cape J. N., Brown A. H. F., Robertson S. M. C., Howson G. and Paterson I. S. (1991). Interspecies comparisons of throughfall and stemflow at three sites in northern Britain. For. Ecol. Manag., 46, 3–4, 165–177.

[3] Dambrine E., Ulrich E., Cenac N., Durand P., Gauquelin T., Mirabel P., Nys C., Probst A., Ranger J. and Zephoris M. (1995). Atmospheric deposition in France and possible relation with forest decline. Forest decline and atmospheric deposition. Effects in the French mountains. Landmann G., Bonneau M. (Eds). Springer. 467 p.

[4] Didon-Lescot J. F. (1996). Forêt et développement durable au Mont-Lozère. Impact d'une plantation de résineux, de sa coupe et de son remplacement sur l'eau et sur les réserves minérales du sol. Thèse de l'Université d'Orléans, 161 p.

[5] Durand P., Neal C. and Lelong F. (1992). Anthropogenic and natural contributions to the rainfall chemistry of a mountainous area in the Cevennes National Park (Mont-Lozère, southern France). J. Hydrol., 130, 71–85.

[6] Hanchi A. (1994). Cycle de l'eau et des éléments biogènes dans un bassin versant forestier: cas d'une hêtraie au Mont-Lozère. Thèse de l'Université de Bourgogne, 232 p.

[7] Harding R. J., Neal C. and Whitehead P. G. (1992). Hydrological effects of plantation forestry in north-western Europe. In Response of Forest Ecosystems to Environmental Changes. Symposium Florence, May 1992. A. Teller, R. Mathy and I. N. R (eds). Elsevier Publications, 445–455.

[8] Hornung M., Rodà F. and Langan S. J. (1990). A review of small catchment studies in western Europe producing hydrochemical budgets. Air Pollution Research Report 28. CEC. 186 p.

[9] Lelong F., Dupraz C., Durand P. and Didon-Lescot J. F. (1990). Effects of vegetation type on the biochemistry of small catchments, (Mont-Lozère, France). J. Hydrol., 116, 125–145.

[10] Lindberg S. E. and Owens J. G. (1993). Throughfall studies of deposition to forest edges and gaps in montane ecosystems. Biogeochemistry 19: 173–194.

[11] Probst A., Lelong F., Viville D., Durand P., Ambroise B. and Fritz B. (1995). Comparative hydrochemical behaviour and element budgets of the Aubure (Vosges Massif) and Mont-Lozère (Southern Massif Central) Norway spruce forested catchments. Forest Decline and Atmospheric Deposition. Effects in the French mountains. Landmann G., Bonneau M. (Eds). Springer. 467 p.

Monitoring and modelling of springflow in the Noor catchment (the Netherlands)

R. Dijksma, H. A. J. van Lanen

Sub-department of Water Resources, Department of Environmental Sciences, Wageningen Agricultural University, Nieuwe Kanaal 11, 6709 PA Wageningen, the Netherlands.

1 Introduction

The Noor catchment is located in the border area between Belgium and the Netherlands near Maastricht and Liège. The catchment consists of permeable Cretaceous deposits overlying impervious Upper-Carboniferous shales and sandstones.

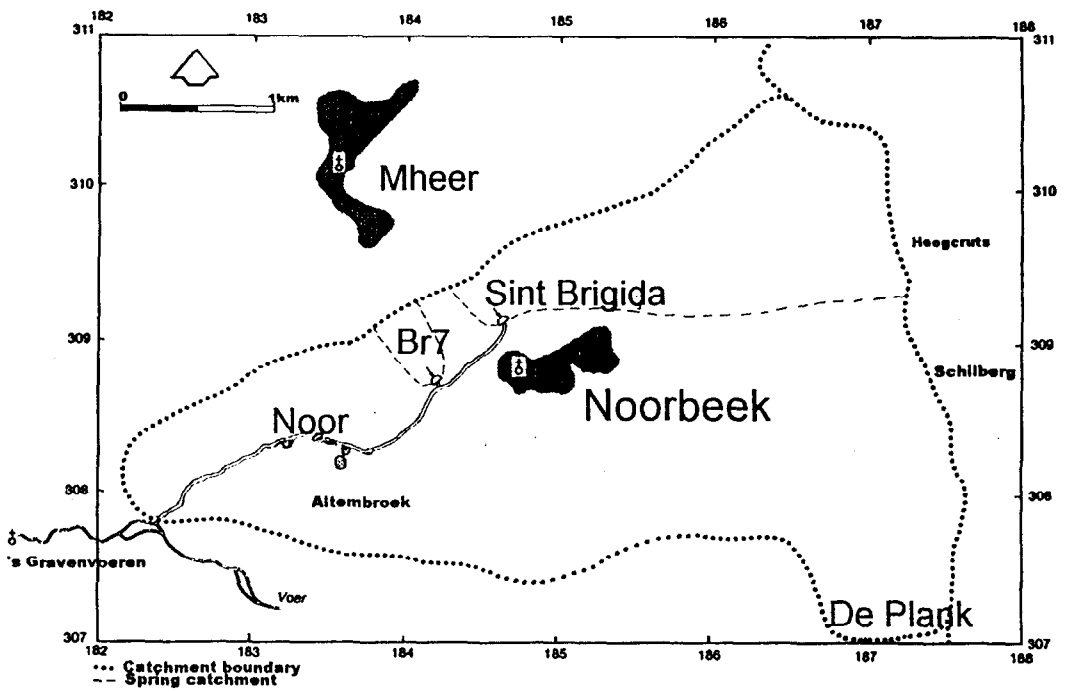

Figure 1: Location of the Sint Brigida spring and Br7 in the Noor catchment.

The lower part of the Cretaceous deposits comprises fine sandy silts with thin-bedded fractured sandstone layers (Vaals Formation) and the upper part comprises chalk (Gulpen Formation). The hydraulic conductivity of the Vaals Formation is limited (k = 0.4 m.day^{-1}), with the exception of the sandstone layers which have a relatively high conductivity (k = 20 – 50 m.day^{-1}). The lower part of the chalk has a hydraulic conductivity of 2.5 m.day^{-1}, whereas in the upper parts the conductivity is supposed to increase significantly (k = 30 m.day^{-1}; Downing et al., 1993). The Cretaceous deposits form a multiple-aquifer system with a thickness of 40–50 m and decreasing hydraulic conductivity with depth. The Pleistocene overburden in the Noor catchment consists of unsaturated loess and river gravels on the plateau and clay with flints on the slopes. The overburden allows ready infiltration of rainfall. Surface runoff is negligible. In the valley, an approximately 5 m layer of low permeable, saturated valley filling (a mixture of predominantly loess, gravels and clay with flints) occurs. The Noor brook is deeply incised in the plateau, which implies that the chalk is eroded in the central part of the valley. Fig. 2 shows a longitudinal section of the Noor catchment, and the position of the Sint Brigida spring and a typical spring (Br7).

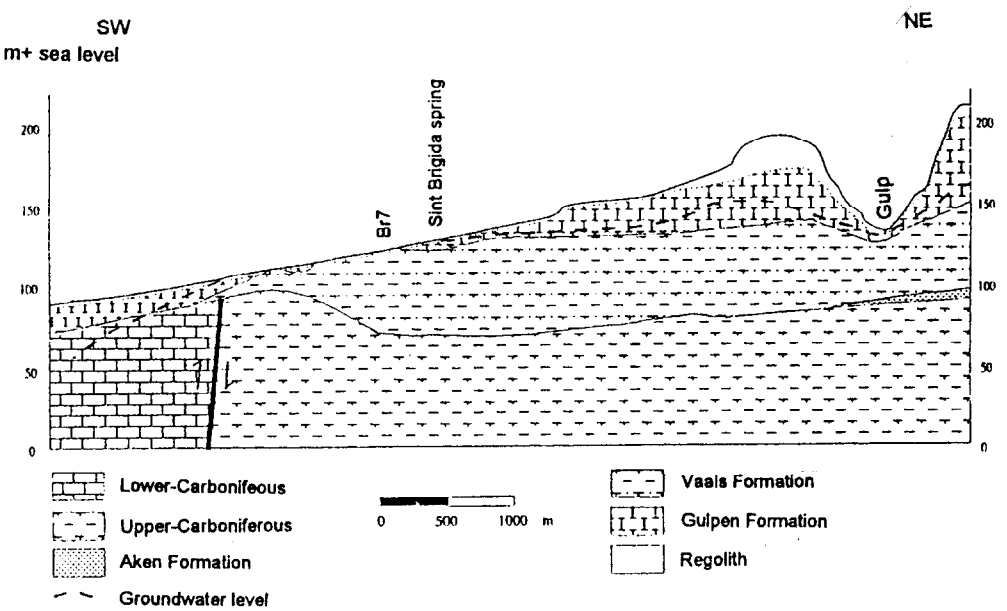

Figure 2: Geological profile of the Noor catchment.

The difference in elevation between the plateau and the valley bottom is about 50–60 m. Deep water tables (30–40 m) occur under the plateau. Rainfall surplus (about 250–300 mm.yr^{-1}) infiltrates on the plateau, then flows through the thick unsaturated zone and the multiple aquifer system towards the valley. Numerous springs and an extended seepage area (a nature reserve) discharge from the groundwater system. Springflow accounts for most of the groundwater discharge (about 60 %). The majority of the springs in the Belgian-Dutch chalk are small (< 2 l.s^{-1}). However, some exceptions are the major chalk spring in Sint Pietersvoeren (80 l.s^{-1}) in the Voer valley (Nota & van de Weerd, 1980) and the Sint Brigida Spring in the Noor catchment (0–30 l.s^{-1}). Since 1991 an intensive groundwater monitoring and modelling program has been carried out in the Noor catchment to investigate the hydrogeological system (Dijksma et al., 1997; Van La-

nen & Dijksma, 1998). In the context of this program the behaviour of the Sint Brigida spring was studied. The springflow strongly fluctuates: the spring even dries up. Furthermore, the nitrate concentration of the spring is above EU drinking water standard of 50 $mg.l^{-1}$. The objectives of this paper are (a) to compare the discharge of the Sint Brigida spring with a typical chalk spring in the Noor catchment and to investigate the reasons for its response, and (b) to analyse the nitrate concentration, which is expected to be positively correlated with discharge (Van Lanen et al., 1993). Knowledge about the springflow and the nitrate concentration is needed for the management of the nature reserve in the wet central part of the valley.

2 Results and discussion

2.1 Observed springflow

Since 1991, precipitation, groundwater levels under the plateau and in the wet valley, discharges of the springs and the brook, and the chemical composition of these waters, have been monitored. Rainfall surplus was calculated, using precipitation, Penman evapotranspiration, land use and soil data. Calculated rainfall surplus varies strongly in the monitoring period. Dry years such as 1991 and 1995 were alternated by wet years (1993, 1994). Table 1 shows the calculated annual rainfall surplus in the period 1991–1996, representing hydrological years (starts on April 1).

Table 1: Annual rainfall surplus in the Noor catchment ($mm.yr^{-1}$).

Year	1991	1992	1993	1994	1995	1996	Average 1991–1996
Rainfall surplus (mm)	185	230	410	405	130	240	270

Eventually, the rainfall surplus feeds the Sint Brigida spring, numerous smaller springs and a seepage area. The Sint Brigida spring collects its water from the north and the east.

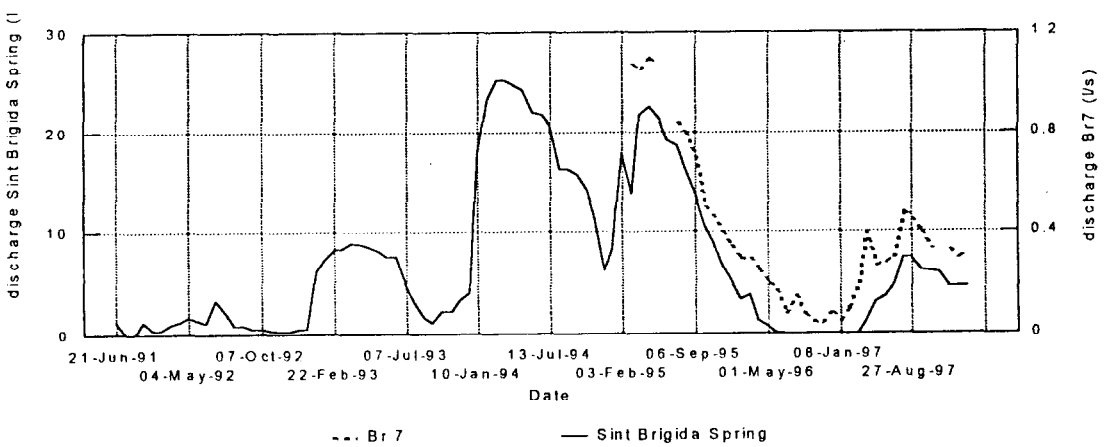

Figure 3: Discharge of the Sint Brigida spring and the typical chalk spring (Br7).

The discharge of this spring was compared with a typical chalk spring (Br7). Discharge measurements of spring Br7 started in 1994. Its catchment is small, compared to the Sint Brigida spring. Fig. 3 shows the discharge of both springs. Both springs respond in wet years (1993 and 1994) with a significant increase of the discharge. A remarkable difference between the springs is that the Sint Brigida spring dries up during dry years (e.g. 1996), despite its relatively large catchment area, while the small spring does not dry up. Also the recession of the spring flow of Br7 is more flat. The difference in response to variations in rainfall surplus is controlled by the area of the catchment and the position of the spring (e.g. its altitude relative to the position of the geological formations).

2.2 Observed nitrate concentrations of the springs

The chemical composition of the springs was measured once a month. It was expected that the nitrate concentration would be positively correlated with discharge because higher spring discharge implies an increased leaching of nitrate in the rootzone. Fig. 4 shows the measured nitrate concentrations of both springs. No correlation between the discharge of the Sint Brigida spring and its nitrate concentration can be found. Obviously a linear increase in the nitrate concentration in the Sint Brigida spring occurs, without any correlation with the discharge. Br7 shows a somewhat different behaviour. The nitrate concentration of this small spring appears to be positively correlated with the discharge. On top of that, an overall increase of nitrate occurs. The behaviour of the Sint Brigida spring is likely to be a result of the size and shape of its catchment area, and the position in the geological framework.

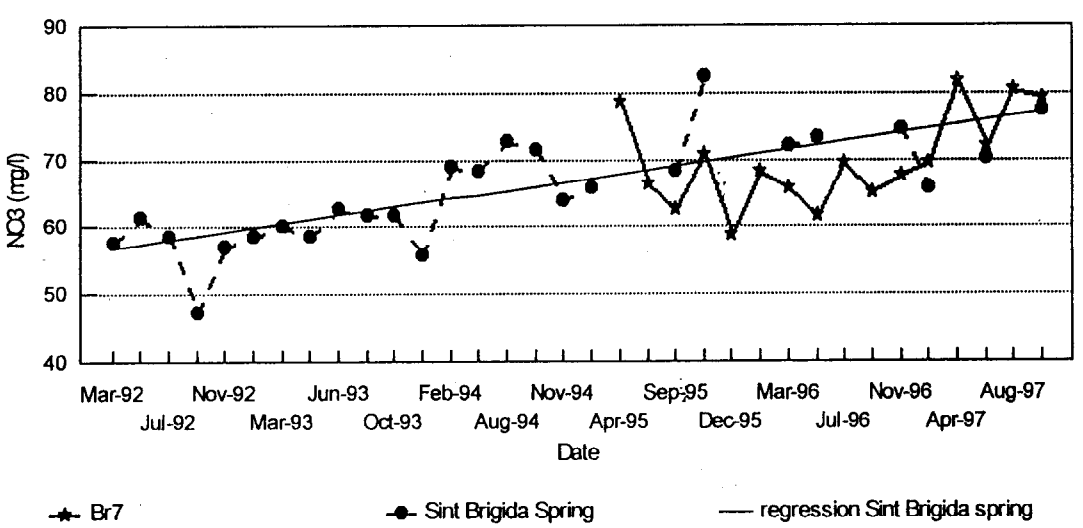

Figure 4: Nitrate concentration of the Sint Brigida spring and the typical chalk spring (Br7).

2.3 Modelling

Several groundwater flow models have been developed (e.g. MODFLOW, FLONET/TRANS) to investigate the hydrogeological system of the Noor catchment and the impact of human interferences. The behaviour of a specific spring, such as the Sint Brigida spring or Br7 is

hard to simulate. Exploration with the models shows a relationship between the discharge of the Sint Brigida spring and the groundwater head under the plateau as presented in Fig. 5.

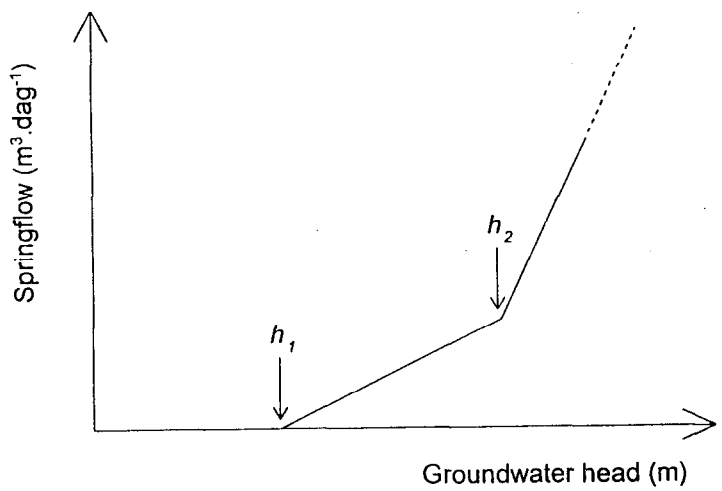

Figure 5: Schematic relation between the discharge of the Sint Brigida spring and the groundwater head under the plateau.

The Sint Brigida spring predominantly drains groundwater from the chalk. Under prolonged dry conditions the groundwater head in the chalk under the plateau drops below h_1, which implies that the spring dries up (e.g. 1991, 1992 and 1996). The relatively high position of this spring (headwater) compared to the other more downstream springs is the main reason for this phenomenon. Then groundwater flows below the spring through the lower chalk and Vaals Formation towards other springs. When the groundwater heads under the plateau are between h_1 and h_2 the Sint Brigida spring receives groundwater, which mainly flows through the lower, less permeable chalk. An increase of the heads causes not more than a restricted increase of springflow. However, under extensive wet conditions the groundwater head may exceed h_2, which results in a substantial increase of springflow (January 1994 and 1995). Under these circumstances remarkable amounts of groundwater can flow through the more permeable upper chalk and feed the spring (Van Lanen et al., 1993). Contrary to the other more typical chalk springs, such as Br7, the Sint Brigida spring has direct contact with the more permeable chalk due to the relatively high elevation. Therefore the spring Br7 does not show the sharp decrease in discharge (expressed in $l.s^{-1}$). Moreover Br7 never dries up because of the lower position in the groundwater system, which means that the relationship between springflow and the groundwater heads is characterised by a line similar to that shown between h_1 and h_2 in Fig. 5. In reality the relationship between springflow and groundwater heads in Fig. 5 is more complex. Several loops around the lines occur dependent on the spatial and temporal distribution of the groundwater heads in the catchment area of the Sint Brigida spring. Furthermore the relationship is not exactly linear and does not show the pronounced inflection points h_1 and h_2 due to a more gradual increase of the hydraulic conductivity of the chalk.

Under wet conditions the Sint Brigida spring receives young groundwater through the upper chalk which passes the older water in the lower chalk. Usually the younger water is more polluted with nitrate than the older water resulting in a positive correlation between

the springflow and the nitrate concentration (Van Lanen et al., 1993). Surprisingly this does not apply to the Sint Brigida spring, where hardly any relationship can be recognised between springflow and nitrate concentrations.

3 Conclusions

The discharge of the Sint Brigida spring is higher than of the other typical chalk springs (e.g. Br7) because of the larger catchment area. The higher position in the hydrogeological system causes a drying up of this spring. The steeper recession of the springflow can be explained by hydraulic conductivity differences of the chalk.

The nitrate concentration of the Sint Brigida spring does not show positive correlation with the discharge. Instead a linear increase occurs. On the other hand, this positive correlation can be recognised in the typical chalk spring Br7.

Acknowledgements

This study has been performed within the framework of research school WIMEK/SENSE, theme A: Behaviour of substances, and the ARIDE project "Climate change and impact on natural resources: 1.1.4.1 European Water Resources". Mr. W. J. Ackerman and Mr. H. F. Gertsen are acknowledged for their support in collecting the field data.

References

[1] Dijksma, R., H. A. J. van Lanen & B. van de Weerd, 1997. Water pathways and streamflow generation in the Noor Catchment. In: D. Viville and I. G. Littlewood (eds), Ecohydrological processes in small basins, Proceedings of the Sixth Conference of the European Network of Experimental and Representative Basins (ERB), Strasbourg, France, 24–26 September 1986. IHP-V, Technical Documents in Hydrology No. 14, 105–110.

[2] Downing, R. A., M. Price & G. P. Jones, 1993. The hydrogeology of the chalk of North-West Europe. Clarendon Press Oxford.

[3] Lanen, H. A. J. van & R. Dijksma, 1998. Water flow and nitrate transport to a groundwater-fed stream in the Belgian-Dutch Chalk. Hydrological Processes (accepted).

[4] Lanen, H. A. J. van, M. Heijnen, T. de Jong & B. van de Weerd, 1993. Nitrate concentrations in the Gulp catchment: some spatial and temporal considerations. Acta Geologica Hispanica 28(2–3): 65–73.

[5] Notà, D. J. G. & B. van de Weerd, 1980. A hydrogeological study in the basin of the Gulp Creek - A reconnaissance in a small catchment area. Fissured rocks and their anisotropic behaviour in catchment studies. Mededelingen Landbouwhogeschool 80–15, Wageningen.

Applicability of a parsimonious nitrate transport model in catchment management

Y. Van Herpe, P. A. Troch, F. P. De Troch

Laboratory of Hydrology and Water Management, University of Gent,
Coupure Links 653, B-9000 Gent, Belgium.

1 Introduction

Nitrate loading on groundwater and surface waters tends to demonstrate a general trend of increase, most notably in the past three decades (Heathwaite et al., 1996). Although nitrate pollution results from several sources, evidence suggests that non-point source pollution from agriculture is the major contributor of the increasing nitrate loss to the aquatic environment (Heathwaite et al., 1993). Further research is still needed in order to obtain a better understanding of nitrate transport in rural catchments. Such an understanding can aid the development of best management practices. In order to accurately evaluate these management strategies, there is still a need for efficient modelling approaches.

Modelling approaches in integrated water management require specialised operational models that operate at the catchment scale and that are appropriate to the specific policy goals and the availability of data sets. The use of these models for policy making requires an understanding of the contributing parameter uncertainties to the variability of the model output. The difficulties of tracing these effects indicate that a model dependent upon fewer parameters is more justifiable at the catchment scale than a complex modelling approach (Anthony et al., 1996).

This paper presents the applicability of a low parameter watershed model as a nitrate decision support tool. The presented model is operational at the catchment scale and consists of a hydrological module and a nitrate transport module. In this study, model performance and behaviour are tested, and the model's ability for predicting nitrate concentrations at the catchment outlet for varying environmental parameters is delineated: the impact of climate and land use changes on the surface water quality is illustrated for an agricultural catchment.

2 Model development

2.1 Runoff generation model

The nitrate transport model reported in this paper is based on the conceptual runoff generation model TOPMODEL (Beven and Kirkby, 1979), assuming simple relationships

between catchment storage deficit and local water table levels, in which the controlling factor is catchment topography. In essence, TOPMODEL combines a series of stores routing water from the surface to the outlet of the catchment. The formulation of the stores used in this paper was presented by Quinn and Beven (1993) and is illustrated in Fig. 1.

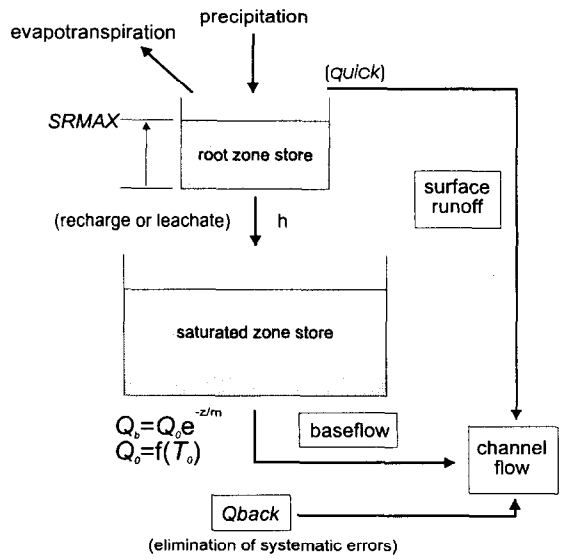

Figure 1: Description of the hydrological model stores and parameters: SR_{max}, m, T_o, *quick* and Q_{back}.

The lumped model adopts only a linear root zone store, with a maximum storage capacity SR_{max} (m), and an exponential saturated zone store. Evaporation from the root zone store is allowed at the estimated potential rate until depletion of the store, and a constant runoff coefficient, *quick* (%), is assumed, generating instantaneous surface runoff estimated as a proportion of the rainfall, whenever the root zone is saturated. Vertical flux from the root zone to the groundwater reservoir occurs by gravity drainage whenever field capacity is exceeded. Output from the saturated zone store is given by the baseflow Q_b

$$Q_b = Q_o \, e^{(-S/m)} \tag{1}$$

with:

$$Q_o = A \, e^{lnT_o - \lambda} \tag{2}$$

where Q_o is the baseflow discharge (m^3/d) when the average catchment storage deficit S (m) equals zero, m is the decay parameter (m) that controls the effective depth of the catchment profile, A is the total catchment area (m^2), λ is the catchment mean topographic index (Beven and Kirkby, 1979), and T_o is the saturated lateral transmissivity (m^2/d). The catchment average storage deficit S for each time step (m/d) is updated by subtracting the unsaturated zone recharge and adding the baseflow from the previous time step:

$$S_t = S_{t-1} - h_t + q_{b,t-1} \tag{3}$$

with h the groundwater recharge (m/d) and q_b the baseflow term (m/d), expressed as the ratio between Q_b and A. Initial flow conditions can be assessed by recession flow data analysis (Troch et al., 1993), and model input consists of catchment mean precipitation and potential evapotranspiration series and discharge data at the catchment outlet.

Because of the high solubility of the nitrate ion, its transport is intimately linked with the hydrological pathways controlling nutrient transport from the land to the stream. In that respect, nitrate transport modelling in catchments where nitrate reaches surface water mainly through diffuse sources should be possible with TOPMODEL. Callewier et al. (1998) extended TOPMODEL with a nitrate transport module (see Fig. 2). The results of the hydrological module are used to control the different functions of the nitrate transport module. The transport module can be considered as a transfer function transforming input from a production function to an output signal representing an estimate of the river nitrate concentration.

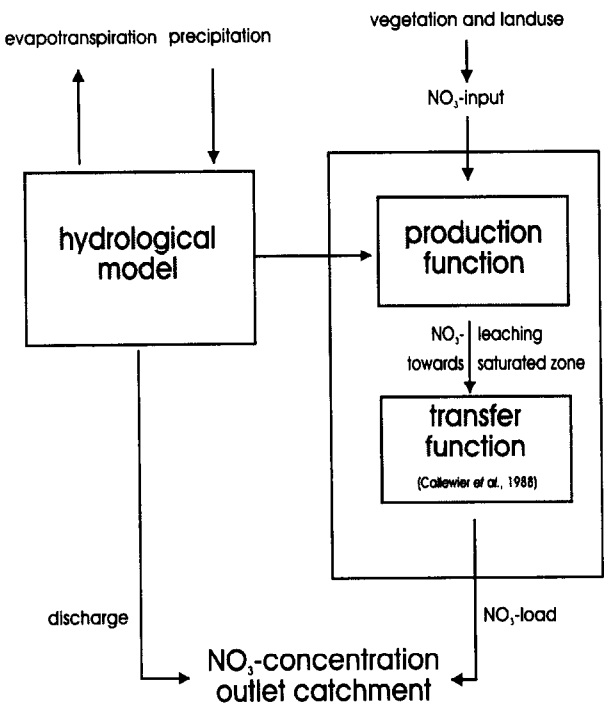

Figure 2: Scheme of the model concept developed by Callewier et al. (1998).

2.2 Nitrate transport module

2.2.1 Production function: transport from the soil surface towards the saturated zone

During rainfall events part of the rainwater percolates and displaces a portion of the nitrate within the soil profile. The nitrate concentration of the leachate depends on the amount of nitrate within the soil profile and is estimated with an empirical leaching model developed by Anthony et al. (1996). The model is derived from the Solute Leaching Intermediate Model (Addiscott et al., 1986) and it expresses the proportion of soil nitrate leached as a function of increasing drainage efficiency:

$$P = 1.111\,\epsilon - 0.203\,\epsilon^3 \quad \text{when } \epsilon \leq 1.35 \tag{4}$$

$$P = 1.0 \quad \text{when } \epsilon > 1.35 \tag{5}$$

$$\epsilon = \frac{H}{\phi} \tag{6}$$

where P is the proportion of the available nitrate leached (-), ϵ (m) is the drainage efficiency, H (m) is the cumulative soil drainage (i.e. the integrated amount of water draining through the soil during a definite time interval) and ϕ (m^3/m^3) is the soil moisture content at field capacity. Hence, in combination with the amount of nitrate present in the soil profile, the amount of nitrate leached during a rainfall event of known intensity can be predicted.

The presented model is applied to 'leaching seasons' starting after the harvest period, with a certain residual nitrate amount in the soil profile, that continuously keeps decreasing during the leaching season and that is adjusted again at the onset of the next leaching season. The simple equations of the leaching model are most suitable to be incorporated into the hydrological model. The only additional parameter needed is ϕ, since the cumulative drainage H is calculated in the hydrological module as the integrated amount of groundwater recharge h. In combination with the nitrate amount leaching, a nitrate concentration in the leachate is obtained for each time step. This concentration serves as input for the transfer function.

2.2.2 Transfer function: transport from the saturated zone towards the surface water

The transfer function is based on the 'flushing hypothesis' (Hornberger et al., 1994; Creed et al., 1996), postulating a relationship between river nitrate concentrations and the extent to which the catchment is saturated. The flushing hypothesis states that when a catchment is a potential source of nitrogen, the release of nitrogen to adjacent waters increases exponentially as the soil saturation deficit decreases. Accordingly, the transfer function states that the nitrate concentration of the baseflow increases proportional to the decline of the catchment saturation deficit or the corresponding rise of the groundwater table. This relationship between nitrate concentration and water table depth is also reported by other authors (Katz et al., 1997; Jiang et al., 1997). The transfer function, however, is not exponential, but depends on the variations in groundwater recharge. The transfer function consists of two components defining the relationship between the saturation deficit (calculated in the hydrological part) and the river nitrate concentration. A detailed formulation of the transfer function and its components can be found in Callewier et al. (1998) and Van Herpe et al. (in press).

A very important aspect of this transfer function is that it does not introduce more uncertainty to the model because there are no new parameters that need to be calibrated.

3 Model analysis and results

For this study, the model was used to simulate nitrate concentrations in the surface water at the outlet of the rural Zwalm catchment. The Zwalm catchment is situated in the sandy loam area of Flanders (Belgium). The drainage area is 114 km^2, and most of the land use is agricultural (arable crops and permanent pasture), while the south of the catchment is forested (9 %) and the degree of urbanisation is about 11 %. The Zwalm data set contains daily hydrologic data and daily river nitrate concentrations for the leaching season 1991–1992. The one-year simulation for the Zwalm catchment was performed with a daily time step, a leaching season starting on the 25^{th} of September and an initial estimated soil nitrate content of 40 kg NO_3^-N/ha.

The analysis approach used to test the performance and behaviour of the model is based on the Generalised Sensitivity Analysis proposed by Spear and Hornberger (1980). Therefore, all model parameters were randomly perturbed within a physically realistic

range, drawn from literature data. In order to sample the parameter range, a set of 10,000 parameters was generated using a uniform sampling strategy, i.e. by allowing all parameters to vary independently. The model is run for each randomly generated parameter set (i.e. 10,000 times) resulting each time in a different model output. The considered model outputs are cumulative saturation deficit, cumulative baseflow and cumulative discharge for the hydrological module, and cumulative leachate concentration and cumulative river concentration for the nitrate transport module. These cumulative model outputs are plotted against each of the parameters, resulting in a fuzzy plot (Fig. 3).

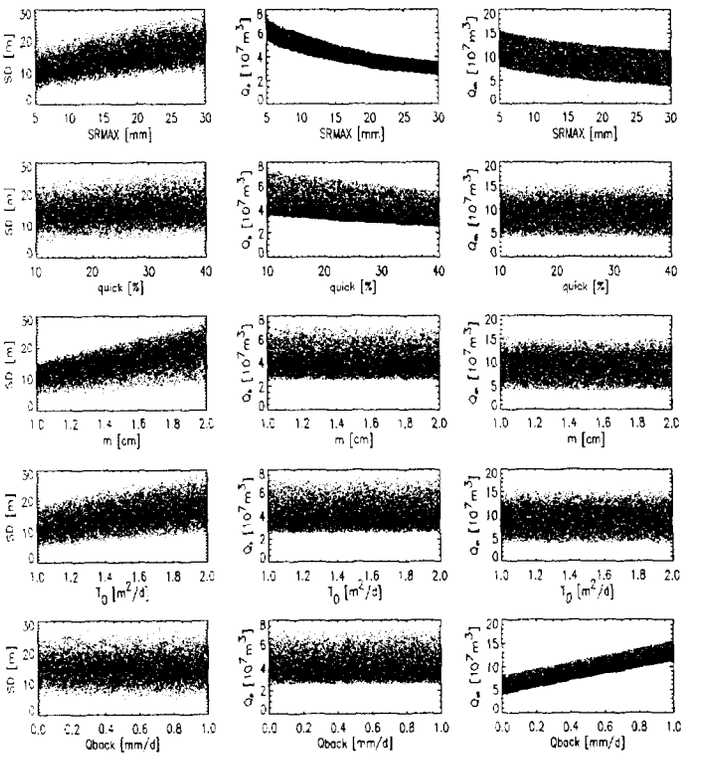

Figure 3: Cumulative fluxes of saturation deficit SD, baseflow Q_b and discharge Q_{ch} plotted against the hydrological parameters: SR_{max}, $quick$, m, T_o and Q_{back}.

The sensitivity degree of the model response to the hydrological model parameters SR_{max} (m), m (m), T_o (m^2/d), $quick$ (%) and Q_{back} (i.e. background flow (m/d), used for eliminating systematic errors) can be derived from the fuzzy plots in Fig. 3. This figure shows cumulative model outputs for saturation deficit, baseflow and discharge, plotted against each of the parameters. Because of interaction with the other randomised parameters, it is not obvious to assess the sensitivity of the model output for all parameters from Fig. 3. The parameter sets are therefore subdivided into discrete classes of the model output by ranking the 10,000 realisations, each existing of a set of randomised parameters with the resulting cumulative fluxes, according to cumulative flux totals and subsequently dividing them into 10 groups of 1000 realisations, thus forming 10 performance classes. For each parameter, the distribution of each defined class can be visualised against the three considered cumulative fluxes, yielding cumulative frequency plots, as shown in Fig. 4. Fig. 4 shows the cumulative frequency plot for the cumulative saturation deficit and the 5 hydrological parameters. Together with the fuzzy plots (Fig. 3), the cumulative frequency

plots (Fig. 4) can be interpreted to determine the sensitivity degree of the cumulative model outputs for each of the hydrological parameters.

As could be expected, the maximum storage capacity of the root zone, SR_{max}, is strongly related to all three of the considered model outputs. Higher values for SR_{max} correspond with higher volumes of water that need to be stored in the root zone before gravity drainage towards the saturated zone can occur. This results in higher values for the cumulative saturation deficit, and, inherently, in lower values for the generated baseflow and discharge. The runoff coefficient, *quick*, manifests a low influence (see Figs. 3 and 4) on the cumulative saturation deficit, but is strongly associated with the cumulative baseflow. Higher values for *quick* generate more surface runoff and less infiltration, resulting in lower baseflow volumes, while the generated discharge is not influenced. In particular for the highest and the lowest performance class (respectively during peak discharges and recession periods), it appears that *quick* affects baseflow generation in a considerable way.

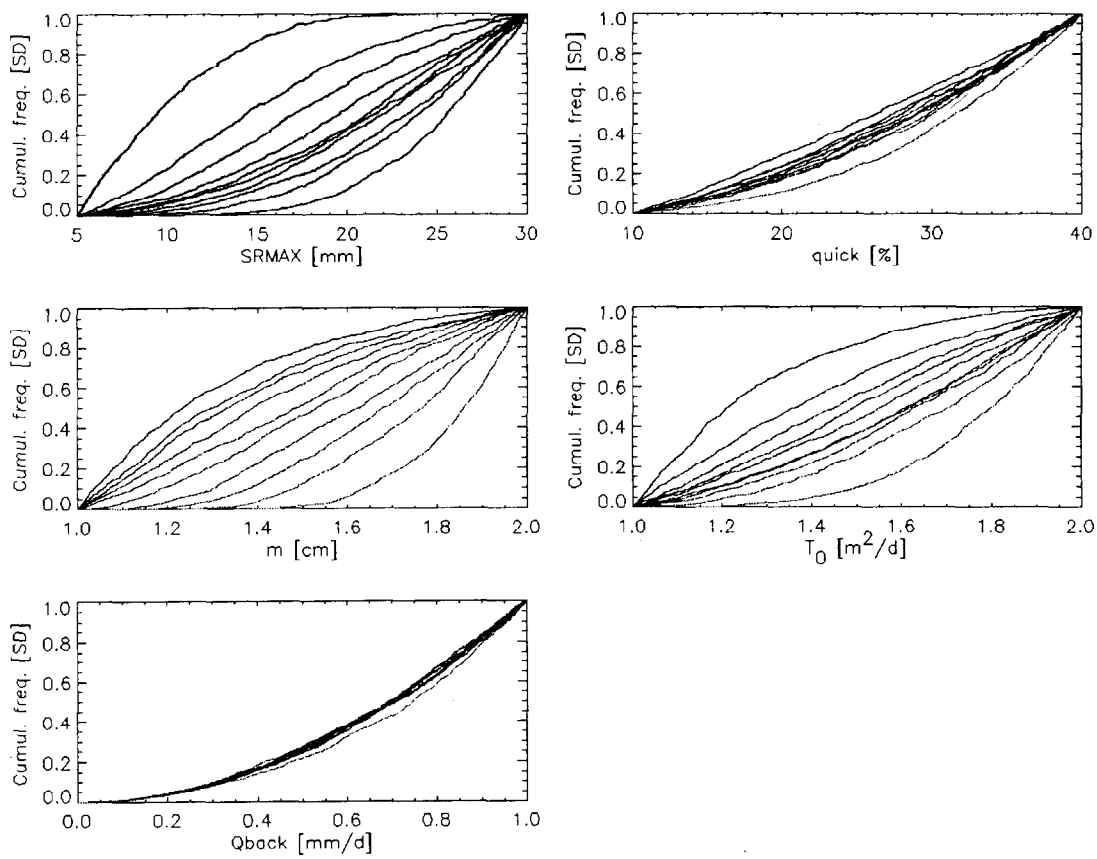

Figure 4: Cumulative frequency plot of each performance class for the saturation deficit SD versus the parameter ranges.

The decay parameter m and the lateral transmissivity T_o have a considerable influence on the cumulative saturation deficit, because higher values for m and T_o correspond with higher values for the saturated hydraulic conductivity, K_s (m/d). This results in faster drainage or increased discrete (i.e. for each time step) baseflow and discharge, which consequently leads to increased values for the saturation deficit. Although m and T_o affect the drainage velocity, the parameters do not seem to influence the cumulative baseflow

and discharge volumes, which can be explained by equations (1) and (2). Since Q_{back} is only used for eliminating systematic errors from the simulated discharge (see Fig. 1), this parameter only affects the cumulative discharge, and has no effect on the cumulative baseflow and cumulative saturation deficit.

Because the results of the hydrological module serve as input for the nitrate transport module, it is important that the hydrological module simulates as correctly as possible. Therefore, for each of these 10,000 model runs, the Nash and Sutcliffe (1970) simulation efficiency E was calculated. Based on this efficiency value, the hydrological module was calibrated with the 'optimal' parameter values. With these values, the sensitivity degree of the model response to the only parameter of the nitrate transport module, the soil moisture content at field capacity, ϕ (m^3/m^3), was assessed. The model outputs subjected to this analysis were the cumulative leachate concentration and the cumulative river concentration. The parameter ϕ is clearly related to the cumulative concentration fluxes: within the parameter interval 0.15–0.40 (m^3/m^3) the cumulative fluxes decrease proportionally with ϕ.

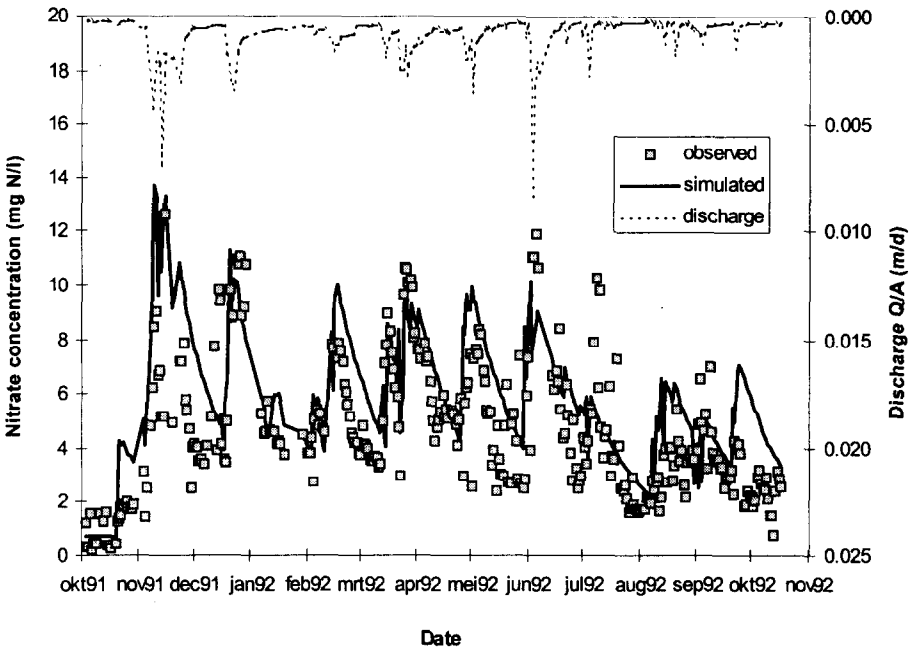

Figure 5: Simulation of nitrate concentrations at the outlet of the Zwalm catchment for one leaching season (October 1991 - October 1992) with corresponding discharges.

The optimal parameter set, derived from the sensitivity analysis, is used for simulating nitrate concentrations at the outlet of the Zwalm catchment (Fig. 5). The model is able to simulate the trend in the observations, with a correlation between observed and computed concentrations of $R = 0.69$. These results clearly illustrate the applicability of the model for simulating nitrate transport at the catchment scale.

4 Model predictions under changing environmental parameters

Watershed models for integrated water management offer the opportunity for systematic analysis of a management policy.

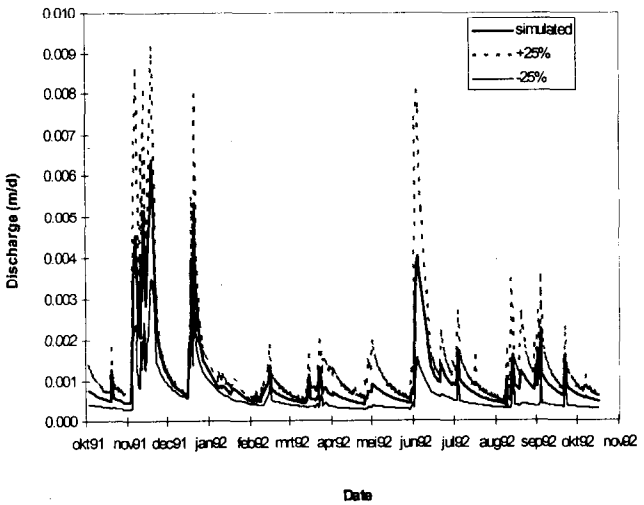

Figure 6: Impact of climate changes (25 % increased and decreased rainfall intensity) on the produced discharge at the outlet of the Zwalm.

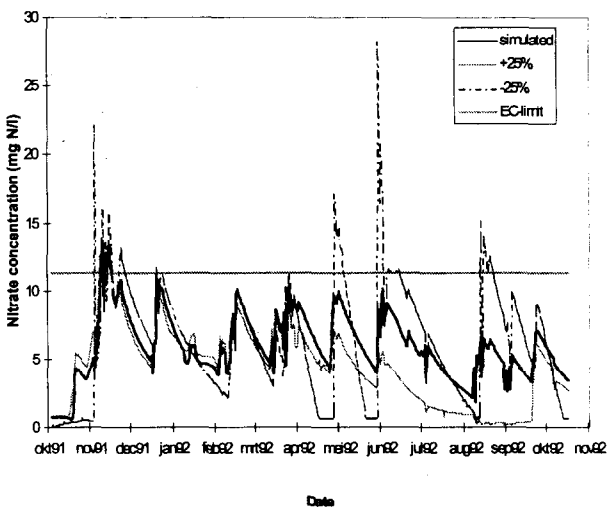

Figure 7: Impact of climate changes (25 % increased and decreased rainfall intensity) on the nitrate concentrations at the outlet of the Zwalm.

Therefore, the model needs to produce reliable simulation results (1) for existing situations and (2) for analyses of catchment management strategies. In other words, models for

nitrate management at the catchment scale need to be able to predict nitrate concentrations at the catchment outlet for varying environmental parameters. The environmental parameters considered for assessing the model's applicability as a management tool were land use, which is one of the key parameters in catchment management, and climate. The impact of climate changes on the quantitative and qualitative characteristics of the surface water at the outlet of the Zwalm catchment was simulated by increasing and decreasing rainfall intensity by 25 %. The results for the produced discharge are shown in Fig. 6, while the resulting nitrate concentrations at the catchment outlet are depicted in Fig. 7, together with an indication of the EC Drinking Water Directive 80/788 limit (11.3 mg NO_3^-N/l).

Land use changes like afforestation and deforestation, changing from undeveloped lands to residential or agricultural lands, and shifts towards more (or less) intensively fertilised crops on agricultural lands, will affect the residual soil nitrate content after harvest, i.e. at the beginning of winter drainage. This will be reflected in the amount of nitrate leached towards the aquatic environment. Hence, the impact of land use changes on the nitrate concentrations of the surface water at the outlet of the agricultural Zwalm catchment was simulated by increasing and decreasing the initial soil nitrate content by 25 %. The results of these changing land use conditions are shown in Fig. 8, together with an indication of the EC Drinking Water Directive 80/788 limit (11.3 mg NO_3^-N/l).

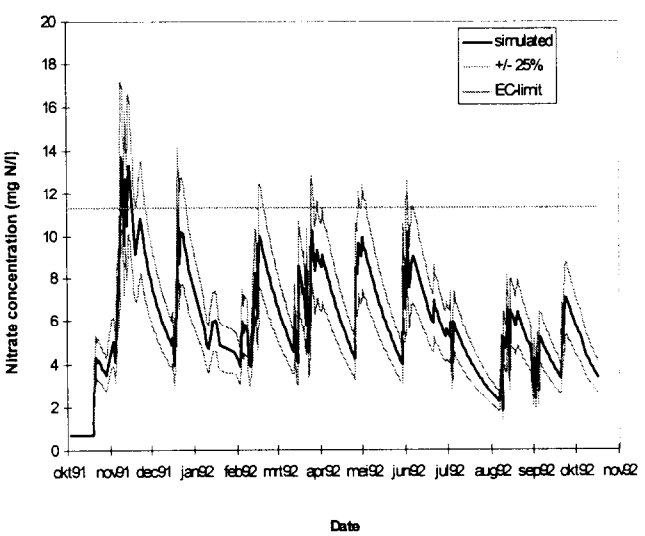

Figure 8: Impact of land use changes (25 % increased and decreased soil nitrate) on the nitrate concentrations at the outlet of the Zwalm catchment.

5 Conclusion

A conceptual catchment scale model for simulating nitrate transport in rural river basins has been applied to a rural catchment under humid temperate conditions. Model performance and behaviour were tested, and model results confirm the findings for another catchment (Callewier et al., 1998). The ability of the model to simulate the impact of climatic and land use changes was also delineated, revealing its ability for systematic analyses of management policies. The simulation results indicate the applicability of the model as a management tool for nitrate decision support.

Current research focuses on refining the runoff generation mechanisms and on implementing a module for calculating initial soil nitrate content based on available land use data and cropping information derived from remote sensing.

Acknowledgements

The authors gratefully acknowledge the support of the Research Fund of the University of Gent (contract n° 01103797).

References

[1] Addiscott, T. M., Heys, P. J. and Whitmore, A. P. (1986). Application of simple leaching models in heterogeneous soils. Geoderma, 38, 185–194.

[2] Anthony, S., Quinn, P. and Lord, E. (1996). Catchment scale modelling of nitrate leaching. Aspects of Applied Biology. Modelling in Applied Biology: Spatial Aspects, 46, 23–32.

[3] Beven, K. and Kirkby M. J. (1979). A physically based, variable contributing area model of basin hydrology. Hydrol. Sci. Bull., 24, 43–69.

[4] Callewier, L., Van Herpe, Y., Troch, P. A. and Quinn, P. F. (1998). Description and application of a conceptual catchment scale nitrate leaching model (in Dutch). Water, 98, 28–34.

[5] Creed, I. F., Band, L. E., Foster, N. W., Morrison, I. K., Nicolson, J. A., Semkin, R. S. and Jeffries, D. S. (1996). Regulation of nitrate-N release from temperate forests: A test of the N flushing hypothesis. Water Resources Research, 32, 3337–3354.

[6] Heathwaite, A. L., Burt, T. P. and Trudgill, S. T. (1993). The Nitrate Issue. In: Nitrate. Processes, Patterns and Management. Edited by Burt T. P., Heathwaite, A. L. and Trudgill, S. T. Wiley, Chisester, UK, 443 pp.

[7] Heathwaite, A. L., Johnes, P. J. and Peters, N. E. (1996). Trends in nutrients. Hydrological Processes, 10, 263–293.

[8] Hornberger, G. M., Bencala, K. E. and McKnight, D. M. (1994). Hydrological controls on dissolved organic carbon during snowmelt in the Snake River near Montezuma, Colorado. Biogeochemistry, 25, 147–165.

[9] Jiang, Z., Wu, Q. J., Brown, L. C. and Workman, S. R. (1997). Water table depth and rainfall timing effect on BR- and NO_3- transport. Journal of Irrigation and Drainage Engineering, 123(4), 279–284.

[10] Katz, B. G., DeHan, R. S., Hirten, J. J. and Catches, J. S. (1997). Interactions between groundwater and surface water in the Suwannee river basin, Florida. Journal of the American Water Resources Association, 33(6), 1237–1254.

[11] Nash, J. and Sutcliffe, J. (1970). River flow forecasting through conceptual models: Part 1 - a discussion of principles. Journal of Hydrology, 10, 282–290.

[12] Quinn, P. F. and Beven, K. J. (1993). Spatial and temporal predictions of soil moisture dynamics, runoff, variable source areas and evapotranspiration for Plynlimon, Mid-Wales. Hydrological Processes, 7, 425–448.

[13] Spear, R. C. and Hornberger, G. M. (1980). Eutrophication in Peel Inlet II. Identification of critical uncertainties via Generalised Sensitivity Analysis. Water Resour., 14, 43–49.

[14] Troch, P. A., De Troch, F. P. and Brutsaert, W. (1993). Effective Water Table Depth to Describe Initial Conditions Prior to Storm Rainfall in Humid Regions. Water Resources Research, 29, 427–434.

[15] Van Herpe, Y., Troch, P. A., Callewier, L. and Quinn, P. F. (in press). Application of a conceptual catchment scale nitrate transport model on two rural river basins. Environmental Pollution.

Water balance, water quality and soil erosion on agricultural lands

in the foothill zone of the Bohemo-Moravian Highland

S. K. Jain[1] , H. Damašková, M. Janeček, M. Tippl[2] , F. Doležal[3], T. Cawley[4]

[1] Department of Engineering Hydrology, National University of Ireland, Galway, Ireland; presently at the National Institute of Hydrology, Roorkee - 247 667, U. P., India. [2] Research Institute for Soil and Water Conservation, Žabovřeská 250, CZ 156 27 Praha 5 - Zbraslav, Czech Republic. [3] Department of Engineering Hydrology, National University of Ireland, Galway, Ireland; presently at the Research Institute for Soil and Water Conservation, Žabovřeská 250, CZ 156 27 Praha 5 -Zbraslav, Czech Republic, dolezal@vumop.tel.cz [4] Department of Engineering Hydrology, National University of Ireland, Galway, Ireland.

1 Introduction

The non-point source pollution of water very often occurs as a consequence of land use activities, such as agricultural cultivation and forest management practices. These activities cause the erosion of soils and the leaching of nutrients. Over the last few decades, the soil erosion and the nutrient leaching became important issues also on the territory of today's Czech Republic, due to unsustainable management practices such as creating and cultivating large fields irrespective of the limitations imposed by the terrain, or growing crops prone to erosion (such as maize for silage) on a large scale in foothill regions. The erosion, together with the nutrient leaching and other pollution processes started to present a danger for large surface water reservoirs such as the Švihov reservoir on the Želivka river. Several experimental catchments have therefore been established in order to estimate the inflow of pollutants into river systems and to investigate the efficiency of various erosion control and water protection measures.

2 Study area

The Černičí catchment is located in Central Bohemia, Benešov district, within a foothill zone of the Bohemo-Moravian Highland. The catchment recipient is a small anonymous stream about 1800 m long. The total area of the catchment is 1.440 km^2, of which 0.942 km^2 is occupied by arable land, 0.202 km^2 by grassland, 0.275 km^2 by forest and 0.021 km^2 by detached groups of houses and gardens (Fig. 1). The area lying upstream of the measured outlet is 1.4213 km^2. The altitude varies between 465 and 520 m a. s. l. The average annual precipitation is about 700 mm, and the average annual air temperature

is about 6.7 °C. About 30 % of the catchment area was drained by underground tile drainage about 20 years ago. The groundwater table is shallow in low-lying parts of the main valley and in one of the lateral valleys. These areas are occupied by sandy-loamy or loamy gley or pseudogley soils (Dystric Planosols and Dystric Gleysols), while the rest of the catchment comprises well-drained loamy sandy Dystric Cambisols on weathered paragneiss and its erosion products.

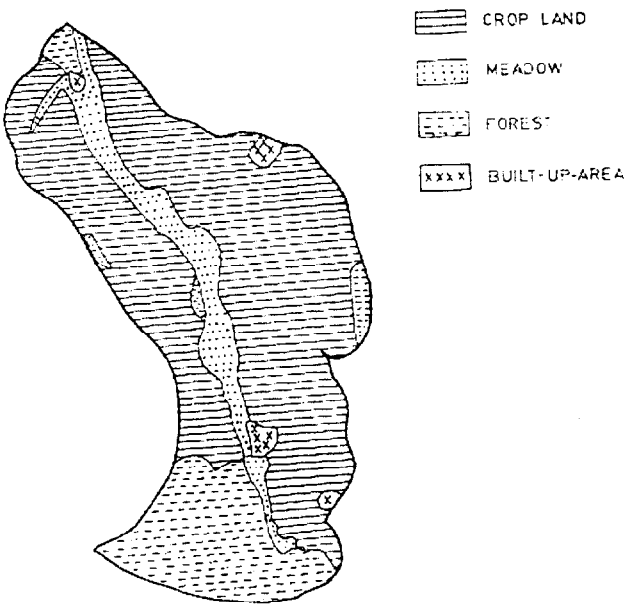

Figure 1: Land use map of the Černičí catchment.

The measurements have been carried out by the Research Institute for Soil and Water Conservation RISWC in Prague since 1990. They comprise, in particular, the monitoring of the stream discharge, drainage discharges at the drain outlets, stream-, drainage- and ground-water quality, the sampling of suspended sediments during flood events, and basic weather, groundwater table and soil water measurements. The weather data used in this study were taken from a nearby (about 5 km) weather station of the Czech Hydrometeorological Institute in Čechtice. The solar radiation was derived by regression from the daily temperature and rainfall data.

3 Model

The model used was EPIC (Sharpley and Williams, 1990) v. 5300, a half-empirical, half-physically-based complex simulation model comprising submodels of weather, surface runoff, soil erosion, soil water movement, plant growth, agricultural operations, nitrogen regime, phosphorus regime and other relevant processes. The time step of the model was one day. The daily runoff and infiltration volumes were estimated using a modification of the SCS curve number technique, the peak runoff rate predictions were based on a modified rational formula. The percolation, lateral subsurface flow and drainage runoff submodels used a storage routing technique. The evapotranspiration was obtained from the Priestley-Taylor equation. Soil erosion by water was estimated from the Universal Soil Loss Equation (USLE), the modified USLE (MUSLE) and the Onstad-Foster equation (AOF).

4 Estimation of input data

All weather data were obtained from Czech sources, except for the rainfall intensity parameters which were left at default levels. The catchment was divided into 18 basic land-use units, called 'fields' (Fig. 2). Each field was modelled separately. The soil data were taken from the Complex Soil Survey database, few unknown properties were left at the default levels. The runoff- and erosion-related soil properties did not vary much over the catchment area and were taken as the same for all fields. A path of concentrated runoff (a 'field channel') was estimated manually for each field (Fig. 2). Geometric characteristics of the fields (area, elevation, field slope and length, channel slope and length) were estimated from a digital terrain model of the TIN type using the GIS softwares ARC/INFO and IDRISI. The simulated crops were clover, maize, pine (a substitute for all forest land), potatoes, rape, rye, spring barley, timothy (a substitute for all grassland and houses with gardens), triticale, winter barley and winter wheat. The EPIC parameters of some crops were modified by trial and error. The application of fertilisers and liming was simulated as automatic. The dates of planting, harvesting and tillage operations were simulated as fixed, corresponding to locally usual dates. The runoff curve numbers corresponding to individual crops and tillage operation were estimated with regard to literature and local knowledge. As for the erosion parameters (in particular the crop management factor C), we relied on the default algorithms of EPIC without any modification. Other unknown parameters were estimated in the best possible way.

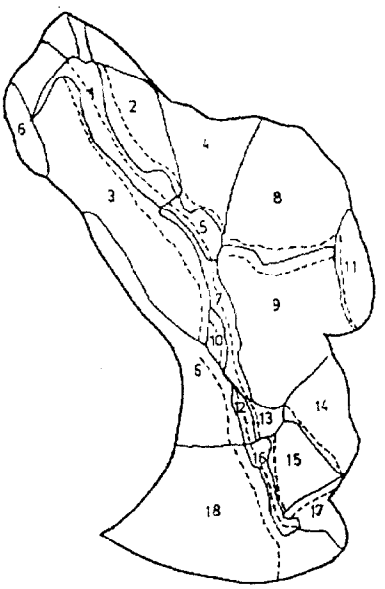

Figure 2: Breakdown of the Černičí catchment into individual fields (the dashed lines indicate the 'field channels', i.e., the paths of concentrated overland flow).

5 Simulation strategy

As the purpose of the simulation was to produce an as-exact-as-possible counterpart to the measured data, the soil and crop management inputs were made as similar as possible to the real situation recorded during the years 1992–1996. The data for 1992–1996 were

actually input twice, first as a fictitious substitute for the unknown data of 1987–1991 and then as true data for 1992–1996. The overall simulated period thus became 10 years (1987–1996), of which the first five years were only used as a warm-up period. The water-balance and water-quality outputs of extensive nature (such as water discharges and nutrients yields) which resulted from the simulation for individual fields were simply summed to give the corresponding outputs for the whole catchment, while the erosion outputs from individual fields were subject to an empirical sediment-routing procedure based on the fields being taken as nodes of a tree structure along which the runoff and the sediment transport were assumed to occur (Fig. 3). The sediment produced by an upstream field was assumed to be passed over by a given field to a downstream field after being multiplied by a sediment delivery ratio, estimated as a function of the field area, land use and elevation difference. In this way, the sediment yields at the catchment outlet were obtained. For comparison, another set of the simulated sediment yields at the catchment outlet was computed by a simple summation of the yields from individual fields, without any routing.

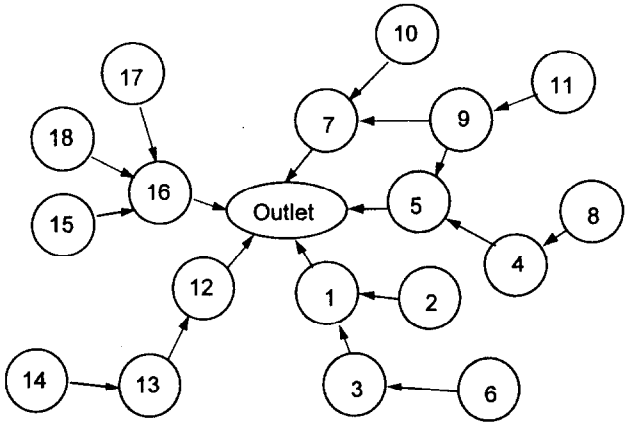

Figure 3: A simplified network of probable sediment routing through individual fields.

The simulated outputs from the whole catchment were compared with the actually measured data. The measured average daily discharges at the catchment outlet were, for this purpose, split into the direct runoff and the baseflow components using an ad hoc semi-empirical procedure. The measured water balance data were extensive enough to be used for a rough backward correction of some of the model inputs. As a matter of fact, only the soil hydraulic conductivity and the minimum depth to groundwater table on some fields had to be corrected. EPIC does not preserve the groundwater balance automatically and has to be calibrated in this respect. On the other hand, the water quality and sediment concentration measurements were too scarce to allow any parameter adjustment. Therefore, no such adjustment was attempted.

6 Results and discussion

Some simulation results are shown below. Even after the adjustment of soil hydraulic conductivities and minimum depths to the groundwater table in some fields, the simulation does not make the output components of the catchment water balance equal to the input, i.e., to the precipitation (Table 1). The component which causes the imbalance is the deep

Table 1: Simulated average annual water balance components of the Černičí catchment, 1992–1996.

Component	mm/yr	l/s	% of PRCP
PRCP = Precipitation	730.0	32.86	100.0
Q = Surface runoff	21.1	0.95	2.9
SSF = Subsurface runoff	17.9	0.81	2.5
PRK = Deep percolation	105.1	4.73	14.4
QDRN = Drainage runoff	3.2	0.14	0.44
ET = Evapotranspiration	599.2	26.97	82.1
Total losses (Q+SSF+PRK+QDRN+ET)	746.6	33.61	102. 3

percolation PRK. Its value could be changed and the imbalance could be eliminated if the input parameters (in particular, the hydraulic conductivities and the groundwater table depths) were adjusted further in an iterative manner. The same conclusion also follows from Table 2 in which the measured and simulated components of runoff are compared. The procedure of direct runoff separation applied to the measured data may not have been accurate enough but, at least, the sum of the two components, i.e., the total runoff at the catchment outlet, has been reliably measured. Hence, as the simulated total runoff is by 44.1 mm/year higher than the measured one, it clearly suggests that the simulated runoff (in particular, the simulated deep percolation) is overestimated, perhaps even more than the formal balance of simulated outputs vs. inputs (as given in Table 1) would suggest. Further investigation is needed to elucidate how much these figures are influenced by an inaccurate estimation of actual evapotranspiration and by that part of the base flow which possibly exfiltrates downstream of the measured outlet.

Table 2: Comparison of the measured and simulated average annual runoff components for the Černičí catchment, 1992–1996.

Component (mm/yr)	measured	simulated
Q = Storm (direct) runoff	26.2	21.1
SSF + PRK + QDRB = Base flow	77.0	126.2
Total runoff	103.2	147.3

In spite of the above reservation, one can conclude that, after some calibration, the long-term water balance of a catchment can be reproduced by EPIC with a reasonable accuracy. The picture becomes different, however, when one looks at the detailed pattern of individual rainfall-runoff events. Fig. 4 compares measured and simulated pseudo-hydrographs of average daily discharges of direct runoff for a typical summer period, while Table 3 illustrates how the peak discharges of total runoff compare. Generally, EPIC does not reproduce individual runoff events. This is to be expected, because of the structure of the model. In addition, Fig. 4 suggests that the simulated runoff often comes one day earlier than the measured one. This may partly be an artefact because the runoff volumes

Table 3: Comparison of the measured and simulated peak discharges for three selected events in the Černičí catchment.

Date of event: measured (simulated)	measured (l/s)	simulated (l/s)
30/5/95 (29/5/95)	366	1081.3
22/7/95 (22/7/95)	280	4291.4
8/7/96 (8/7/96)	62	3446.4

Table 4: Comparison of measured and simulated concentrations (g/l) of suspended sediment during some flood events (for the whole catchment).

Date of event:	30/5/95	22/7/95
Measured average concentration during the flood:	74.44	10.00
Simulated average daily concentration obtained by a simple summation of erosion from individual fields:	78.06	8.03
Simulated average daily concentration obtained by sediment routine:	9.48	11.92

were obtained by integration of hydrographs between neighbouring midnights while the standard time of precipitation measurement was 7:00 a. m. However, this may also mean that some sort of routing of runoff from individual fields may be necessary, in spite of the small size of the catchment.

A comparison of measured and simulated concentration of suspended sediments in the stream water during two extreme runoff events is given in Table 4. It suggests that the sediment routing procedure adopted may underestimate the true sediment yield, because it gave a realistic concentration in one of the events while, in the other event, the measured concentration was considerably higher than the one predicted by the routing procedure and even approached the value obtained by direct summation of amounts of eroded soil on individual fields. The measured data are, of course, too scarce for a definite conclusion.

Similarly, the data on concentrations of nutrients in the stream water, which was only sampled during flood events, do not allow to say how well EPIC reproduces the reality. A first-glance conclusion from Table 5 is that EPIC overestimates the concentrations of phosphorus and underestimates the concentrations of nitrogen. However, one must realise that, in this case, even the input data for EPIC were not very reliable: nothing was known about true rates of fertiliser application and very little was known about chemical properties of the soil. Thirdly, the comparison given in Table 5 only relates to flood events, while the concentrations at low and medium flows remain unexplored.

Other results of measurement and simulation, not shown here in detail, have confirmed that the vegetation canopy is the most efficient erosion-control measure. The most harmful erosion events occurred due to the coincidence of high-intensity rainfalls with insufficiently protected soil surface on large fields and on steep slopes, e.g. when potatoes or maize for silage were grown. The crop rotations used by two different agricultural enterprises farming in the catchment resulted in different average values of the USLE crop management factor C and, thus, in different erosion risk.

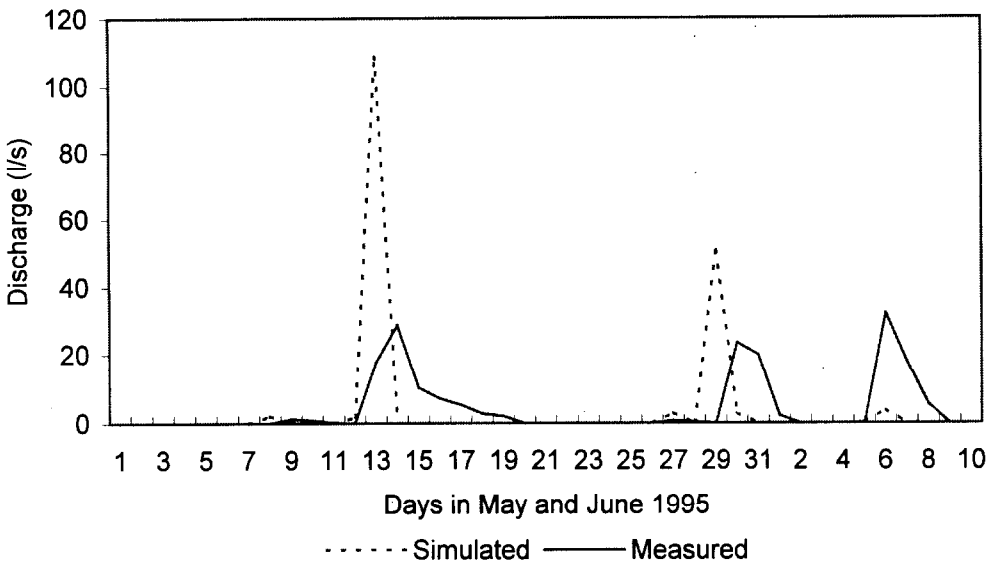

Figure 4: Comparison of simulated and measured average daily direct runoff discharges of water from the whole Černičí catchment, May–June 1995.

Table 5: Comparison of measured and simulated concentrations of nutrients dissolved in the stream water at the catchment outlet during some flood events.

Date of event:	30/5/95	6/6/95	23/7/95
A-NO_3 (mg/l), measured:	13.67	8.16	43.50
A-NO_3 (mg/l), simulated:	1.58	2.43	3.78
Soluble P (mg/l), measured:	0.545	0.254	0.172
Soluble P (mg/l), simulated :	0.653	0.990	0.750

7 Conclusions

As one may have expected, EPIC is not capable of reproducing individual events exactly because, to a great extent, it was not designed for this purpose. Its subroutines for simulation of various components of the catchment water balance (other than surface runoff) are relatively simple and may give inaccurate results even in terms of the average annual water balance, unless they are locally calibrated. This pertains, in particular, to the deep percolation component. However, as its core is built on solid empirical grounds, EPIC gives a correct overall semi-quantitative picture of how various factors influence surface runoff, sediment yield and stream water quality. It provides a rather detailed, albeit hypothetical, insight into spatial and temporal structure of the phenomena which would be otherwise difficult to achieve by measurements.

Both the measurements and the simulations confirm that the vegetation canopy is the most efficient erosion-control measure. It would also be of great importance, for proper validation of the adopted sediment-routing algorithm, to monitor runoff and sediment/nutrient yields coming from different parts of the catchment.

In general, acquiring experience in studies like this one helps build a culture of modelling without which further progress is unthinkable. On the other hand, our study points out that the extent, accuracy and frequency of stationary measurements of erosion-related phenomena on the small-catchment scale in the Czech Republic is insufficient.

Acknowledgements

The main part of this study was done as the first author's M. Sc. project at the Department of Engineering Hydrology, National University of Ireland, Galway, under supervision of the fourth and the fifth authors. A part of the field work was supported by the EU Copernicus programme, contract n° CIPA-CT-93-0241. The assistance of Messrs O. Haltuf and P. Pražák in obtaining field data is gratefully acknowledged. We also thank the authors of EPIC for providing us with the code and the accompanying documentation.

References

[1] Cunnane, C. (1997) 'Hydrological forecasting models for small agricultural catchments'. Main Technical Report. EU Copernicus Programme, Contract no. CIPA-CT-93-0241. Dept. Engineering Hydrology, National University of Ireland, Galway, Ireland.

[2] Jain, S.K. (1997) 'Evaluation of catchment management strategies by modelling soil erosion/water quality in EPIC supported by GIS'. MSc thesis. Dept. Engineering Hydrology, National University of Ireland, Galway, Ireland.

[3] Sharpley, A. N., and J. R. Williams (1990) 'EPIC - Erosion/Productivity Impact Calculator: 1. Model documentation, 2. User's guide.' U. S. Department of Agriculture Technical Bulletin No. 1768.

Reconsideration of three-component hydrograph separation models

and proposition of a combination of environmental tracing with time domain reflectometry measurements

C. Joerin, A. Musy, F. Pointet

Soil and Water Management Institute, Swiss Federal Institute of Technology, 1015 Lausanne, Switzerland.

1 Introduction

During recent years, considerable efforts have been expended in the pursuit of a thorough understanding of the processes responsible for the generation of storm runoff in streams. Among the experimental methods used for these investigations, environmental tracing has probably been the most used and has provided the most interesting results. Hydrograph separation using mass balance equations for water and chemical tracers to determine runoff sources in streamflow is now a widely used technique in hydrology. Nevertheless during the last ten years, its assumptions have been discussed and reconsidered. In the particular case of two-component hydrograph separation, several studies (Kennedy et al. 1986, Dewalle et al. 1988, Swistock et al. 1989, Bazemore et al. 1994) raised doubts about the validity of the assumption that the soil water does not contribute significantly. Therefore, it appears that three-component models, which distinguish groundwater and soil water, can improve the hydrological interpretation of hydrograph separation.

In the particular case of the Haute-Mentue watershed, Iorgulescu (1997) developed a three-component mixing model based on two chemical tracers (silica and calcium). This model considers the following components: direct precipitation, soil water (acid soils) and groundwater (in contact with the carbonate bedrock). The application of this model to Haute-Mentue hydrographs demonstrates that the contribution of soil water is strongly related to the antecedent moisture conditions of the basin (Iorgulescu 1997). In wet antecedent moisture conditions the contribution of soil water to total runoff may reach 58 % and subsurface flow (acid soil water and groundwater) 80 %.

In the hydrological literature, several mechanisms have been suggested to explain the important contribution of pre-event water: 'translatory flow', 'groundwater ridging', 'transmissivity feed-back', 'macropore flow', 'mixing in surface storages' (see Buttle 1994 for a review). In order to test these different hypotheses or to propose possible mechanisms responsible for these results, it appears that the application of environmental tracing, or more particularly of mixing models, is not enough. In fact, mixing models identify volumes but not water pathways. The same water (same age or same chemical characteristics) can

follow different pathways or, conversely, a given process can involve different kinds of water (McDonell 1990).

Furthermore the physical interpretation of the application of mixing models in terms of hydrological processes is quite difficult because it is affected by the uncertainty of hydrograph separation results. In fact, according to the spatial and temporal variability of water content, it is difficult to determine a unique chemical signature for each component, so results present some uncertainty. Consequently it seems important to be able to consider this uncertainty for the physical interpretation of hydrograph separation.

In this context the present study proposes first a method for the systematic uncertainty analysis of three-component mixing models. Then in order to study hydrological processes more specifically, an approach, which associates environmental tracing and soil water content measurements using Time Domain Reflectometry (TDR), is proposed. This approach begins with the identification of hydrological behaviour at a large scale and then investigations are conducted to establish the contributing area in order to study specific mechanisms and to discover which physical parameters control them.

2 Methods

2.1 Environmental tracing

2.1.1 Sampling

The outlet of the Bois-Vuacoz basin is equipped with a flow measuring structure (H-Flume) and with a submerged probe (pressure transducer) flow meter ISCO. An automatic ISCO sampler connected to the flow meter was programmed to take a sample every five millimetres of runoff. A recording tipping-bucket raingauge (200 cm^2) is situated in the studied basin. Bulk samples of open precipitation were collected at the outlet of the raingauge. Furthermore bulk throughfall was sampled by a trough (300 x 10 cm^2) situated at about 900 metres downstream of the Bois-Vuacoz outlet. The soil water was sampled at only two different sites in the Bois-Vuacoz basin during the studied period. This is not enough to adequately define the component of 'acid soil water', so for the hydrograph separation presented below the chemical signature of this component was defined according to all soil samples collected in the whole Haute-Mentue basin (at 15 different sampling locations) since 1993. The soil water was collected either by ceramic suction cups (unsaturated zone) or by zero tension lysimeters (saturated zone).

2.1.2 Uncertainty analysis approach

The knowledge about watershed hydrological behaviour and also the behaviour of a chemical tracer within the catchment is partial. Therefore the development of a three-component mixing model such as that proposed for the Haute-Mentue necessitates some subjective assumptions. It follows that there will be uncertainty associated with hydrograph separation. It is possible to distinguish two types of uncertainty: a fundamental uncertainty, which is affected by model assumptions; and a statistical uncertainty, due to temporal and spatial variability of the chemical signatures of different components. Only the latter can be formally quantified with the methodology of Bazemore et al. (1994). The former should be investigated by alternative hypotheses. In the context of the present study, the Soil and Water Management Institute developed a program (AIDH: Analyse d'Incertitude des Décompositions d'Hydrogramme) for a systematic analysis of statistical uncertainty (Joerin 1997). The latter was largely inspired of the study of Bazemore et al. (1994). In fact, the program AIDH is based on a Monte Carlo approach. However the program AIDH

presents the advantage that distributions of component chemical signatures are not necessarily normal. Therefore it is possible to determine the form of distribution function from the water samples collected in the field. In order to examine the fundamental uncertainty, hypotheses tests will be adopted. The program AIDH will be applied to four different mixing models. These models are all based on the same tracers (silica and calcium) but assumptions concerning their behaviour (spatial and temporal variability) are different (Fig. 1). Definitions of the chemical signatures of the different components go from the most general case (case 1: no spatial and no temporal variability specified) to the most specific one (case 4: spatial and temporal variability).

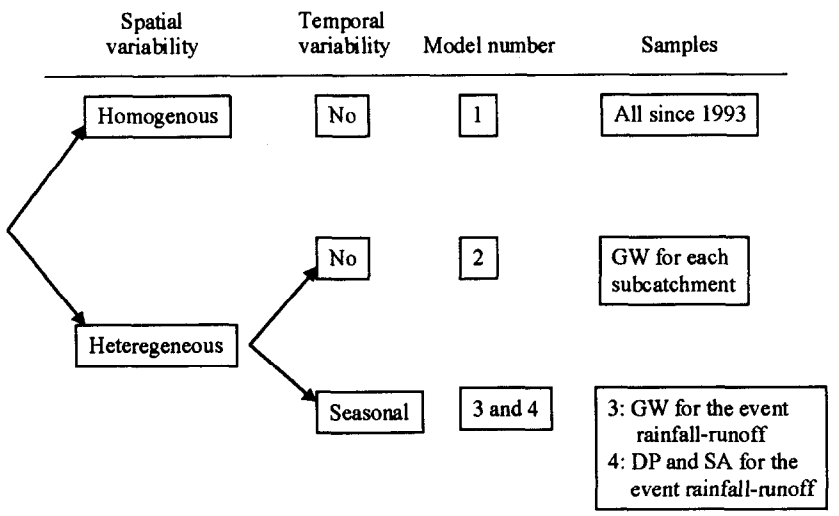

Figure 1: Presentation of models and their hypotheses concerning component chemical definition.

A comparison of the quality and the physical feasibility of the results will allow the most appropriate model to be identified or, in others words, the most appropriate chemical definition for the components. This test may also give some indications about the tracers behaviour.

2.2 Time domain reflectometry

TDR technique is used in this study to measure soil moisture in an area of approximately 500 m^2 at Bois-Vuacoz (Fig. 2: TDR probe = — 9.5, Temperature probe = —•, Coaxial cable (5 m) = — , Coaxial cable (15 m) = — , Coaxial cable (25 m) = — , Level 1 multiplexer = Mux 1, Level 2 multiplexer = Mux 2 to 9, Cable tester, datalogger and battery = Control centre). Thanks to multiplexing, the system records the apparent length of 64 probes computed from the plotted pulse with the software Pc208e from Campbell Scientific with a frequency of one hour. Each probe is composed of two wires, which are 30-cm long. The soil water content is calculated with the three-phase model of Roth et al. (1990).

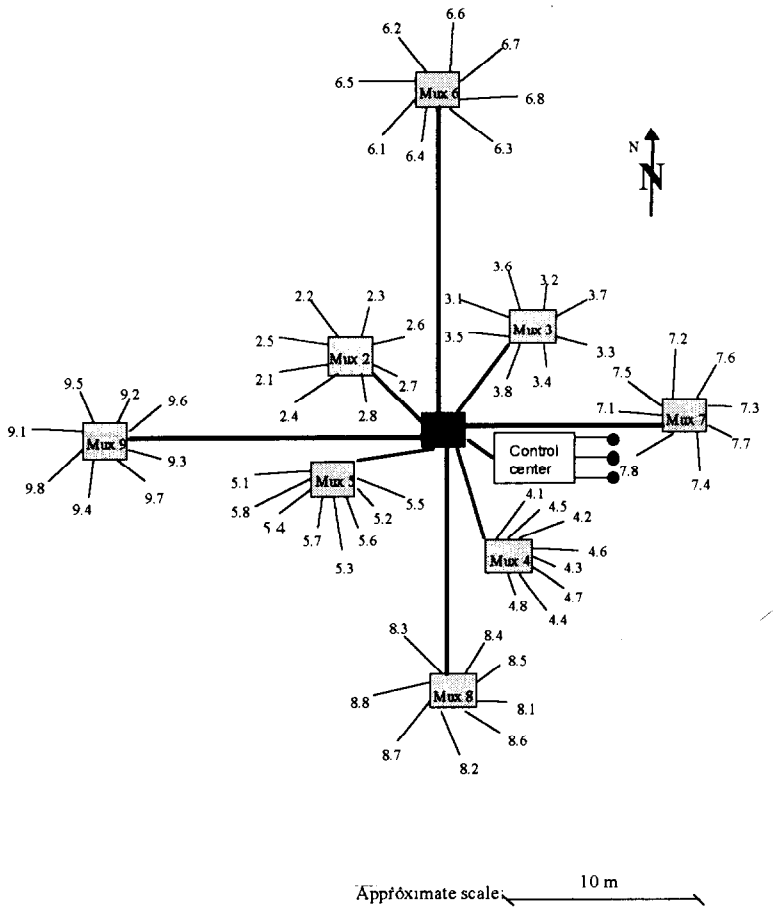

Figure 2: The configuration of the TDR probe net at Bois-Vuacoz.

3 Results and discussion

3.1 Uncertainty analysis

For the most general component definitions (model 1 and 2), the dispersion of component contributions (expressed in percent) obtained by the application of the AIDH program to the separation of the Haute-Mentue hydrograph is important. For example, for the first model the difference between the smallest and the biggest contribution calculated by the Monte Carlo method for a component can reach 50 %. Nevertheless the modification of component chemical definition between the first and the fourth model allows this variability to be reduced (Fig. 3). Finally hydrograph separation of the fourth model was clearly identified as the most certain and moreover it presents the most coherent hydrological behaviour (e.g. less contributions < 0). The chemical definition of components of the fourth model is based only on samples collected before and during the studied rainfall-runoff event (Fig. 1). Therefore the fact that the fourth model gives the most coherent results suggests indirectly that the temporal variability of component chemical composition is important. The improvement of hydrograph separation from the case one, where chemical definition is considered as invariable in space and time, to the fourth case should be considered as information contribution concerning components.

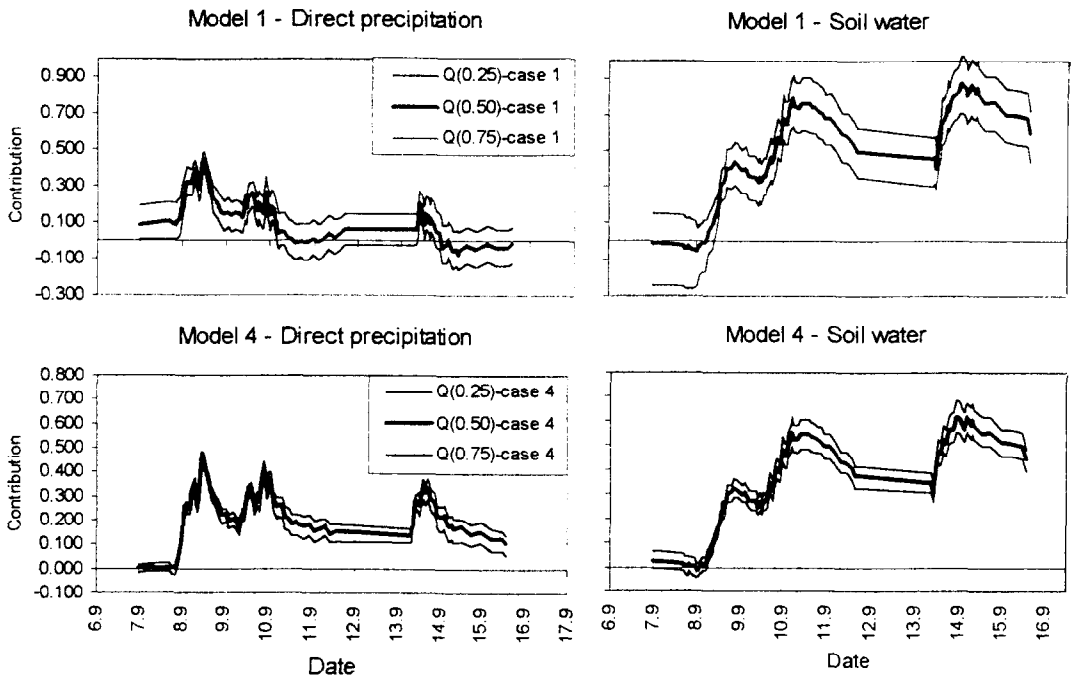

Figure 3: Contribution of direct precipitation and soil water at Bois-Vuacoz for three floods observed in September 1993 and representation of uncertainty (quartile 0.25, 0.50 and 0.75).

According to this analysis it appears that despite uncertainty in the results, it is possible to determine clearly general hydrological behaviour at the catchment scale with the application of environmental tracing. In fact, even with the application of the most general model (model 1: consideration of no spatial and no temporal variability of component signature), the origin of flows during the flood are well identified. But in order to improve the physical interpretation by the reduction of uncertainty in the results, it is possible to consider information concerning tracer behaviour and spatial and temporal variability of component chemical signatures.

Nevertheless, given the limited knowledge of tracer behaviour in the watershed and more particularly in the soil, it seems difficult to improve the chemical definition of components beyond what was possible here in moving from model 1 to model 4. As we have seen before, temporal variability of tracer concentration seems important but it is difficult to characterise it with the sampling techniques available. Moreover mixing models do not generally take the temporal variability of component chemical composition into account. Consequently, it seems opportune to explore and develop a new approach to use environmental tracing for hydrological processes identification. Moreover, geochemical models provide a global description of the system (watershed). Intra-basin processes cannot be inferred by environmental tracing alone. In fact several processes or combinations of processes may be responsible for the observed chemical behaviour. An alternative approach may be a combination of environmental tracing with hydrometric field measurements.

3.2 Combination of environmental tracing with time domain reflectometry

The period considered (5th November to 2nd December 1997) for this analysis presents relatively wet conditions. In October it rained 76.3 mm. Nevertheless, a relatively long period without rain occurred between the 24th October and the 3rd November. So the chemical signature of 'groundwater component' can be reasonably defined according to base flows observed just before the studied period. The hydrograph decomposition was obtained by the application of the AIDH. The quality of the separation obtained by the application of the AIDH program to the studied events of November 1997 is good (Fig. 4b). In fact the uncertainties are rather limited and thus it is possible to identify clearly the general hydrological behaviour of the Bois-Vuacoz basin. Most relevant observations are that the groundwater dominates the flow almost all the time (GW 36–99 %) and the soil water contribution increases during the series of four events between the 8th November and the 13th November (Fig. 4a and 4b). Moreover the during 13th November the peak flow soil water dominates the flood (SW 46 %, GW 41 %, DP 13 %). These observations correspond well with patterns proposed by Iorgulescu (1997). He suggested that these patterns depend on the variation and extension of contributing areas within the basin. In dry conditions storm flow can be explained as a mixture of pre-event base flow and precipitation. In the same time the basin becomes wetter the contribution of soil water increases. Finally in wet conditions soil water dominates storm flow.

Concerning TDR measurements, it appears that the spatial variability of soil moisture at the local scale is very important. Pointet (1998) studied this spatial variability with a regionalised variables approach (Matheron 1970) and suggested that soil moisture is a random variable at the local scale (< 20 m). Differences between the time series dynamics are also important and it is possible to distinguish two patterns. In the first case (e.g. probes 4.4, 4.7, 4.6, 4.2 in Fig. 4c), the soil moisture increases more strongly than in the second one (e.g. probes 4.8, 4.1, 4.5, 4.3 in Fig. 4c). In the first case the soil water content is initially clearly lower than in the second one but the soil moisture maxima of both series are very close. Nevertheless the time since the beginning of the precipitation to reach maximum soil moisture is similar in both cases, varying between 15 and 17 hours. In wet conditions differences of soil moisture are less important than in dry conditions. The decrease of soil moisture is also completely different. In the first case this dynamic is clearly stronger and faster than in the second one. These differences of behaviour are observed between very close sites (the distance between probes in Fig. 4c varies between 1 and 8 metres). The spatial variability and the difference of dynamic of soil moisture seems to be due to phenomena such as preferential flows.

It is interesting to compare the soil moisture evolution with the hydrograph separation. Among the three components the dynamic of soil water contribution is obviously the most similar to soil moisture. In fact these two series follow the same evolution and furthermore they reach their maximum virtually at the same time (maximum of soil water contribution on the 13th November at 0:34; maximum of soil moisture on the 13th November at 1:34). Overall TDR observations confirm partially the relative importance of the 'soil water' component. After important precipitation the soil water content increases strongly and can reach moisture close to the saturation (in comparison with the figure 4c the porosity at Bois-Vuacoz is around 0.5 m^3/m^3). This behaviour, which occurs at the same time that the streamflow increases, seems to be favourable for subsurface flows, and more particularly for lateral flows through the soil. So according to environmental tracing and TDR results, it seems possible to confirm the importance of the soil water contribution and that of subsurface flow to flood generation in wet conditions. In the present situation it is still difficult to associate these flows with particular hydrological processes.

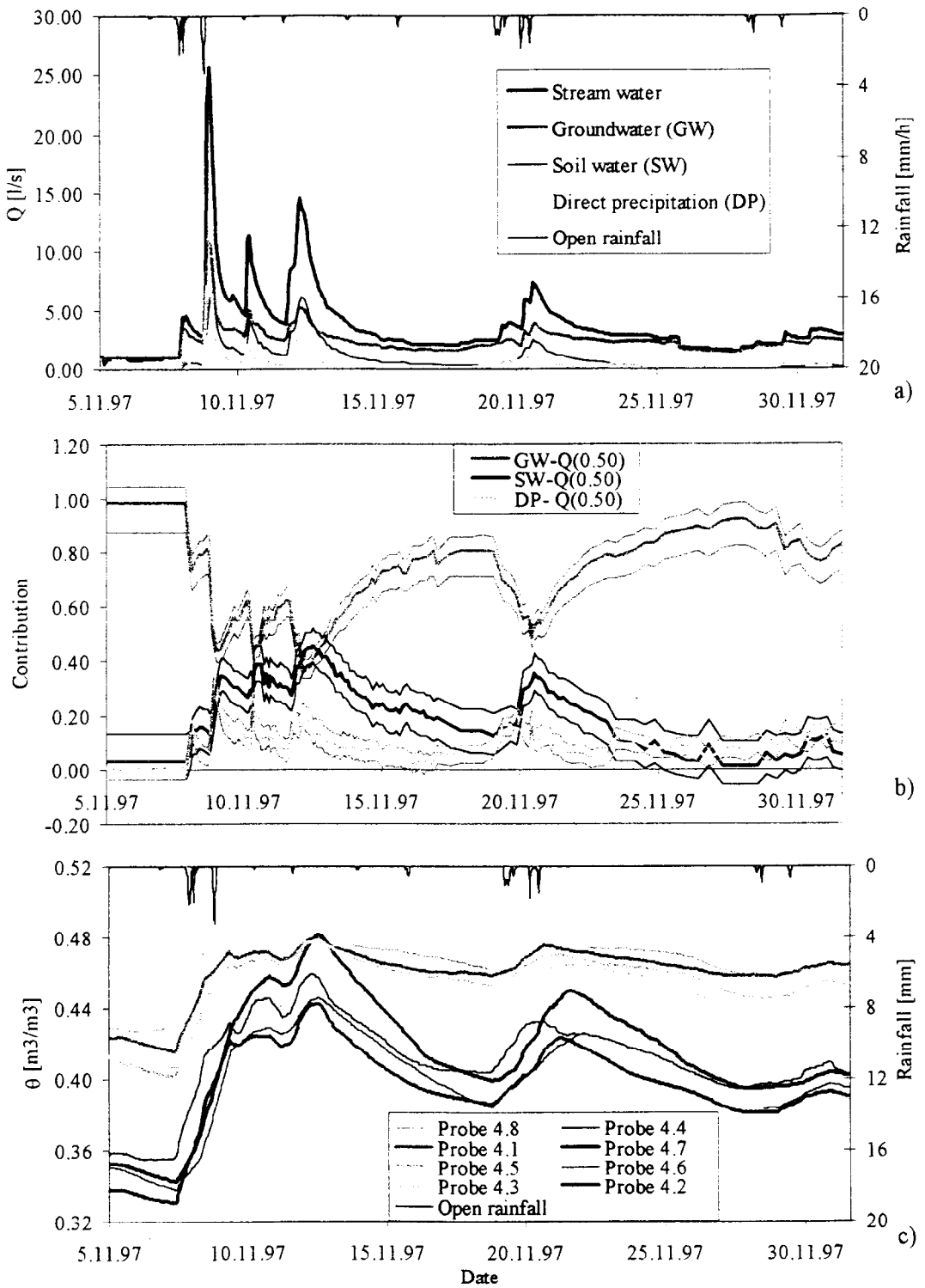

Figure 4: Bois-Vuacoz a) Hydrograph separation, b) Component contribution and representation of uncertainty (quartile 0.75, 0.50 and 0.25) and c) Soil moisture.

Nevertheless, the TDR experiment indicates clearly that conditions of subsurface flows are not homogeneous within hill slopes. Consequently hydrological processes, in addition to soil moisture, depend probably on very local characteristics. According to hydrological mechanisms proposed in the literature and field observations some hypotheses can be proposed in order to explain the rapid and important soil water contribution. In wet conditions it seems that preferential flows extend through the hill slope and deliver rapidly a significant amount of water to the stream. Several physical mechanisms or properties can be responsible for these preferential flows. More particularly in the case of the Haute-Mentue, they are probably due to either macropores or differences of soil properties (e.g. hydraulic conductivity, porosity) or micro-topography as proposed by Iorgulescu (1997). He suggested that, when the water table is close to the soil surface, micro-topography and changing boundary conditions create 'local flow paths' on hill slopes. Then local source areas are connected to the permanent network by surface pathways (see also Bazemore et al. 1994).

4 Conclusions

First, this study developed a methodology for the uncertainty analysis of geochemical mixing models. This methodology was built on the Haute-Mentue example, but it can be transposed to other tracers and other watersheds. In spite of investigations which try to identify tracer behaviour in space and in time, the water-soil-substratum system is so complex that there will always remain some uncertainty concerning the chemical definition of the components. Therefore, in future uncertainty analysis should be always associated with mixing models in order to consider it in physical interpretation of hydrograph separation. Despite the limitation of geochemical mixing models, as presented in the discussion above, they remain a reasonable technique for studying the general behaviour of a catchment. Nevertheless, if we intend to identify hydrological processes inside the catchment, it will be necessary to require the application of others techniques.

The approach adopted during this study, the combination of several techniques of measurements (e.g. environmental tracing and TDR), seems interesting in the context of the study of hydrological processes. In fact it is virtually impossible to identify the specific hydrological behaviour of a basin with the application of only one type of measurements. Each sort of measurement has a specific area of exploitation and consequently interpretation of a single sort of measurement is limited. For example basin scale environmental tracing does not allow the specification of the mechanism by which soil water is delivered to the river during the flood. Therefore it appears that a better hydrological processes identification may be obtained by the association of several types of measurements (e.g. tracers for a global view and TDR for a more local view). A good way to begin such an approach is certainly the application of environmental tracing in order to determine the general behaviour and then to concentrate on local measurements on specific areas. The choice of point or internal measurements depends on the mechanisms being investigated.

Acknowledgements

This research was supported in part by the Swiss National Research Foundation (Grant 21-43308.95) and by OFES (Grant 95.00449) in the framework of the EU funded Project VAHMPIRE.

References

[1] Bazemore, D. E., Eshleman, K. N. and Hollenbeck, K. J., (1994). The role of soil water in stormflow generation in a forested headwater catchment: synthesis of natural tracer and hydrometric evidence. J. Hydrol., 162: 47–75.

[2] Buttle, J. M., (1994). Isotope hydrograph separations and rapid delivery of pre-event water from drainage basins. Progress in Physical Geography, 18,1: 16–41.

[3] Buttle, J. M. and Peters, D. L., (1997). Inferring hydrological processes in a temperate basin using isotopic and geochemical hydrograph separation: a re-evaluation. Hydrol. Processes, 11: 557–573.

[4] Dewalle, D. R., Swistock, B. R. and Sharpe, W. E., (1988). Three-component tracer model for storm flow on a small Appalachian forested catchment. J. Hydrol., 104: 301–310.

[5] Iorgulescu, I., (1997). Analyse du comportement hydrologique par une approche intégrée à l'échelle du bassin versant. Application au bassin versant de la Haute-Mentue. PhD Thesis, Ecole Polytechnique Fédérale de Lausanne, Lausanne, 216 pp.

[6] Joerin, C., (1997). Analyse d'incertitude des modèles de mélange géochimique - Application à la décomposition des hydrogrammes de la Haute-Mentue, Master Thesis, Ecole Polytechnique Fédérale de Lausanne, Lausanne, 69 pp.

[7] Kennedy, V. C., Kendall, C., Zellweger, G. W., Wyerman, T. A. and Avanzino, R. J., (1986). Determination of the components of stormflow using water chemistry and environmental isotopes, Mattole river basin, California. J. Hydrol., 84: 107–140.

[8] Matheron, G. F., (1970). La théorie des variables régionalisées et ses applications, Tech. Rep. Fascicule 5, Les cahiers du centre de morphologie mathématique de Fontainebleau. Ecole Supérieure des Mines de Paris.

[9] McDonell, J. J., (1990). A rationale for old water discharge through macropores in a steep, humid catchment. Wat. Resour. Res., 26: 2821–2832.

[10] Pointet, F., (1998). Analyse de la variabilité spatiale et temporelle de la teneur en eau du sol: application au bassin versant expérimental de la Haute-Mentue. Travail de diplôme, Ecole Polytechnique Fédérale de Lausanne, Lausanne, 79 pp.

[11] Roth, K., Schulin, R., Flühler, H. and Attinger, W., (1990). Calibration of time domain reflectometry for water content, measurement using composite dielectric approach. Wat. Resour. Res., 26: 2267–2273.

[12] Swistock, B. R., De Walle, D. R. and Sharpe, W. E., (1989). Sources of acidic storm flow in an Appalachian headwater stream. Wat. Resour. Res., 25(10): 2139–2147.

Biogeochemistry of forest catchments with contrasting lithology

P. Krám[1], J. Hruška[1] , Ch. T. Driscoll[2]

[1]Czech Geological Survey, Department of Environmental Geochemistry, Klárov 3, CZ 118 21 Prague 1, Czech Republic. [2]Syracuse University, Department of Civil and Environmental Engineering, 220 Hinds Hall, Syracuse, New York, USA.

Abstract

Biogeochemical patterns were studied in two forested catchments in the Czech Republic, one underlain by leucogranite, the other by serpentinite. The objective was to compare and contrast element pools and fluxes in the catchments with similar topography, vegetation, climate, and atmospheric deposition, but different lithology. The leucogranite site showed low concentrations of exchangeable base cations on the soil exchange complex and in stream water. Supplies of base cations from atmospheric deposition and soil processes were smaller than inputs of sulfate on an equivalence basis, resulting in low pH and high concentrations of aluminum in drainage water. In contrast, high weathering rates at the serpentinite site resulted in magnesium as the dominant cation on the soil exchange complex and in drainage water. The catchment exhibited near neutral stream water pH, despite elevated inputs of acidic deposition.

1 Introduction

Lithology may have a strong influence on element cycling (Cleaves et al. 1974, O'Brien et al. 1997, Hornbeck et al. 1997). There is considerable interest in the biogeochemistry of areas underlain by granite because typically low weathering rates limit the supply of base cations (Ca, Mg, Na, K) resulting in sensitivity to acidic atmospheric deposition (Chadwick et al. 1991). Serpentinite is intriguing because in addition to its acid neutralization properties, its peculiar chemistry with enrichment of Mg, Fe, Ni, Cr, Co and B, and undersupply in Ca, K, P, Mo and Zn leads to an unusual chemical environment for vegetation (Roberts and Proctor 1992).

In this study, the influence of lithology on the response of forest ecosystems to acidic deposition was tested at two experimental catchments in the Czech Republic. The site selection criteria for the experimental catchments included proximity to each other, similar climate, atmospheric deposition, topography, vegetation cover and differing lithology.

2 Methods and site description

The Slavkov Forest (Slavkovský les), located in the western part of the Czech Republic is a mountainous region with drainage waters exhibiting diverse chemical compositions. The areas surrounding the highest peaks are underlain by leucogranite and they have podzolic soils. Drainage waters are highly acidic, with elevated concentrations of Al and Be (Krám et al. 1995, 1997, 1998, Krám 1997). The landscape is also characterized by peat bogs located on gentle hillslopes. Waters derived from these systems are highly acidic, with elevated dissolved organic carbon concentrations and relatively low Al concentrations (Hruška et al. 1996, 1997). The other chemical water type is associated with serpentinite, characterized by Mg-rich alkaline drainage waters (Krám et al. 1997, Krám 1997).

The two experimental catchments are located 7 km apart at the following latitudes and longitudes (Lysina 50°03'N, 12°40'E, Pluhův Bor 50°04'N, 12°46'E). The catchment area of Lysina is 0.27 km^2 over an elevation range of 829–942 m. It is underlain by a coarse-grained leucogranite. Predominant soils are Spodosols. The catchment consists of a mosaic of Norway spruce (*Picea abies*) stands (Fig. 1). The catchment area of Pluhův Bor is 0.22 km^2 with an elevation range of 690–804 m. It is underlain by serpentinite bedrock consisting primarily of antigorite (Mg-silicate). The dominant soils are Inceptisols. Pluhův Bor is almost entirely forested with Norway spruce plantations (Fig. 1).

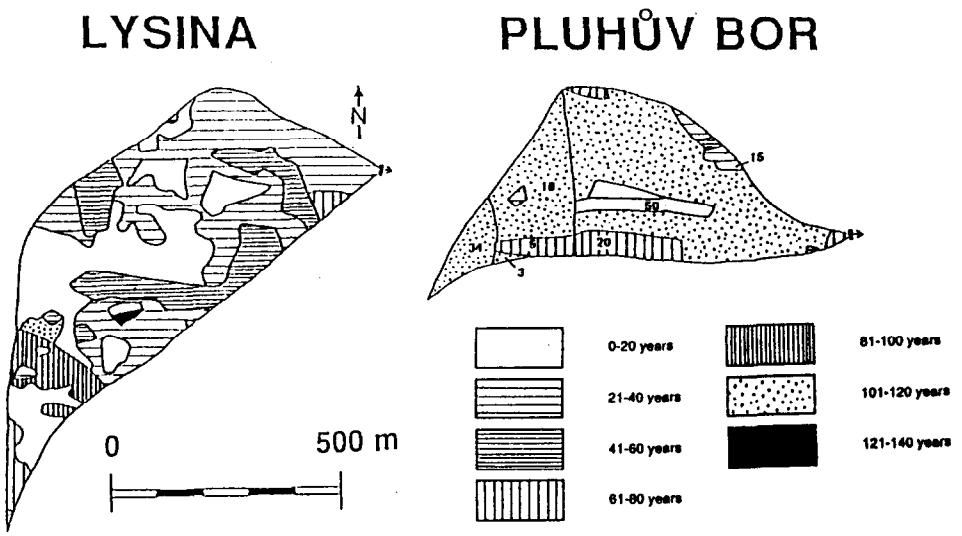

Figure 1: Stock age map of Norway spruce (*Picea abies*) stands at the study sites. Numbers denote percentage of admixed Scots pine (*Pinus sylvestris*). V-notch weirs are situated in the eastern part of the catchments.

Bulk precipitation was collected bi-weekly in a clearing within the forest at Lysina. Bulk precipitation was not measured at Pluhův Bor due to the absence of clearings. Throughfall was collected monthly in each catchment. The outflow from the catchments was monitored continuously using V-notch weirs and water level recorders. Streamwater was collected weekly for chemical analysis. The flow from the catchment was monitored continuously from September 1989 at Lysina and from November 1991 at Pluhův Bor. In each catchment, two lysimeter pits were excavated in 1993. One zero-tension lysimeter was inserted just beneath the organic horizon and beneath the first mineral horizon in each pit (depth 5–30 cm below the surface). Soil solution was sampled at approximately monthly intervals beginning in June 1994. Soils were sampled at nine locations at Lysina

and at four locations at Pluhův Bor. Spruce tissue samples were obtained from four representative trees, which were cut within each catchment. Details of laboratory methods were described in Krám et al. (1997).

3 Results and discussion

For the 1992–1994 water years mean measured rainfall was 999 mm yr^{-1} at Lysina, and stream runoff was 442 mm yr^{-1} at Lysina and 244 mm yr^{-1} at Pluhův Bor (Krám 1997). An assessment of the contribution of throughfall for the mature forested areas in conjunction with bulk deposition for open areas (30 % at Lysina, 6 % at Pluhův Bor) resulted in a water input to the soil of 814 mm yr^{-1} at Lysina and 630 mm yr^{-1} at Pluhův Bor.

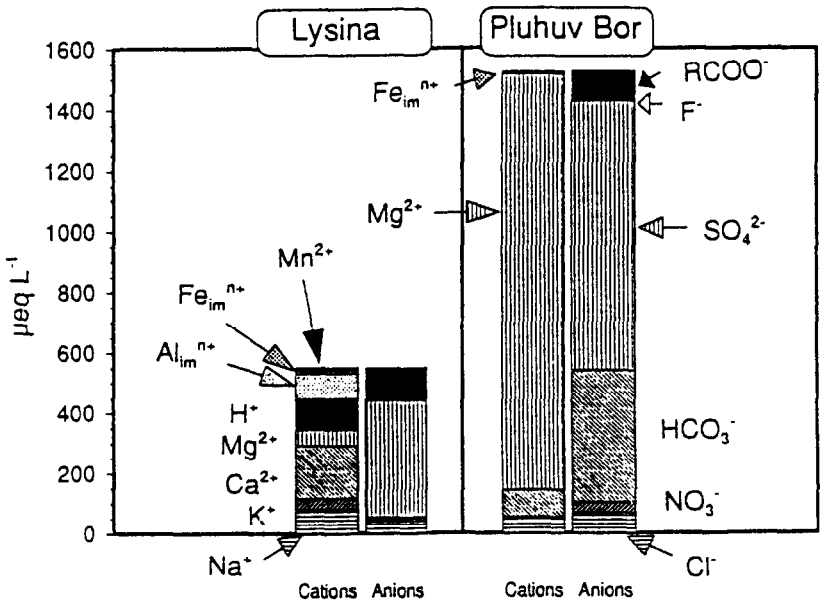

Figure 2: Mean charge balance in stream water at Lysina and Pluhův Bor. Al_{im} is inorganic monomeric AL, Fe_{im} is inorganic monomeric Fe, $RCOO^-$ is naturally occurring organic anion.

Bulk precipitation to the study catchments was characterized by large inputs of NH_4^+, NO_3^-, H^+ and SO_4^{2-}. Overall, the bulk deposition of ionic solutes showed a strong anthropogenic influence. Throughfall fluxes were greater than bulk precipitation inputs for all solutes except for NH_4^+. Throughfall fluxes were dominated by SO_4^{2-}, H^+, NO_3^-, and K^+. The high throughfall fluxes of SO_4^{2-} reflect the high loading of dry deposition of sulfur to the region. Dry deposition was a significant source of acidic deposition as indicated by a SO_4^{2-} throughfall/bulk precipitation flux ratio of 3.4 (108 vs. 32 mmol m^{-2} yr^{-1} at Lysina, 1992–1994).

At Lysina, acidic throughfall (pH 3.8) below the spruce canopy was further acidified by organic acids leached from the O horizon, resulting in low pH (3.6) of soil solution in the O and E horizons. In contrast, the acidic throughfall (pH 3.9) at Pluhův Bor was neutralized by the upper soil as reflected by the increases of soil solution pH in the O (pH 4.6) and A horizons (pH 5.4). Magnesium, the dominant cation in soil solution at Pluhův Bor, ranged between 300 and 1700 μmol l^{-1}. In contrast, concentrations of Mg^{2+} in soil solution at Lysina were low (5-14 μmol l^{-1}).

Weathering of feldspars in the Lysina catchment resulted in stream water with relatively high proportions of dissolved Si (78– 315 μmol l^{-1}), Na^+ and Ca^{2+} (Figs. 2-3). At Pluhův Bor, however, the relatively high weathering rate of antigorite contributed to the high concentrations of Mg^{2+} and dissolved Si (231–481 μmol l^{-1}), and low Na^+, Ca^{2+} and Al concentrations (Figs. 2–3). Elevated concentrations of SO_4^{2-} in stream waters at both sites were consistent with high inputs of SO_4^{2-} from atmospheric deposition (Fig. 2, Fig. 4). Bicarbonate (HCO_3^-) was the second most important anion in stream water at Pluhův Bor, but was negligible at Lysina (Fig. 2). At Lysina, stream pH varied between 3.8 and 4.5, with a discharge-weighted mean pH of 3.9, and the Gran acid neutralizing capacity (ANC) varied between -196 to -30 μmol l^{-1} in the 1992–1994 water years (Fig. 4). Organic anions (estimated by difference in charge balance) comprised about 19 % of total anionic charge at Lysina, and 7 % at Pluhův Bor (Fig. 2).

Stream water at Lysina was characterized by unusually high concentrations of Al (16–81 μmol l^{-1}, discharge-weighted mean 57 μmol l^{-1}) (Fig. 3). The inorganic monomeric Al (Al_{im}) was the dominant Al fraction at Lysina, ranging from 50 to 90 % of Al. Aquo Al^{3+} (toxic form) was approximately 40 %, and Al-F complexes (relatively non-toxic) were roughly 35 % of Al_{im} during high-flow events. During baseflow, aquo Al^{3+} decreased to 20 % and Al-F accounted for 75 % of Al_{im}. In contrast, stream pH ranged between 6.1 and 8.2, and ANC between 101 and 2560 μmol l^{-1} in the catchment underlain by serpentinite, and concentrations of Al were low (1–11 μmol l^{-1}) (Figs. 3–4).

Quartz was a dominant mineral in all soil horizons at both Lysina and Pluhův Bor. Other major minerals in the mineral soil at Lysina were albite, orthoclase, amorphous Al, and muscovite. Major minerals in the mineral soil at Pluhův Bor were amorphous Al, albite, amphibole, orthoclase, antigorite, and talc. Concentrations of exchangeable base cations and soil pH were markedly different. Pluhův Bor exhibited high concentrations of exchangeable Mg, base saturation increased with depth, reaching essentially 100 % in the C horizon. In contrast, the catchment at Lysina showed low concentrations of exchangeable base cations, the base saturation decreased with depth to less than 5 % in the lower mineral soil and the soil exchanger was dominated by exchangeable Al. The mineral soil (0–40 cm) exchangeable Mg pool at Pluhův Bor (9020 $mmol_c$ m^{-2}) was 120 times larger than at Lysina (76 $mmol_c$ m^{-2}). Exchangeable Ca pools in the same layer were 899 $mmol_c$ m^{-2} at Pluhův Bor and 370 $mmol_c$ m^{-2} at Lysina. Soil pH_w was similar in the forest floor at the two sites (Lysina: 3.7, Pluhův Bor: 3.8), but values in the mineral soil followed the patterns of base saturation. Soil pH_w increased with depth to near-neutral values at Pluhův Bor, while pH_w exhibited acidic values throughout the profile at Lysina.

Among the base cations, Ca exhibited the highest concentrations in the tree tissue at both sites and the highest concentrations were found in the bole bark (Lysina: 175 mmol kg^{-1}, Pluhův Bor: 209 mmol kg^{-1}). At Pluhův Bor, foliage had relatively high Ca concentrations (163 mmol kg^{-1}). The Ca concentration in foliage at Lysina was about 43 % of the value at Pluhův Bor. Concentrations of Mg in spruce tissues at Lysina were low. Foliar concentrations of Mg were extremely low (14 mmol kg^{-1}), even lower than Mg concentrations in bole bark (30 mmol kg^{-1}), and branches (21 mmol kg^{-1}). In contrast, the Mg concentrations in foliage (112 mmol kg^{-1}), bole bark (65 mmol kg^{-1}), and branches (41 mmol kg^{-1}) were very high at Pluhův Bor. Concentrations of K were higher in all vegetation tissues at Lysina than at Pluhův Bor. At both sites, the highest K concentrations were found in the foliage (Lysina: 141 mmol kg^{-1}, Pluhův Bor: 84 mmol kg^{-1}). Very high concentrations of Ni were observed in spruce tissues at Pluhův Bor. Nickel was especially concentrated in the bole bark (0.34 mmol kg^{-1}) and foliage (0.2 mmol kg^{-1}).

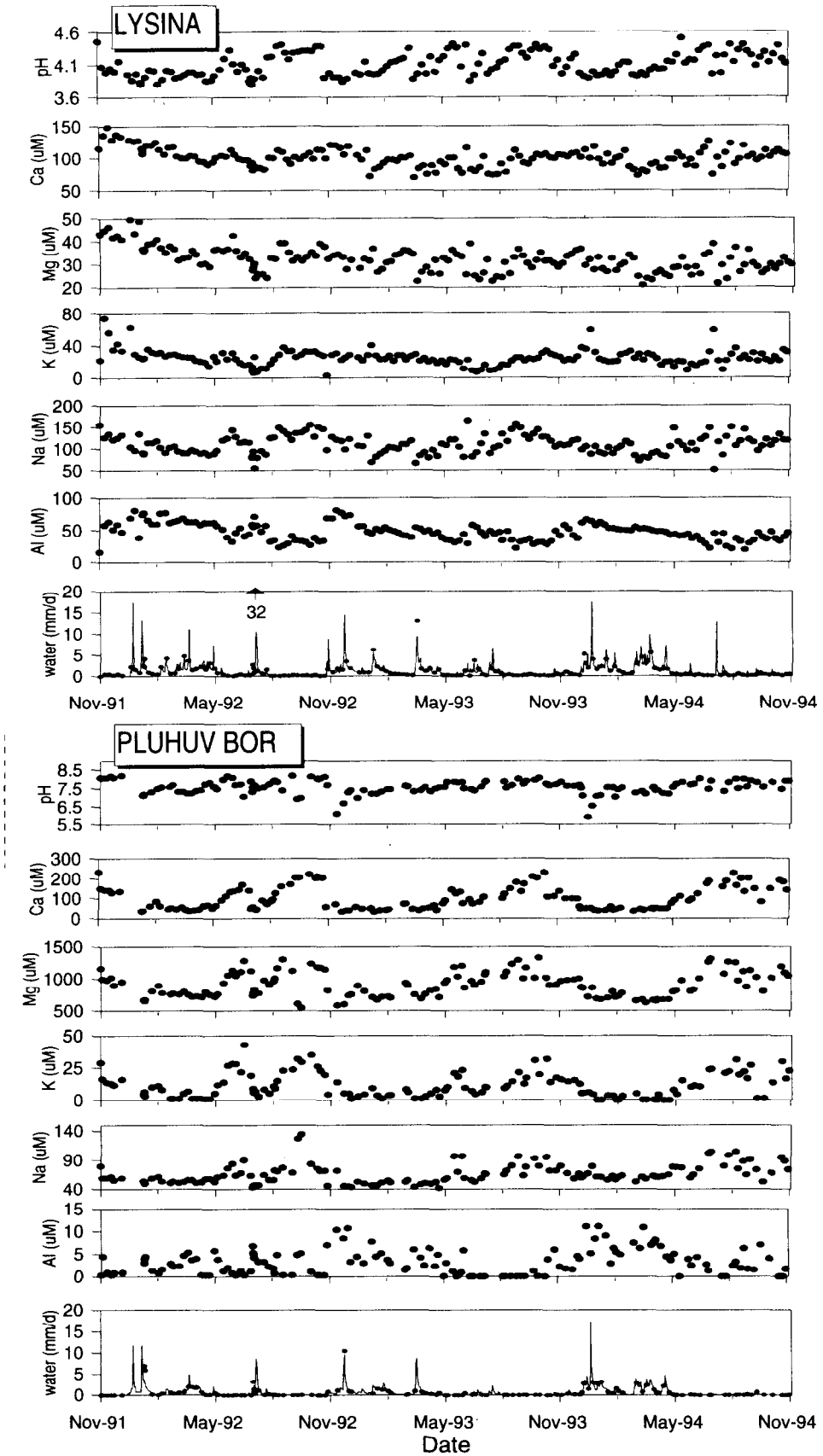

Figure 3: Temporal patterns of stream water pH and concentrations of cations, mean daily runoff (curve) and instantaneous runoff at the time of sampling (circle or arrow) at the study sites in 1992–1994 water years (November–October).

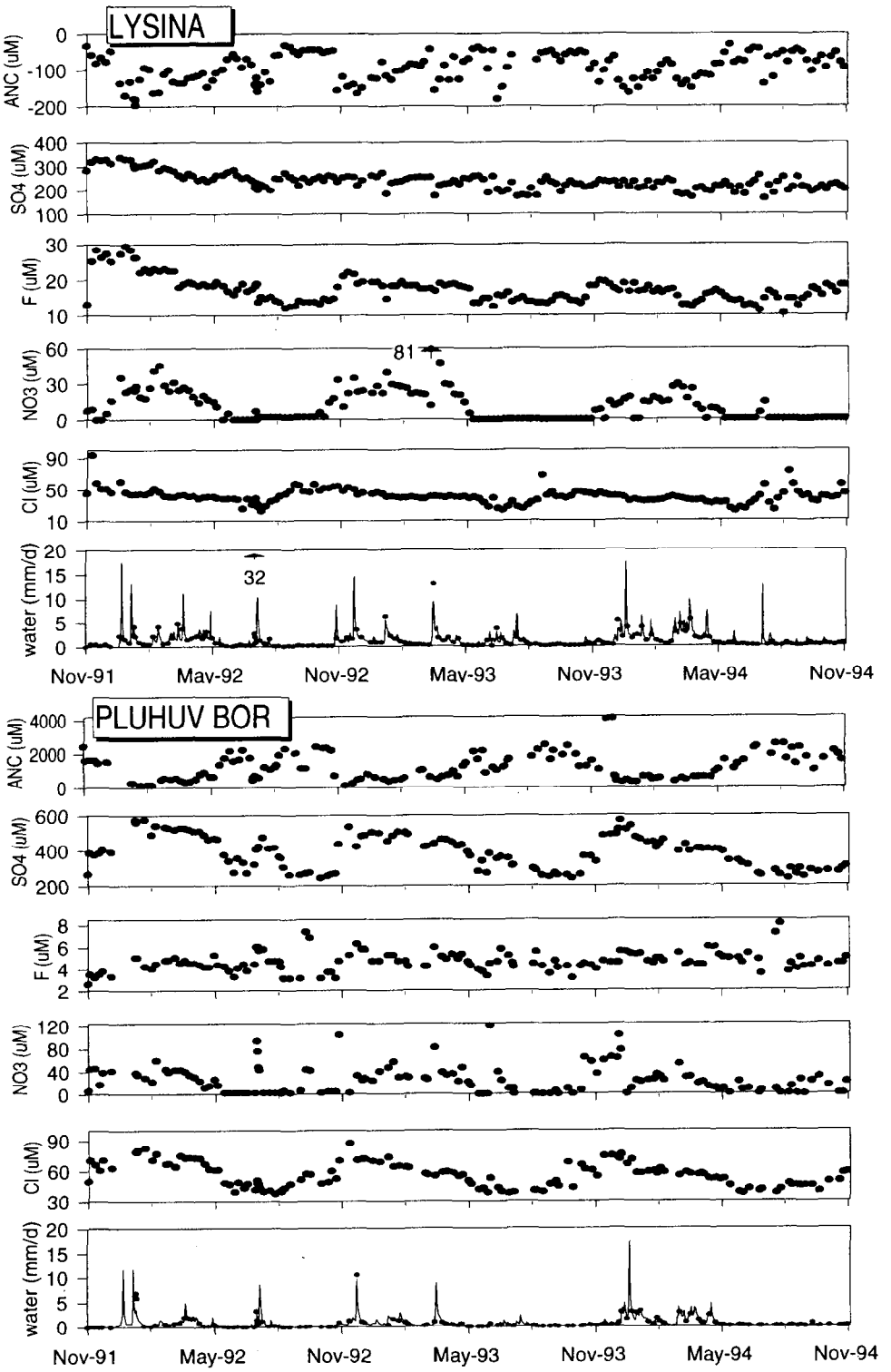

Figure 4: Temporal patterns of stream water ANC and concentrations of anions, mean daily runoff (curve) and instantaneous runoff at the time of sampling (circle or arrow) at the study sites in 1992–1994 water years (November–October).

4 Conclusions

The experimental catchments served as valuable end-members of ecosystem sensitivity to severe levels of acidic deposition.

Soils at Lysina showed small pools of exchangeable base cations, and low soil and soil solution pH. Weathering and exchange processes in the catchment were unable to neutralize the high inputs of atmospheric acidity, resulting in elevated stream H^+ and Al concentrations. Concentrations of potentially toxic Al (inorganic monomeric Al_{im}; and mainly Al^{3+} species) were extremely high in Lysina stream water. Elevated concentrations of Al reflected a limited supply of base cations from granitic bedrock and podzolic soils, which were unable to neutralize strong acid inputs from atmospheric deposition. Visible symptoms of forest decline by needle yellowing were probably caused by Mg deficiency at Lysina.

The Pluhův Bor catchment, underlain by the faster weathering serpentinite, showed extremely large pools of exchangeable Mg but smaller pools of other base cations. Exchangeable concentrations and pools of soil Ca were relatively large at Pluhův Bor, despite the fact that Ca was found only in trace amounts in the serpentinite. Weathered amphibole veins may be a major primary source of soil Ca. Foliar Ca was in the upper optimum range in Norway spruce. Much of the Ca is probably returned to the soil via canopy leaching and litterfall. Slow tree growth appears to be caused by K deficiency, Mg oversupply and/or Ni toxicity at Pluhův Bor.

Acknowledgements

Support for this research was provided by the Czech Geological Survey, the Grant Agency of the Czech Republic, Syracuse University, and the U.S. National Science Foundation. We appreciate the field monitoring of Z. Dedek and V. Kmínek. Most of the chemical analyses were done by M. Mikšovský, L. Dempírová, H. Vitková, and V. Valný. Mineralogical analyses were done by P. Ondruš and F. Veselovský. We appreciate the technical help of B. Wenner, P. Baresh, and C. Johnson.

References

[1] Chadwick, M. J.; J. C. I. Kuylenstierna and C. A. Gough (1991) 'The Stockholm Environmental Institute map of relative sensitivity to acidic deposition in Europe'. In: J. P. Hetteligh; R. J. Downing and P. A. M. de Smet (eds.) Mapping critical loads for Europe, CCE Tech. Rep. 1, National Institute of Public Health and Environmental Protection, Bilthoven, p. 49–57.

[2] Cleaves, E. T.; D. W. Fisher and O. P. Bricker (1974) 'Chemical weathering of serpentinite in the Eastern Piedmont of Maryland'. Geological Society of America Bulletin, Vol. 85, 437–444.

[3] Hornbeck, J. W.; S. W. Bailey; D. C. Buso and J. B. Shanley (1997) 'Streamwater chemistry and nutrient budgets for forested watersheds in New England: variability and management implications'. Forest Ecology and Management, Vol. 93, p. 73– 89.

[4] Hruška, J.; C. E. Johnson and P. Krám (1996) 'The role of organic solutes in the chemistry of acid-impacted bog waters of the western Czech Republic'. Water Resources Research, Vol. 32, p. 2841–2851.

[5] Hruška, J.; C. E. Johnson; P. Krám and C.-Y. Liao (1997) 'Organic solutes and the recovery of a bog stream from chronic acidification'. Environmental Science and Technology, Vol. 31, p. 3677–3681.

[6] Krám, P. (1997) 'Biogeochemistry of forest catchments in the Czech Republic with contrasting lithology under conditions of acidic deposition'. PhD dissertation, Syracuse University, Syracuse, New York, 179 p.

[7] Krám, P.; J. Hruška; C.T. Driscoll and C.E. Johnson (1995) 'Biogeochemistry of aluminum in a forest catchment in the Czech Republic impacted by atmospheric inputs of strong acids'. Water, Air, and Soil Pollution, Vol. 85, p. 1831–1836.

[8] Krám, P.; J. Hruška; B. S. Wenner; C. T. Driscoll and C. E. Johnson (1997) 'The biogeochemistry of basic cations in two forest catchments with contrasting lithology in the Czech Republic'. Biogeochemistry, Vol. 37, p. 173–202.

[9] Krám, P.; J. Hruška and C. T. Driscoll (1998) 'Beryllium chemistry in the Lysina catchment, Czech Republic'. Water, Air, and Soil Pollution, Vol. 105, p. 391–397.

[10] O'Brien, A. K.; K. C. Rice; O. P. Bricker; M. M. Kennedy and R. T. Anderson (1997) 'Use of geochemical mass balance modelling to evaluate the role of weathering in determining stream chemistry in five Mid-Atlantic watersheds on different lithologies'. Hydrological Processes, Vol. 11, p. 719–744.

[11] Roberts, B. A. and J. Proctor (eds) (1992) 'The ecology of areas with serpentinized rocks. A world view'. Geobotany 17. Kluwer Academic Publishers, Dordrecht.

Determination and sampling of fog and cloud water in the Krkonoše Mountains National Park, Czech Republic

J. Kubizňáková

Institute of Landscape Ecology, Academy of Sciences of the Czech Republic, Na sádkách 7, CZ 370 05 České Budějovice, Czech Republic.

Abstract

The imission situation and meteorological conditions in the Krkonoše Mountains National Park were studied during the autumn of 1995. Mean concentrations were about 19 $\mu g/m^3$ for SO_2 (with maximum 194), 80 $\mu g/m^3$ for ozone (with maximum 120), 5.7 $\mu g/m^3$ for nitrogen dioxide (with maximum 63.5) and 32.2 $\mu g/m^3$ for total solid particles-TSP (with maximum 102). Simultaneously, unique measurements of fog and cloud water were made for first time in the Czech Republic at so high an elevation. Three fog collectors were applied and tested. The composition of liquid samples were determined for major anions (chlorides, sulphates and nitrates) and cations (Na, K, Mg, Ca, Al, Fe and Mn). The mean value of liquid water content for the time of the campaign was 0.241 g/m^3, ranging from 0.240 to 0.350 g/m^3, which is typical for low clouds. Variations in wet deposition were observed for the forest ecosystem. Some regional and local sources of air pollution were estimated by synoptic characteristics.

1 Introduction

The impact of acidifying atmospheric pollutants on coniferous forest ecosystems in Europe is very well known. Much of the area at high elevations in Bohemia (about 600 m a. s. l.) is forested by spruce which comprises about 24.3 % of the whole afforested area. In many forested parts visible pollution damage and dying of the coniferous trees has been detected. There has not been a permanent and full automatic monitoring of air pollutants. In the past it has been believed that the Krkonoše Mountains have very low levels of atmospheric pollutants. The local air pollution was underestimated in this western part of the National Park.

Different physical processes produce various forms of water input (rain, snow, dew, fog, drizzle, hail) to the surface hydrological system. Especially in the Czech Republic, passive sampling, analyses and evaluation of horizontal deposition were carried out. Thus a unique international measurement campaign was undertaken in the Krkonoše Mountains. This campaign confirmed the large contribution of horizontal precipitation to bulk wet deposition in some experimental plots. The mountain forests intercept greater amounts of

cloud and fog water than surrounding lowlands (orographical effect). Also increased input of chemicals and water from horizontal flux was observed. Enhanced ozone and sulphate concentration, air pollution and UV radiation were detected.

The total deposition to forest ecosystem was estimated by adding both vertical and horizontal deposition for major ions (total deposition of nitrogen, sulphur, chloride and basic cations). Such estimates are higher than estimates from the imission situation and deposition velocity. Estimated atmospheric inputs were also applied for assessment of risk for coniferous forest in this elevated part of Bohemia. A new approach for the estimation of total deposition and its assessment of risk is described in (Kubizňáková et al., 1991, Kubizňáková, 1999).

2 Experimental methods and determination

2.1 Monitoring areas

All monitoring plots were situated in the western part of the Krkonoše Mountains, not far from one large emission source (about 50 km). Most plots were situated in the first preservation zone in the most protected area of National Park. There were situated on boundary of two trunk rivers (Labe and Jizera). Labská station is the highest monitoring station which is located above the forest line. Some characteristics of the plots are given in Table 1.

Table 1: Characteristics of monitoring plots.

Area	Types of Area	Altitude m a. s. l.	Angle exposit.	Slope 100 v/c	Mean temp. (°C)	Total precip. (mm)	Frost days/yr.	Mean conc. SO_2	Co-ordinate
Labská	Mts. plain	1360	110	15	2.3	1800	>180	8	15° 33'E 50° 46'N
Harrachov	Pass	850	30	5	4.0	1200	160	15	15° 27'E 50° 49'N
Pudlava	Leeward slope basin	1160	160	25	3.8	1000	140	-	15° 34'E 50° 45'N
Mumlava	Summit	1210	220	7.2	3.2	1600	160	-	15° 29'E 50° 45'N
Alžbětinka	Mountain slope	1175	320	14	3.6	1500	>160	-	15° 32'E 50° 45'N

2.2 Monitoring equipment and the imission situation

The imission situation and local meteorology has been automatically and continually measured by means of analysis for SO_2, TSP, NO_x, O_3, CO, methane, hydrocarbons, and micrometeorological parameters. The air temperature at 3 and 10 m above the earth, wind direction and speed, air pressure and humidity and radiation were measured only at Labská station. The sensors and monitors at Horiba have been maintained into a mobile van by the Czech Hydrometeorological Institute, which was the same as in steady

automatic air pollution monitoring. Campaign has been started since 19th September to 10th October in 1995 at about 200 m from Labská cottage. Half-hourly averages were calculated as integrated 30 second interval data. Common joint calibrations of all assembled instruments were done before the start of campaign in Jelenia Gora, Poland.

Table 2: Review of air pollution and air water quality measurements on each plot. Distribution of sampling collectors at various plots. Remark: * At Labská operated mobile imission monitoring van from CHMI. Abbreviation: BD = bulk deposit collector, TH = throughfall collector, PCC = passive cloud water collector CR, PCD = passive cloud water collector BRD, ACC = active cloud water collector, SF = stemflow collector, OB = storage rain gauge , OTH = throughfall gauge.

Monitoring plots	BD	TH	PCC	PCD	ACC	SF	OB	OTH
Alžbětinka	2	3	2	-	-	1	-	-
Labská*	1	-	1	1	1	-	-	-
Mumlavská hora	2	3	2	-	-	1	-	-
Pudlava	2	3	1	-	-	1	1	-
Harrachov	1	-	1	-	-	-	1	1

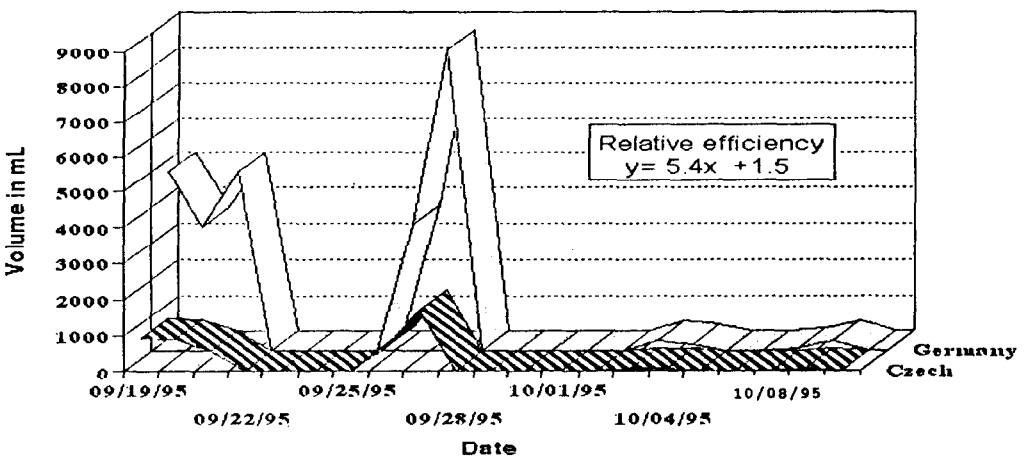

Figure 1: The occurrence, course and volume of precipitation in two passive cloud collectors(Czech - PCR and German - PCG).

2.3 Sampling collectors for atmospheric water

The review of sampling equipment is shown in Table 2. The liquids from sampling collectors (cloud and fog) were taken the same day, but the bulk deposition, throughfall and stemflow were usually collected weekly.

Throughfall is the part of the incident precipitation that reaches the forest floor after having passed through the canopy tree. The part of the incident precipitation caught by branches and trunks and deposited immediately around the base of the tree is called

stemflow. The stemflow collectors were made from silicon rubber paste. They were wound in spiral form around the stem of trees. All water samples have been collected to PET bottles.

The sampling of atmospheric precipitation and throughfall was by means of washed polyethylene funnels (with area 95 cm^2), as described by Kubizňáková et al. (1991).

Cloud- and fog-water passive collectors were constructed (nylon fibre 0.15 mm, 300 m length). Three types of cloud water collectors were placed at Labská station for comparison: one active collector and two passive collectors. The active cloud collector - ACC with PTFE fibre 0.7 mm (from Institute of Hydrodynamics) is described by Tesař (1993). Also one German passive string cloud collector - with PTFE fibre was tested as described in Mohnen and Kadleček (1989).

The temporal variation and the total amount of precipitation were determined by three commercial Polish rain gauges. One rain gauge was also situated under spruce canopy for the time and volume recording. The same procedure and determination with all liquid samples was provided. Also further six passive home-made collectors (PCR) were situated in surrounding forests plots.

Intercomparison of collecting efficiencies is shown in Fig. 1. The entrapped amount of water depends on stand condition, the micrometeorological situation, and also on the construction of the collector.

Some problem exists with the quantification of horizontal deposition in some gauges. Nevertheless such wet form of deposition creates dominant contribution to hydrological cycle in this mountain area (at elevation about 1100 m a. s. l.). There are only relative and comparative data between similar plots. During the whole campaign the humidity was very high. Liquid water content measurements were carried out by a German group. They used continuous measurement with a laser forward scattering technique using a Gerber Particulate Volume Monitor for droplet diameters 3–45 mm.

Table 3: Equipment and analytical methods for chemical determinations of air water samples.

Component	Method	Equipment
pH	Potenciometry, pH meter	Radelkis OP-265/1
H^+	Calculated from pH	
Conductivity	Conductometry	Radelkis OK 102/1
Acidity	Automatic burette	Radelkis OP-930/1
Anions	Isotachophoresis (ITP)	URJV ZKI-01
Cations	ICP spectrometer	Unicam PU-7450
LWC	Laser scattering technique	Gerber Monitor PVM-100

2.4 Chemical determination

After sampling of the atmospheric water, volume, pH and conductivity were measured by pH/conductometer. The samples were stored at 4°C for further chemical analyses. Major anions (chlorides, sulphates and nitrates) and cations (Na, K, Mg, Ca, Al, Fe and Mn) were analysed in the Laboratory of Environmental Chemistry, Institute of Landscape Ecology (ASCR), České Budějovice. The survey of applied analytical instruments is given in Table 3. International calibration and quality assurance/quality control (QA/QC) was carried out for each analytical method.

2.5 Trajectory analysis

To investigate the incidence of long range transported air pollutants, isobaric backward air trajectory analysis was carried out by Department of Meteorology and Environment Protection, Charles University, Prague using Grid Point Value (GPV) on wind data in the 850 hPa pressure level. The time interpolation of wind velocity was performed by linear interpolation of previous and observed wind data.

3 Results and discussion

3.1 Meteorological situation

Average campaign air temperature was about 5.0°C (3 m) and 4.7°C (10 m), and solar radiation was about 64.2 W/m^2. The mean value of liquid water content during the campaign was 0.241 g/m^3 ranging from 0.240 to 0.350 g/m^3 which is characteristic of low clouds. Wind velocity from 1.1 up to 5.5 m/s and wind direction - NW quadrant (180°–270°) has dominated.

The monitoring campaign was divided into three periods, according to the meteorological conditions and gaseous and liquid composition of atmospheric situation.

3.2 Air quality data

The data of air pollutants are the main subject of reference Kubizňák and Kubizňáková (1996, 1997). There is presented only average values. Maximum of acidic pollutants from long distance sources appeared mainly during the period from 1st to 8th October. Average whole campaign concentration of sulphur dioxide was about 19 $\mu g/m^3$ (maximum 194), of ozone about 80 $\mu g/m^3$ (maximum 120), of nitrogen dioxide 5.7 $\mu g/m^3$ (maximum 63.5), of methane 1272 $\mu g/m^3$ (maximum 1621), carbon monoxide 661 $\mu g/m^3$ (maximum about 4850). The total solid particles (TSP) were estimated to be about 32.2 $\mu g/m^3$ (maximum 102). During a day were found a few short episodes. The relationship between wind direction and gaseous pollutants concentration showed prevailing NW and SE sources of pollution from the Turow power plant (Kubizňák and Kubizňáková, 1997, Kubizňáková, 1998). The mean concentration of TSP is roughly constant for all wind directions. Episodic concentration of gaseous NO_2 has recorded as very low, and belong to probably mainly local gas heating source at Labská station. So far estimated concentrations of SO_2 were inserted about 10 $\mu g/m^3$ at Labská and Harrachov plots too, but our results have shown concentration about two times higher.

3.3 Cloud and fog water composition

During the monitoring campaign have been only a few opportunities for own cloud chemistry measurement. During campaign time was cloudless for about 60 % at Labská station. Nevertheless the liquid water content reached the value 25 mg/m^3 or longer than 15 minutes to get a sufficient amount of cloud water for the analytical determinations. In Table 4 are presented average recalculated concentrations of ionic species in liquid phase for cloud- and fog-water during campaign periods.

First period from September 21st to 27th proceeded prolonged precipitation. The last period of campaign was very sunny with prevailed dry deposition, but the highest air pollution. In all localities and every period, the sulphate and nitrate concentrations were higher in cloud than in fog water samples. The Cl/Na ratio for liquid samples was about 0.8. Chloride is probably enriched with sub-cloud scavenging by sea-salt sodium chloride uniformly distributed over the boundary layer. The excess chloride results from

Table 4: Average chemical composition of cloud- and fog-water during campaign. a - chloride, b - nitrate, c - sulphate.

Site	Al	Ca	Fe	K	Mg	Na	Mn	H^+	pH	a	b	c
I. Period: Campaign determination from 19th to 23rd September in μeq/l												
Pudlava	0.72	7.32	0.11	1.92	1.57	3.32	0.00	39.81	4.40	1.7	13.9	25.6
Alžbětinka	0.37	2.30	0.113	0.15	0.59	0.52	0.01	211.35	3.68	0.6	9.8	5.8
Mumlavská h.	0.96	7.64	0.26	0.42	3.65	0.72	0.01	218.78	3.66	1.3	37.1	14.5
Labská	2.20	24.30	1.01	2.66	3.86	4.53	0.02	-	-	6.3	58.0	75.5
II. Period: Campaign determination from 24th September to 1st October in μeq/l												
Harrachov	0.91	10.02	0.19	0.55	1.74	6.16	0.04	5.25	5.28	3.4	14.6	18.1
Pudlava	2.39	9.60	0.19	2.81	4.69	15.50	0.10	169.82	3.77	4.9	32.8	21.3
Alžbětinka	2.02	10.83	0.35	0.57	3.47	2.82	0.03	245.47	3.61	5.5	54.4	21.4
Mumlavská h.	9.52	22.73	1.91	5.48	27.62	131.4	0.04	158.49	3.80	58.0	309.6	133.3
Labská	5.71	25.92	2.15	3.58	9.67	14.47	0.18	-	-	14.4	144.1	83.8
III. Period: Campaign determination from 2nd October to 8th October in μeq/l												
Harrachov	0.02	0.43	0.02	0.07	0.9	0.45	0.00	38.02	4.42	7.8	6.6	6.3
Alžbětinka	0.77	3.19	0.13	0.51	3.72	12.37	0.03	192.75	3.72	9.4	13.4	9.7
Mumlavská h.	6.54	20.75	1.55	1.05	10.75	21.61	0.19	457.09	3.34	22.0	182.2	83.1
Labská	0.50	5.05	0.14	0.92	3.42	11.82	0.04	-	-	3.6	41.6	22.6

the inflow of cold/warm maritime air mass at the mountain area. The ratio of nitrate and sulphate indicates that acids have relative contribution to wet deposition. We conclude that nitric acid predominated in cloud and fog in this mountain area. The salts of aluminium, iron and manganese as well as pH-value of solution could be considered as main factor catalytic oxidation and affecting the formation of sulphates in aqueous solution. The range of pH was associated with the cloud of a frontal type. Frequency distribution of fog and cloud pH-values is presented in Fig. 2. The subinversion of fog presented pH = 3.8–3.9 and cloud with low water content had values of pH from 3.1 to 3.3. Higher values of pH (pH> 4.5) show on wet only deposition. In cloud water at Mumlavská hora plot, the maximum concentration of sulphates achieved 483.3 meq/l and concentration of nitrates 239.6 meq/l.

The passive German collectors had approximately 5.5 times higher efficiency in collected volume than our passive collector (see equation in Fig. 1) and 1.5 times higher than one active collector. Chemical compositions of waters were very unpredictable, the highest concentrations of ions have had samples from active collectors.

3.4 Wet deposition

Precipitation volumes were characterised by three rain gauges. Bulk, throughfall and stemflow were determined, but they are not the subject of this communication. Details are also in (Kubizňák and Kubizňáková, 1996). Frequency distribution of pH-values is shown in Fig. 3. In plot Alžbětinka during the second period, there were found the highest concentrations of sulphates (239.3 mg/l) and also the lowest pH-values (about pH=2.6). This forested area is very damaged and has started dying.

In altitudes above the forest line, the volume-weighted mean pH of all liquid samples it seems to be increase in consequence:

$$\text{Stemflow} \cong \text{Cloud} < \text{Throughfall} < \text{Bulk} << \text{Snow}$$

Values of pH and concentrations of sulphates in throughfall and stemflow samples show on predominant dry deposition. The amount of major ionic species in cloud-fog, bulk and throughfall and stem flow shown essential differences in relationship to volume and concentration. In all localities and periods, the sulphates and nitrates concentrations were the highest in the cloud and fog water samples (FP) than in throughfall and bulk. Some differences between cloud and stemflow in chemical compositions were found relatively low.

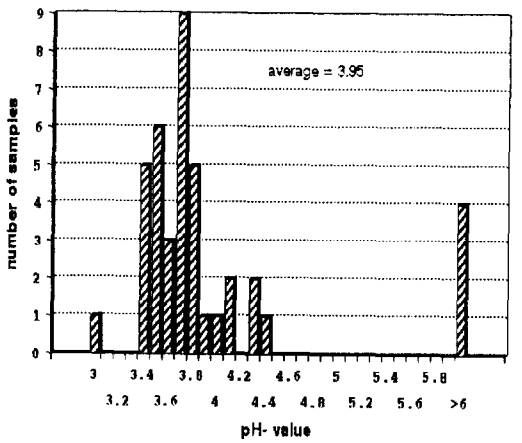

Figure 2: Frequency distribution of pH-values in various campaign samples. Fog and cloud water.

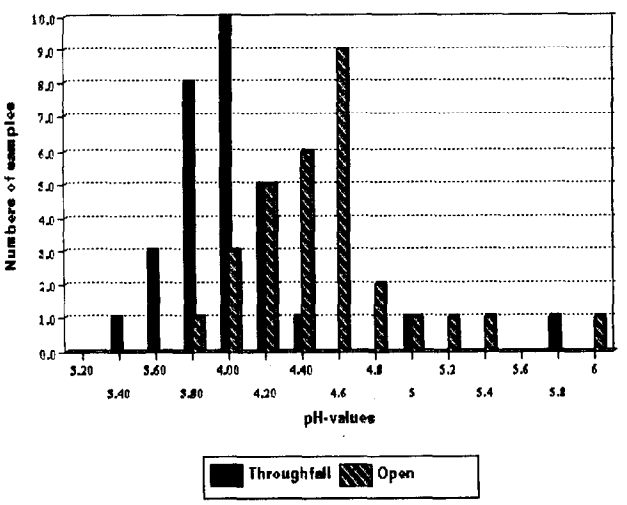

Figure 3: Frequency distribution of pH-values in various campaign samples. Bulk and throughfall water.

Low temperatures caused freezing of water in all equipment. The records of peaks from 1st October to 2nd October are mainly from melted snow. In the last period of the campaign, the composition of snow corresponded to lower concentration of ions and increased pH values. The highest air pollution was recorded in the last week.

4 Conclusion

Temporal and spatial variation in the amount and composition of both horizontal and vertical deposition were studied. Horizontal wet deposition to mature forest prevàils to vertical wet deposition and creates dominant contribution at high elevations in the Krkonoše Mountains. The evidence has been determination of higher volume in throughfall than in open deposition.

Complex and intensive monitoring measurements of air characteristics were undertaken. Nevertheless whole monitoring time, the weather was not only quite ideal stable for very intensive cloud chemistry measurements. The most continual campaign measurements were interrupted by frost and the last week was very sunny with very small occurrence of fogs. Therefore active and passive collectors were tried with different efficiency and intercepting material. It seems, that our cheaper passive collector should be very convenient for sampling of cloud and fog water in remote area of a forest. Also Laboratory of Environmental Chemistry in ILE has had responsible result in international calibration of quality assurance/quality control (QA/QC) carried out for all applied analytical methods.

Some results were used to quantify the estimation of risk assessment from total and potential wet and dry deposition to forest ecosystem and calculation of critical loads in National Park (Kubizňáková et al., 1997), where there is still visible damage of spruce forest.

Spatial variations have shown also a contribution from local emission source e.g. Labska chalet to total surrounding contamination. The pollution decreased from west to east, from higher elevation to lower. There are many orographic effects as land cover, elevation, slope, exposure, that will need more longer or permanent observation.

Acknowledgement

The campaign was included into co-operation programme COPERNICUS within the international joint research project EASE (Emission Abatement Strategy and Environment (CIPA-CT93-0071 DG-12 HSMU). The EASE project has received a major part of its funding from EC. Thanks of the Czech Ministry of Environment has also contributed financial support for air pollution campaign measurement. Several regional authorities and academic institutes had also made considerable contribution for easier course of that campaign. The own intensive monitoring of air pollution and meteorological situation has been also ensured by thank and co-operation of Czech Hydrometeorological Institute (CHMI).

References

[1] Kubizňáková J., Buřičová V., Huderová L., Kubizňák J., Musil J. (1991) Bulk Atmospheric imput into various sites of forest ecosystems Mts. Šumava. A preliminary Report. Proc. of Symp. "Research and Decline in Eastern Central Europe and Bavaria". Passau, Germany, July 1991, 472–477.

[2] Kubizňák J., Kubizňáková J. (1996) Atmospheric impact to permanent forest plots and air situation in western part of Krkonoše Mts., Institute of Landscape Ecology, Acad. Sci. Czech Rep., České Budejovice, 56 p.
[3] Kubizňák J., Kubizňáková J. (1997) Stav ovzduší v KRNAPu během mezinárodní měřící kampaně (In Czech). Proc. of Conf. "Ovzduší 97", Luhačovice, Czech Rep., 51–54.
[4] Kubizňáková J., Novotná M., Kubizňák J. (1997) Rizika z kyselých depozic aneb škodlivé účinky kyselých dešťů (In Czech). In: Hodnocení rizik pro životní prostředí. ERA '97, 144–149.
[5] Kubizňáková J. (1998) Kvalita ovzduší na Labské v roce 1995 (In Czech). Proc. of Conf. "Geoekologiczne problemy Karkonoszy", KPN and UNESCO-MAB, Tom 1, Poznaň, Poland, Acarus, 109–116.
[6] Kubizňáková J. (1999) Assessment of Atmospheric Pollution on Spruce Canopy. In: Biomarkers: A Pragmatic Basis for Remediation of Severe Pollution in Eastern Europe. D. B. Peakall, C. H. Walker, P. Migula (Eds.), NATO Science Series, Vol. 54, Kluwer Publishers, London, 272–277 and 311.
[7] Reports of EASE Project 1994, 1995, 1996, 1997, London ICMT 1994–97.
[8] Tesař M. (1993) Cloud and fog water deposition in the Šumava Mts. (Czech Republic). A model astimate of water flux and deposition of chemical compounds to mountainous spruce stand. Acta Universitatis Carolinae, Geologia, 37, 57–72.

Water residence time in the Strengbach catchment (Vosges massif, France)

B. Ladouche[1*], D. Viville[2], T. Bariac[1]

[1]Laboratoire de Biogéochimie Isotopique, (LBI-CNRS/INRA/UPMC), Case 120, 4 place Jussieu, 75252 Paris, France (*Present address: BRGM, Direction de la Recherche, 1039 rue de Pinville, 34000 Montpellier, France). [2]Centre d'Etudes et de Recherches Eco-Géographiques, (CEREG-ULP/CNRS), 3 rue de l'Argonne, 67083 Strasbourg Cedex, France.

1 Introduction

Environmental isotopes are commonly used in the field of investigations and research projects to provide an improved qualitative understanding of the hydrological systems and processes that are involved in the water transfer. The use of isotope data for quantitative interpretation requires a conceptual model. By studying the relation between input and output time series of tracer concentrations conclusions can be obtained from parameters of the model that describes the transformation of the input to the output signal. For example, with used of lumped parameter models, in which the investigated system is treated as a whole, the relation between input and output time series of tracer concentrations is described by a convolution integral which allows estimation of the water residence time of the investigated system (Maloszewski and Zuber, 1982, Zuber, 1986). The use of environmental isotopic tracers to estimate water residence time in hydrological systems has been applied to several cases (Herrmann et al., 1990; Stewart and McDonnell, 1991; Maloszewski et al., 1995; Rodhe et al., 1996; Amin and Campana, 1996).

Supposing that the assumptions are valid (i.e. linear system, both time invariant flow and transit time distribution), the main difficulty of the lumped parameter approach consists to determine an appropriate input function. Indeed, the input concentration needed for model calculations is that of the infiltrating water which contributes to the recharge of the aquifer. This concentration is not equal to the one measured in the precipitation. Output concentrations calculated by the models depend strongly on the assumption related to the infiltration coefficient. So, a proper estimation of the input function is very important for quantitative interpretation.

The input function can be determined independently of infiltration coefficients α_i in rare cases (Stichler et al., 1986) but, generally, only two infiltration coefficients (summer and winter periods) are considered as input functions. Some authors often consider that recharge of the aquifer in summertime is reduced and α_i coefficients values are 0 (Davis et al., 1967) or 0.05 (Maloszewski and Zuber, 1982). But α_i can also be expressed as runoff

coefficient between runoff and precipitation for the considered periods (Maloszewski et al., 1992).

The objective of this study is to determine water residence time on the Strengbach catchment (Vosges massif, France) for the 1989–1995 observation period. The Flowpc model (Maloszewski and Zuber, 1994) has been used and infiltrating water which contributes to the recharge of the aquifer has been estimated by a deterministic approach based on a simplified hydrological balance.

2 Description of the used approach

In order to calculate the residence time of the water, the hydrological system of the Strengbach catchment can be described by two reservoirs (Fig. 1): the upper unsaturated reservoir (R_1 = soil reservoir) with a shorter residence time (i.e. week to month) feeding the lower groundwater reservoir R_2. In this schema, we assume that the monthly runoff at the outlet is both due to a portion of the input precipitation γP and by the flow ϕ which can be considered as the baseflow.

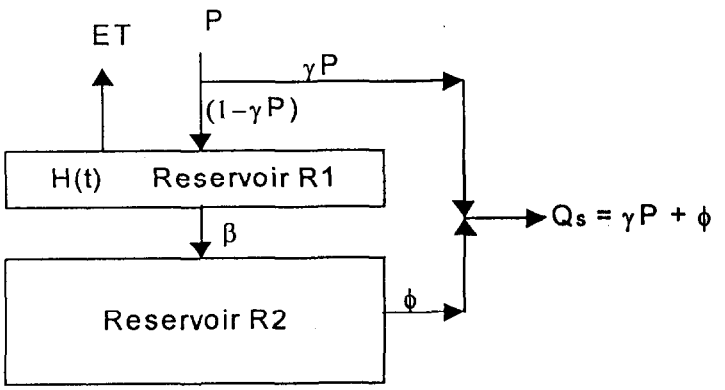

Figure 1: Conceptual representation of Strengbach catchment.

A deterministic approach based on a simplified hydrological balance (Humbert 1982) was used to describe the behaviour of reservoir R_1. The water stored in this reservoir $H(t)$ depends on atmospheric inputs $(1-\gamma)P$ and on losses by evaporation ET and deep seepage β. This model requires only two input variables: the monthly mean corrected (by γ coefficient) precipitation and the monthly potential evaporation PET.

A simple mixing model was applied to calculate the isotopic signature of the input function associated to the flux β. Calculations performed with the δ_P input assume that there is a complete mixing with the water stored in the reservoir $H(t-1)$:

$$\delta_\beta(t) = \delta_{R_1}(t) = \frac{H(t-1)\,\delta R_1(t-1) - (1-\gamma)\,P(t)\,\delta_P}{H(t-1) + (1-\gamma)\,P(t)} \qquad (1)$$

where $\delta R_1(t-1)$ is the $\delta^{18}O$ value of the water in unsaturated reservoir R_1 at the time $t-1$; $(1-\gamma)P(t)$ and $\delta P(t)$ are the rainfall amount and the corresponding $\delta^{18}O$ value of the water which infiltrates in the reservoir R_1 at the time t.

Lumped parameter models are used to calculate the tracer concentrations in spring and streamwater (output signal) based on concentrations calculated at the exit of the reservoir R_1 (input function). For a steady state flow through the aquifer (reservoir R_2)

and a non-radioactive isotopic tracer, the input-output relation can be described by the convolution integral (Maloszewski and Zuber, 1982):

$$C_{\text{out}}(t) = \int_0^{\infty} C_{\text{in}}(t-\tau)\, g(\tau)\, d\tau \tag{2}$$

where $C_{\text{in}}(t)$ and $C_{\text{out}}(t)$ are the tracer input and output functions, τ is the turnover time and $g(t)$ is the transfer function. In this formulation, the transfer function (i.e. weighting function) describes the distribution of the transit time of the water in the system.

Calculations were performed with the commonly used weighting functions derived from exponential and dispersive models. Flow parameters - τ (turnover time) for exponential model and τ and $D/\nu x$ (dispersion parameter) for dispersive model - were obtained by fitting calculated to measured output concentrations.

3 Field and data description

3.1 Site

The Strengbach forested catchment is located on the eastern side of the Vosges massif (north-eastern France). This small catchment (0.8 km^2) ranges in altitude from 883 m to 1146 m a. s. l. and mainly lies on a base-poor granitic bedrock. Soils are acidic and coarse-textured. This catchment is forested mainly with Norway spruce (65 % of the area) and mixed beech and silver fir take up the rest. The climate is temperate oceanic-mountainous; mean annual precipitation is 1400 mm evenly spread throughout the year and mean annual runoff is of 850 mm with high flow in the cold season and low water at the end of summer. An automatic weather station located at an elevation of 1100 m a. s. l. at the catchment provided the necessary data for evaporation determination.

3.2 Sample collection

During the 1989–1995 observation period intensive water ^{18}O sampling was performed at various time intervals in the Strengbach catchment: (1) streamwater at the outlet was collected at 1 week intervals; (2) groundwater sampling was collected from a spring at 1 week intervals during the 1992–1995 period; (3) precipitation was sampled at various intervals with a rainfall gauge located at the outlet. The time series of $\delta^{18}O$ content in precipitation had be completed by using data collected at Karlsruhe (IAEA/WMO) from 1986 to 1989. Oxygen-18 analysis was carried out by the standard CO_2 equilibration method (Eipstein and Mayeda, 1953) and expressed as d-deviation in per mil with an accuracy of 0.1 ‰ (2σ).

The monthly outflow β and the corresponding $\delta^{18}O$ value δ_β were calculated for the October 1986–September 1995 period. Reservoir R_1 value has been estimated to be a maximum of 100 mm for a soil of a 900 mm thickness (Biron, 1994) and R_1 reservoir has been considered as empty for initial condition in September 1986.

4 Results

The annual fluctuation of the $\delta^{18}O$ content in precipitation is 10 ‰ (-5 to -15 ‰) while signals vary only of 0.5 to 1 ‰ (-9 to -10 ‰) in spring and streamwater (Fig. 2). The amplitude of the isotopic signature in precipitation appears considerably attenuated in the signature of the aquifer. The original fluctuation range has been considerably reduced by about 95 %. This result suggests that the rainfall amounts, which recharge the aquifer, are

not important compared to the storage water in the groundwater system. This qualitative interpretation suggests that the mean water residence time in the catchment is at least of the order of one year.

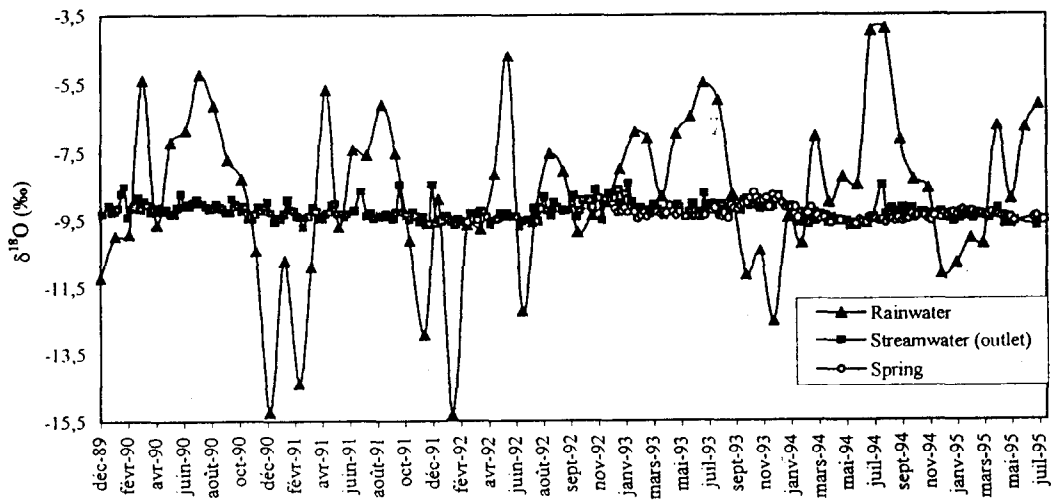

Figure 2: Comparison of the $\delta^{18}O$ values in precipitation and the observed output $\delta^{18}O$ values in the aquifer (spring) and in the streamwater (outlet).

Spring and stream isotopic signals do not differ that much; this means that stream is mainly composed by groundwater. Slight differences are due to flood periods when rain contribution is greater than usually.

Mean spring isotopic δ_{gw} ^{18}O content was -9.3 ‰ (mean value for January 1992–July 1995 period, n =167 samples, 2σ = 0.2 ‰). For October 1986-September 1995, the weighted mean of oxygen-18 content in precipitation was of - 8.5 ‰. The mean $\delta^{18}O$ value of the groundwater is depleted compared to the weighted mean of the precipitation. This result means that the winter precipitation contributes to the aquifer recharge more than the summer precipitation. The contribution of the summer precipitation to the aquifer recharge has been estimated with (Grabczack et al., 1984) :

$$\alpha = \frac{\alpha_{\text{summer}}}{\alpha_{\text{winter}}} = \frac{\sum_{\text{winter}} \delta_i P_i - \delta_{gw} \sum_{\text{winter}} P_i}{\delta_{qw} \sum_{\text{winter}} P_i - \sum_{\text{winter}} \delta_i P_i} \tag{3}$$

where α_{summer}, α_{winter}, are the infiltration coefficients, δ_{gw} is the mean $\delta^{18}O$ value of the groundwater and P_i and δ_i the monthly amount and concentration in precipitation, respectively.. For the observation period, the infiltration coefficient α is of 0.26 .The winter precipitation contributes about four times more to the aquifer recharge than summer precipitation.

Exponential and dispersive models have been applied to spring samples. Flow model calculations were performed with γ = 0.1 meaning, in the adopted conceptual model to describe the catchment, that monthly runoff at the outlet is composed of 10 % of rain fallen during the month. This hypothesis is realistic because intensive isotopic investigations in May 1994 and July 1995 have shown the dominant (= 90 %) role of old water in storm and snowmelt runoff generation (Ladouche, 1997).

The best fit between observed and calculated output tracer concentrations was obtained for mean residence time $\tau = 41 - 43$ months for the exponential model and $\tau = 30 - 32$ months and $D/\nu x = 0.55$ for the dispersive model (Fig. 3).

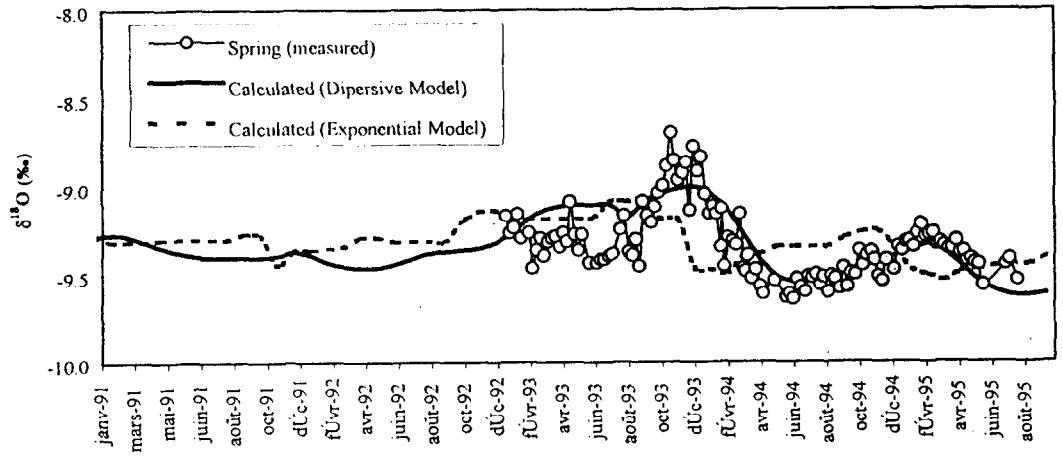

Figure 3: Measured (circle) and fitted ^{18}O concentrations for spring water calculated with the use of dispersive model (solid line; $\tau = 31$ months, $D/\nu x = 0.55$) and exponential model (dashed line; $\tau = 42$ months).

Concentration simulation with the dispersive model is very satisfying for 1994 and 1995 compared to the observed values, but is slightly different (less than 0.3 ‰.) for the previous period. Simulation of the concentrations with the exponential model is less satisfying than with the dispersive version.

Exponential and dispersive models have been also applied to stream samples and the best fit obtained between observed and calculated output tracer concentrations was obtained for $\tau = 44 - 46$ months for the exponential model and $\tau = 31 - 32$ months and $D/\nu x = 0.8 - 0.9$ for the dispersive model. These values are very close to those obtained in springs.

Determination of mean residence time allows estimation of the water volume stored in the aquifer of the Strengbach catchment. For a mean 20.4 $l.s^{-1}$ discharge and for residence times varying between 31 and 42 months, the equivalent of the volume expressed in water depth varies between 1850 and 2500 mm. In any cases, a great thickness of fractured bedrock may be involved to store such amount of water in the aquifer.

5 Conclusions

Environmental isotopes (^{18}O) have been used to calculate water residence time in the Strengbach catchment on the period 1989–1995 on a monthly base with FLOWPC model. The simulation results obtained with the dispersive version of the model indicate a residence time of 31 months.

References

[1] Amin, I. E., Campana, M. E.: A general lumped parameter model for the interpretation of tracer data and transit time calculation in hydrologic systems. J. of Hydrol., 179, 1996, 1–21.

[2] Biron, P.: Le cycle de l'eau en forêt de moyenne montagne: flux de sève et bilans hydriques stationnels (basssin versant du Strengbach à Aubure, Hautes-Vosges). Thèse de doctorat Univ. Louis Pasteur, Strasbourg, 1994, 244 p.

[3] Davis, G., Dincer, T., Florkowski, T., Payne, B., Gattinger, T.: Seasonal variations in the tritium content of groundwater of the Vienna basin. Isotopic Hydrology, IAEA, (eds), Vienna, 1967, 451–473.

[4] Eipstein, S., Mayeda, T.: Variation of ^{18}O content of waters from natural sources. Geochimica et Cosmochimica Acta, 4, 1953, 231- 224.

[5] Grabczack, J., Maloszewski, P., Rozanski, K. and Zuber A. : Estimation of the input function with the aid of stable isotopes. Catena, 11, 1984, 105–114.

[6] Herrmann, A., Finke, B., Schoëninger, M., Maloszewski, P. and Stichler, W. : The environmental tracer approach as a tool for hydrological evaluation and regionalization of catchment systems. In Regionalization in Hydrology, Proceeding of the Ljubljana Symposium, IAHS Publ. N 191, 1990, 45–58.

[7] Humbert, J.: Cinq années de bilans hydrologiques mensuels sur un petit bassin versant des hautes Vosges (1976–1980): le bassin versant du Ringelbach. Recherches Géographiques à Strasbourg, 19-21, 1982, 105–122.

[8] Ladouche, B.: Etude des flux hydriques par le traçage isotopique naturel à l'échelle d'un bassin forestier (Strengbach, Vosges). Thèse Univ. Paris VI, 1997, 194 p.

[9] Maloszewski, P., Zuber, A.: Determining the turnover time of groundwater systems with the aid of environmental tracers. 1- Models and their applicability. J. of Hydrol., 57, 1982, 207–231.

[10] Maloszewski, P., Rauert, W., Trimborn, P., Herrmann, A., Rau, R.: Isotope hydrological study of mean transit time in an alpine basin (Wimbachtal, Germany). J. of Hydrol., 140, 1992, 343–360.

[11] Maloszewski, P. and Zuber, A.: Lumped parameter models for the interpretation of environmental tracer data. User's guide of Flowpc program, GSF Inst. Für Hydrol. Oberschleissheim, Germany, 1994, 52 p +25 p fig.

[12] Maloszewski, P., Moser, H., Stichler, W. and Trimborn, P. : Isotope hydrology investigations in large refuse lysimeters. J. of Hydrol., 167, 1995, 149–166.

[13] Rodhe A., Nyber, L. and Bishop, K. : Transit time for water in a small till catchment from a step shift in a oxygen 18 content of the water input. Water Resour. Res., 32(12), 1996, 3497–3511.

[14] Stewart M. J. and McDonnell J. J.: Modeling baseflow soil water residence times from deuterium concentration. Water Resour. Res., 27, 1991, 2691–2693.

[15] Stichler, W., Maloszewski, P. Moser , H.: Modeling of river water infiltration using oxygen-18 data. J. of Hydrol., 83, 1986, 355–365.

[16] Zuber, A.: Mathematical models for the interpretation of environmental radioisotopes in groundwater systems. In P. F. J.-C. Fontes. Handbook of environmental isotope geochemistry, Vol. 2, Elsevier, Amsterdam, 1986, 1–59.

Macro- and mesoscale hydrological modelling in the Elbe river basin

W. Lahmer

Potsdam Institute for Climate Impact Research, Telegrafenberg, D 14412
Potsdam, Germany.

Abstract

A GIS-based modelling approach is used for hydrological simulation calculations in the German part of the Elbe river basin (96,428 km^2, macroscale) and in the Stepenitz subbasin (575 km^2, mesoscale). The approach includes variable spatial aggregation and disaggregation methods necessary to study the regional impacts of climate and land use changes on the hydrological cycle. The adequate interpolation of climatic input variables turns out to play a key role in large scale hydrological modelling. The results obtained for various water balance components and for two land use change scenarios demonstrate that the developed concept can be applied to river basins of different size and characteristics and is especially suited for regional impact studies.

Key words: Hydrological modelling at different scales, GIS- coupling, spatial aggregation and disaggregation methods, water balance calculations, land use and climate change

1 Introduction

Global change phenomena and processes take place and have to be investigated at all spatial scales, from local to global. Stronger emphasis on regional and local scales is needed at the land surface where the most important sources and drivers of global change are located, as for instance areas with changing land use/land cover, industrial complexes, cities, traffic with emissions of trace gases, different types of waste, etc. It is primarily at these scales that political and technical measures and action can and must be taken to avoid critical developments and to reduce negative or undesired effects. The regional scale is crucial for an improved understanding not only of the different causes of global change and the contributing processes, but also of its impacts on the environment and society.

River basins are preferred land surface units for regional scale studies because they represent natural spatial integrators/accumulators of water and associated material transports at the land surface. For the present hydrological study, the German part of the Elbe river basin covering an area of nearly 100,000 km^2 was chosen (see Fig. 1). It is the driest of the five largest German river basins, so that water stress and water deficiencies occur earlier and more frequently in the case of droughts than in other parts of Germany.

The approach used in the present study applies methods of a GIS-based modelling concept, which were developed at the mesoscale, to a macroscale river basin. It is based

on variable spatial disaggregation and aggregation techniques, which allow an effective simulation of the regional hydrological cycle. It consequently uses the GIS-based derivation of model parameters from generally available spatial data. The application in the Elbe river basin and in some of its sub-basins demonstrate that the disaggregation of a study region into subareas of similar hydrological behaviour represents an effective modelling concept. The simulation calculations performed in these basins of various size and characteristics show that the developed concept can be generally applied.

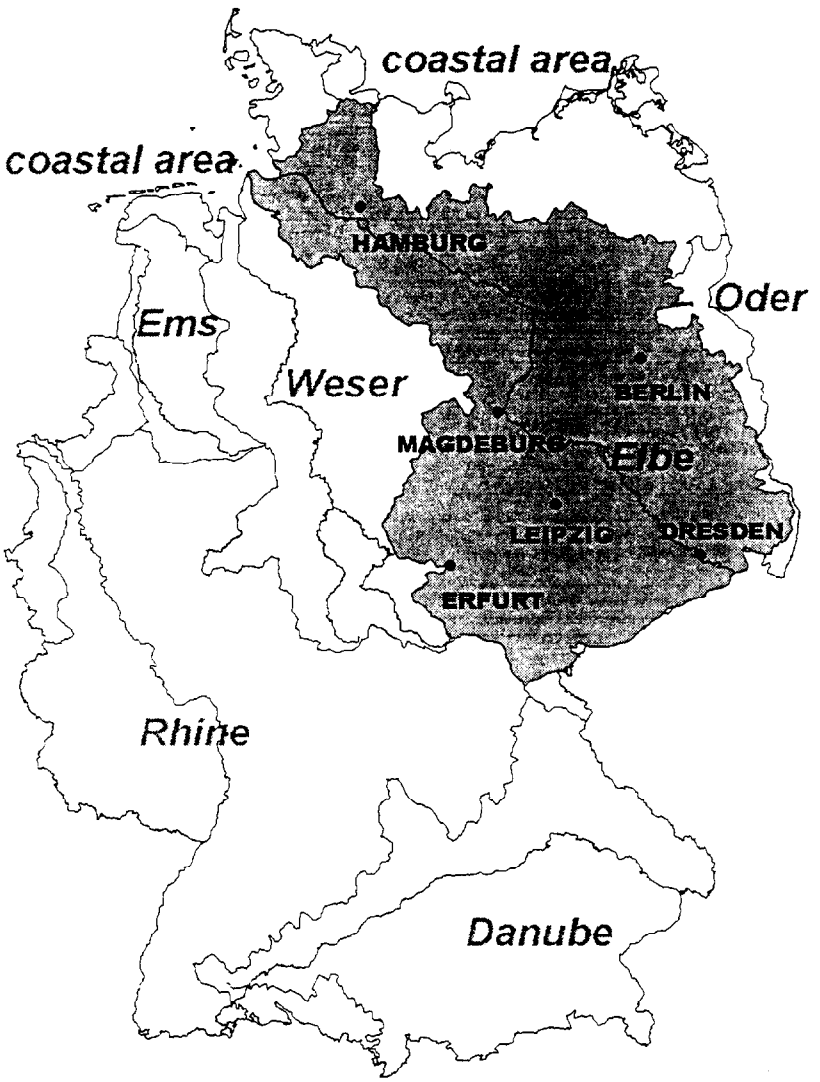

Figure 1: The German part of the Elbe river basin, covering an area of nearly 100,000 km^2.

The results presented in the following cover spatially distributed values of various water balance components for the whole Elbe basin (Lahmer 1997) and some more detailed analyses for the Stepenitz river basin, a tributary basin of 575 km^2 about 200 km north of Magdeburg (see Fig. 1). These analyses also include some first results in modelling land use changes.

2 Methodology

The concept of fully distributed physically based models has been questioned in recent years, because their application is constrained by the availability of required input data and their use in prediction at the regional level is often of limited value (e.g., Gleick 1986, Beven 1993). Therefore, simplified (conceptional) models with physically meaningful parameters are needed which can be applied at different scales. Such models must be able to use directly the information provided by various digital maps and to handle different temporal and spatial discretization levels. In addition, they must enable simulations based on spatial units of various size and heterogeneity.

The modelling concept applied in the Elbe river basin is based on results obtained in the Upper Stör basin, a mesoscale river basin of about 1,100 km^2 in the northern part of Germany (north-east of Hamburg, see Fig. 1), where some essential problems of large- and mesoscale hydrological modelling were successfully addressed (Lahmer et al. 1997, Becker and Lahmer 1997). The spatially distributed and temporal dynamic modelling performed with the modelling system ARC/EGMO (Pfützner et al. 1997) resulted in the following general conclusions:

- It is appropriate to distinguish two domains of hydrological processes, that of vertical and that of lateral fluxes, because then different disaggregation, aggregation, and scaling techniques can be applied in both domains to simplify modelling, if required.
- Mixed landscapes should be subdivided (disaggregated) into units of unique hydrological regime (hydrotopes or Hydrological Response Units HRU), which significantly differ in their hydrological process characteristics, in particular in vertical processes modelling, for two reasons: (i) in contrast to aggregated (lumped) modelling, important areal process differentiations can be described appropriately; and (ii) the physical soundness of the applied models is better preserved and model parameters can be more directly derived from real land surface characteristics.
- Polygons of different form and size are best suited to represent the mosaic structure of real landscapes. In regions with similar climate such spatially distributed polygons can be combined (aggregated) into larger modelling units (e.g. hydrotope classes) to simplify large scale modelling and to reduce computing time (fractional area concept). The 'intra patch' areal variability of parameters can be represented adequately by areal distribution functions.
- In lateral flows modelling, simple approaches like single storage reservoirs or simplified diffusion type models have turned out to be most efficient. They can be applied to large river basins and sub-basins.

2.1 Spatial disaggregation to elementary units

One basic problem in meso- and macroscale hydrological modelling is the disaggregation of the landscape into areas characterized by a significantly different hydrological process behaviour. With respect to the vertical processes, differences in land use, vegetation type, soil characteristics, groundwater depth and topography are most important. The degree in spatial disaggregation depends on the resolution of the available data and must be determined for each study region, in order to take into account properly the discontinuities of the landsurface. The principles of spatial disaggregation applied in the Elbe river basin follow the special needs of large scale modelling (Lahmer and Becker 1998) and will be outlined in the following.

The basis of all simulation calculations performed with ARC/EGMO is the so called 'elementary unit map', generated by a Geographic Information System (GIS) from all

necessary digital information (land use, vegetation cover, soil characteristics, topography, ground water level, river net, sub-basins etc.) in the pre-processing stage. This map consists of 'elementary units' (EUs), which represent the smallest modelling units of the modelling approach and can be considered homogeneous with respect to their hydrological behaviour. In general, the resolution of the EU map is directly determined by the resolution of the used basic maps.

Since for macroscale applications the number of EUs may be rather high, some maps should be spatially aggregated already in the pre-processing stage. In the case of the whole German part of the Elbe river basin, the CORINE land use map was the basic map for data preparation, due to its high resolution and hydrological importance. The available 28 land use classes were pre-classified into the 6 classes given in Table 1, taking into account the hydrological and ecological sensitivities of the underlying sub-classes. The aggregated land use class 'urban areas', for example, now includes the original 7 sub-classes 'closed urban areas', 'open urban areas', 'industrial areas', 'street and railway systems', 'ports', 'airports', and 'recreational areas'. The dominant land use class in the Elbe basin is 'arable land' (fractional area of 53.37 %) followed by 'forests' (27.48 %) and 'meadows' (9.47 %). All important characteristics of the aggregated land-use classes (like degree of sealing, root depth, interception capacity, and degree of covering) are provided by relational tables coupled to the digital map and can be directly used in the GIS-based simulation calculations.

Table 1: Pre-classified land use classes for the German part of the Elbe river basin, including the original classification of the used CORINE land use map, the number of elementary units defining the aggregated classes and their fractional areas.

CORINE	aggregated land use classes			
classification	nr.	name	nr. of EUs	fractional area (%)
1,2,3,4,5,6,11	1	urban areas	9212	6.69
10,18,26,35	2	meadows	8739	9.47
12,19,20,21,27	3	arable land	23429	53.37
16,23,24,25,29	4	forests	17487	27.48
40,41	5	open water bodies	4278	1.43
7,8,9,30,32	6	pasture	892	0.96

Combining the pre-classified land use map with the soil map (55 different soil types in up to 8 layers), the digital elevation model (DEM, 1 x 1 km resolution), the groundwater level map (pre-classified into 3 classes with < 1 m ('shallow', 15.7 % fractional area), 1–2 m (6.54 %) and > 2 m ('deep', 76.64 %) groundwater level depth), and the map of 93 sub-basins results in a map of 64,550 elementary units. In Fig. 2 a section of about 85 x 70 km of this map is shown, demonstrating the various size (up to 216 km^2, with a mean size of about 1.5 km^2) and shape of these modelling units. The EU-map emphasizes one of the advantages of the polygon-based disaggregation approach, which results in larger spatial units in homogeneous parts of the basin and in smaller spatial units in parts of high heterogeneity. This aspect is especially important in simulating land use/land cover changes (as performed in the Stepenitz sub-basin, which was disaggregated into 30,675 EUs), which normally is restricted to rather small and widely distributed parts of the study region.

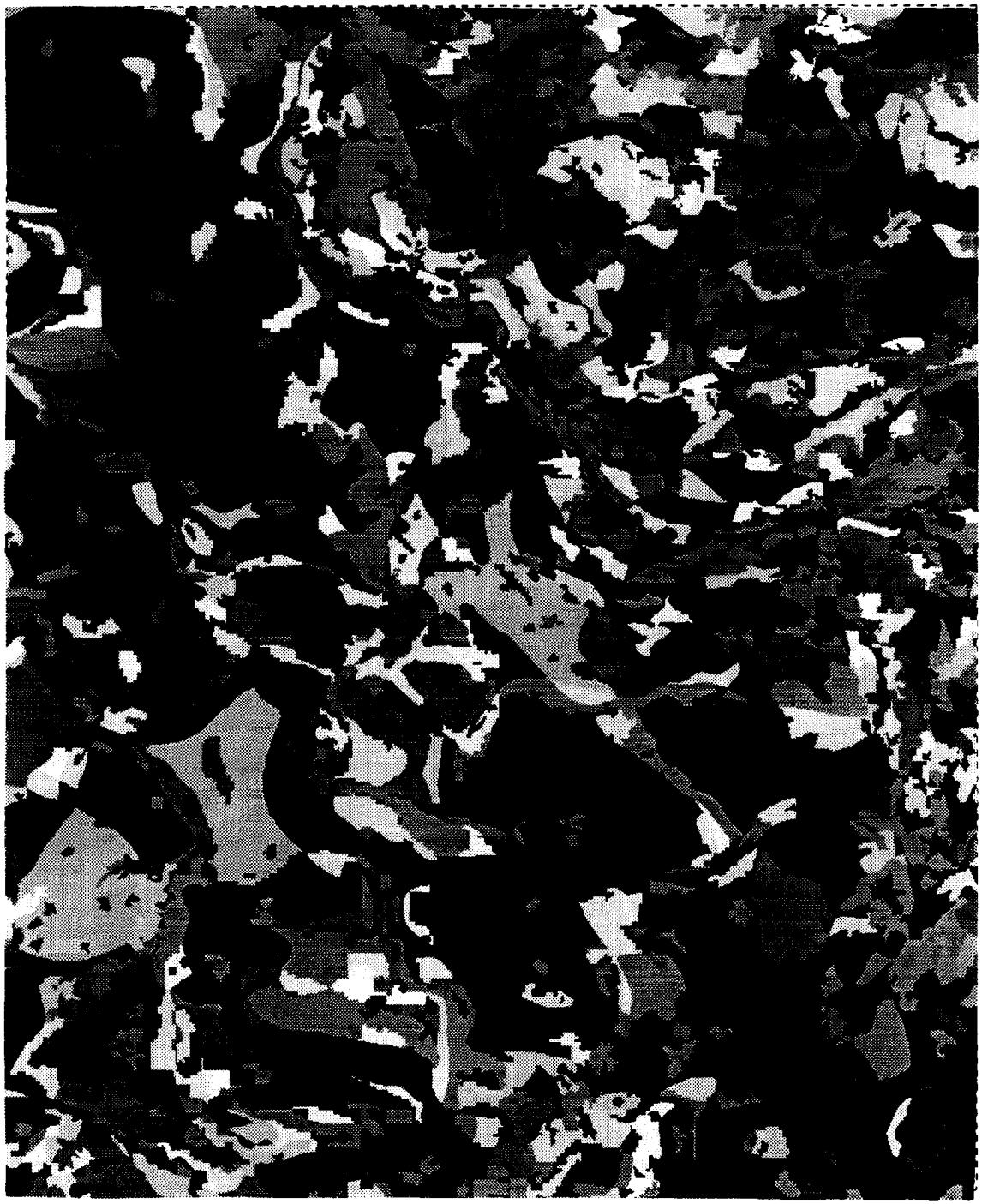

Figure 2: Section of about 85 x 70 km of the elementary units (EU) map generated for the German part of the Elbe basin. The total map consists of 64.550 EUs.

2.2 Spatial aggregation to hydrotope classes

Calculations based on elementary units represent the most precise approximation to reality, since they correspond strongly to the original spatial discretization. However, in case of meso- or macroscale applications it is often more effective to aggregate the EUs to larger spatial units, since their number (and the corresponding simulation times) can be rather high. This is an important aspect in climate or land use impact studies, where long time periods (50 to 100 years or even more) must be simulated on a daily basis using different scenarios. On the basis of earlier studies (Lahmer et al. 1997, Becker and Lahmer 1997), the EU maps of the Elbe basin and the Stepenitz sub-basin were aggregated to hydrotopes (spatially connected EUs characterized by a unique hydrological regime) and hydrotope classes (location independent combinations of similar hydrotopes within a larger areal unit; 'semi-distributed modelling approach') which refer to essential (hydrologic, geographic) characteristics of the study region. Since different EU-characteristics can be used for their definition (depending on the scale and the problems to be solved), simulations based on hydrotope classes are flexible with respect to the definition of each class and the number of classes.

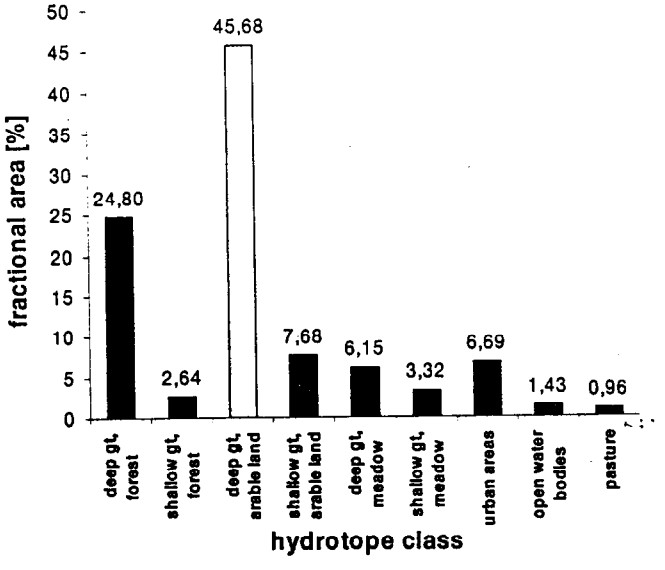

Figure 3: Fractional areas of the 9 hydrotope classes used for the simulation runs in the Elbe river basin, gt - groundwater table.

One important task is to define a reasonable and adequate hydrotope classification for each specific study region. This classification should include hydrological aspects and separate areas differing considerably in their evapotranspiration and runoff behaviour. In addition, the dominant characteristics of the study region should be taken into account. In case of the Elbe basin, a classification into 9 hydrotope classes was chosen. For the dominant land use classes arable land, forests and meadows (see Table 1) areas with shallow and deep groundwater table (gt) were distinguished. In addition, the classes open water bodies, urban areas, and pasture were classified, due to their high evaporation and runoff formation characteristics, respectively. The classification given in Fig. 3 shows that the agricultural and forested areas on deep groundwater table (fractional areas of 45.68 % and 24.80 %) are the dominant hydrotope classes in the Elbe river basin. The

simulation calculations in the Elbe basin which will be discussed in the following chapter were performed either on the basis of the 64,550 elementary units or the 9 hydrotope classes (corresponding to 766 hydrotopes) given in Fig. 3.

3 Results

3.1 Spatial interpolation of meteorological input variables

The spatial distribution of meteorological input variables plays a key role in meso and large scale hydrological modelling, due to its high influence on the calculated water balance components. The interpolation method used in the present study ('extended quadrant method') has proven to be very effective in interpolating meteorological point data for every time step (one day) of the simulation period. Dependencies of the variables on elevation can be taken into account as well. For the water balance calculations in the Elbe basin 33 climate and 107 precipitation stations were used for the spatial interpolation of precipitation, mean temperature, relative humidity, and sunshine duration.

Results of such interpolations are shown in Fig. 4 for precipitation and in Fig. 5 for the climatic water balance (difference between precipitation and potential evaporation calculated according Turc 1961 and Wendling and Schellin 1986). The daily interpolation patterns calculated on the basis of 64,550 EUs are aggregated to annual means for the period 1983–1987, respectively. The location of the used climate and precipitation stations are given as well. Mountaineous regions in the southern and western parts of the basin show high precipitation rates of up to 900 mm or more. The climatic water balance is strongly dominated by the precipitation distribution and clearly indicates the driest and thus most vulnerable sub-areas of the Elbe basin, which are found in the central and north-eastern part. In these sub-areas the mean annual precipitation is about 400 mm and the climatic water balance is zero (or even negative). Thus, this map indicates regions in the Elbe basin characterized by water deficit. In general, the spatially distributed maps of meteorological input variables demonstrate the quality of the interpolation algorithm used. They also emphasize the importance of a high density meteorological network in case of large heterogeneities of these variables, in order to calculate realistic distributions of water balance terms.

3.2 Calculation of water balance components

Water balance calculations in the Elbe river basin were performed on a daily basis for the period 1983–1987, both for EUs and the 9 hydrotope classes given in Fig. 3. Among the various hydrological processes taking place in complex landscapes, evapotranspiration, groundwater recharge and surface runoff are most essential. The results obtained for these water balance components are characterized by (i) the spatial distribution of the meteorological input variables and (ii) the heterogeneities of the underlying elementary units with respect to land use, soil, and groundwater level.

As an example for the macroscale application in the Elbe basin, mean annual values of evapotranspiration for the period 1983–1987 are given in Fig. 6. The calculations performed on the basis of 64,550 elementary units demonstrate that the gross structure of the spatial distribution is dominated by the meteorological input (especially precipitation and temperature). Fine structures, on the other hand, are mainly due to differences in land use. Open water bodies show the highest evaporation values (up to 700 mm/y), followed by riparian and wetland areas. Due to their higher direct runoff formation, settlements are characterized by relatively low evaporation values.

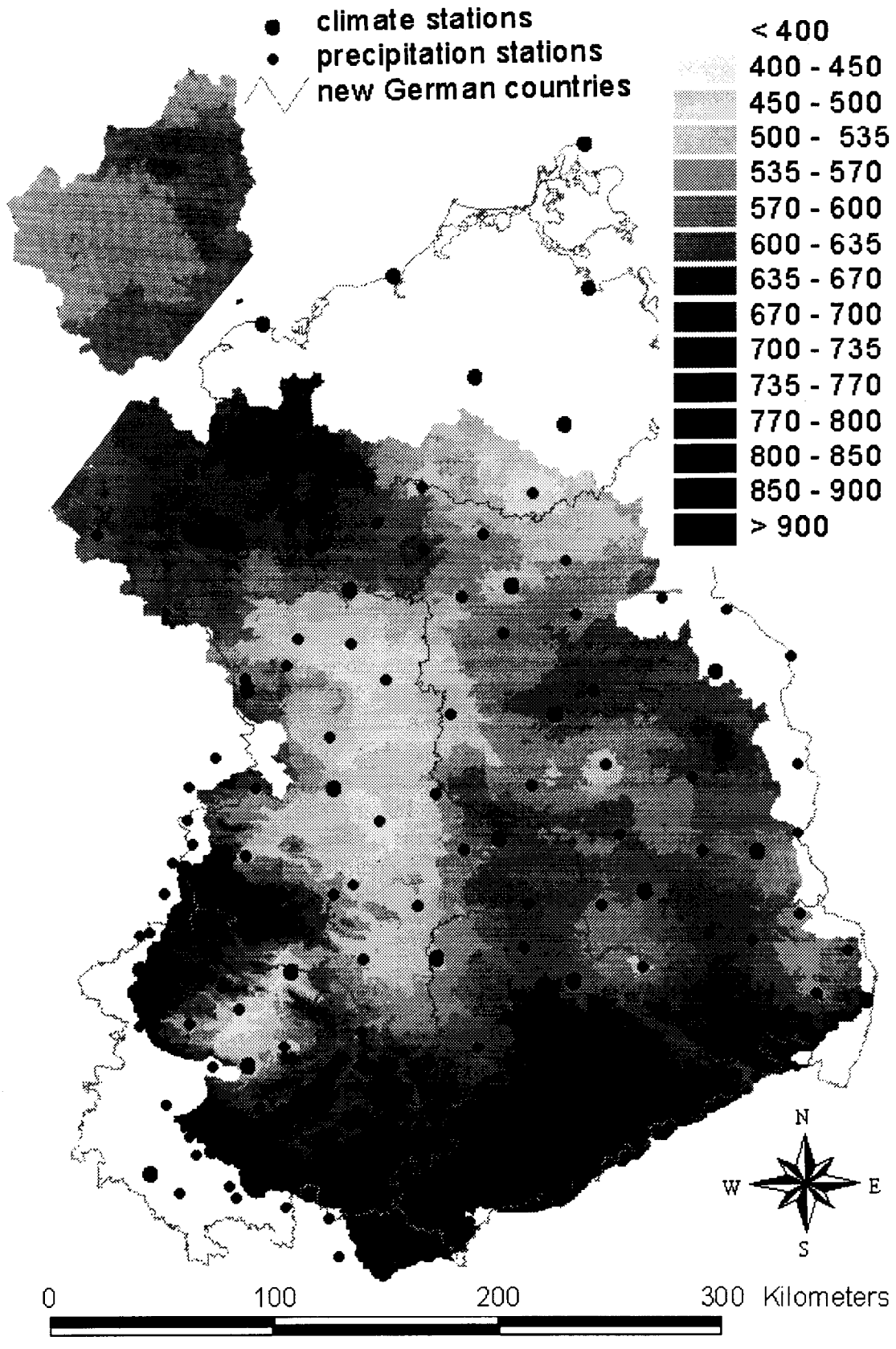

Figure 4: Mean annual precipitation (mm) in the Elbe river basin for the period 1983–87, calculated from 33 climate and 107 precipitation stations on the basis of 64,550 elementary units.

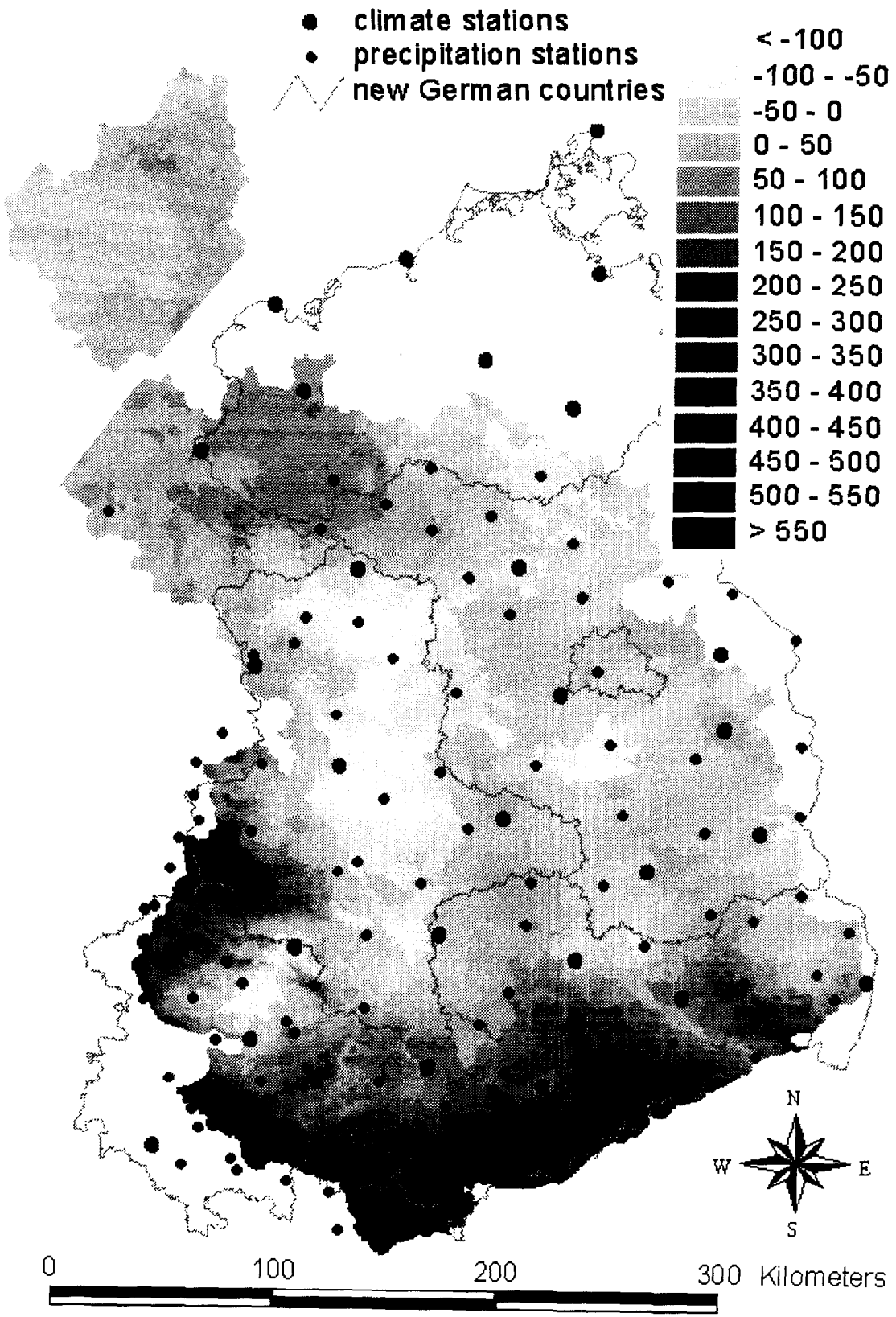

Figure 5: Spatial distribution of the climatic water balance (mm) in the Elbe river basin for the period 1983–87 (mean annual values calculated on the basis of 64,550 elementary units).

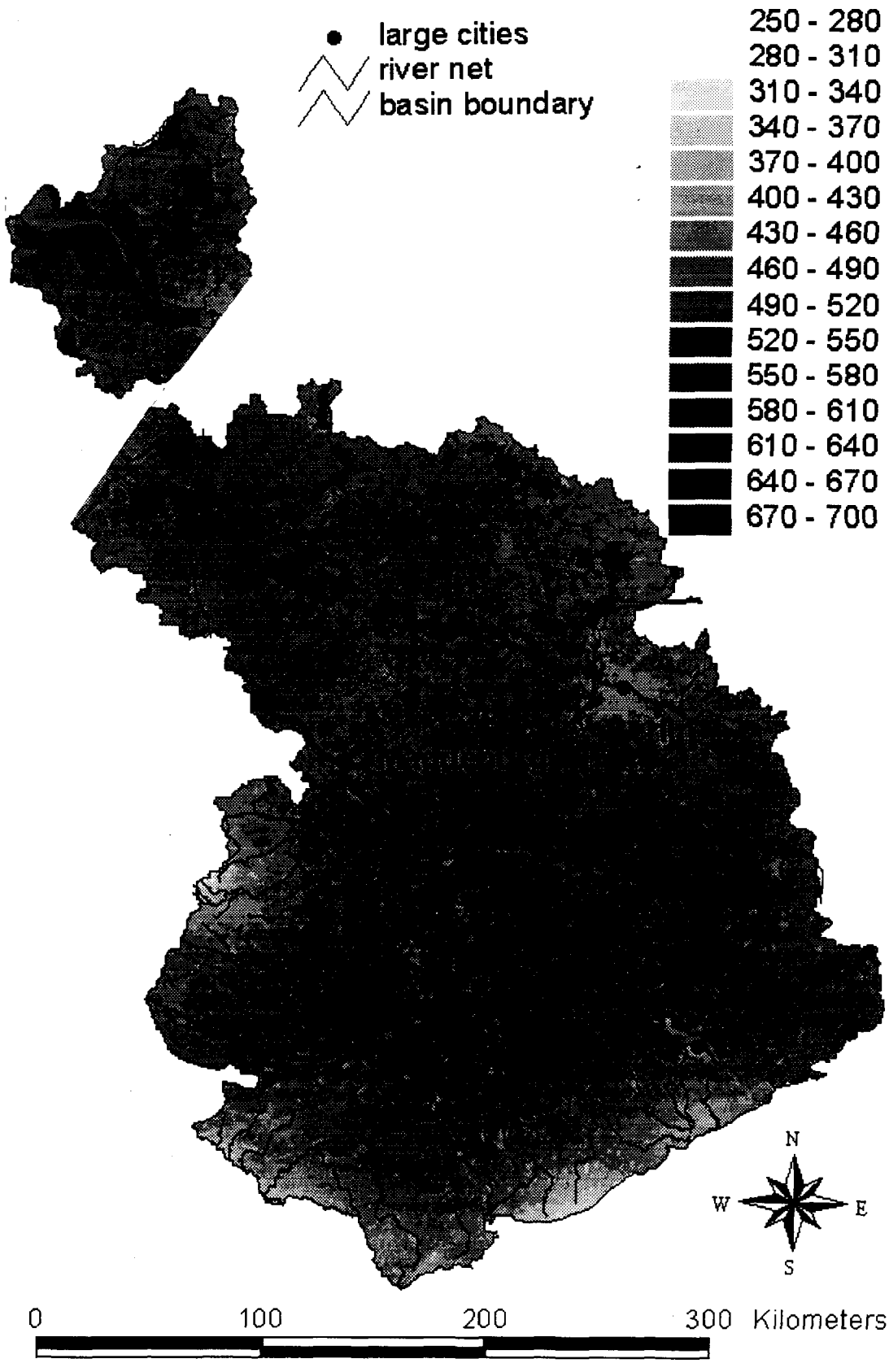

Figure 6: Mean annual evapotranspiration (mm) in the Elbe river basin for the period 1983–87, calculated on the basis of 64,550 elementary units.

Examples for the other two water balance components mentioned above will be given for the meso-scale Stepenitz river basin, where similar calculations were performed in order to analyse the current hydrological state for comparisons with land use scenario calculations. The GIS-based data pre-processing of the basic maps used for this basin resulted in a map of 30,176 elementary units. These units were spatially aggregated into the 10 hydrotope classes (corresponding to 557 hydrotopes in 64 sub-basins) given in Table 2. The only difference to the classification used for the Elbe basin is the differentiation of areas with low (20 %; e.g. settlements, industrial areas, railway tracks etc.) and high sealing (100 %; e.g. highways and other streets). The meteorological input is based on 9 climate and 24 precipitation stations in and around the basin.

Table 2: Hydrotope classes in the Stepenitz river basin used for the calculation of water balance components, including the number of elementary units (EUs) defining these classes and their fractional areas (gt = groundwater table).

hydrotope class	nr. of EUs	fractional area (%)
deep gt, arable land	8240	51.27
shallow gt, arable land	1045	15.13
deep gt, forest	3165	9.25
shallow gt, forest	1015	3.49
deep gt, meadow	2706	9.65
shallow gt, meadow	673	3.72
areas with low sealing	1061	2.23
areas with high sealing	3690	1.15
pasture	465	1.22
open water bodies	8116	2.89

In Figs. 7 and 8 the spatial distributions of the water balance components of percolation (leading to groundwater recharge) and surface runoff calculated on the basis of these hydrotope classes are shown for the period January 1983 to June 1988. Again, the results simulated on a daily basis are aggregated to annual means. In contrast to the results in the Elbe basin, the distributions are strongly characterized by the differences in land use, vegetation cover, soil properties and especially groundwater level of the underlying hydrotope classes. This is due to a more homogeneous meteorological input for this rather small basin and less pronounced heterogeneities of landscape characteristics (especially elevation, which ranges up to only 154 m as compared to 1134 m in the Elbe basin).

Percolation rates are low for areas with high evaporation (areas with shallow groundwater table, forests, wetlands) and high for areas with low evaporation (areas with deep groundwater table, arable land, sealed areas). Large parts of the basin show negative percolation rates corresponding to the high evapotranspiration losses of areas with shallow groundwater table. The distribution of surface runoff formation is characterized by high values for sealed areas, areas with shallow groundwater table and wetlands. In addition, this map demonstrates another advantage of the polygon-based modelling approach, because even small spatial units (like streets) are represented as subareas generating low evaporation, no percolation and high surface runoff. Using a raster-based concept, such units cannot be represented at all in maps of water balance components if they are smaller than the grid size. This aspect is very important in simulating land use changes, as these changes normally happen on widely distributed sub-areas of small or medium size in a basin.

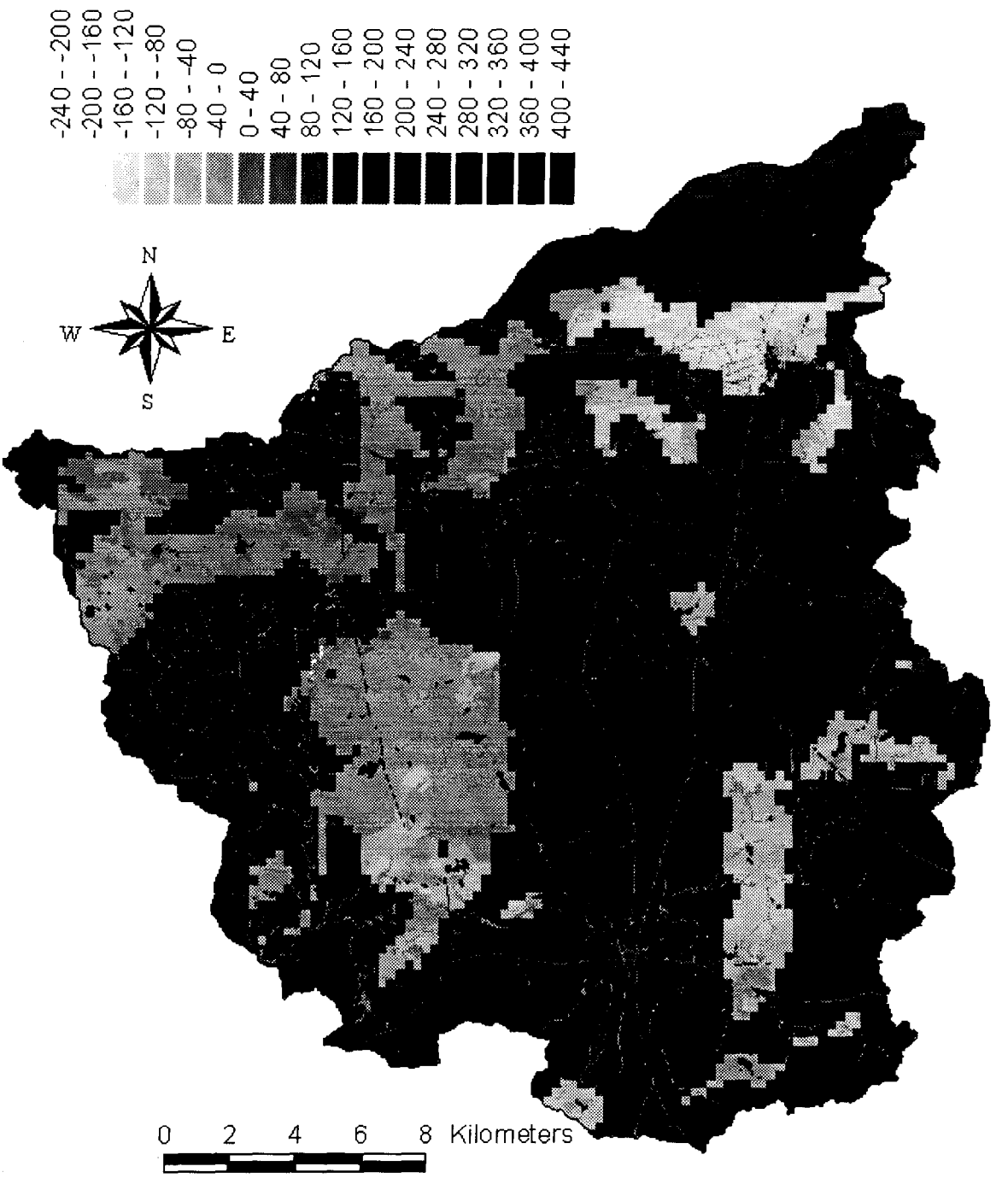

Figure 7: Mean annual percolation (mm) in the Stepenitz river basin, calculated on the basis of 10 hydrotope classes for the period January 1983 to June 1988.

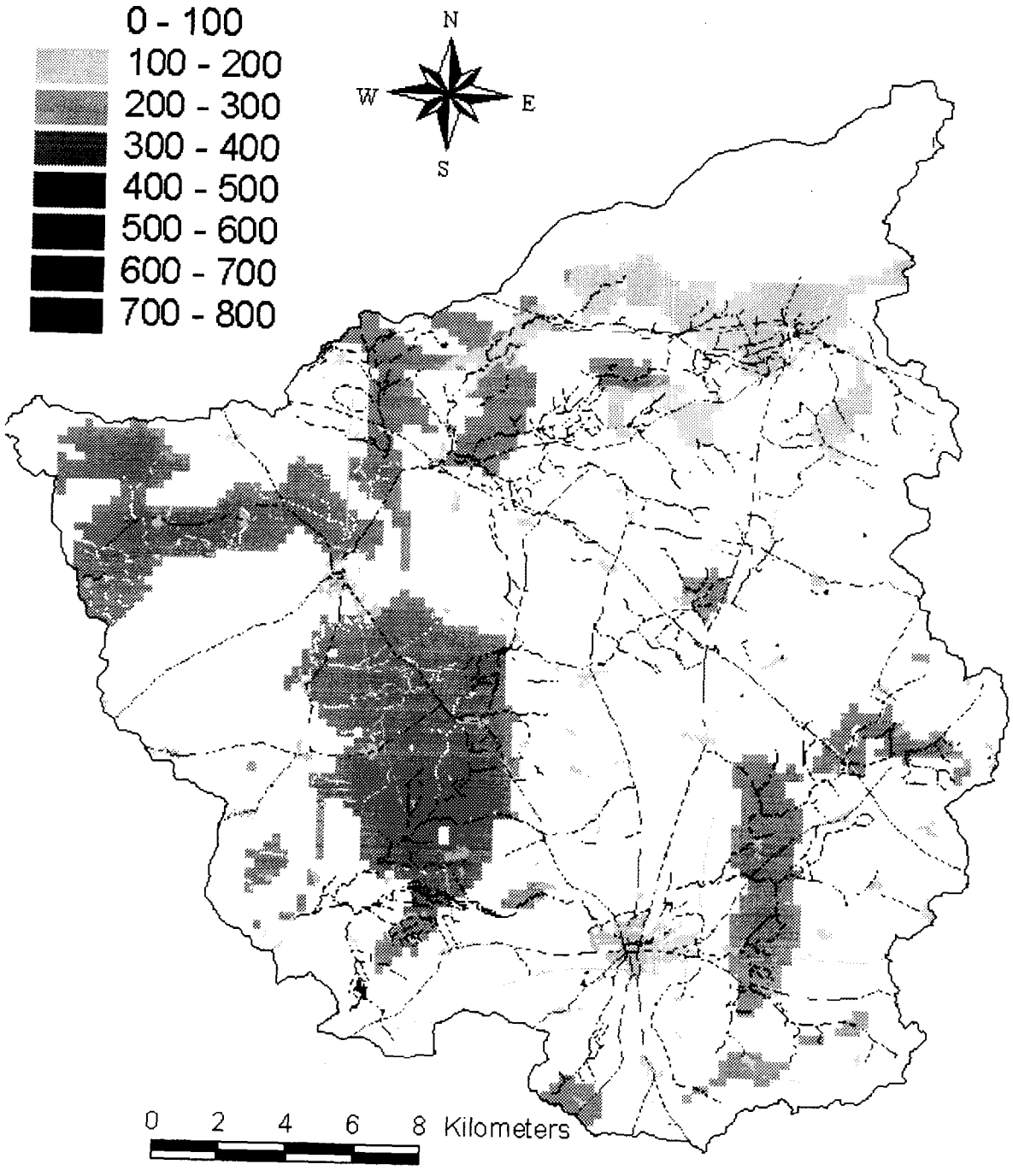

Figure 8: Mean annual surface runoff formation (mm) in the Stepenitz river basin, calculated on the basis of 10 hydrotope classes for the period January 1983 to June 1988.

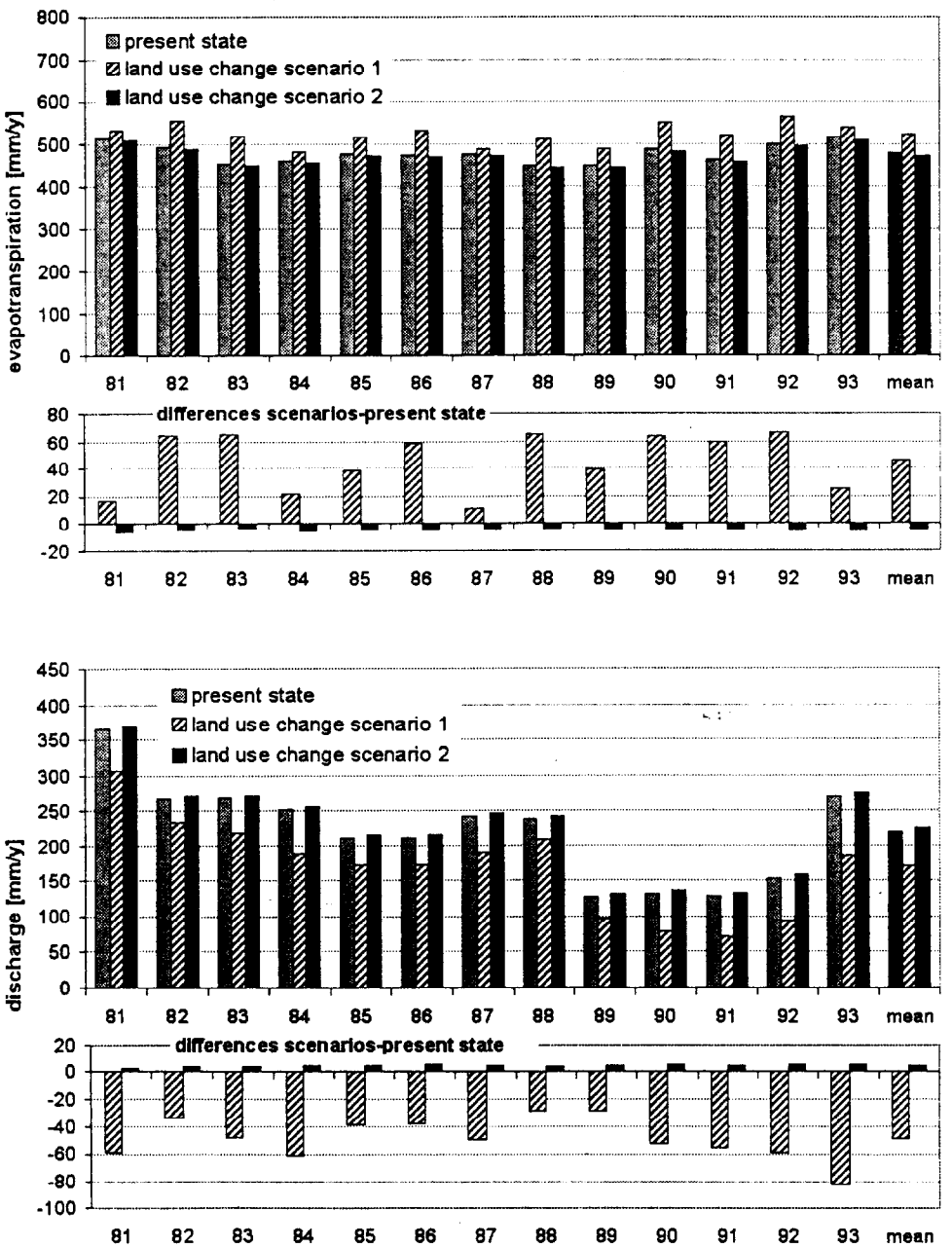

Figure 9: Annual sums of evapotranspiration (top) and discharge (bottom) for the present state and two scenarios of land use change in the Stepenitz river basin, as well as the differences between the two scenarios and present state. Mean values (mean) for the period 1981–93 are given on the right hand site.

3.3 Simulating land use changes

The simulation of land use (and/or possible climate) changes in a region plays a growing role in today's hydrological modelling. First results of such simulation calculations will be given for the Stepenitz river basin, where the influences of different land-use scenarios on the water balance are currently analysed. Land use changes are manifold and include, for example, an increase of urbanized areas, forestation and deforestation, closure of agricultural land due to political decisions, or the conversion of special areas (used for other purposes so far). Modelling these changes also has to deal with a severe scaling problem, since the basic maps available at different scales differ considerably both with respect to their spatial resolution and their degree of classification. For large scale applications, for example, the available land use map may provide some basic land cover classes like 'forests' or 'agricultural areas' without differentiating sub-types of these classes, which may be necessary for a detailed analysis of land use change. For mesoscale applications, on the other hand, the classification may be much more detailed (e.g. providing 'deciduous forest', 'coniferous forest' and 'mixed forests') but still not sufficient for a realistic simulation. This data situation strongly influences the modelling approaches to be used, because a low degree in classification implies the use of mean parameters to describe e.g. evapotranspiration and runoff generation.

In order to analyse the effects of land use changes on the regional water balance, two land use change scenarios were developed and applied in the Stepenitz river basin. Scenario 1 assumes the complete conversion of arable land (about 66.4 % of the total area for the present state) into forest. Though it represents an extreme (and unrealistic) scenario, it provides insight into the model sensitivity and the possible rate of change in the hydrological response of the basin. Scenario 2 assumes an increase in the degree of sealing for areas classified as 'low sealed' (e.g. settlements; see Table 2) from moderate, i.e. 20 % (present state), to complete (100 %). This concerns just 2.23 % of the total basin area. For the scenario analyses, climate conditions as observed during the period 1981–93 were used as reference.

In Fig. 9 the simulated basin response is represented for this period in terms of annual sums of evapotranspiration and basin discharge for the real land use conditions and the two scenarios of change. Due to the rather different size of the affected areas, the response is much more pronounced for scenario 1 than for scenario 2. As expected, there would be a clear increase in basin evapotranspiration of up to 15 % for scenario 1, in particular in the drier period 1988–92. Accordingly, basin runoff would be reduced by up to 44 %, in particular during and after dry years, which could result in critical consequences for the environment and the water supply. Scenario 2 would produce a slight increase in discharge (about 4 % on the average) and a corresponding decrease of 1 % in evapotranspiration.

These first results indicate that the developed modelling approach is sensitive enough to cope with a change in land use/land cover as small as about 2 %. Nevertheless, the two scenarios described here are not 'realistic', as they are not derived from socio-economic analyses or political decisions. In addition, they just represent 'static' scenarios, which do not reflect the dynamic development of specific land use changes, covering years or decades. Therefore, the modelling concept will be extended for future studies, in order to include 'transient' scenarios as well.

4 Conclusions

The results obtained in the German part of the Elbe river basin and the Stepenitz sub-basin provide a better understanding of the spatial and temporal data necessary for a physically based hydrological modelling at different scales. They also demonstrate the usefulness of the developed GIS-based modelling concept, which directly uses model parameters derived from generally available spatial data and provides spatial and temporal results of various water balance components. The disaggregation of the study area based on the available spatial maps, followed by an aggregation of areas with equal or similar hydrological behaviour has turned out to be an effective method to study long-term impacts of climate and land use changes in a river basin. In addition, the use of an interpolation algorithm to provide adequate spatial distributions of climatic input variables has proven to be a key issue in hydrological modelling at larger scales.

In order to study human impacts on the hydrological cycle in river basins of various size, both high resolution data and an appropriate modelling approach are necessary. Only then the hydrological effects of climate and/or land use changes can be modelled at various spatial and temporal scales. First results of a meso-scale land use change analysis demonstrate that the developed concept is especially suited for regional impact studies, since high resolution data are available at this scale.

Summary

Global change phenomena must be investigated at all spatial scales, but it is the regional scale that is crucial for an improved understanding not only of the different causes of global change and the contributing processes, but also of its impacts on the environment and society. River basins are preferred land surface units for regional scale studies because they represent natural integrators of water and associated material transports at the land surface. For the present hydrological study, the German part of the Elbe river basin covering an area of nearly 100,000 km^2 was chosen. More detailed analyses, including first steps towards the modelling of land use changes, were performed in the Stepenitz sub-basin (575 km^2, mesoscale).

The GIS-based modelling approach used in the present study includes variable spatial aggregation and disaggregation methods, which are especially suitable to study regional impacts of climate and land use changes on the hydrological cycle. The approach consequently uses the GIS-based derivation of model parameters from generally available spatial data and includes an effective interpolation algorithm for climatic input variables, which turns out to play an key role in large scale hydrological modelling. Though the principles of spatial aggregation and disaggregation applied in the Elbe river basin follow the special needs of large scale modelling, the concept can be applied to river basins of different size and heterogeneity.

The data pre-processing of the available spatial data results in a map of 64,550 (Elbe) and 30,176 (Stepenitz) elementary units, respectively, which represent the smallest modelling units of the modelling approach and can be considered homogeneous with respect to their hydrological behaviour. These units are spatially aggregated to about 10 hydrotope classes during the simulation runs, in order to enable long-term simulation runs on a daily basis. This aggregation step considerably simplifies large scale modelling and reduces computing time, without a remarkable loss in simulation quality.

The results obtained for various water balance components like evapotranspiration, groundwater recharge and surface runoff formation in the Elbe basin and the Stepenitz sub-basin demonstrate that the aggregation of a study region into subareas of similar

hydrological process behaviour represents an effective modelling concept. In the case of the Elbe basin (macroscale), the spatial distributions of these water balance components are dominated by the meteorological input (especially precipitation and temperature), whereas they are strongly characterized by the differences in land use, vegetation cover, soil properties and especially groundwater level of the underlying hydrotope classes in case of the Stepenitz sub-basin. This is due to a more homogeneous meteorological input for a smaller basin and less pronounced heterogeneities of various landscape characteristics.

In order to analyse the effects of land use changes on the regional water balance, two simple land use change scenarios were developed and applied in the Stepenitz river basin. The simulated basin response represented in terms of evapotranspiration and basin discharge demonstrates that the modelling approach is sensitive enough to cope with land use/land cover changes of realistic size. Future scenarios of more realistic character will be derived from socio-economic analyses for the region and include a dynamic development of specific land use changes as well.

References

[1] Becker, A. and Lahmer, W. (1997): Large Scale Hydrological Modelling. Final report within the research program "Regionalization in Hydrology" of the German Research Society (DFG) (in German, unpubl.).

[2] Beven, K. J. (1993): Prophesy, reality and uncertainty in distributed hydrological modelling. Adv. Wat. Resour. 16, 41–51.

[3] Gleick, P. H. (1986): Methods for evaluating the regional hydrologic impacts of global climatic changes. J. Hydrol. 88, 99–116.

[4] Lahmer, W. (1997): Spatially distributed modelling of water balance components in the German part of the Elbe basin using large-scale aggregation principles. Report to the Potsdam Institute for Climate Impact Research, October 1997 (in German, unpubl.).

[5] Lahmer, W. and Becker, A. (1998): Basic principles for a GIS-based large-scale hydrological modelling. In: Modelling of water and nutrient transport in large catchments. PIK-Report No. 43, PIK 1998, 55–66 (in German).

[6] Lahmer, W., Becker, A., Müller-Wohlfeil, D.-I. and Pfützner, B. (1997): A GIS-based Approach for Regional Hydrological Modelling. Accepted for IAHS publication (International Conference on Regionalization in Hydrology, Braunschweig, March 1997).

[7] Pfützner, B., Lahmer, W. and Becker, A. (1997): ARC/EGMO - a program system for GIS-based hydrological modelling. Short documentation to version 2.0. Potsdam Institute for Climate Impact Research (in German, unpubl.).

[8] Turc, L. (1961): Évaluation des besoins en eau d'irrigation, évapotranspiration potentielle, formule simplifiée et mise à jour. Ann. agron 12, 13–49.

[9] Wendling, U. and Schellin, H. G. (1986): Neue Ergebnisse zur Berechnung der potentiellen Evapotranspiration. Z. für Meteorologie 36, 3, 214–217.

Analysing the role of phreatic level dynamics on the streamflow response

in a Mediterranean mountainous experimental catchment

(Vallcebre, Catalonia)

J. Latron, F. Gallart, C. Salvany

Institute of Earth Sciences 'Jaume Almera', CSIC, Solé i Sabarís s/n., 08028 Barcelona, Spain.

1 Introduction

The study of catchment runoff generation mechanisms notably started in the early 1960s when several authors (Cappus, 1960; Hewlett and Hibbert, 1967) showed with field data that infiltration excess overland flow identified by Horton (1933) was not in many cases the leading mechanism but was only a particular case of streamflow generation. Many field studies under temperate climates have since confirmed the predominance of other runoff-generating processes, mainly subsurface flow and saturation excess overland flow.

However, as Dunne (1978) suggested, all these mechanisms are complementary rather than contradictory, and dry areas like Mediterranean regions provide frequent examples of the occurrence of all the above mentioned mechanisms due to both high rainfall intensities and varying antecedent conditions.

Former studies on the interaction between soil moisture, groundwater and streamflow response in the study area show the role of infiltration excess runoff in dry periods (Latron and Gallart, 1995; Latron et al., 1997) and stressed the main role of saturation excess runoff generation mechanisms (Llorens and Gallart, 1992; Latron et al., 1997), the role of terraced topography on the generation of saturated areas (Gallart et al., 1994), and the delay of the saturation and drying of semi-permanent saturated areas when compared to the mean soil water reserve (Rabadà et al., 1993, Gallart et al., 1997).

The present work tries to exploit the extensive piezometric network installed in 1995 in order to describe the dynamics of the phreatic system and to discuss some non-linearities observed especially during the wetting-up transitions, which remain a challenge for hydrological modelling in seasonal climates (Piñol et al., 1997).

2 The study area

The Cal Rodó catchment (4.17 km^2) is located in the southern margins of the Pyrenees, at altitudes between 1100 and 1600 m a. s. l. Bedrock is dominated by red smectite-rich mudstones locally prone to badlands formation and massive limestone beds. The

climate is mountain Mediterranean with a mean annual temperature of about 9°C and a mean annual rainfall of about 850 mm. Water deficit occurs usually in summer, but can be advanced or delayed depending on the usual climatic variability of Mediterranean climates. Most of the hillslopes (35 % of the catchment surface area) were terraced in the past for cultivation and are now used for cattle stockbreeding or forestry. Forest (*Pinus sylvestris*) covers nowadays 60 % of the catchment. Soils are loamy and well structured, with a thickness that varies up to 3 m because of the terraced micro-topography. The present general arrangement of the instruments in the Cal Rodó catchments (Fig. 1) consists of 4 runoff gauging points, 7 rainfall recorders, 1 weather station, 3 tensiometric profiles, 9 TDR (time domain reflectometry) soil moisture measurement points, 3 weekly-measured wells, and 4 continuous recording piezometers.

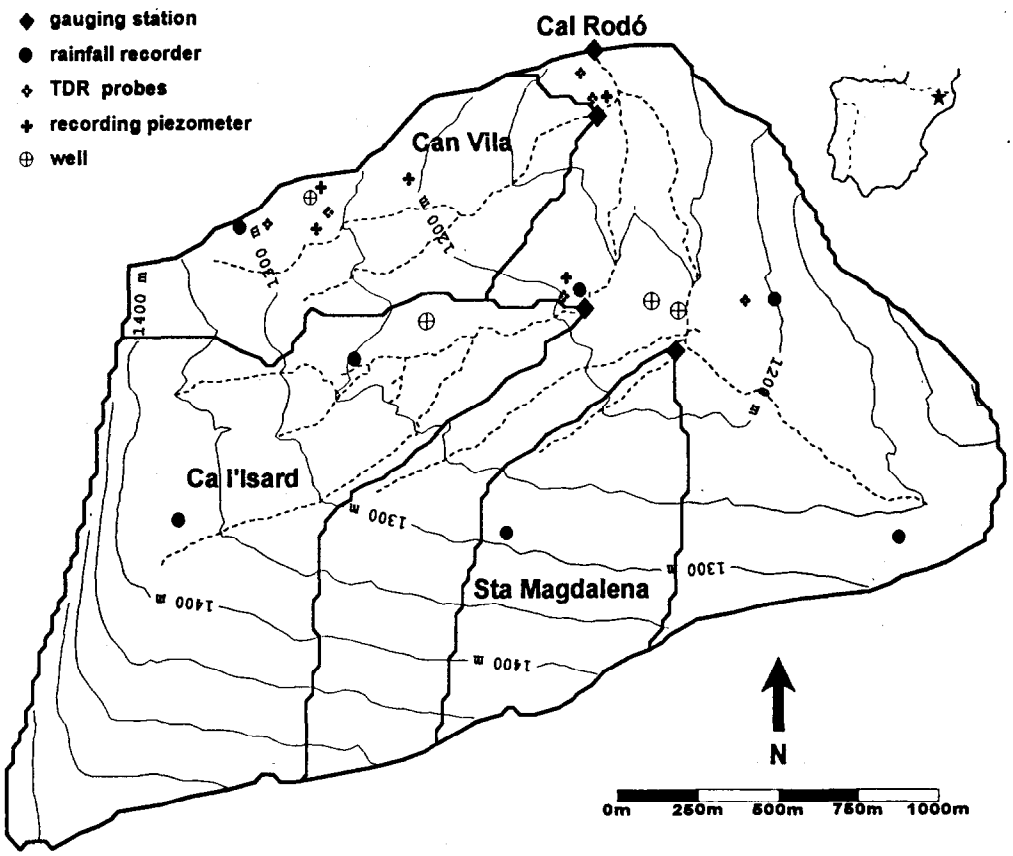

Figure 1: General arrangement of the measuring network.

3 Soil moisture and phreatic levels

Soil moisture values measured down to 80 cm show a wide range (0.15 to 0.60 cm^3/cm^3), are temporally well correlated and are spatially controlled mainly by vegetation cover and position in the hillslope; forested or upslope areas being drier than grassed or downslope ones. The points with less variation correspond to the deeper situations in the profiles and downslope locations where saturation is frequent. Position in the hillslope, by means of the topographic index (Beven and Kirkby, 1979), vegetation cover and soil depth have been

used to estimate catchment water reserves from soil water content point measurements in order to validate internal state variables of hydrological models.

Free shallow aquifers can be found in these soils over clayey bedrock even on steep hillslopes because of the low hydraulic conductivities. Phreatic level variations show in general a greater inertia than soil moisture values, thus being better correlated with deeper points in the profiles and downslope situations. Nevertheless, continuous recording piezometers demonstrated that phreatic levels react usually very quickly to rainfall events of sufficient magnitude to produce relevant runoff. This highly dynamic behaviour was observed before and justified the use of recording piezometers (Latron et al., 1997). The rapid response is a rule except when the rainfall event occurs after a long drought period that depleted the phreatic level (Fig. 2). In these dry antecedent conditions, the reaction of the phreatic level to rainfall can be delayed by 120 hours.

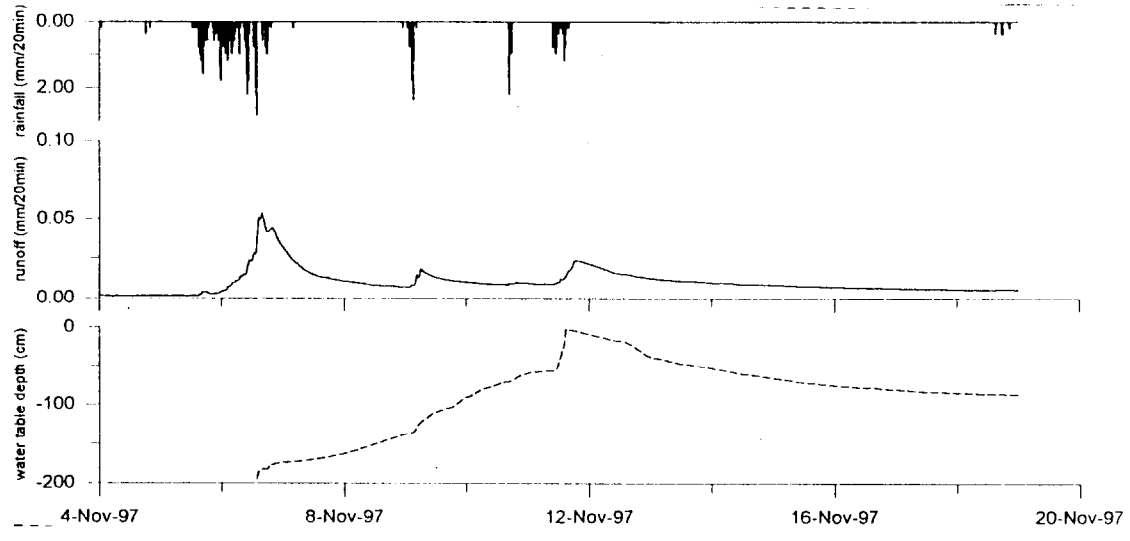

Figure 2: Streamflow and water table response to the first rainfall event after a dry period (Can Vila catchment). Compare the water table response to rainfall for the different events.

4 Runoff events

A close relationship between phreatic levels and runoff coefficients has been demonstrated before for these catchments (Latron et al., 1997). Nevertheless, the continuous record of phreatic levels allows better analysis that makes possible the identification of anomalies of this general rule. In a very simplistic manner, runoff from a catchment driven by subsurface flow can be approximated by some negative exponential function of water reserve (Beven and Kirkby, 1979). The plot on Fig. 3 shows the log-linear relationship between phreatic levels and runoff volumes at daily scale. Although with scatter, the general trend of the points fits an exponential function if a few outliers are excluded. These outliers coincide with events over 'dry' antecedent conditions prior to rainfall and correspond to days with runoff volumes much higher than those that could be predicted by the phreatic level, and thus by saturation mechanisms based models. For these events the low soil moisture contents and the deep location of phreatic levels strongly reduce subsurface and saturation excess contributions to streamflow.

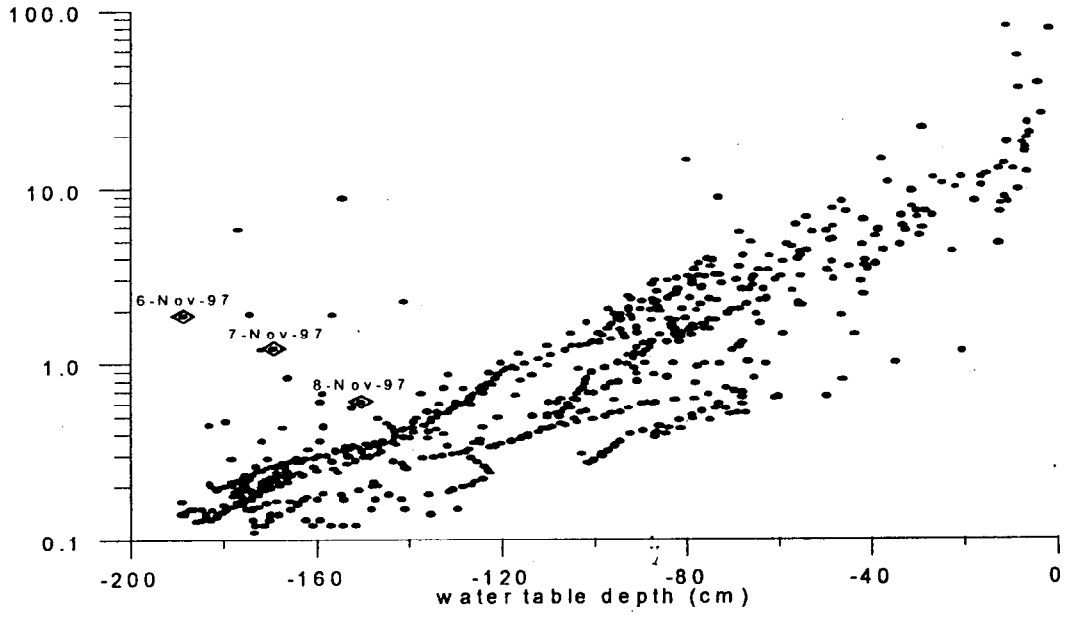

Figure 3: Relationship between daily runoff (Can Vila catchment) and water table depth. Days corresponding to Fig. 2 are indicated.

5 Conclusions

The hydrological functioning of the Cal Rodó catchments is usually controlled by subsurface flow and saturation excess overland flow, as it corresponds to humid temperate environments. Nevertheless, the continuity of subsurface water transfer is interrupted almost every year, after a water deficit period, when the Mediterranean character of the climate becomes evident and stress infiltration excess runoff generation mechanisms. Between these two kinds of behaviour there is a threshold, subject to hysteresis delays, that represents a progressive substitution of the processes.

The analysis of the mechanisms active during the dryer and transition periods is not a merely academic exercise, as it can provide a bridge to understand the behaviour of catchments in rather dry areas, or to allow the simulation of the likely hydrological consequences of a drying climate.

Acknowledgements

This work has been carried out within the VAHMPIRE Project, supported by EC Environment and Climate Research Programme (ENV4-CT95-0134).

References

[1] Beven, K. J., Kirkby, M. J. (1979): A physically-based variable contributing area model of basin hydrology. Hydrological Sciences Bulletin, 24 (1), 43–69.

[2] Cappus P. (1960): Bassin expérimental d'Alrance - Etude des lois de l'écoulement - Application au calcul et à la prévision des débits. La Houille Blanche n° A, 493-520.

[3] Dunne T. (1978): Field studies of Hillslope Flow Processes. in: Kirkby M. J. (Ed), 'Hillslope Hydrology', Wiley-Interscience Publ., 227–293.

[4] Gallart, F., Llorens, P., Latron, J. (1994): Studying the role of old agricultural terraces on runoff generation in a Mediterranean small mountainous basin. Journal of Hydrology 159: 291–303.

[5] Gallart, F., Latron, J., Llorens, P., Rabadà, D. (1997): Hydrological functioning of Mediterranean mountain basins in Vallcebre, Catalonia: some challenges for hydrological modelling. Hydrological Processes 11: 1263–1272.

[6] Hewlett J. D., Hibbert A. R. (1967): Factors affecting the response of small watersheds to precipitation in humid areas. In: W. E. Sopper & H. W. Lull (Eds), Forest Hydrology, Pergamon, Oxford (UK), 275–290.

[7] Horton R. E. (1933): The role of infiltration in the hydrological cycle. Trans. Amer. Geophys. Union. 14, 446–460.

[8] Latron, J., Gallart, F. (1995): Hydrological response of two nested small Mediterranean basins presenting various degradation states. Physics and Chemistry of the Earth. Vol. 20, n° 3–4: 369–374.

[9] Latron, J., Llorens, P., Gallart, F. (1997): Spatial and temporal patterns of runoff generation processes in mountainous Mediterranean basins (Vallcebre, Catalonia). In: D. Viville & I. Littlewood (eds), Ecohydrological processes in small basins. Proceedings of the Sixth Conference of the European Network of Experimental and Representative Basins (ERB), Strasbourg, 24–26 September 1996. IHP-V Technical Documents in Hydrology, 14, UNESCO, 93–98.

[10] Llorens, P., Gallart, F. (1992): Small basin response in a Mediterranean mountainous abandoned farming area: research design and preliminary results. Catena, 19: 309–320.

[11] Rabadà, D., Gallart, F., (1993): Monitoring soil water content variability in the Cal Parisa basin (Alt Llobregat) with TDR. Experimental design and first results. in: Llorens, P. & Gallart, F. (eds), Assessing hydrological changes. Proceedings of the Fifth Conference of the European Network of Experimental and Representative Basins (ERB), Barcelona. Special issue, Acta Geologica Hispanica, 28 (2-3): 85–93.

[12] Piñol, J., Beven, K., Freer, J. (1997): Modelling the hydrological response of mediterranean catchments, Prades, Catalonia. The use of distributed models as aids to hypothesis formulation. Hydrological Processes 11: 1287–1306.

Water quality of the Łasica river (Central Poland)

M. Lenartowicz

University of Warsaw, Faculty of Geography and regional Studies, Division of Hydrology, Krakowskie Przedmieście 30, 00-927 Warsaw, Poland.

Abstract

The paper presents the results of investigations on river water quality in an area of Kampinos National Park in Poland. From several field measurements sessions, two have been selected. One of them was arranged in the winter (December 1997), the second one during the vegetation season (June 1998). The following parameters were measured at 18 points; pH, total hardness, carbonate hardness, chloride, nitrate, nitrite, ammonium, phosphates and sulphates. The results of discharge measurements and chemical analyses of water are presented and discussed. The study shows that even protected catchments are not free from the influence of human activity. Water quality is a good indicator of all processes of natural and human origin, and it varies spatially in accordance with the physico-geographical conditions in different parts of the catchment.

1 Introduction

The quality of flowing water is a good indicator of the complexity of processes currently acting in a catchment above the sampling point. Water quality changes with natural conditions, processes and human activity. Identification of those processes is the first step to recognize a complex system of the catchment, its current state and sensitivity.

2 Study area

The Łasica River (catchment area of 493 km^2) is located in central Poland, within the territory of The Kampinos National Park and its protection zone. The natural borders of the catchment are the Bzura River from the west, the Vistula River from the north, the City of Warsaw from the east and the glacial plains from the south. The sources of some tributaries of the Łasica are in the City of Warsaw. The annual precipitation total is about 550 mm (November to April - 200 mm, May to September - 350 mm). The whole catchment consists of 5 sequential hydrological spatial units extending from east to west: the escarpment of the glacial plain; a zone of the wetlands; a southern belt of dunes (height up to 100 m a. s. l.); the depression of the Łasica River; and a northern belt of dunes (height up to 110 m a. s. l.). Dominant soils are light sands, alluvial sands,

peats in the depressions and only in the southern parts clays and silts. The Łasica River flows toward the west in the local depression and has mostly left side tributaries flowing from the glacial plain. The main tributaries are the Zaborowski and Olszowiecki Channels from the left side and so called Ł-9 channel from the right side. Comparing to left-side tributaries of the Łasica River, its length and catchment area are much smaller. The outlet of the Łasica River to the Bzura River is controlled. Two pumping stations work intensively during high water stages. In the first half of the 20^{th} century the wetlands were partly changed by agricultural drainage. Since that time almost all natural streams have features of artificial channels. All along the Łasica River over 15 hydrotechnical constructions (mostly weirs) slow down the outflow from the catchment. In recent years some steps to re-naturalize the Łasica River have been undertaken, so far without any visible effects.

The forest is dominated by pine trees (80 %). The wetlands are partly covered by alder carrs and birch forests. The dunes are landscapes of intensive infiltration and relatively low mineralization of the groundwater. In contrast, the wetlands are areas of very high evapotranspiration, especially in the vegetation season, and relative high mineralization of the groundwater. The highest mineralization of the groundwater was documented in the rural areas and surrounding farming regions (Kazimierski et al, 1995). The location of the sources of the Łasica River and some tributaries close to Warsaw have a significant influence on the quantity and quality of the water resources in the catchment (Ciepielowski and Wawrzoniak, 1997).

3 Water quality

The chemical features of the river water in the catchment of the Łasica have been already studied by Ciepielowski and Wawrzoniak (1997). Since 1997 State Inspectorate for Environment Protection has measured water quality once a month in 9 profiles but the results have not been published.

In this study the following parameters of the water from 18 sections (Table 1) were measured: pH, total hardness, carbonate hardness, concentration of chloride, nitrate, nitrite, ammonium, phosphates and sulphates. Analyses were made using field tests (e.g. pH), or performed in the laboratory (e.g. chloride). Together with water sampling, discharge measurements were made. From several measurement sessions two were selected, from December, 1997 and June, 1998.

3.1 Discharge

In December 1997, discharge at the mouth of the catchment was 1.8 m^3/s (in June 1998 only 0.4 m^3/s). Changes in the runoff along the Łasica River are shown on Fig. 1. In the area where river flows through the wetlands the evapotranspiration in summer was very high and caused great losses in runoff. The same situation could be observed in the catchments of the Zaborowski and Olszowiecki Channels (Fig. 2 and Fig. 3).

3.2 pH

Values of pH measured in June 1998 had bigger scatter than the values from December 1997 and varied from 6.5 to 8.0 (Fig. 4). The Łasica River has its sources in the wetlands in the eastern parts of the catchment. These are landscapes of relative high acidification and this affects lower reaction of water in the upper part of the catchment. The river water mixes downstream with the water of tributaries and groundwater flowing from the glacial plain, leading to more neutral pH levels.

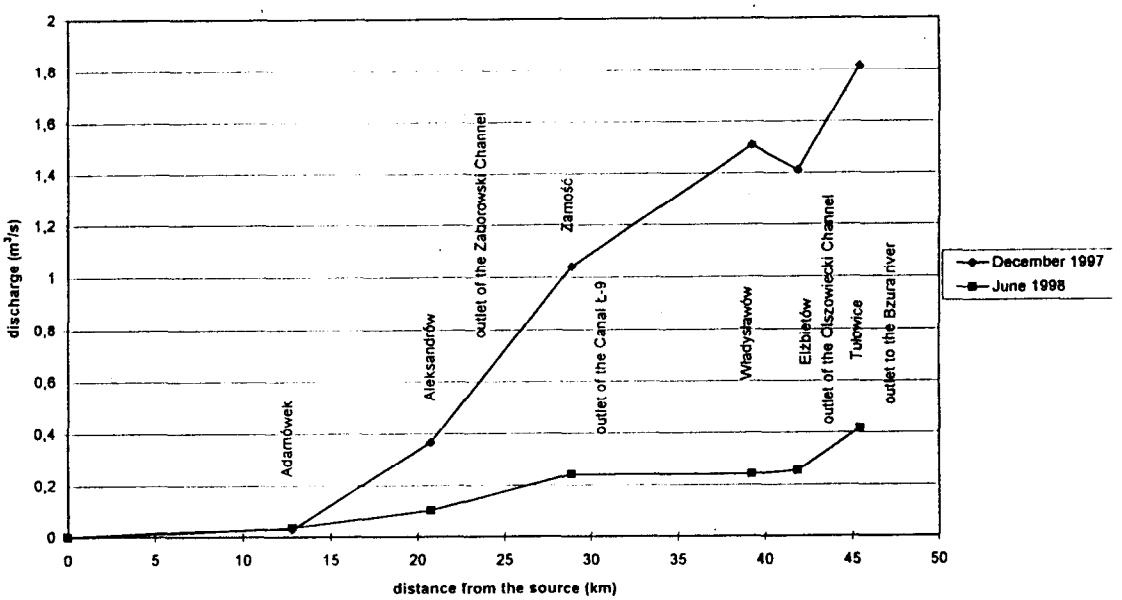

Figure 1: Changes in the river discharge down the Łasica River.

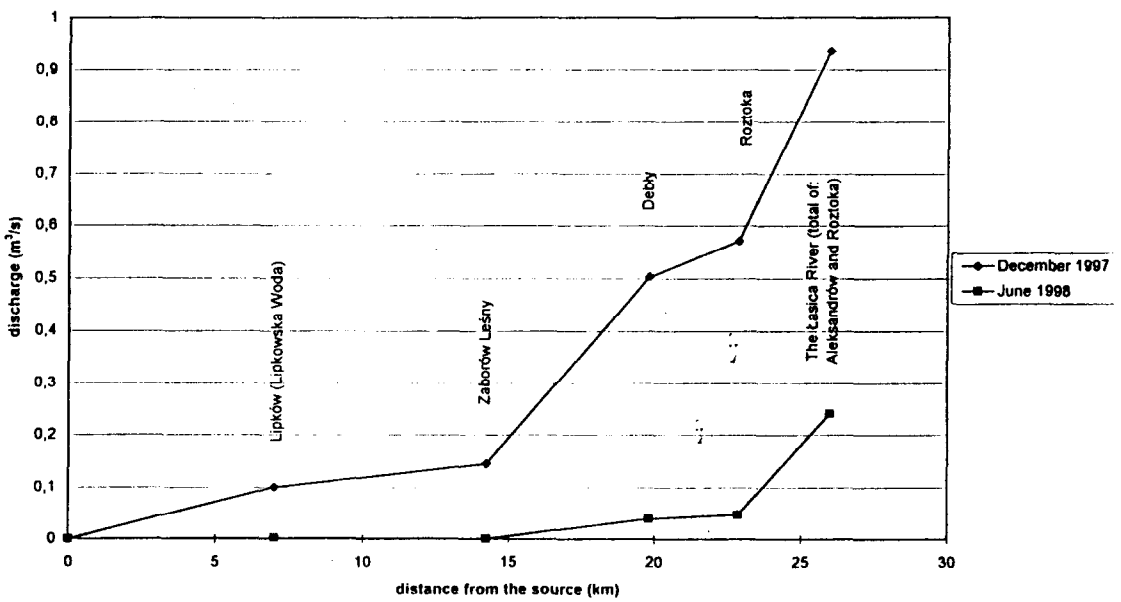

Figure 2: Changes in the river discharge down the Zaborowski Channel.

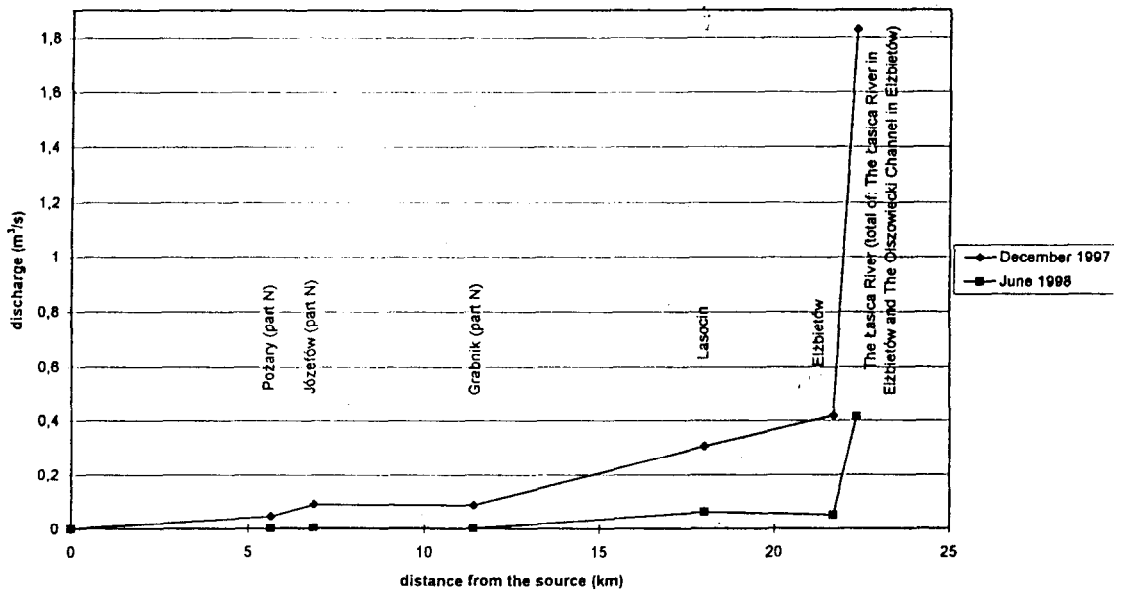

Figure 3: Changes in the river discharge down the Olszowiecki Channel.

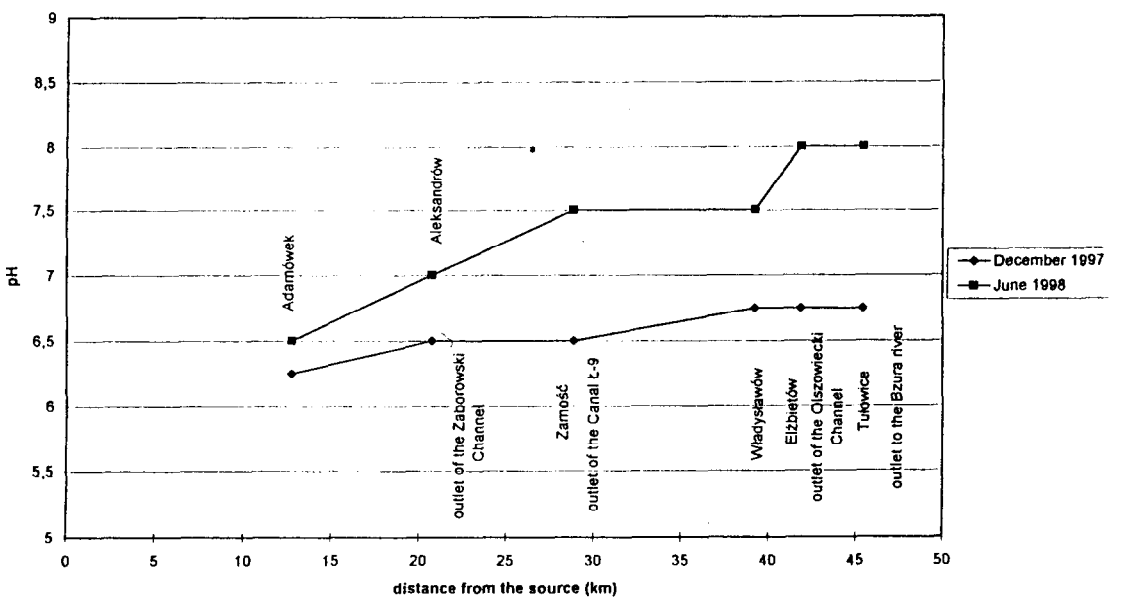

Figure 4: Changes in pH down the Łasica River.

Table 1: Location of the measurement profiles.

River	Profile		Distance from the source (km)
Łasica	Adamówek	12.75	
Łasica	Aleksandrów	20.73	
outlet of Zaborowski Channel		23.54	
Lipkowska Woda	Lipków		6.99
Zaborowski Channel	Zaborów Leśny		14.23
Zaborowski Channel	Debły		19.81
Zaborowski Channel	Roztoka		22.87
Łasica	Zamość	28.85	
outlet of L-9 Channel		30.05	
L-9 Channel	Wędziszew		7.83
L-9 Channel	Cisowe		16.77
Łasica	Władysławów	39.22	
Łasica	Elżbietów	41.86	
outlet of Olszowiecki Channel		42.79	
Olszowiecki Channel N.	Pożary		5.64
Olszowiecki Channel N.	Józefów		6.86
Olszowiecki Channel N.	Grabnik		11.41
outlet of Olszowiecki Channel S.			16.26
Olszowiecki Channel S.	Józefów		3.99
Olszowiecki Channel S.	Grabnik		8.35
Olszowiecki Channel	Lasocin		18.02
Olszowiecki Channel	Elżbietów		21.70
Łasica	Tułowice	45.42	
outlet of the Łasica river to Bzura		48.48	

The change of the type of environment between the upper and lower part of the catchment is very distinct. In its middle part, the Łasica River flows through pastures and grasslands. Mineralization of the groundwater in this area is higher due to the fertilizers and substances used for soil de-acidification.

3.3 Total hardness and carbonate hardness

Values of total hardness varied from 4.2°d to 16°d and carbonate hardness from 2.4°d to 10.6°d (Fig. 5 and Fig. 6). Similar to pH values, hardness of the river water rose downstream due to mixing of water flowing from the glacial plain from the south. Measured values were lower in June 1998 than in December 1997. One exception was observed at Adamówek in the upper part of the catchment where the total hardness of the water, and the carbonate hardness, were the lowest. The main cause of the sharp rise in hardness is the confluence of the Łasica River with tributaries where the values of total hardness were not lower than 12°d and reached over 20°d in the parts of catchment close to the glacial plain and farming areas. During the cold season the influence of soft water from the swamps with peats which are drained by the river is minimized. Due to frost penetration recharge from the peats does not occur.

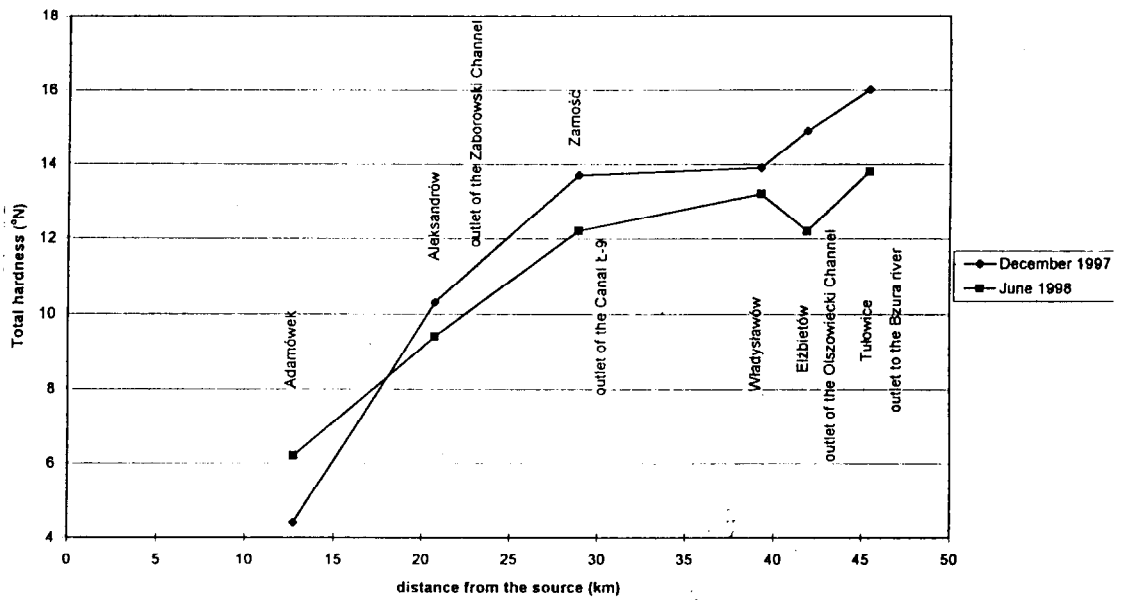

Figure 5: Changes in the total hardness down the Łasica River.

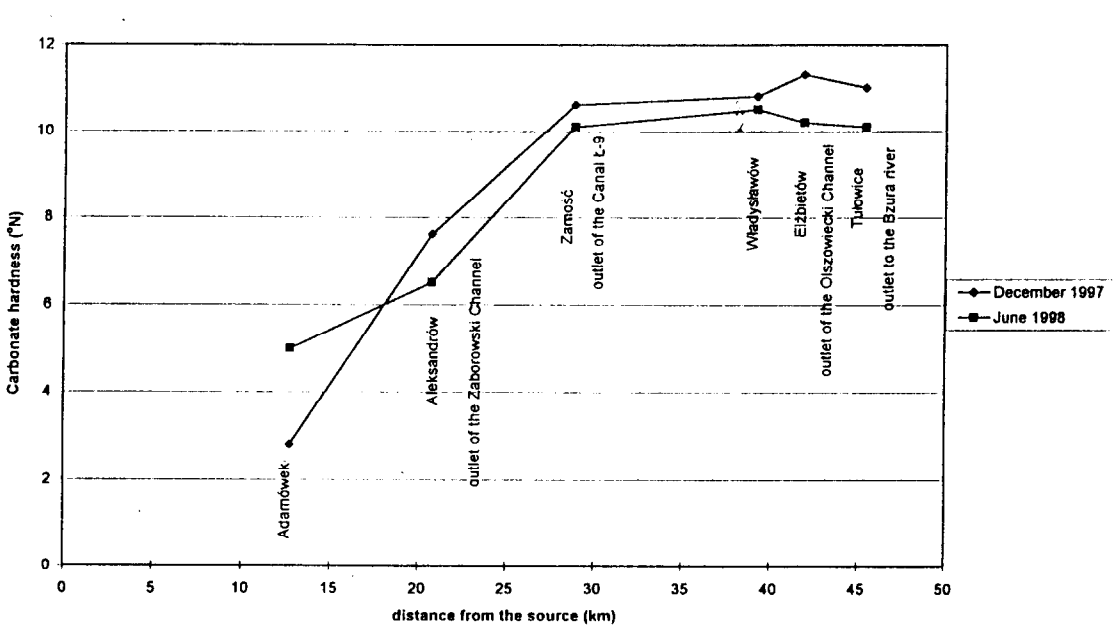

Figure 6: Changes in the carbonate hardness down the Łasica River.

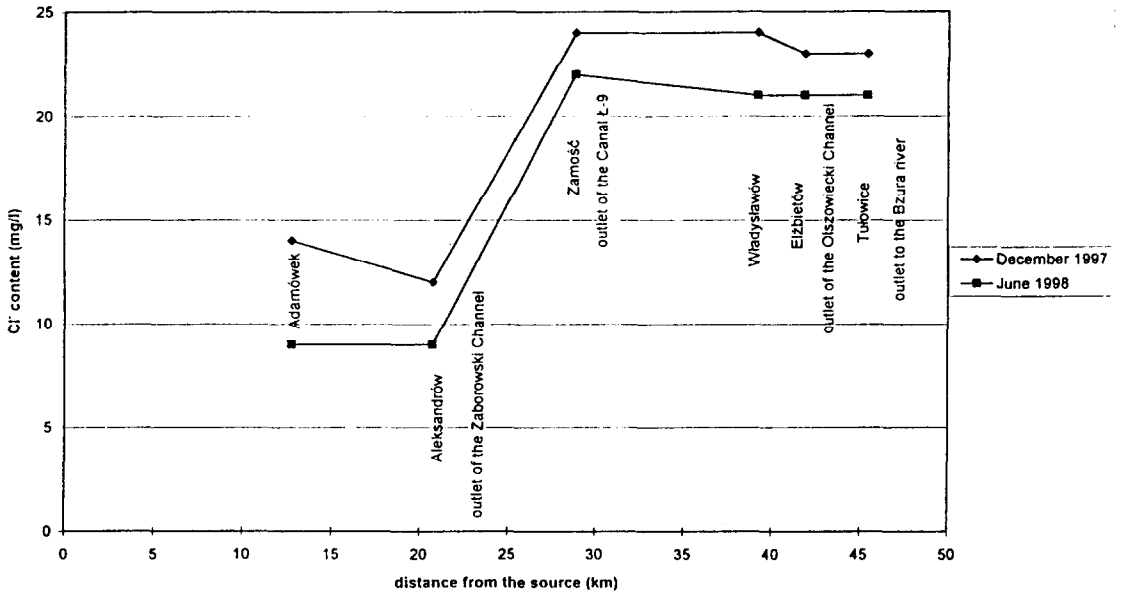

Figure 7: Changes in content of chloride down the Łasica River.

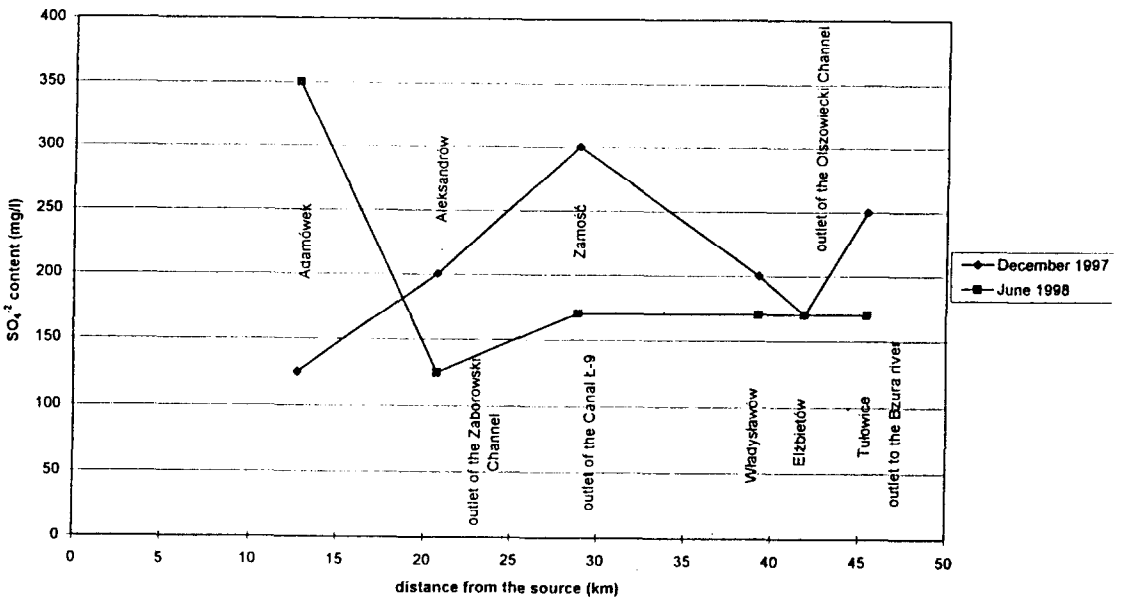

Figure 8: Changes in content of sulphate down the Łasica River.

It is a very important factor between the profiles in Władysławów and Elżbietów. In the farming areas between Adamówek and Zamość observed increase of hardness is more sharp than in the areas where the Łasica river flows through the pine forest (between Zamość and Władysławów).

3.4 Chloride

Chloride concentration showed a degree of stability all along the Łasica River. Measured concentrations varied from 9.0 to 24.0 mg/l. The differences between winter and vegetation season were relative low and varied from 2.0 to 5.0 mg/l (Fig. 7). Very interesting is sharp rise of the concentration in the outlet of the Zaborowski channel where concentrations of chloride reached 100.0 mg/l in the upper part of the catchment (Lipków). Left-side tributaries of Zaborowski Channel flow from rural areas on the glacial plain. Those streams collect water from operating wastewater treatment plants. The higher concentration of chloride round the year shows a season-independent causes of this fact. Before and after the outlet of the Zaborowski Channel, concentration of chloride in the water of the Łasica river is more or less constant.

3.5 Sulphates

The presence of sulphates in surface water and shallow groundwater is mostly connected with biogeochemical processes of organic matter decomposition and oxidation. High sulphate concentrations in surface water can be the result of human activity (e.g. wastewater treatment plants).

Sulphate concentration in the Łasica river varied between 125 mg/l and 350 mg/l (Fig. 8). The higher concentrations were observed in summer in the areas of wetlands. This was especially characteristic for the catchments of the Łasica river tributaries where the concentrations reached 400 mg SO_4/l. The sulphates concentrations profile for the Łasica River shows an increase downstream of the outlets of its tributaries (e.g. The Zaborowski Channel) and wetlands areas. The low temperatures in winter slow down the biochemical processes, and the concentration of sulphates in the wetland areas decreases. In the winter, when the confluence of the Łasica River in its middle part comes mostly from shallow groundwater, the observed content of sulphates can be even higher than in summer. Year-round high concentrations in the upper part of the catchment show the influence of wastewater treatment plants (in upper part of the Zaborowski Channel in Lipków) and groundwater pollution in the rural areas close to the City of Warsaw. Moving downstream, the concentration of sulphates, decreases very quick. In many profiles the Polish norm of sulphate content in drinking water (200 mg/l) was exceeded.

3.6 Ammonium, nitrate and nitrite

Ammonium, nitrate and nitrite are the main nitrogen compounds. Their presence in the surface water is an indicator of pollution. Wetlands, where biochemical processes of organic matter degradation act, can be the source of nitrogen compounds. In the process of nitrification, ammonium is oxidized to nitrite and nitrate (at pH = 7 and in the presence of O_2). According to Stumm and Morgan (1996) the main source of ammonium are fertilizers and processes of organic matter decay. Nitrate comes mostly from fertilizers and nitrite is a product of nitrification, denitrification and nitrate reduction. Typical progress in the transformation of ammonium to nitrite and nitrate in a small river affects the highest concentration of ammonium in the source part of the river and its quick decrease downstream.

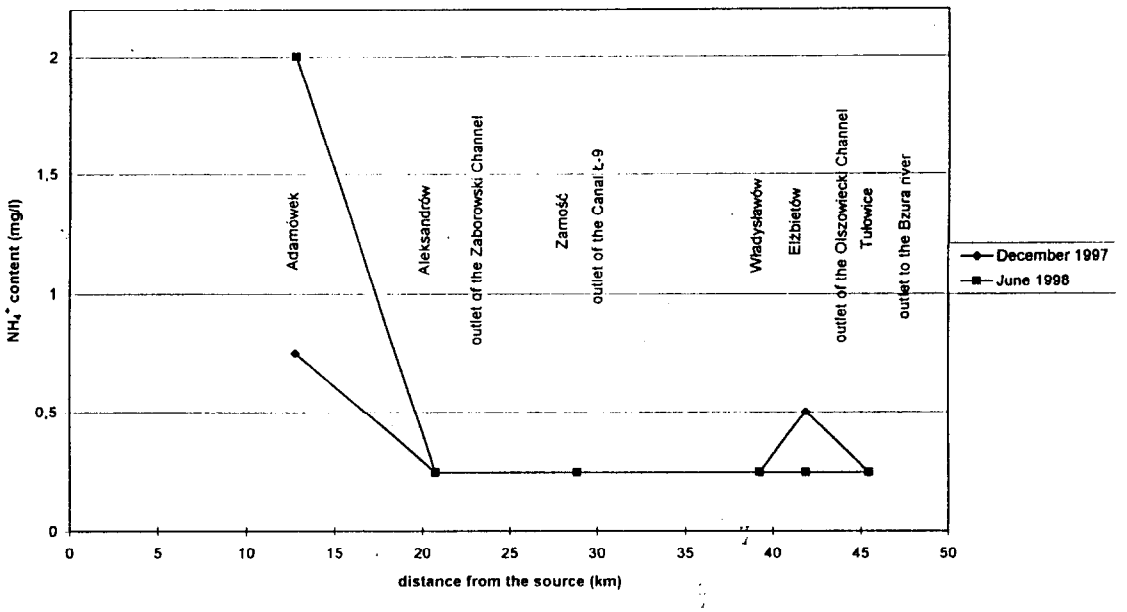

Figure 9: Changes in content of ammonium down the Łasica River.

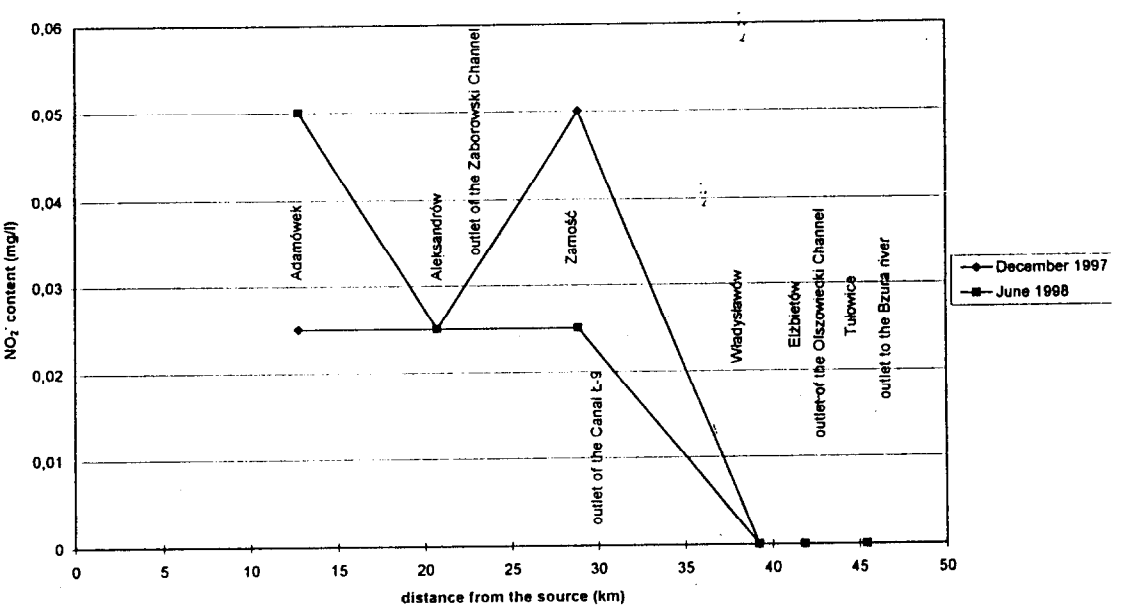

Figure 10: Changes in content of nitrite down the Łasica River.

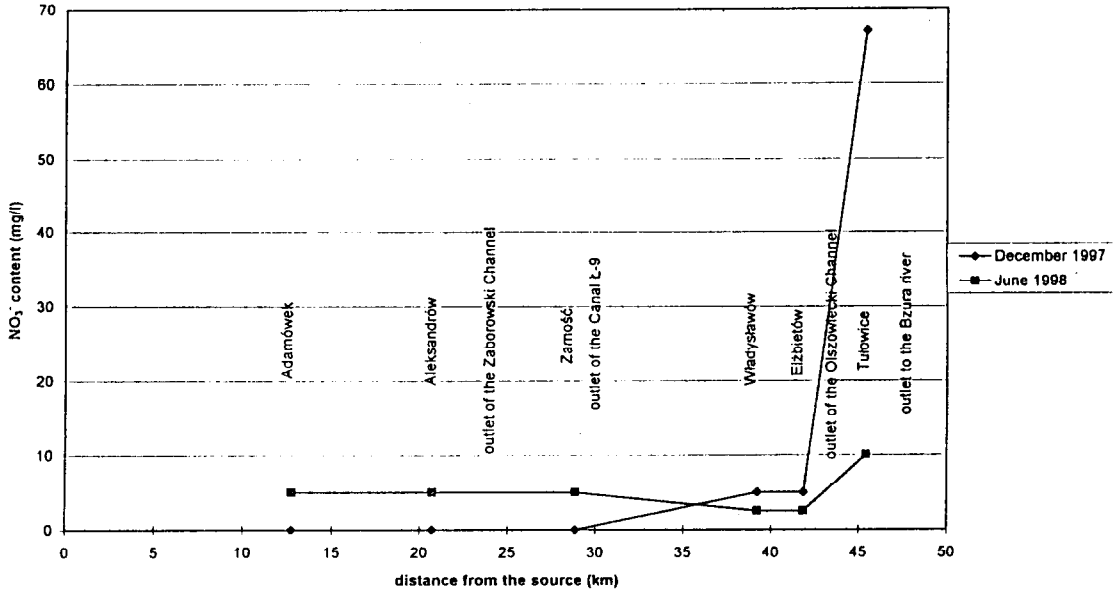

Figure 11: Changes in content of nitrate down the Lasica River.

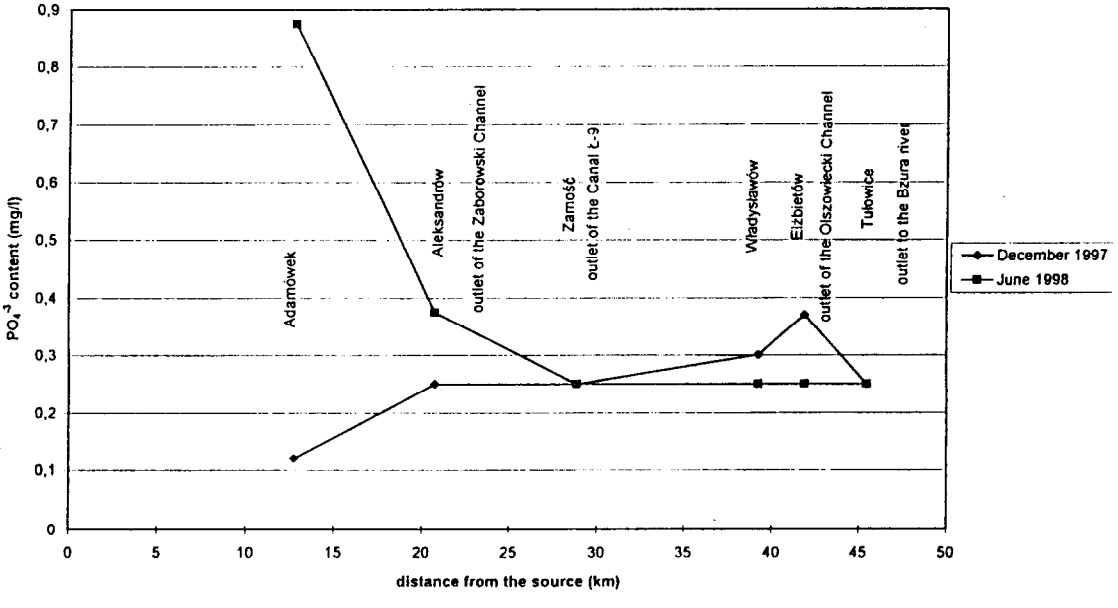

Figure 12: Changes in content of phosphates down the Lasica River.

The concentration of nitrite rises very sharply in the upper part of the river and decreases downstream. Nitrate content rises from 0 mg/l to its maximum close to the mouth of the river. Changes in concentration of ammonium, nitrite and nitrate down the Łasica River are very similar to typical concentration profiles. However, it is modified by the influence of tributaries and farming areas in the middle and southern part of the catchment. The concentration of ammonium varied between 0.25 mg/l and 2.0 mg/l (Fig. 9). The highest concentration was observed in the upper part of the river. The maximum concentration of nitrite was observed in Adamówek in the upper part of the river (June,1998), and in Zamość in the middle part of the river (December 1997). Values varied between 0 and 0.05 mg/l (Fig. 10). Downstream from Władysławów, nitrite was not present in the river water in December or in June.

Concentration of nitrate rose slowly downstream in the Łasica River but in December all the way down to Zamość it was equal to 0 mg/l (Fig. 11). A very sharp rise of the concentration up to 67 mg/l (Polish norm of nitrate content in drinking water is 10 mg/l) in Tułowice shows the possibility of strong pollution. So high concentrations were not even observed in June 1998 while, as a rule in summer, nitrate content in the river water is significantly higher.

3.7 Phosphates

The main sources of phosphates in the water are fertilizers and sewage discharge. Their presence in river water is an indicator of pollution. Concentration of phosphates varied between 0.12 mg/l and 0.87 mg/l (Fig. 12). In summer, the highest values occurred in the upper part of the catchment (Adamówek), decreased downstream and stayed constant as far as the mouth of the river. Compared to summer, winter concentrations of phosphates were lower in the upper part of the catchment and higher in the lower part. Content of phosphates was higher in the tributaries of the Łasica River. The main source of phosphates are the farming areas and wastewater treatment plants in the southern part of the catchment. The Polish norm of phosphate content (0.2 mg/l) was exceeded in almost all profiles, in accordance with results of Ciepielowski and Wawrzoniak (1997). In this situation necessary steps should be undertaken, especially in the case of the Zaborowski and Olszowiecki Channels which are strongly polluted in the upper parts close to the farming and rural areas.

4 Conclusions

The results of chemical analyses of the water are mostly in accordance with the results obtained by other authors in the similar types of landscapes. The high concentrations of phosphates, nitrate and nitrite were observed in the upper part of the catchment and in the streams flowing from the glacial plain (farming region). Within the National Park the concentrations are significantly lower except the regions with the strong groundwater outflow from the farming areas. This could be explained by the mechanism of river self-purification, which is less efficient during drought periods and intensive evapotranspiration. During the vegetation season concentrations of phosphate, nitrate and nitrite are usually lower in the whole catchment. Locally higher concentrations of the nitrate are caused by operating of wastewater treatment plants in the southern part of the catchment.

There are differences in natural water composition between the southern and northern parts of the Łasica catchment. The southern part is under the influence of streams flowing from the glacial plain, made up of loam and loamy sands. The pH of water and concentrations of calcium, chloride and sulphate are higher in this area (Wicik, 1997).

Along the streams, flowing to the north, composition of their water is modified and close to their outlets to the Lasica river is more typical for conditions in the valley. Features of the water in the northern part of the catchment are different to those from the southern part. The value of pH and the concentrations of calcium, chloride and sulphates are lower. As an implication, composition of water in the Lasica River changes from source to outlet. After connection with the tributaries from the south the hardness of water, and the concentrations mentioned above, are increased.

Farming and land improvement practices cause increased concentrations of nitrates, nitrites and phosphates. It leads in the short-term to degradation of the swamp ecosystems related to the lowering of groundwater level. Although the catchment of the Lasica River is a strictly protected areas, agriculture influence, even if remote spatially, is still evident.

References

[1] Ciepielowski A. and Wawrzoniak T. (1996) 'Quality of the flowing waters in Kampinos National Park' (in Polish). In: Magnuszewski A. and Soczyńska U. (eds.), 'Hydrologia u progu XXI wieku' materiały z Konferencji Hydrologicznej Mądralin k/Warszawy 24–27. 10. 1996.

[2] 'Hydrographical Atlas of Poland' (1980). IMGW Warsaw.

[3] Kazimierski B. et al. (1995), 'Protection plan of the Kampinos National Park - Protection of water ecosystems and water resources - Water conditions study' (in Polish). NFOŚ, Warsaw.

[4] Stumm W. and Morgan J. J. (1996) 'Aquatic Chemistry'. A Wiley-Interscience Publication, New York - Chichester - Brisbane - Toronto - Singapore.

[5] Wicik B. (1997), 'Chemical features of the landscapes within the Kampinos National Park' (in Polish). Prace i Studia Geograficzne t. XXI, WGiSR UW, Warszawa.

Rainfall interception modelling with the Brook model

in a Mediterranean mountainous catchment with spontaneous afforestation by Pinus sylvestris

P. Llorens[1], J. Buchtele[2]

[1]Institute of Earth Sciences "Jaume Almera", CSIC. Solé i Sabarís, s/n. 08028 - Barcelona, Spain. [2]Insitute of Hydrodynamics, Academy of Sciences of the Czech Republic, Pod Pat'ankou 5, CZ 16612 Praha 6, Czech Republic.

1 Introduction

In the framework of the VAHMPIRE project the hydrological modelling of Vallcebre catchments (East Pyrenees, Spain) has been performed working with the following hydrological models: SHETRAN, TOPMODEL, BROOK, SACRAMENTO and TOPKAPI.

From this set of models only two have rainfall interception submodels able to be analysed. These two models are SHETRAN and BROOK. The paper presents the first results of this modelling exercise with BROOK (Federer, 1993). It includes a comparison between modelled and measured rainfall interception for the study period of September 1994–June 1997. The same analysis has been made also for SHETRAN (Llorens & White, 1998).

2 The study area

At the Vallcebre experimental catchments (ERBES030) one of the study topics is the role of spontaneous afforestation of abandoned agricultural fields in the hydrological behaviour of catchments. In this Mediterranean mountainous area, spontaneous afforestation by scattered patches of Pinus sylvestris has occurred after the abandonment of agricultural fields in the 1950s, increasing considerably the surface covered by forest.

Two experimental plots, one grassed and another forested, were installed in 1993 in order to study the Soil–Vegetation–Atmosphere transfers in such heterogeneous catchments. The forested plot consists of a dense monospecific Pinus sylvestris patch of overgrown pines. At this experimental plot we record, at 5-minute steps, the water fluxes in the forest canopy which are necessary to determine the interception process: bulk precipitation, throughfall and stemflow (Llorens et al., 1997).

3 The Brook model

BROOK is a physically-based and one-dimensional model, which concentrates on the detailed simulation of evapotranspiration processes, vertical water flow in soils and runoff generation, and is a useful research tool for the study of catchment water balances. In the BROOK model rainfall interception is one of the five evapotranspiration components. Evaporation of interception rain (or snow) is calculated considering: (i) the canopy capacity, (ii) the average storm duration, (iii) the canopy resistance set to zero and (iv) the aerodynamic resistance based on the canopy height. Aerodynamic resistance (Shuttleworth & Gurney, 1990) depends on Stem Area Index SAI which is a parameter derived from Leaf Area Index LAI and canopy height.

The calibration of the BROOK model at the Vallcebre subcatchment named Cal Rodó (4 km^2) (Buchtele et al., 2000) was performed for the period September 1994–December 1995, and validated over the period January 1995–June 1997.

As the Cal Rodó catchment has a 60 % of the total area covered by pines, some of the canopy parameters, such as SAI and LAI, are 'calibrated' (by an iterative process) using both the flow records and the catchment land use map (Latron et al., 1997). The other parameters related to rainfall interception are default parameters provided by the model designer and obtained from the Hubbard Brook catchments for a conifer forest vegetation cover (Federer, 1993).

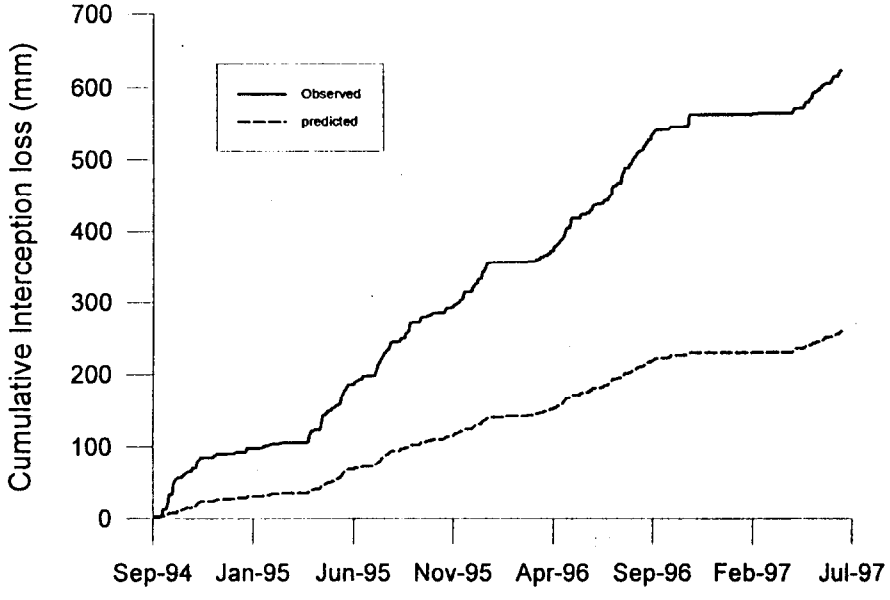

Figure 1: Cumulative observed and predicted by BROOK model interception losses for the period September 1994 - June 1997.

4 Results and discussion

The comparison between predicted and observed rainfall interception illustrates the difficulty of validating model predictions when the model is not spatially distributed, as in the case of BROOK. This problem, which arises due to the comparison of predicted lumped results, i.e. at catchment scale, with field measurements at a point, is enhanced because the study catchment is inhomogeneous in its geoecological characteristics (soils, vegetation cover, etc.).

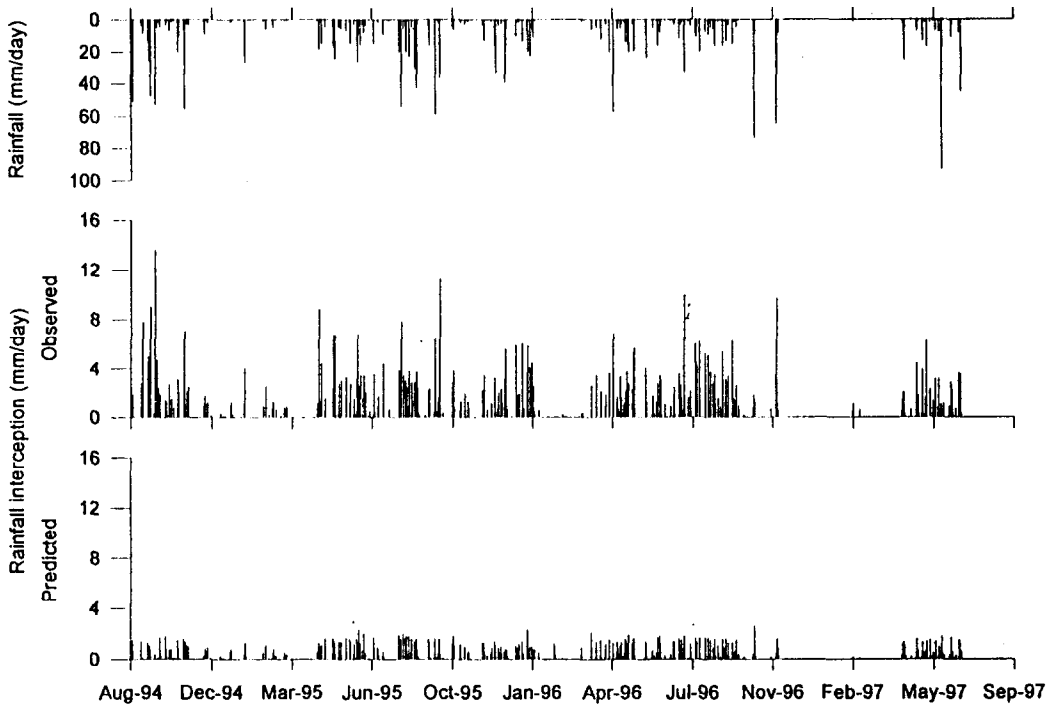

Figure 2: Temporal evolution of observed and predicted by BROOK model rainfall interception.

Keeping in mind this uncertainty a comparison between interception predicted for the Cal Rodó basin and interception observed at the forest experimental plot is presented. Fig. 1 shows cumulative observed and predicted interception losses for the whole study period (September 1994–June 1997), showing the clear underestimation of rainfall interception by the BROOK model.

Table 1: Summary of observed I_o and predicted by BROOK model I_p interception losses for the period September 1994 - June 1997.

rainfall P	observed interception I_o/P		predicted interception I_p/P		$I_o - I_p$	
(mm)	(mm)	(%)	(mm)	(%)	(mm)	(%)
2417.0	622.6	25.8	258.0	10.7	364.6	58.6

These differences are about 365 mm in absolute values, which represents a predicted interception of only 41 % of observed interception. When observed interception losses during the period are 26 % of the total rainfall the predicted interception is only a 11 %, implying a difference of 15 % with respect to rainfall (Table 1).

Considering that observed and predicted values correspond to different realities, we can suppose that the total observed interception (623 mm) corresponds to a catchment with a forest covering the 100 % of its area. If we have a catchment with a forest cover of 60 % (as

in Cal Rodó) the total rainfall interception would be 60 % of the former observed value, assuming in this approach that grasses do not intercept rain. This rough estimation yields an interception loss of about 374 mm. Taking into account this approach the differences between predicted and observed values diminished to 166 mm , that represents a predicted interception of 56 % of the observed one.

Even roughly considering the heterogeneity of the catchment, the differences between predicted and observed values are significant. Fig. 2 presents the temporal evolution of rainfall, observed and simulated interception losses during the period September 1994–June 1997. This figure shows that even the model follows the temporal pattern of rainfall, as it is designed to calculate the rainfall interception rate for each rainy day, although it clearly underestimates the measured rainfall interception. This illustrates the difficulty of an adequate parameterization, in these environmental conditions, at a daily time scale.

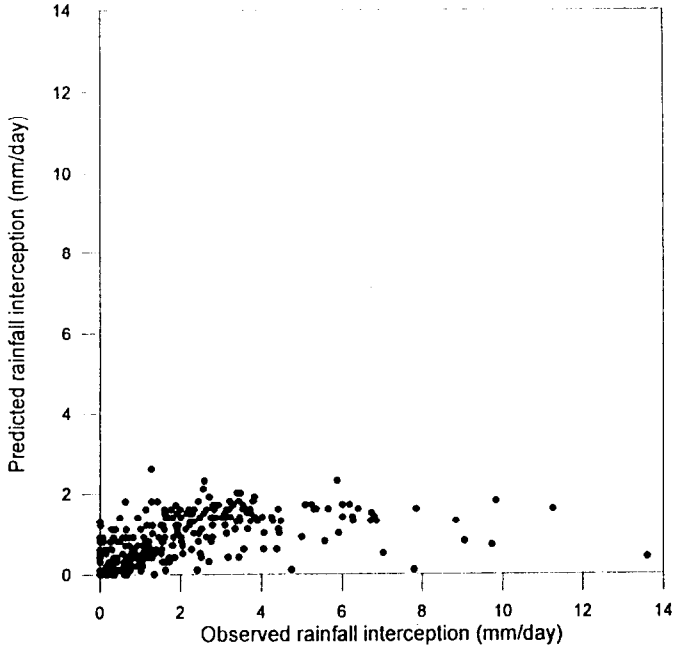

Figure 3: Observed Vs predicted daily interception for the studied period.

As shown in Fig. 3, simulated interception is limited to about 2 mm per day. There is an approximately linear relationship between observed and predicted interception losses for values of interception lower than 2 mm, but this linearity disappears for observed values higher than 2 mm. The predicted interception loss has a highest value of 2.6 mm although the observed one raises to values as high as 14 mm.

The obtained results show that differences between observed and BROOK predicted interception losses could not be related only to a possible lack of representativity experimental data. Eventhough, a more detailed analysis of the role of each vegetation cover would be done to achieve the comparison, the main task to do furthermore is to critically analyse each set of parameters used in this model run and to use a new parameters set more adjusted to the heterogeneity of the Vallcebre catchments. Recently performed experiments indicate that the improvement would be possible.

Acknowledgements

The present work is on the Spain side financed by the EC project: VAHMPIRE (ENV4-CT95-0134) and in the Czech Republic supported by Grant Agency of the Czech Republic (grant 205/99/1561).

References

[1] Buchtele, J.; Buchtelová, M.; Gallart, F.; Latron, J.; Llorens, P.; Salvany, C. & Herrmann, A. (2000): Rainfall-runoff processes modelling using SACRAMENTO and BROOK models in the Cal Rodó catchment (Pyrenees, Spain). In: V. Eliáš and I.G. Littlewood (eds), Catchment Hydrological and Biogeochemical Processes in Changing Environment. Proceedings of the Seventh Conference of the European Network of Experimental and Representative Basins (ERB), Liblice, Czech Republic, September 22–24, 1998.

[2] Federer, C. A. (1993): BROOK 90 - A simulation model for Evapotranspiration, Soil Water and Streamflow. USDA Forest Service, Durham, New Hampshire, USA.

[3] Latron, J.; Llorens, P. & Gallart, F. (1997): Data set n° 6. VAHMPIRE internal report.

[4] Llorens, P.; Poch, R.; Latron, J. & Gallart, F. (1997): Rainfall interception by a Pinus sylvestris forest patch overgrown in a Mediterranean mountainous abandoned area. I. Monitoring design and results down to the event scale. J. Hydrology, 199: 331–345.

[5] Llorens, P. & White, S. M. (1998): From point measurement to catchment data sets for internal validation of models. II-Example of rainfall interception. Ann. Geophysicae, 16(2): C498.

[6] Shuttleworth, W. J. & Gurney, R. J. (1990): The theoretical relationship between foliage temperature and canopy resistance in sparse crops. Q. J. R. Meteorol. Soc., 116, 497–519.

Sixteen years field monitoring of debris supply from an incised stream channel network

(Gallina experimental basin, North western Italy, 1982–1997)

F. Maraga, F. Di Nunzio, F. Godone, R. Massobrio, E. Viola

National Research Council of Italy, CNR-IRPI, Strada delle Cacce, 73, 10135 Torino, Italy.

1 Introduction

Long-term field investigations of debris supply by bed load transport at the outlet of a small experimental basin show the value of data collection for bed load analysis, description and prediction.

This report explains the results obtained from different field facilities managed in an alpine catchment in north-western Italy related both to bed load sediment volumes and to bed load transport mechanisms.

Since 1982 the 1.08 km^2 experimental basin Valle della Gallina in the Piedmont Alps has been monitored to measure simultaneously the hydrogeological balance and sediment yield from volcanic rocks exposed to meteorological disintegration and decomposition.

Apart from the scientific instruments, and mushroom harvesting, there is no human activity in the catchment.

2 The experimental basin

The experimental basin location and its stream channel network is presented in Fig. 1. Soil erosion has cut a dense stream channel network (52 km/km^2) that reaches into the bedrock and develops rill channels on the slope divides.

The soil is 1 m think on average, coarse-grained genetically produced by weathering of loose 'eluvium' and 'colluvium' materials from volcanic Tertiary rocks, which forms the uniform impermeable bedrock underlying the catchment. The bedrock outcrops over about 1 % of the basin area and frequently forms the channel beds (Bellino and Maraga, 1995). Vegetation consists of shrubs and chestnut trees covering 77 % of the basin area, except on the slope divides.

Mean annual temperature is 11.2°C, ranging between 21.0°C (July) and 1.2°C (January) from summer to winter (Bellino and Di Nunzio, 1996).

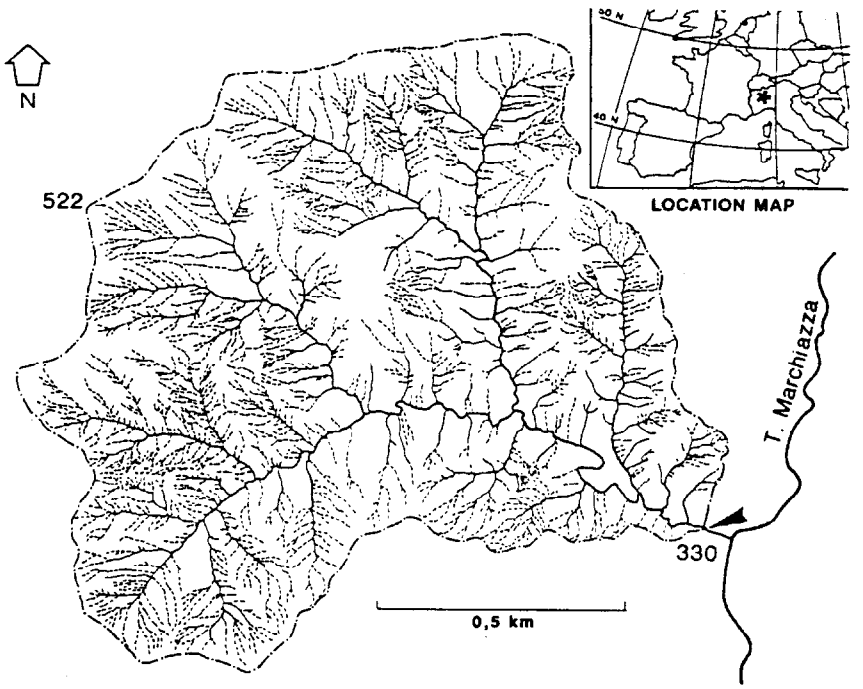

Figure 1: Location map of Valle della Gallina experimental basin (1.08 km^2) and their catchment with stream channel network drawn from aerial photographs. The elevation maximum and minimum are indicated as well as the position of the hydrometric and sedimentologic station (arrow).

Rainfall distribution is in accordance with the continental piedmont pattern in Mediterranean conditions (Caroni, 1979). Mean annual rainfall is 1266 mm, with a first maximum in the spring (April–May) and a second maximum in the autumn. In the summer (July) rainstorms are frequent.

Runoff showed a large range of peak flows from 0.005 m^3s^{-1} (18 July 1989) to 6.440 m^3s^{-1} (19 September 1995), the mean discharge being 0.02 m^3s^{-1}.

The mean annual discharge of 0.02 m^3s^{-1} corresponds to the limit exceeding 20 % of frequencies in runoff patterns investigated by annual and monthly discharge duration analysis, computed at intervals of 5 minutes, to detect also short-duration floods. April and October show the highest discharges rates, with a frequency of 10 % in discharge values higher than 0.15 m^3s^{-1}, whereas in the months of June and September the discharge rates higher than 0.15 m^3s^{-1} are less than 2.5 % frequent.

Main channel has a mean slope of 0.06 and the difference in height is 192 m between the higher basin elevation (522 m) and the measuring station at the basin outlet.

The debris delivery is mainly driven by the bed load processes of sand-gravel sized material created by disintegration of the bedrock and introduced into the channel network from the channel heads and directly from their banks. Suspended load is irrelevant in comparison with the bed load sediment transport.

The grain-size distribution of the bed load normally ranges from 0.006 to 256 mm, with a modal size in the 16–32 mm class. Some debris in the 256–512 mm class is transported by occasional bigger flows. The specific weight of the transported loose material varies between 1.4 to 1.6, depending on the grain-size distribution.

Physiographic and hydrologic characteristics of the Valle della Gallina experimental basin are summarised in Table 1.

The results presented here were obtained from 1982 to 1997 by measuring the annual sediment supply, water runoff and by simultaneous monitoring of water discharge and bed load transport.

Table 1: Physiographic and hydrologic characteristics of the Valle della Gallina experimental basin (Alps, North-western Italy).

Lithology	rhyolites
Area	1.08 km^2
Vegetation cover	77 %
Elevation (maximum-minimum)	522–330 m a.s.l.
Annual temperature (1982–1989)	11°C
Annual Precipitation (1982–1997)	1266 mm
Runoff coefficient	0.60
Mean discharge (1982–1997)	0.02 m^3s^{-1}
Maximum peak discharge (19 Sept. 1995)	6.44 m^3s^{-1}
Basin slope	0.49
Main channel length	1.57 km
Main channel slope	0.06
Annual bed load runoff (1982–1997)	38 m^3
Bed load grain size range	0.06–512 mm

3 Measurements

Records on the bed load runoff were collected in the terminal segment of the main channel at the hydrologic station located at the outlet of the basin.

The terminal main channel segment runs straight for about 50 m and slopes 0.08, and is incised in a channel cutting about 4 m into the bedrock, 7 m wide at the bank full and 5 m at the bottom. The in-channel bed load is characterised by a thin movable bed composed of coarse material with a variable thickness from 0.1 to 1.5 m, depending on irregularities of the bedrock. This segment makes up the delivering channel to the debris materials produced by bedrock weathering in the basin and collected by the transport in the channel network towards the outlet of the catchment.

In the furthest downstream stretch of the segment a sedimentation trap has been created by a cement wall 1m high built up from the rigid channel bed 8 m upstream from the hydrometric section. In continuity with the wall, cement covers the channel bedrock in the portion between the wall and the hydrometric section, regulating the bed to 1 m high on the banks. This was done to prevent alteration of the original dimensions of the channel bed and to facilitate measuring the sediment volumes with an accuracy of 0.01 m^3 to the maximum capacity of the trap of 35 m^3.

The accumulated material is sampled using a mechanical shovel to maintain the trap's efficiency in collecting material deposited there.

The sediment flowing through the terminal segment is defined for each transport event by the volume of sediments caught in the trap and the grain sizes of the material.

3.1 Topographic survey

The terminal reach is equipped with bench marks nailed in the bedrock of the stream banks, in the crest of the wall and in the edges of the debris trap, which are regularly used to survey the height of the gravel bed and the material caught in the trap. The surveys were taken with the aid of instrumentation enabling the measurements to be automatically recorded on memory modules. The investigations involving detailed topographic surveys of the bed surface start from 1984 (Fig. 2).

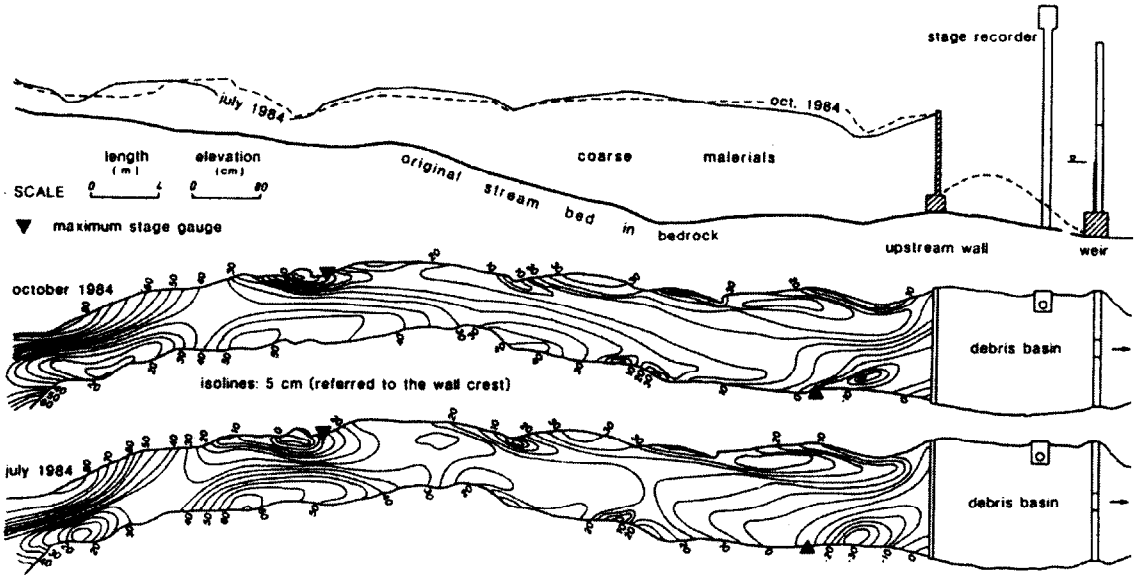

Figure 2: Main channel instrumented reach at the outlet of the basin. Talweg profiles and bed forms (elevation isolines) are presented before and after bed load transport (modified from Anselmo and Maraga, 1985).

Channel bed surfaces (300 m^2) are periodically surveyed at an average of 300 points for each survey, the points being more closely spaced where the bed forms are present, so as to obtain a very accurate picture of local geometrical characteristics.

The bench marks are always surveyed from two station bases; in this manner it is possible to obtain a precision of 0.15 m at the horizontal position and of 0.2 m at the vertical position.

Field data are numerically and graphically processed with software specifically developed to define the topographic features of the channel bed surface by plotting the contour lines or generating the regular terrain grid. Any variations in the channel bed morphology are quantified by their horizontal and vertical changes.

The morphological data on the bed load carried away from the terminal main channel reach were taken by the comparison of the detailed topographic surveys made before and after the following sediment transport events, which occurred after 1984: between November 1986 and July 1987, with 33 m^3 of sediment delivery and a maximum peak flow of 5.25 m^3s^{-1}; between July 1987 and September 1987, with 35 m^3 and a maximum peak of 2.93 m^3s^{-1}; between September 1987 and June 1991, with 139 m^3 and a maximum peak of 5.79 m^3s^{-1}; between June 1991 and October 1991, with 28 m^3 and a maximum peak of 1.83 m^3s^{-1}.

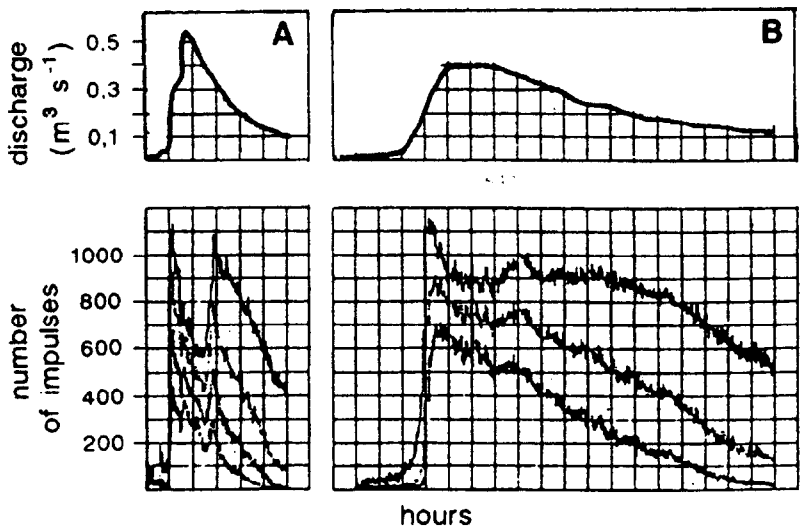

Figure 3: Debris bed load pulses enhanced by geophone related to selected peak flows of 13 October (A 0.53 m^3s^{-1}) and 25 November 1990 (B, 0.39 m^3s^{-1}) (volumes trapped in A unknown, in B 0.29 m^3). Above: the hydrographs. Below: the sediment transfer drawn by the microseismic impulses number per minute exceeding predetermined threshold values of ground oscillation velocity at the same occasions of above hydrographs.

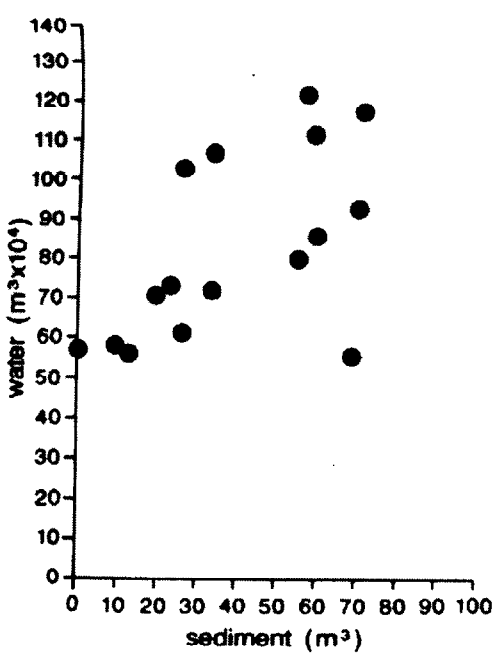

Figure 4: Annual water and sediment runoff relationships. Except one point the debris bed load is produced above a line starting at 560 m^3x10^4 of water volume, with sediment runoff volumes from 0 to 12 m^3.

3.2 Geophones experience

A field experiment for continuous monitoring of bed load runoff was operated in the main channel terminal reach from July to November 1990 by seismology devices, at the same time with the water runoff monitoring.

The sensors were seismic detectors with a natural frequency of 1 Hz, generating a voltage proportional to the ground oscillation velocity with a sensitivity of 240 V $m^{-1}s^{-1}$. Five seismometers were placed on the channel banks for up to 150 m upstream of the hydrologic station. Another seismometer was placed in the stream-bed debris, buried to a depth of 0.3 m immediately upstream of the concrete weir of the sedimentation basin. Individual sensors were connected to the recorder. Seismometer position in the gravel bed just upstream the concrete wall of sedimentation basin obtained the better response on the sediment runoff (Govi et al., 1993).

During seismic monitoring, seven floods were recorded at peak flows from 0.14 to 0.86 m^3s^{-1} and five of them occurred with sediment delivery.

Data were analysed to determine the average velocity of ground oscillations induced by water and sediment runoff and to count the number of impulses per minute exceeding threshold values of velocity starting from the step of average oscillation velocity at peak flow of 0.14 m^3s^{-1}.

Data processed from the sensor embedded at the concrete weir proved able to distinguish water discharges with and without bed load transport.

The velocities approximate the synchronous hydrographs, while the number of impulses per minute display singularities in comparison with the synchronous hydrographs of the floods with sediment transport.

In fact, microseismic anomalies related to sediment delivering floods strengthen the view that the bed load process occurs by pulses during a flood flow. Two or three microseismic impulse peaks are delayed on the hydrograph and were associated with bed load pulses, the first coming at the rising limb of the hydrograph and the others occurring during the recession limb (Fig. 3).

4 Results and discussion

Data on the sediment volumes have been regularly collected since January 1982. During the 1982–1997 the annual specific sediment load was 36 m^3km^{-2}, with a maximum of 65 m^3km^{-2} measured in 1987.

Temporal analysis points out sediment runoff versus water runoff do not concord during a single flood flow and nor in annual response, because at the same water volume different sediment volumes occur or no sediment is delivered (Fig. 4).

A specific hydrologic analysis on the peak flows distribution and their influence on sediment transport and transport distances could be executed in order to define the counting discharge limits in water volumes calculation.

Sediment and water volumes therefore indicate similarity on the linear evolutionary trend, indicating a divergent pattern over the years (Fig. 5).

Over sixteen years of observation the cumulative sediment-water volume pattern indicate a deficiency of sediment supply from the catchment. This indication suggest at long time physical conditions not able to promote soil production nor hydrographic evolution, then exhaustion of sediment delivery.

Topographic data collected from 1984 to 1991 revealed vertical changes in the movable bed elevation, which are produced by alternating processes of cutting and filling. The surveys demonstrate a mechanism of sediment delivery characterised by a wave form

propagation in the channel, about ten times longer than the width of the channel bed. Cut and fill at the bed results in a temporary bed load process involving a thickness of 0.1–0.3 m of the gravel bed.

Finally, seismic monitoring data recorded in 1990 reveal that bed load transport changes in intensity during the same flood flow event. Particularly, two or three minor delivery pulses are detected after the peak flow.

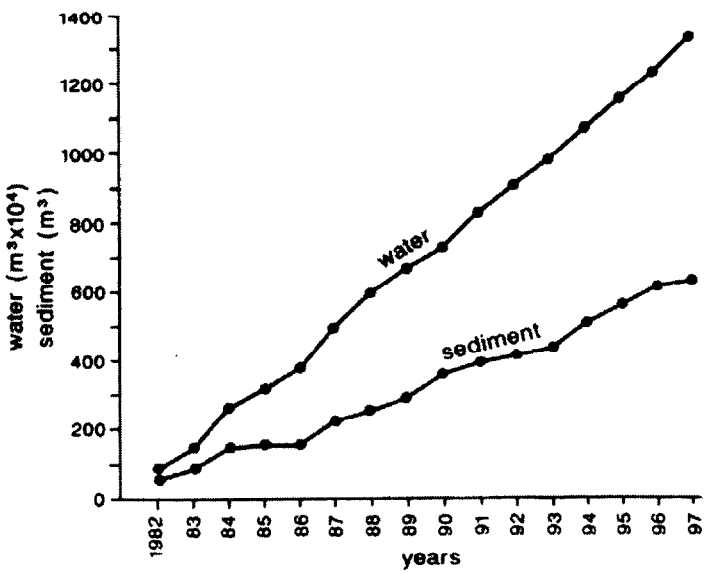

Figure 5: Annual water and sediment runoff trends shown by the cumulative curves. The debris bed load curve shows some steps of increase independently of water volumes.

5 Hydrologic remarks

The behaviour of the sediment runoff by bed load debris transport in relation to water runoff is described in the Valle della Gallina experimental basin as follows:

- water runoff directly correlate with sediment runoff enhancing significant discrepancies;
- a discharge threshold equal to 0.11 m^3s^{-1}, compared with a mean discharge of 0.02 m^3s^{-1}, must be overcome in order to generate processes of mobilisation and bed load transport of the debris fraction equal or smaller than the mean grain size;
- discharge threshold equal to 0.33 m^3s^{-1}, must be overcome in order to generate processes of mobilization and bed load transport of the debris fraction larger than the mean grain size;
- sediment delivery have a pulsate pattern both during a single flood flow process and at the scale of bed form evolution along the channel;
- at an equal discharge efficacious for debris mobilisation, the possibility of sediment transport depend on the availability of material in the movable bed up to a distance upstream of the trap wall equal to six times the bed width.

The continuity of data collection is aimed to develop hydrologic forecast studies by recording the cyclic variations of sediment runoff and analysing their relationship with waste mantle evolution, soil erosion, sediment production from a forested mountain catchment in the Mediterranean Alps.

Acknowledgements

This paper was prepared with collaboration of: C. Tantaro (word editing) and P.G. Trebò (figures scanning), CNR-IRPI, Torino, Italy. In the framework of experimental researches carried out in the Po basin by funds of National Researches Council of Italy.

References

[1] Anselmo V. and Maraga F. (1985) 'Cobble movement and sediment transport in a streambed'. Proc. CNR-PAN meeting Progress in mass movement and sediment transport studies, Torino, Italy, Dec. 5–7, 245–264.

[2] Bellino L. and Maraga F. (1995) 'Temps de saturation en bassin versant'. Proc. International Meeting Young Researchers in Applied Geology, Peveragno (CN) Italy, 11-13 Oct. 1995, 254–259.

[3] Bellino, L., Di Nunzio, F.(1996) 'Analisi dei dati di temperatura in un piccolo bacino sperimentale (Valle della Gallina, Lozzolo, VC)' (in Italian). CNR-IRPI, Torino, Internal Report, M. I. 96/15.

[4] Caroni E. (1979) 'Rainfalls of Eastern Biellese region' (in Italian). Bul. of Associazione Mineraria Subalpina, XVI, N. 4, 889–909.

[5] Govi M., Maraga F., Moia F.(1993) 'Seismic detectors for continuous bed load monitoring in a gravel stream'. Hydrol. Sciences J., 38 (2), 123–132.

Sediment yield from badlands catchments:

analysis and interpretation at different basin and time scales for the Draix catchments, (Alpes-de-haute-Provence, France)

N. Mathys

Cemagref Grenoble, Division Erosion Torrentielle, Neige et Avalanches,
2 rue de la Papeterie, BP 76, 38402 Sain-Martin-d'Héres Cedex, France.

1 Introduction

In the Southern French Alps, the Black Marls formation, called in French 'Terres Noires', covers large areas. This formation is very susceptible to weathering and erosion with a 'badlands' topography, and causes high solid transport. In order to obtain data to quantify and analyse this phenomenon, Cemagref and RTM, the operational service in charge of uplands natural hazards survey and mitigation, have equipped since 1984 several small catchments at Draix, 15 km north-east of Digne. This paper presents the main results obtained for erosion during nearly 15 years, focusing on statistical analysis of sediment yield during storm events and on annual sediment yield rates. The possibility of correlation between erosion and hydroclimatologic or morphometric parameters is investigated in order to predict erosion at the outlet of a marly basin. These results should be of great use for extrapolation to other basins on similar lithology.

2 Measurement site, equipment and available data

Five basins have been equipped since 1982 for the measurement of rainfall, liquid discharges and both bedload and suspended solid transport. These basins have different areas, from 1300 m^2 to 1 km^2. Only four are still monitored now, three in denuded areas with vegetation cover rate from 21 to 56 %; the last one was afforested at the end of the last century, within the frame of RTM works, and is now 87 % of its surface area is covered with pine forest (Table 1). Five pluviographs measure the precipitation of the study area and at the outlet of each catchment a set of different devices allows the measurement of liquid discharge and sediment transport (Fig. 1).

Rainfall and discharge, with self-gauging flumes, are measured continuously, at a one-minute time step. Deposits in the sediment traps (coarse solid transport) are measured if possible after each flood, or after a small group of floods. Suspended sediment transport

is sampled with discontinuous samplers in the flume downstream of the sediment traps (Cambon et al., 1990). However, because of heavy sediment load, up to 300 or 500 g/l, the samplers are often out of order and the lack of suspended sediment data may be frequent.

Because of these difficulties in maintaining the samplers and of the concentration fluctuations observed, a continuous measurement of solid discharge was searched. As the concentrations of suspended sediments were too high for most of the available devices, a prototype, based on the backscattering of light by particles in suspension was designed for this experimental site. The optical fibre sensor, installed in 1995, is strong, simple, and non intrusive in the flow. It gives good measurements of the concentration but is sensitive to the grain size distribution (Bergougnoux et al., 1996).

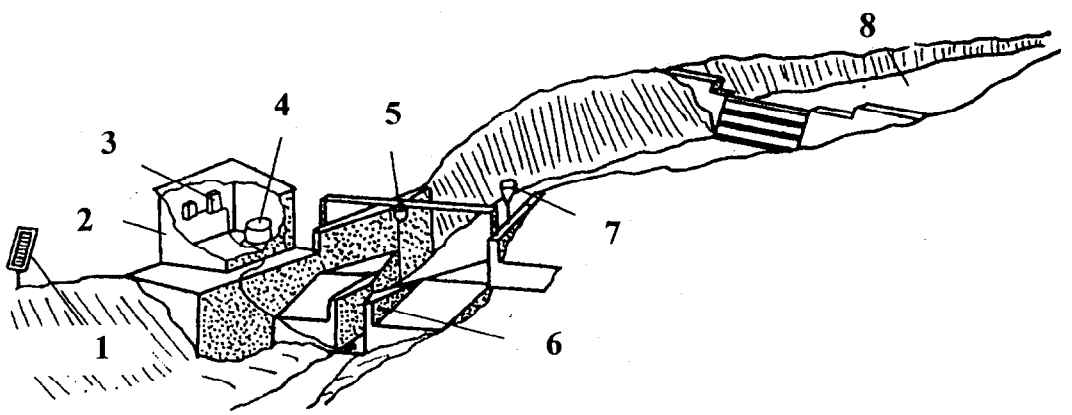

Figure 1: Equipment of a gauging station. 1 - solar batteries, 2 - shelter, 3 - data logger, 4 - sampling equipment, 5 - limnigraphs, 6 - selfgauging station, 7 - pluviographs, 8 - sediment trap.

Table 1: Characteristics of the basins.

Basin name	Area (ha)	Denudation rate (%)	Average slope	Observed since
Roubine	86	79	75	1983
Moulin	8	54	30	1988
Laval	0.133	68	58	1984
Brusquet	108	13	53	1987

3 Statistical analysis of the sediment yield

As shown in Fig. 1, sediment production is measured both with deposited volumes in the trap and sediment concentration of samples downstream through the gauging station. When bad site conditions or a short duration between two floods lead to deposit measurement for more than a single flood, different interpretations may be applied to separate this amount for each flood of the period. Sampling is ordered by a program of the data recorder taking account of water level variation and time lag between two samples. The

concentration of each sample is obtained by weighing after drying at 105°C in an oven. This gives a discontinuous measurement of sediment load. For all the floods sampled, no relationship was founded between discharge and sediment concentration but for a single flood a hysteresis curve is very often observed and can be used to make a concentration evaluation for the points of the hydrograph that were not sampled. After this interpolation, sediment concentration is calculated for each point of the hydrograph and total discharge is separated in liquid and solid discharge. The integration of the whole solid hydrograph for the duration gives the total amount of sediments exported during the flood event (Mathys and Meunier, 1989). The erosion variables studied are, for each flood completely measured and sampled; average concentration C_{moy}, maximum concentration C_{max}, total volume V_{mes} of suspended sediment, total volume V_{dep} of deposits, total erosion production Poi_{tot}. As the density of deposit is about 1.7 and density of suspended material 2.7, $Poi_{tot} = 1.7\,V_{dep} + 2.7\,V_{mes}$. When erosion can only be evaluated for a period with several storm events, only V_{mes}, V_{dep} and Poi_{tot} are significant. The descriptive variables studied were numerous, either related to rainfall characteristics, maximum intensity at different time step (I_{01}, I_{15}, I_{30} for 1, 15, 30 min time step), kinetic energy calculated with a Wishmeier formula, total depth H_{tot} or partial depth above an intensity threshold (H_{05}, H_{10} for part of the rain with an intensity higher than 5, 10 mm/h), or on runoff characteristics, peak discharge Q_{max}, total runoff volume, etc.

4 Summary of selected observations

Except in winter, the floods are very short ('flash floods'), quick and intense. They are very heavily loaded. As shown in Table 2, the peak discharges are very high for such small basins. On September 8th 1994, a storm event, widespread on the study area, caused a flood of about 20 m^3/s on the Laval basin and more than 2 m^3/s on the Brusquet basin, though it is a forested basin.

Table 2: Summary of selected observations.

Basin name	Maximum peak discharge		Maximum concentration	Maximum deposit in 1 flood
	l/s	m^3/s/km^2	g/l	m^3
Roubine	80	60	260	2.5
Moulin	1900	24	420	50
Laval	20000	23	650	700
Brusquet	2300	2.3	30	

In the Laval catchment (0.133 ha), the fine sediment concentration is very high, frequently more than 300 g/l (on average twice a year). The annual maximum fine sediment yield of a flood ranges between 113 m^3 (1991) and 750 m^3 (1997). The maximum volume for a deposit during a single flood (700 m^3) occurred in July 1987, during a storm event with a hail sequence. In the Moulin catchment (8 ha), the maximum concentration is lower - 420 g/l - and only a few floods exceed 300 g/l. The maximum volume for a single flood reaches 40 m^3 for fine sediments and 50 m^3 for coarse material in the sediment trap. On the Roubine catchment (86 ha) only 20 % of the floods exceed 100 g/l and the maximum concentration remains always below 300 g/l (Richard and Mathys, 1997).

5 Main results at the scale of an event or a few events

5.1 From the Roubine elementary gully to the Laval catchment, a size scale effect

The main results can be summarised by two multiple non-linear regression models using either two or three variables :

Roubine	$Poi_{tot} = 0.69\, H_{tot}^{0.85}$	$I_{01}^{1.18}$		N = 64	$R^2 = 0.97$
Laval	$Poi_{tot} = 4515\, H_{tot}^{0.87}$	$I_{01}^{0.51}$		N = 65	$R^2 = 0.76$
Roubine	$Poi_{tot} = 0.64\, H_{tot}^{0.90}$	$I_{01}^{1.14}$	$Q_{max}^{1.24}$	N = 60	$R^2 = 0.99$
Laval	$Poi_{tot} = 5303\, H_{tot}^{0.48}$	$I_{01}^{0.21}$	$Q_{max}^{0.34}$	N = 65	$R^2 = 0.97$

These models, calibrated over the 1984–1988 period were validated over the period 1989–1990, and successfully used and controlled in the following period. We can observe that on Roubine the two models give similar results whereas on Laval the 3-variables model, including Q_{max}, is much better than the 2-variables model with only rainfall parameters. This is the first scale effect; Roubine can be considered as an elementary erosion unit where scouring processes are well correlated to rainfall erosivity but in the Laval catchment, the phenomenon of transport or deposit in the reaches of the torrent leads to the necessity of adding a discharge parameter to obtain a good explanation of the sediment production at the outlet. This effect is confirmed when relative proportions of transported and suspended volumes are compared; in the Roubine, 85 % of the total erosion is stored in the sediment trap and only 40 % in the Laval. That means that the marl platelets are disintegrated during the transport in the reaches of Laval when most of the sediments are still coarse at the outlet of Roubine (Borgès, 1993).

5.2 The medium basin of Moulin, as indication of a threshold in the size scale effect

The Moulin, an intermediate size (8 ha) catchment, allowed the study of erosion at a medium scale.

Moulin	$Poi_{tot} = 147\, H_{tot}^{0.88}$	$I_{05}^{0.74}$		N = 104	$R^2 = 0.69$
Moulin	$Poi_{tot} = 310\, H_{tot}^{0.55}$	$I_{01}^{0.26}$	$Q_{max}^{0.39}$	N = 104	$R^2 = 0.76$

On this catchment, we can consider that the transport of sediment by the flow plays a role on sediment export, but less important than in Laval. Deposited volumes represent 53 % of total erosion, much less than for the Roubine, but sediment are less desegregated than in Laval, as the distance and duration of transport are shorter. We can observe that the ratio of coarse material decreases rapidly with the basin size and assess that over a few km^2 most of the particles of marls are transported in suspension.

5.3 Observations on the erosion from vegetated plot, an indication on elementary processes

Studies have been undertaken at Draix since 1991 on the effects of vegetation by herbaceous seeding. For the measurement of efficiency of vegetation trials, two small gullies (310 and 606 m^2) were equipped with a sediment trap at their outlets. Deposited volumes after each storm were measured before and after seeding. Statistical analysis of 28 storm events in the 2 years before seeding shows that, as for Roubine, rainfall depth and intensity explain most of the sediment yield. A single and simple parameter, the rainfall depth of the period over a threshold of intensity (15 mm/h) explains more than 70 % of variance. Erosion on the 310 m^2 plot is well correlated (R^2 = 0.92) to Roubine erosion over the same period, whereas the 606 m^2 gulley shows a greater dispersion (R^2 = 0.69), (Crosaz, 1994). The slope of the gullies seems to be of great influence on material export, as in the steeper slopes of the first all the particles of marls are quickly transported at the bottom whereas for the other one, there is temporary storage of eroded material inside the basin.

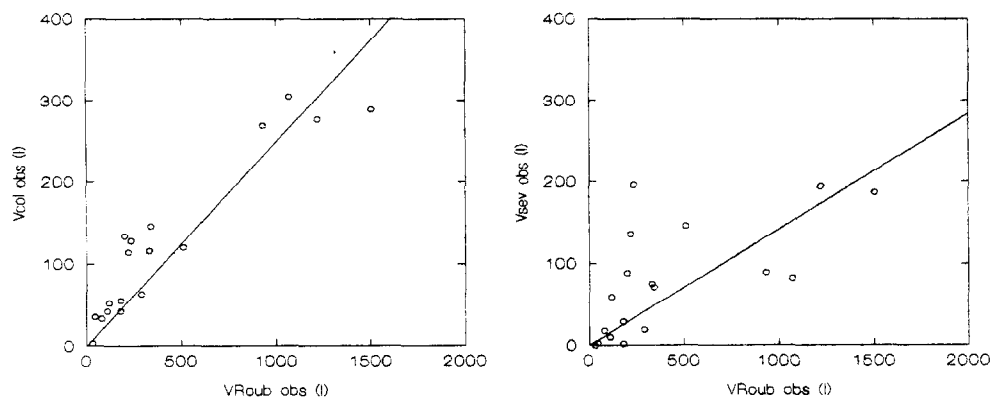

Figure 2: Erosion on the two small gullies compared to erosion on Roubine at the scale of a few storms.

5.4 Using statistical results at the event scale to fill in missing observations

To obtain the total annual sediment yield, it is necessary to add suspended material volumes to deposited (in sediment traps) volumes. Except when storms occur before the emptying of full sediment traps, the deposited volumes are easily well measured, but the lack in suspended sediment volumes are frequent. The above results allow complete estimation either at a storm event scale, with regression formulas using hydrologic variables, or at an annual scale, using the result of the suspended/deposited ratio (Mathys et al., 1996).

6 Annual sediment yield analysis

6.1 Annual results of the observation period

Annual volumes, for the denuded surface area of each catchment are given in Table 3.

Table 3: Annual erosion, mean m and standard deviation s.

	85	86	87	88	89	90	91	92	93	94	95	96	m	s
Roubine	118	262	163	174	89	138	132	350	163	310	174	222	191	76
Moulin				66	25	141	99	185	114	174	81	156	113	49
Laval	91	159	166	103	64	181	135	311	176	270	139	263	171	72
Brusquet				2	2	2	3	8	7	17	1.4	6.8	5	5

Erosion values over 100 t/ha/year are measured on the three denuded catchments. This represents an ablation of the marl bedrock (density 2.6) higher than 4 mm per year, which is the value found for the most erodible soils in the world (Walling, 1988; Mahmood, 1987). Mean annual erosion rate is nearly the same in Roubine and Laval, which have similar mean slope, and lower in Moulin, which has a lower slope. For the Brusquet, 87 % covered with forest, sediment yield reported for the denuded area is 40 times lower than that measured on the Laval basin, 220 times lower if it is reported to the total area of the watersheds.

6.2 Statistical law of annual erosion

The annual erosion rate on denuded basin varies in a large range, from 64 to 270 for the Laval for example. The annual values can be adjusted to a Gumbel law and the 10-years return period erosion estimated to 220–270 t/ha/year (Laval and Roubine).

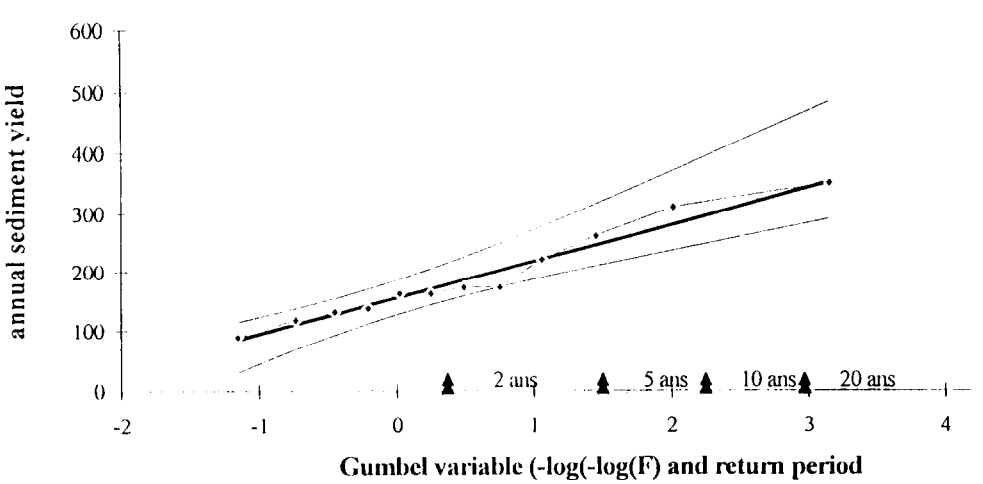

Figure 3: Statistical law of annual Laval sediment yield.

6.3 Relation between annual sediment yield and annual rainfall

Table 4 shows that annual erosion is better correlated to annual rainfall for the Laval than for the Roubine. The more intense part of annual precipitation explains better erosion on Roubine, showing the dominating effect of the scouring phenomenon at this scale. For the Laval, P_{05}, related to the rainfall events producing runoff, is a good parameter to predict annual sediment yield and may take into account both scouring and transporting material (Figs. 4, 5).

Table 4: Correlation coefficients between annual erosion and annual rainfall depth without (P) or with (P_{05}, P_{10}, ...) an intensity threshold (5, 10 mm/h ...).

	P	P_{05}	P_{10}	P_{15}	P_{20}
Roubine	0.68	0.74	0.75	0.78	0.79
Laval	0.85	0.93	0.91	0.89	0.87

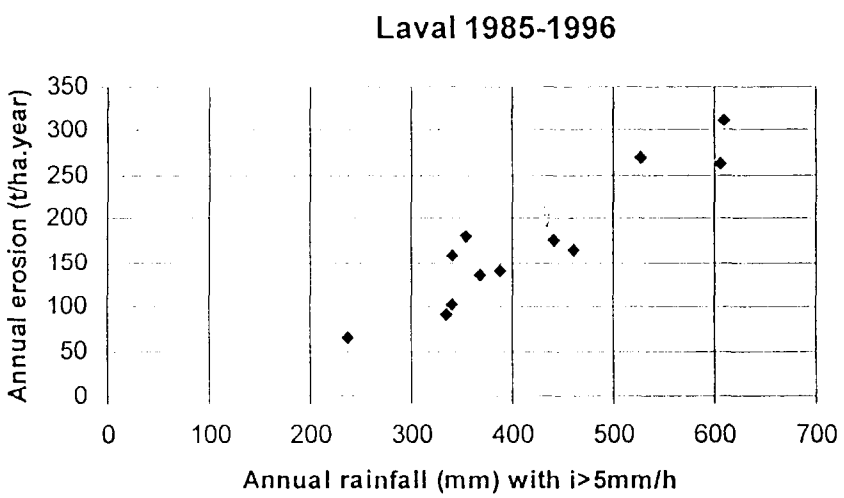

Figure 4: Relation between annual erosion and annual rainfall above 5 mm/h. Laval 1985–1996.

7 Conclusion

The measurements of erosion at the outlet of these basins show that specific sediment yield is considerably reduced on the forested basin compared to the denuded ones. On the badlands zone, annual mean erosion rate seams to be un-correlated to the catchment size and influenced by the basin slope. The factors predicting sediment yield of storm events show the influence of the size on the processes involved ; mainly scouring and slope quick transport for elementary gullies, scouring, transporting, deposit and re-transporting at a scale of nearly 1 km^2. The effect of transport in the reaches begins to be observed as soon as a main channel is present, as for the Moulin (8 ha). A more detailed analysis of the processes occurring inside the basins is necessary now to improve the knowledge and modelling of sediment production on such areas. This is important to enable extrapolation

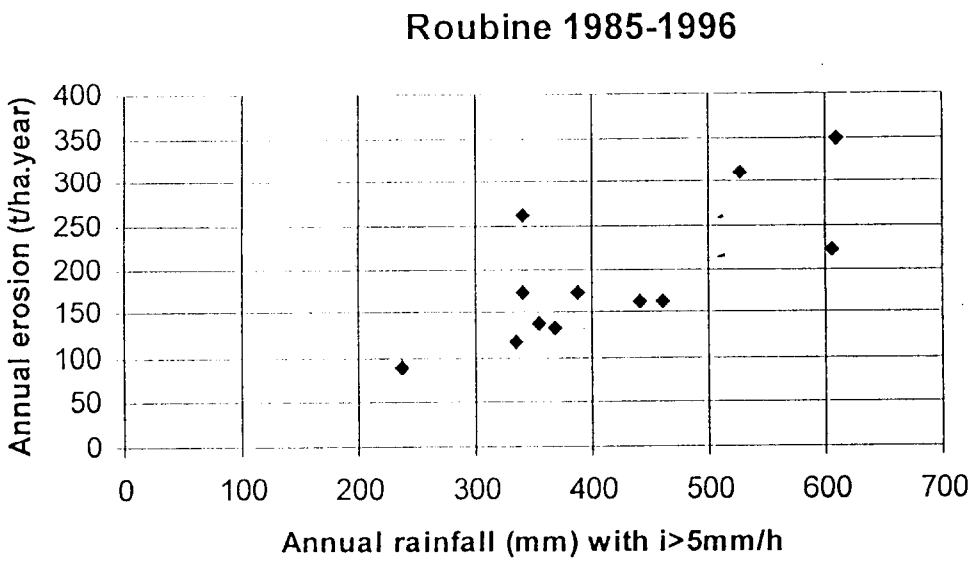

Figure 5: Relation between annual erosion and annual rainfall above 5 mm/h. Roubine 1985–1996.

of the results. As there is a strong socio-economic dimension for quantifying erosion, mainly to sediment management through the Durance basin, it would be necessary to widen the significance of representativity.

References

[1] Bergougnoux L., Misguich-Ripault J., Firpo J-L. and André J., 1996, Monte Carlo calculation of backscattered light intensity by suspension: comparison with experimental data. Appl. Opt., 35, 1735–1741.

[2] Borgès A.-L., 1993, Modélisation de l'érosion sur deux bassins versants expérimentaux des Alpes du sud. Thèse de l'université Joseph Fourier, Grenoble, spécialité mécanique, soutenue le 19 février 1993. 205 pages + biblio. + figures + annexes.

[3] Cambon J.-P., Mathys N., Meunier M., Olivier J.-E., 1990, Mesure des débits solides et liquides sur des bassins versants expérimentaux de montagne. IAHS publ. n° 193, 231–238.

[4] Crosaz Y., 1994, Le matériel végétal, un outil pour la protection des sols. 11èmes journées du Réseau Erosion, Paris, 20-22 septembre 1994. Bulletin n° 15 du Réseau Erosion, 449–460.

[5] Mahmood K. (1987). Reservoir Sedimentation. Impact, Extent and Mitigation. World Bank. Tech. Paper., 71, 118 p.

[6] Mathys N., Meunier M., 1989, Mesure et interprétation du processus d'érosion dans les marnes des Alpes du sud á l'échelle de la petite ravine. Colloque transport solide, la Houille Blanche n° 3/4, 1989, 188–192.

[7] Mathys N., Brochot S., Meunier M., 1996, L'érosion des Terres Noires dans les Alpes du sud : contribution à l'estimation des valeurs annuelles moyennes (bassins versants expérimentaux de Draix, Alpes de Haute-Provence). Revue de géographie alpine, tome 1984, n° 2, 1996, 17–27.

[8] Richard D., Mathys N., 1997, Historique, contexte technique et scientifique des BVRE de Draix. Caractéristiques, données disponibles et principaux résultats acquis au cours de dix ans de suivi. Actes du séminaire 'les bassins versants expérimentaux de draix, laboratoire d'études de l'érosion en montagne', Draix-le Brusquet-Digne, France, 22–24 octobre 1997, 11–28.

[9] Walling D.E. (1988), Measuring sediment yield from river basins. In: R. Lal (editor), Soil Erosion Research methods, Soil Water Conserv. Soc., Iowa, 39–79.

Hydrogeological and geochemical investigations of agricultural nutrients

on a typical groundmoraine site in NE-Germany - model based scenario studies of groundwater pollution

C. Merz[1], K. C. Kersebaum[2] and A. Wurbs[3]

Center for Agricultural Landscape and Land Use Research; [1]Institute of Hydrology. [2]Institute of Landscape Modeling. [3]Institute of Land Use Systems and Landscape Ecology, Eberswalder Str. 84, 15374 Münchenberg, Germany.

1 Introduction

Agricultural land-use is the main non-point source pollution of groundwater in Germany. About 40 % of surface water contamination through nitrogen is caused by exfiltrating groundwater (Flaig & Mohr, 1996). Therefore the development of sustainable land-use systems to improve or preserve groundwater quality is of great relevance.

On the typical sandy soils of North Germany nitrate leaching is a serious problem due to small water-holding capacity and low denitrification rates. Integrated and organic farming systems were compared regarding their effects to reduce nitrate concentrations in a small catchment with high nitrate contamination. To assess the vulnerability of the whole soil/aquifer system regarding nitrate dynamics a model chain was realized by linking the deterministic models HERMES, SIFRONT and FEFLOW considering the complete soil profile from the root zone to the aquifer. Scenarios were calculated to assess the effects of agricultural management on a regional scale.

2 Methods

The investigation area, a small hydrological catchment, is located in Brandenburg 40 km east of Berlin. The hydrogeology is characterized by morphologically formed groundmoraines of the last boulder period. The unconfined aquifer consists of glacial sandy and gravel sediments. The depth to the water table varies from 10 m to 15 m in the northern part of the site to less than 1 m at the western border.

Two agricultural management systems were established in 1989 on a field of 24 ha, where high amounts of slurry were applied during the previous decade (1970–1987). Intensive measurements of nitrate concentrations were carried out between 1989 and 1996 in the root and unsaturated zone. Sampling of seepage water and sediment was carried out by static Cone Penetration Testing CPT. Additionally a network of 50 groundwater

observation wells was installed at the experimental site and its surroundings on a total area of 40 ha between 1989 and 1991 to investigate the geochemical composition of the groundwater at different depths. From 1992 onwards each observation well was sampled in spring and autumn respectively.

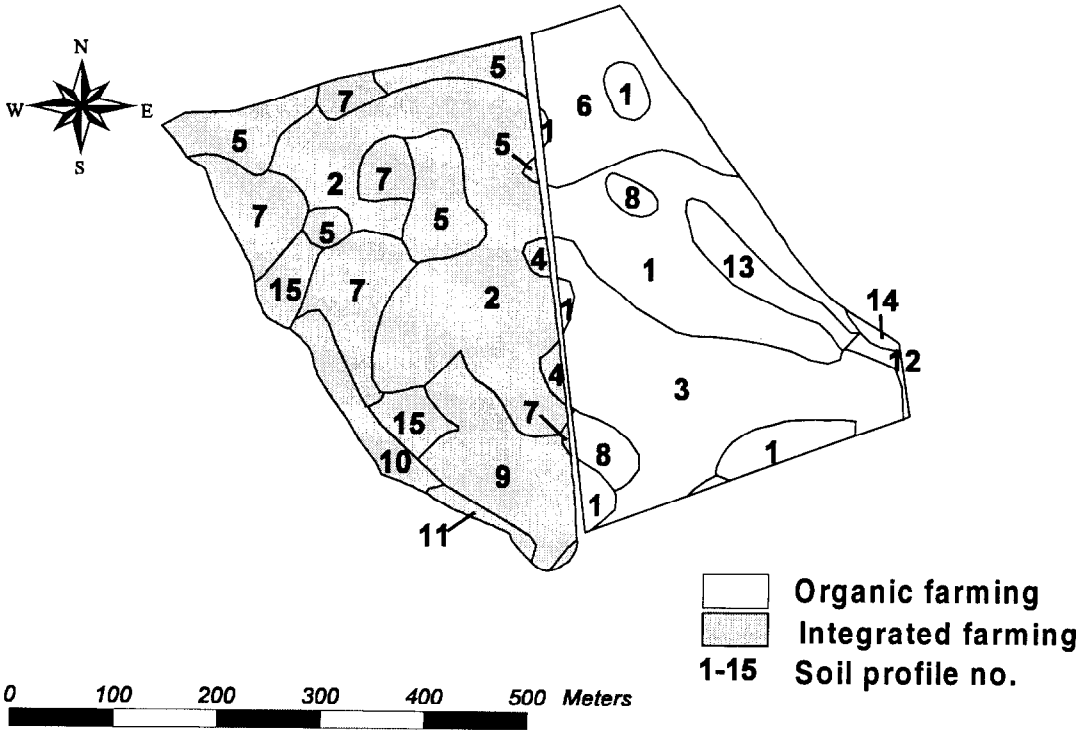

Figure 1: Spatial distribution of the soil types and farming systems on the investigation site (profile data and crop types - Table 1).

The nitrogen dynamics and transport in the root zone, in the unsaturated zone and in the aquifer were simulated by three models which were linked by their output and input files. The HERMES model (Kersebaum & Richter, 1991; Kersebaum, 1995) simulates nitrogen dynamics in the soil-plant system of the root zone. The input data required by the model are: soil information (texture class, organic matter content, groundwater table depth), daily weather data (precipitation, temperature, vapour pressure deficit, irradiation) and agricultural management data (crop, sowing and harvest dates, fertilization, yield). The daily fluxes of seepage and nitrogen were used as input by the model SIFRONT (Michel, 1991), which simulates nitrate transport and denitrification from the root zone to the groundwater table. Nitrate losses in the unsaturated zone were calculated as well as travel times to determine the spatio-temporal nitrate flux at the interface between unsaturated and saturated zone. The results for nitrate flux were used as input to the groundwater model FEFLOW-3D. FEFLOW-3D (Wasy, 1993), a Finite Element subsurface flow system (FEM), represents an interactive, graphics-based modeling system for confined or unconfined groundwater flow and contaminant transport (Diersch & Gründler, 1993). Measured nitrate distribution and groundwater contour lines for 1989 were used as initial input conditions. Observed concentrations of the groundwater influx at the border of the investigation site and the spatially distributed results of SIFRONT simulations (groundwater recharge and nitrate concentrations) were used as boundary conditions. For the mathematical model a network of 19800 finite elements was constructed in 9 calculation layers.

Table 1: Soil types and selected profile data used to simulate nitrogen dynamics of the investigation site. FC - field capacity, WP wilting point, acc. to Bodenkundliche Kartieranleitung, 1994).

Profile no.	Soil type	Depth (cm)	Texture class	FC (Vol %)	WP (Vol %)
1	Cambic	0–30	silty sand	30	9
	Arenosol	30–40	silty sand	26	8
		40–200	medium sand	16	6
2	Cambic	0–30	slight silty sand	22	6
	Arenosol	30–40	slight silty sand	19	5
		40–180	medium sand	16	6
		180–200	sandy silt	31	11
3 + 4	Luvic	0–30	very silty sand	33	9
	Arenosol	30–80	silty sand	26	8
		80–200	medium sand	16	6
5 + 6	Leptic	0–30	silty sand	30	9
	Podzol	30–60	slight loamy sand	20	6
		60–160	slight silty sand	19	5
		160–180	medium sand	16	6
		180–200	loamy sand	20	6
7 + 8	Eutric	0–30	slight silty sand	22	6
	Podzoluvisol	30–60	slight silty sand	19	5
		60–140	fine sand	16	6
		140–200	medium sand	14	4
9	Arenosol	0–20	slight silty sand	22	6
		20–60	slight silty sand	19	5
		60–200	clay loam	35	11
10	Stagnic	0–30	slight loamy sand	26	7
	Podzoluvisol	30–60	slight loamy sand	22	6
		60–150	slight loamy sand	22	6
		150–200	slight loamy sand	22	7
11 + 12	Gleysol	0–30	slight loamy sand	26	7
		30–70	slight loamy sand	22	6
		70–200	medium sand	19	6
13	Kolluvisol	0–30	slight loamy sand	26	7
		30–80	slight loamy sand	22	6
		80–100	silty loamy sand	30	11
		100–200	fine sand	18	6
14 + 15	Cambisol	0–30	loamy sand	22	9
		30–60	very loamy sand	28	12
		60–80	slight loamy sand	22	6
		80–200	fine sand	18	6

Table 2: Selected management of the investigation site and representative weather data. PET - potential evapotranspiration, * given as calcium ammonium nitrate, ** green manure (oil radish), *** green manure (contains: *Lolium multiflorum*, *Trifolium incarnatum*, and *Vicia villosa* (Rothmaler, 1990)).

Crops	year	Measure	integrated farming system	organic farming system	rainfall (mm)	PET (mm)
Winter rye	1989	fertilizer: org.			384	582
		min.	120 kg N ha^{-1} *			
		pesticide:	1,0 l ha^{-1} Sportak			
Potatoes	1990	fertilizer: org.	300 dt ha^{-1} manure	300 dt ha^{-1} manure	606	502
		min.	100 kg N ha^{-1} *			
		pesticide:	2,0 l ha^{-1} UVON			
Winter rye	1991	fertilizer: org.			357	687
		min.	100 kg N ha^{-1} *			
		pesticide:	1,0 l ha^{-1} Sportak			
Maize	1992	fertilizer: org.	**	***	419	686
		min.	105 kg N ha^{-1} *	200 dt ha^{-1} manure		
		pesticide:				
Lupines	1993	fertilizer: org.	lupines ploughed under	lupines ploughed under	625	633
		min.				
		pesticide:	40 kg N ha^{-1} *			
Oats	1994	fertilizer: org.			712	671
		min.	40 kg N ha^{-1} *			
		pesticide:	1,0 l ha^{-1} Sportak			
Winter rye	1995	fertilizer: org.			507	603
		min.	100 kg N ha^{-1} *			
		pesticide:	2,0 l ha^{-1} Camposan			
			0,5 l ha^{-1} Tilt			

To assess the potential remedial effects of the two farming systems on a regional scale scenario simulations with HERMES were accomplished using 3 dominant soil types (Luvic Arenosol, Hapic Luvisol and Cambisol) of a region in East-Brandenburg (district of Märkisch-Oderland with 42700 ha arable land) and a time series of 8 years from a representative weather station (1989–1995). For each farming system two typical crop rotations were defined, which were simulated 8 times with shifted starting dates to avoid individual combination effects of annual weather and crops.

3 Model results

Mineral nitrogen contents in the soil (about 130 kg N ha^{-1}) were very high at the beginning of the experiment due to the high amount of slurry applied in the past. Following the changes of the management system the amount of mineral nitrogen in the root zone decreased significantly which is shown in Fig. 2a for the integrated plot.

The results of the spatially distributed simulation show a high temporal and spatial variability of the nitrate concentrations of the seepage water corresponding to the weather conditions and soil properties (Fig. 2b).

The spatially distributed nitrate concentration of the seepage water at the bottom of the root zone during the period 1989–1995 was simulated. Over this period the areally weighted average of nitrate leached from the organic managed part of the field (244 kg N ha^{-1}) was lower than on the integrated part (319 kg N ha^{-1}). The amount of

percolation water on the organic part was also reduced (644 mm versus 911 mm) due to a longer soil cover with crops and a higher average of water holding capacity of the soil types. The overall averaged nitrate concentration in the seepage water at the bottom of the root zone was calculated to decrease between 1989 and 1995 from 244 mg NO_3 l^{-1} to 92 mg NO_3 l^{-1}.

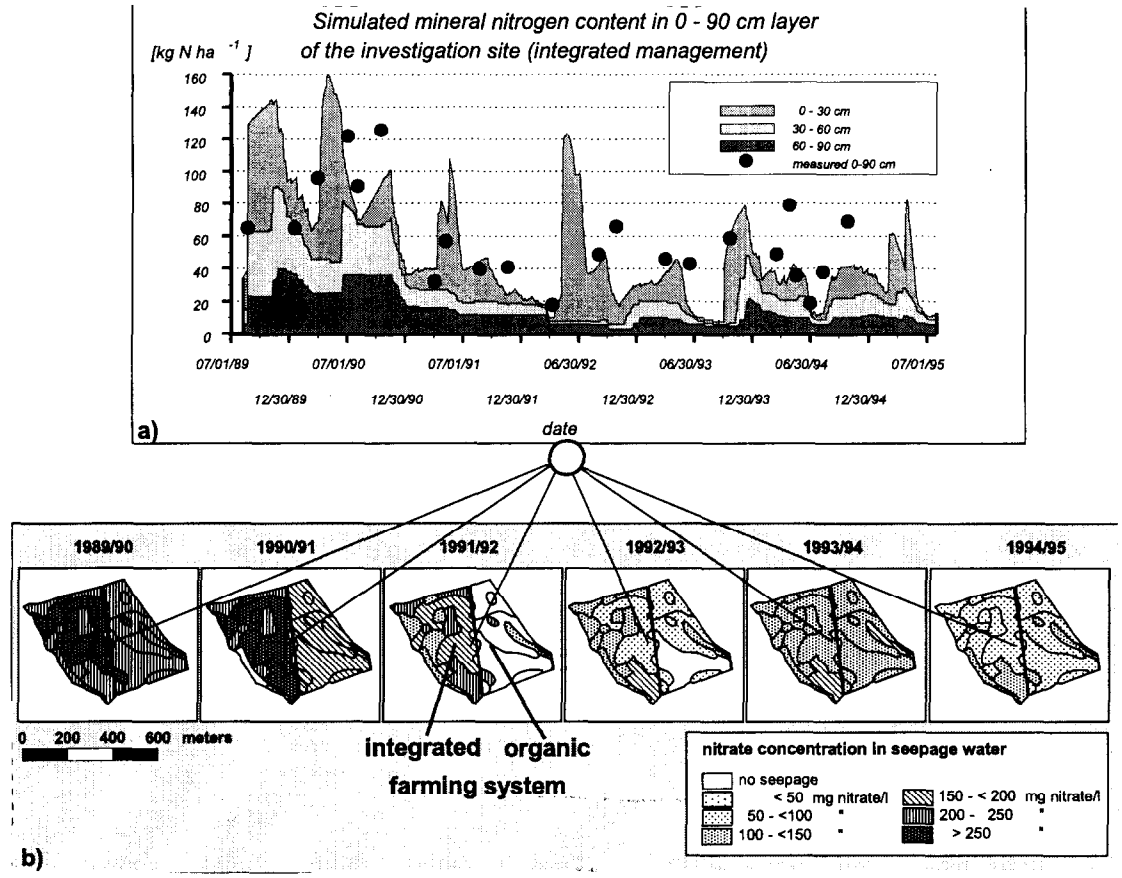

Figure 2: a) Simulated mineral nitrogen in 0–90 cm of the integrated management plot and b) spatio-temporal distribution of nitrate concentrations in seepage water of both farming systems (1989–1995).

The denitrification potential in the unsaturated zone was calculated with SIFRONT for the complete soil profiles using a DOC depending Michelis Menten kinetic. For a soil profile with 5 m thickness subject to 100 mm percolation over a long period, the model simulated that only 5 % of the infiltrated nitrate was degraded in a sandy soil. In a loamy sand soil profile nearly 30 % of the nitrate was eliminated by denitrification (Voigt & Michel 1997). The simulation of nitrate transport and degradation was carried out considering the spatial distribution of soil units as well as the different depths to the water table (0.5 m to 9.0 m). The results of SIFRONT indicate that changes of nitrate amounts in seepage will reach the groundwater 11 years at the latest after changing the agricultural management (Fig. 3).

To simulate the spatial distribution of nitrate in the groundwater before 1989 different input scenarios of nitrate were calculated with FEFLOW to achieve the measured nitrate concentrations. Scenario simulations were used due to the lack of information about the nitrate input conditions prevailing during the period from 1970 to 1989. Based on these

scenarios the period from 1989 to 1996 was calculated by FEFLOW to simulate the nitrate migration in the groundwater (Fig. 4). Time variable nitrate and percolation amounts from the unsaturated zone were linked to FEFLOW-3D by spatial flux conditions (Cauchy-term). Compared to the measured distribution of nitrate in the groundwater there is only a small difference to the calculated results for 1996.

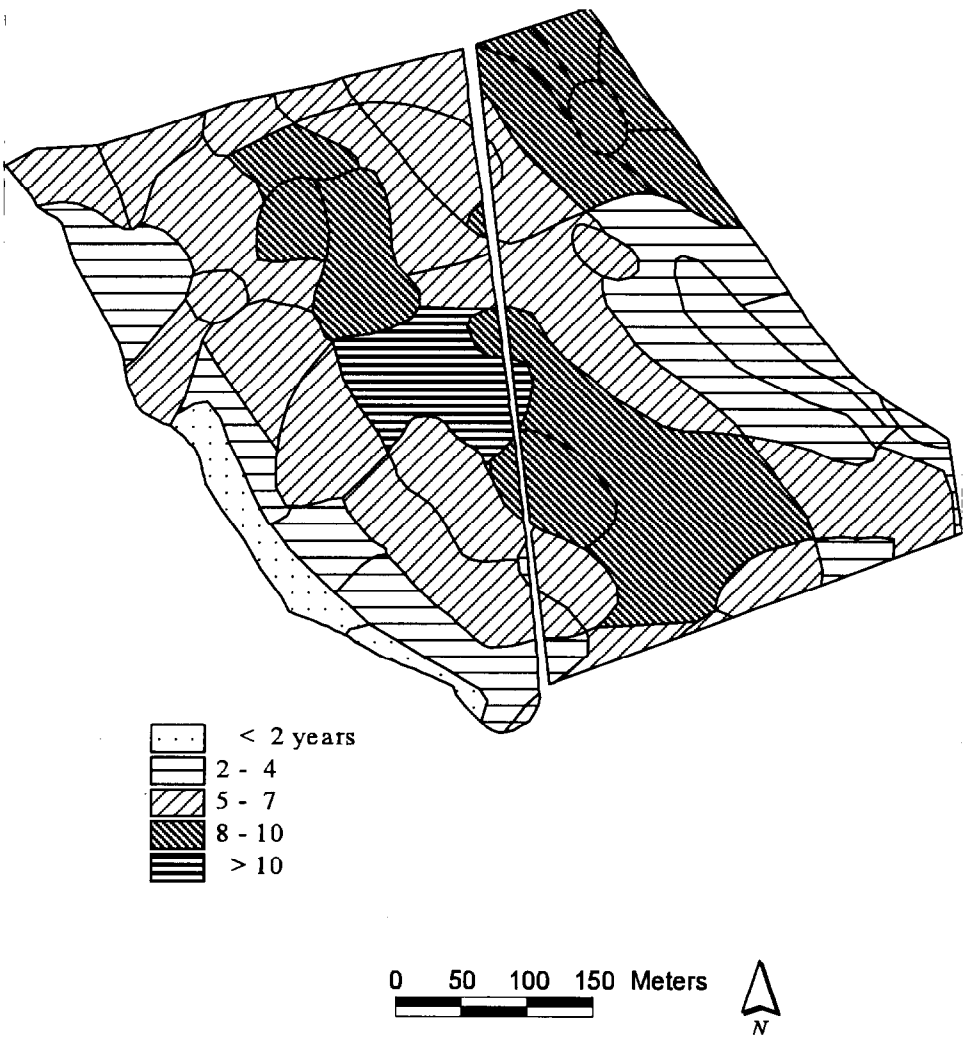

Figure 3: Travel times of seepage water from the root zone to the aquifer calculated by SIFRONT.

The results of the scenarios show the dominating effect of soil type on the total amount of nitrate leaching over the simulated period of eight years (Fig. 5). Compared to this, differences between the organic farming system and the integrated system are relatively small under the climate conditions of North-East Germany. Nevertheless, the average annual amount of nitrogen leaching in organic farming systems was estimated to be 22–37 % lower than in integrated farming systems over the period of the crop rotation (Fig. 5). Regarding the concentrations, differences between both systems were leveled due to the lower amounts of seepage in the organic farming system. It has to be emphasized that on sandy soils neither the integrated nor the organic system achieved seepage concentrations below the European drinking water standard of 50 mg NO_3 l^{-1} (11.3 mg NO_3-N l^{-1}).

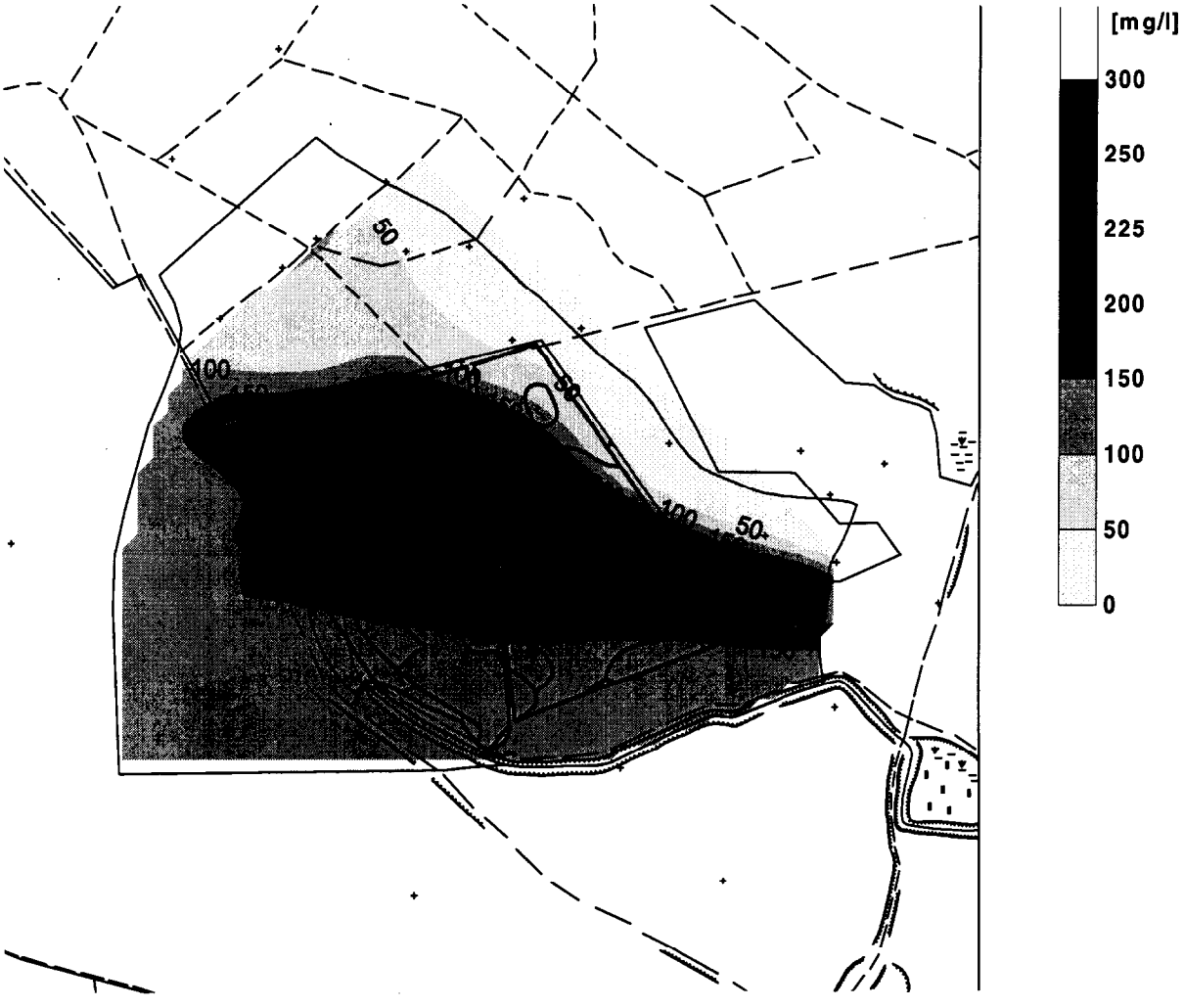

Figure 4: Distribution of nitrate concentrations in the aquifer in 1996 calculated by FEFLOW (1970–1996).

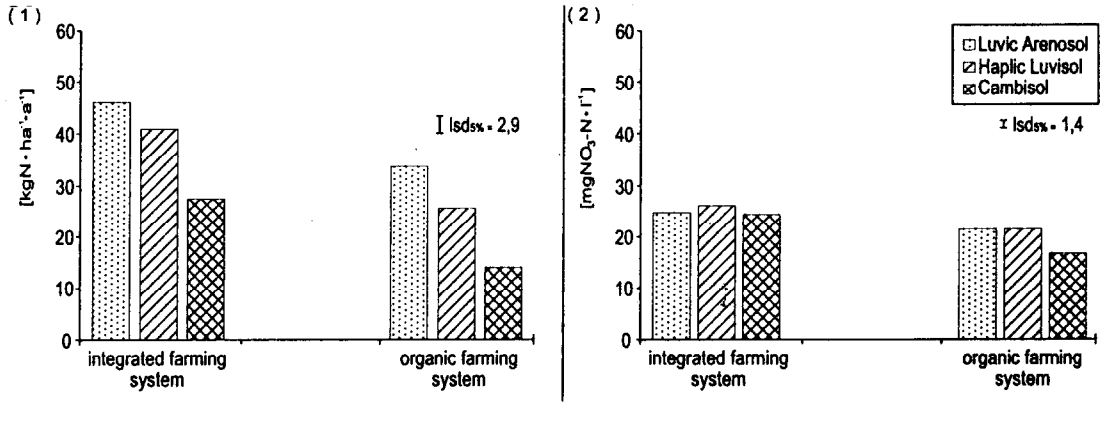

Figure 5: Average annual amount of N-leaching from the root zone (1) and N-concentrations in 2 m soil depth in integrated and organic farming systems for different soil types (480–550 mm of annual precipitation).

4 Conclusions

The application of models allows simulation of the effects of alternative crop rotations and management systems on groundwater water quality. Due to high temporal and spatial variability of state variables in sandy soils, a good correlation between measurements and simulations is difficult to achieve on a field or regional scale. Nevertheless, the simulation as well as the measurements show a similar trend between the two management systems.

The simulation results indicate that measured differences between plots in the root zone have to be interpreted very carefully because management effects are often overlaid by alternating soil properties. Calculations with the models SIFRONT and FEFLOW show that, under the special conditions of the site investigations, significant remedial effects for the contaminated aquifer can be expected at the earliest 9 years after the management has been changed.

On sandy soils the amount of N-leaching from the root zone seems to be reducible by the establishment of organic farming systems under a variety of environmental conditions. Nevertheless, the nitrate concentrations are highly affected by the different amounts of seepage water of the farming systems.

Under the typical conditions of climate and soils of North-East Germany the organic farming system shows only little advantages compared to the integrated system on a regional scale. The decision for the best management practice has to include site specific aspects e.g. climate and soil properties. In a watershed context a reduction of nitrate pollution by 15 % requires a conversion of 50 % of the area to organic farming. Therefore suitable economic and political boundary conditions have to be established based on scenario calculations.

Acknowledgements

The authors wish to thank the Federal Environmental Agency, the German Federal Ministry of Nutrition, Agriculture and Forestry and the Ministry of Nutrition, Agriculture and Forestry of Brandenburg state for their financial support of this project.

References

[1] Bodenkundliche Anleitung (1994): Kartieranleitung der AG Boden. Hrsg. Bundesanstalt für Geowissenschaften und Rohstoffe und Geologische Landesämter der Bundesrepublik Deutschland, 4. Auflage: 392 S.

[2] Diersch, H. J., and R. Gründler (1993): GIS based groundwater flow and transport modeling - The simulation system FEFLOW. in On Application of Geographic Information Systems in Hydrology and Water Resources. International Conference. Vienna, Austria.

[3] Flaig, H., and H. Mohr (1996): Der überlastete Stickstoffkreislauf. Nova Acta Leopoldina Nr. 289: Bd 70: 168 p.

[4] Kersebaum, K. C., and J. Richter (1991): Modeling nitrogen dynamics in a plant soil system with a simple model for advisory purposes. Fertilizer Research 27: 273–281.

[5] Kersebaum, K. C. (1995): Application of a simple management model to simulate water and nitrogen dynamics. Ecological Modeling. 85: 145–156.

[6] Michel, R. J. (1991): Entwicklung eines Modells zur zeitlichen und örtlichen Verfolgung von Sickerwasserfronten in der Aerationszone und Anwendung zur Beurteilung der vertikalen Wasserbewegung unterschiedlicher Böden im Winterhalbjahr. Abschlussarbeit Postgradualstudium. TU Dresden: 15 p.

[7] Rothmaler, W. (1990): Exkursionsflora von Deutschland, Gefässpflanzen. Band 3: 639 S.

[8] Voigt, H.-J., and R.-J. Michel (1997): Ein einfacher Ansatz zur Abschätzung der möglichen Denitrifikation in der Aerationszone. Mitteilungen der Deutschen Bodenkundlichen Gesellschaft 85 III: 1421–1424.

[9] Wasy (1993): Interactive, graphics-based finite simulation system FEFLOW for modeling groundwater flow and contamination transport processes. User's manual. Wasy Ltd. Berlin, Germany.

A model for determining flood waves in small basins up to 100 km^2

P. Mita , C. Corbus

National Institute of Meteorology and Hydrology, Sos. Bucuresti - Ploiesti 97, Bucuresti, 71552, România.

Abstract

The paper presents a model for flood waves for small basins from 5 km^2 up to 100 km^2. This model is based on using analytical functions for flood waves. The analytical functions correspond to the relations between the various elements of flood waves (increasing and decreasing durations, maximum discharge, volumes in the increasing and decreasing periods) and the characteristics of the rainfall which causes them (duration, amount, intensity). Such relations were obtained for a large number of hydrometric stations within representative basins, between 5 km^2 and 90 km^2, in the mountainous area in the west of Romania. The floods simulated using the suggested model are close to the recorded floods, which leads to the conclusion that the model is acceptable.

1 Introduction

In a previous paper we presented a model for computing flood waves for small river basins up to 100 km^2 (Mita and Corbus, 1996). In this paper we present a model for determining flood waves in basins from 5 km^2 to 100 km^2.

The methodology of computing the flood waves for this kind of basin is similar to that for basins smaller than 5 km^2. Thus, this model is also based on analytical functions for computing the flood wave hydrograph. This hydrograph is considered to be made up of the hydrograph of surface runoff (including the hypodermic runoff) and the hydrograph of base flow. The functions are the mathematical expressions of relationships between the characteristics of the flood waves and of the precipitation. From these relations, the model parameters were thus determined.

The data which are the basis of this paper are values recorded at representative basins in the mountainous area in the west of Romania over a period of 20 years.

2 The analysis of dependency of the characteristics of flood waves on the characteristics of precipitation

First, Fig. 1 presents schematically the characteristics of the flood waves and of the rainfall which were considered in the present study.

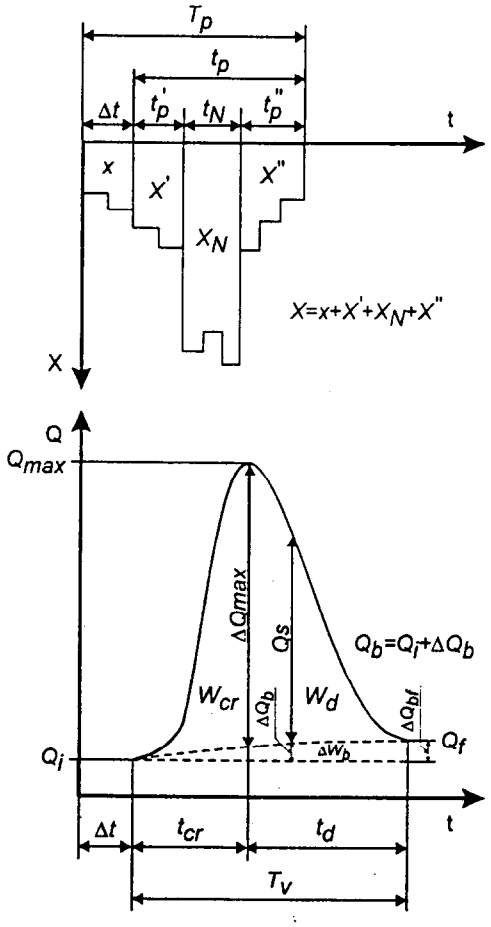

Figure 1: Flood wave and rainfall characteristics.

- Δt - the time interval between the beginning of the rainfall and the beginning of the flood
- t_{cr}, t_d, T_v - flood increase, decrease and total duration
- $Q_{\max}$ - maximum discharge of the flood
- $\Delta Q_{\max}$ - the maximum discharge of the surface runoff
- Q_i, Q_f - initial and final discharge
- ΔQ_{bf} - variation of the base flow discharge with Q_i, at the end of the flood
- W_{cr}, W_d - increase and decrease volume of the surface runoff
- ΔW_b - variation of the volume of the base flow with the volume corresponding to Q_i
- t_p - the time interval between the beginning of the rainfall and the beginning of its nucleus
- t_N - duration of the rainfall nucleus
- t_p'' - the time interval between the end of the rainfall nucleus and its end
- t_p - the time interval between the beginning of the flood and the end of the rainfall
- T_p - total duration of the rainfall
- x, X', X_N, X'' - amount of rain fallen during the time interval Δt, t_p', t_N and t_p'' respectively
- X - total amount of the rainfall registered during the time interval T_p

- Q_i - surface runoff discharge
- Q_b - flood base flow discharge
- ΔQ_b - variation of the base flow discharge with Q_i

The analysis of dependency of the characteristics of flood waves on the characteristics of precipitation was initially carried out for each hydrometric station separately regarding the area, relief, soil, vegetation etc. The following relations were thus obtained:

- $\Delta t = f(x, X_a)$
- $t_{cr} = f(\Delta t + t_p' + t_N)$
- $t_d = f(T_p, X_p)$
- $\Delta Q_{\max} = f(i_p, X_a)$
- $W_{cr} = f(x + X' + X_N, X_a)$
- $W_d = f(X_p, X_a)$
- $\Delta Q_{bf} = f(x + X' + X_N, X_a)$
- $\Delta W_b = f(X_p, X_a)$

where i_p is the rainfall intensity from its beginning to the end of the maximum nucleus.

Fig. 2 presents, as an example, the $\Delta Q_{\max} = f(i_p, X_a)$ graphical relation obtained for the Boroaia hydrometric station from Moneasa representative basin. This sub-basin, has the following morphometric and vegetation characteristics: area - 14.3 km^2; sub-basin slope - 40.3 % and afforestation coefficient - 100 %.

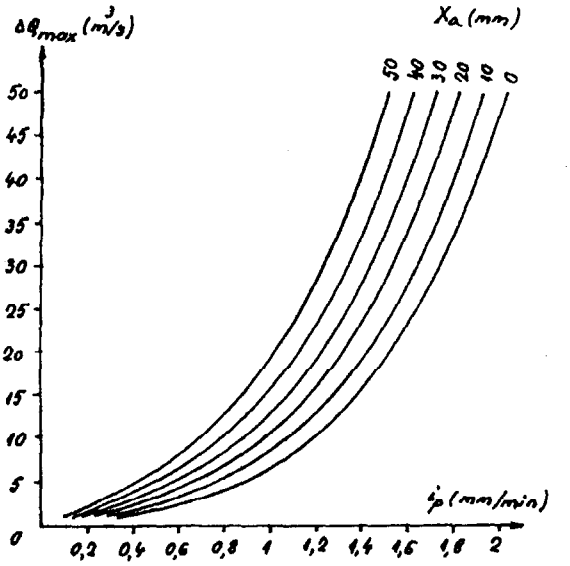

Figure 2: The $\Delta Q_{\max} = f(i_p, X_a)$ relation for the Boroaia hydrometric station.

3 Regionalizations of the characteristics of flood waves

On the basis of relations between the characteristics of flood waves and precipitation, regionalizations of the characteristics of flood waves were obtained which consider besides the flood generation factors (or only such factors) also the basin area and other factors of the natural environment.

Thus, regionalizations for all the above-mentioned characteristics of flood waves were obtained:

- $\Delta Q_{\max} = f(i_p, X_a, F, C_p)$, were F represents the basin area; C_p - afforestation coefficient
- $t_{cr} = f(\Delta t + t_p' + t_N, F)$
- $t_d = f(T_p, X_p)$
- $\Delta Q_{\max} = f(i_p, X_a)$
- $W_{cr} = f(x + X' + X_N, X_a)$
- $W_d = f(X_p, X_a)$
- $\Delta Q_{bf} = f(x + X' + X_N, X_a)$
- $\Delta W_b = f(X_p, X_a)$

Fig. 3. presents as example some of these regionalizations.

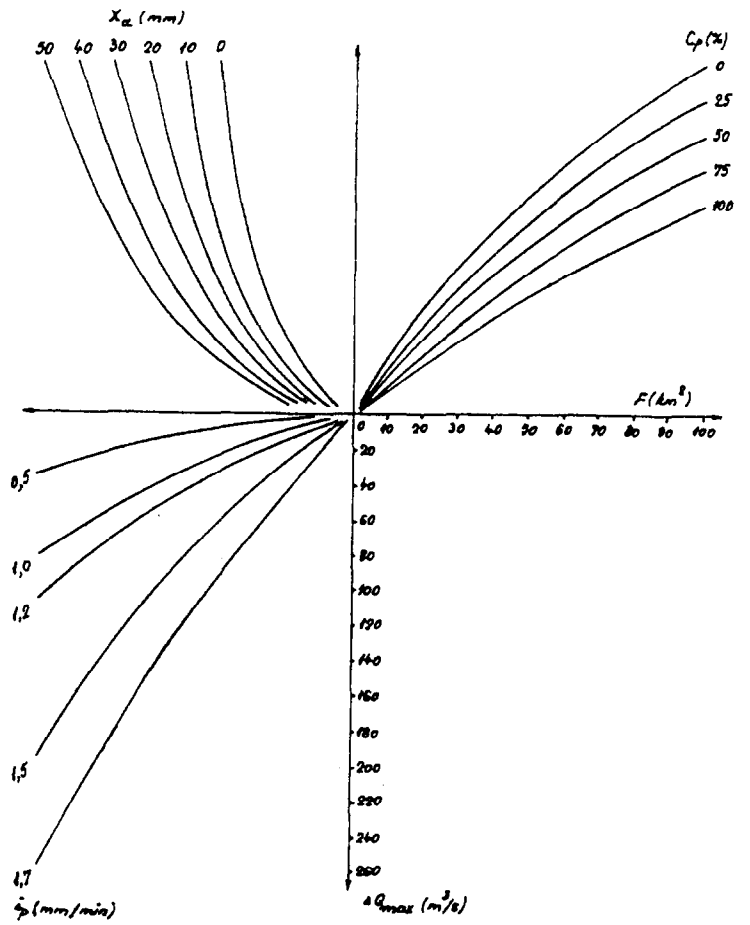

Figure 3: Coaxial synthesis relation $\Delta Q_{\max} = f(i_p, X_a, F, C_p)$.

We chose the coaxial graphs as means of analysis of the regionalizations of the flood waves as they are more operational at the determination of the values of these characteristics depending on the factors which determine them.

All the parameters necessary for the suggested model are thus more easily obtained in order to determine the flood waves for various situations regarding precipitation, vegetation, basin area from 5 km^2 to 100 km^2.

4 The modelling of the hydrograph of the surface runoff

In order to model this hydrograph, a model based on a rational function (in combination with the polynomial and rational functions) unique for the whole flood is proposed:

$$Q_s(t) = \frac{A + Bt}{1 + Ct + Dt^2} \tag{1}$$

where t is time; A, B, C and D - parameters which determine the form of the hydrograph of the surface runoff.

The proposed analytical model can be used in computing the ordinates of the hydrograph of the surface runoff in the hypothesis that the following elements which characterise the flood are specified: t_{cr}, t_d, $\Delta Q_{\max}$, W_{cr} and W_d.

The A, B, C and D parameters are determined by solving the equation system which results by using the following three conditions:

- the function graph has to pass through the point of co-ordinates $t = t_{cr}$ and $Q_s(t) = \Delta Q_{\max}$
- the abscissa of the maximum point of the analytical function to be $t = t_{cr}$
- the definite integrals $\int_o^{t_{cr}} Q_s(t)\,dt$ and $\int_o^{t_d} Q_s(t)\,dt$ to be equal with the volume of the surface runoff calculated through the formula W_{cr} and W_d.

5 The modelling of the hydrograph of the base flow

In order to model the hydrograph of the base flow a polynomial function was used:

$$Q_b(t) = Q_i + \Delta Q_b(t) \tag{2}$$

with

$$\Delta Q_b(t) = et^2 + bt \tag{3}$$

where t is time, a and b - parameters which determine the form of the hydrograph of base flow.

The proposed analytical model can be used in computing the ordinates of the hydrograph of the base flow using the hypothesis that the following elements which characterise the flood are given: t_{cr}, t_d, ΔQ_{bf} and ΔW_b.

The a and b parameters are determined by solving the equation system which results by passing the following conditions:

- the function graph has to pass through the point of co-ordinates $t = T_v$ and $\Delta Q_b(t) = \Delta Q_{bf}$
- the definite integral $\int_o^{T_v} Q_b(t)\,dt$ to be equal with the variation of the volume of the base flow given by ΔW_b.

Solving the above mentioned equation system the final form of the hydrograph of the base flow results:

$$Q_b(t) = Q_i + \left(\frac{t}{T_v}\right)^2 \left(\frac{\Delta W_b}{T_v} - \Delta Q_{bf}\right) + \frac{t}{T_v}\left(-\frac{\Delta W_b}{T_v} + 2\Delta Q_{bf}\right) \tag{4}$$

6 Application

An example of a practical application of the proposed model is presented for the flood of 26 August 1995, 15:00 hours, registered in the Moneasa basin at the Ranusa hydrometric station.

Given the rainfall characteristics, the elements which characterise the two component hydrographs corresponding to the base flow and surface runoff are computed.

Using the flood characteristic elements, the hydrographs of the base flow and surface runoff are then analytically computed. Gathered together, the two hydrographs form the total hydrograph of the flood. The result is presented in Fig. 4.

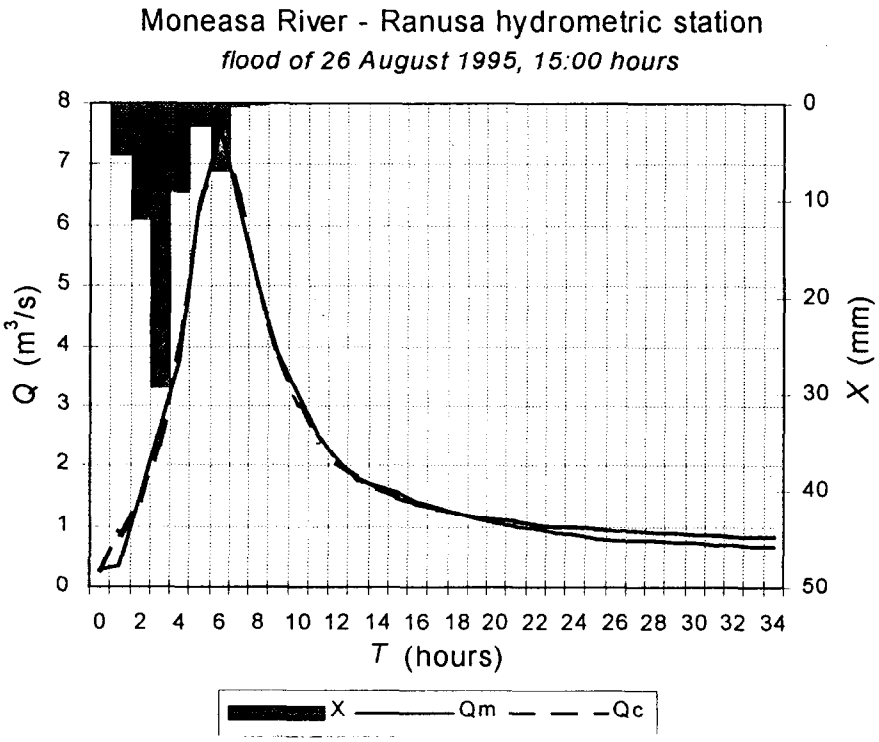

Figure 4: Measured Q_m and calculated Q_c discharges using the proposed model.

7 Conclusions

The relations obtained at the hydrometric stations between the characteristics of flood waves and of precipitation lead to the conclusion that the characteristics of precipitation were properly chosen, i.e. the ones that determine the best the various characteristics of flood waves.

The regionalizations of the characteristics of flood waves can be considered as operational instruments for the determination of values of these characteristics depending on the factors which determine them. At the same time, relations were obtained for the determination of model parameters for the computing of flood waves under different conditions regarding precipitation and the entire variation of area, from 5 km^2 to 100 km^2.

The results obtained for the use of regionalization of the characteristics of flood waves presented in this paper are close to the ones obtained from the earlier regionalizations of those characteristics for this area.

The close values of the characteristics of flood waves simulated as against the recorded ones also show that the model parameters were properly determined, but at the same time that the suggested model was well chosen for the computing of flood waves the small basins of such area.

References

[1] Lauterbach, D. (1965): Ein Verfahren zur Berechnung von Hochwasserganglinien für die Bemessung von Speicherraumen. Besondere Mitteilungen zum Gewasserkundlichen Jahrbuch, nr. 3, Berlin.

[2] Mita, P., Corbus, C. (1996): A model for determining flood waves in small basins. In: D. Viville and I. G. Littlewood (eds), Ecohydrological Processes in Small Basins. Proceedings of the Sixth Conference of the European Network of Experimental and Representative Basins (ERB), September 24–26, Strasbourg, France. Unesco IHP-V Technical Documents in Hydrology, No. 14, 181–186.

[3] Sokolovski, D. L. (1959): River flow. Ghidrometeorologhiceskoe izdatelstvo, Leningrad.

The quantitative influence of karst on the surface runoff in the Moneasa representative basin

P. Mita[1], I. Oraseanu[2], C. Corbus[1]

[1]National Institute of Meteorology and Hydrology, Sos. Bucuresti - Ploiesti 97, Bucuresti, 71552, România. [2]S. C. Prospectiuni S. A. Company, Str. Caransebes 1, Bucuresti, 78768, România.

Abstract

The paper presents methods of determining the influence of karst on the surface runoff in the representative basin of Moneasa, which is located in the West of Romania. The relation between the specific multiannual mean discharge, $\bar{q}$ (l/s/km^2), and the basin mean altitude, $\bar{H}$ (m), was derived using data from hydrometric stations in karst uninfluenced areas of the Moneasa basin and also from neighbouring basins. This relation shows quantitatively the substantially less surface runoff within a sub-basin in the representative basin of Moneasa and the existence of an important supplementary contribution in another sub-basin. Labellings carried out in the karstic areas indicated the directions of the underground runoff, clarifying both the discharge loss areas and their occurrence areas. Discharge measurements performed at a karstic spring confirmed quantitatively the discharge loss and contribution in various areas. A discharge balance carried out for the whole area both on the basis of the relation, $\bar{q} = f(\bar{H})$, and of the discharge measurements, clarified the discharge loss and contribution areas.

1 General presentation of the problem

The objective of this paper is to establish through different means the way the karst in the representative basin of Moneasa influences the surface runoff. The Moneasa representative basin is situated in the western part of the country, in the low altitude Codru - Moma Mountains. The highest peak in these mountains, Izoi Peak, is 1,097 m. The area of this basin at the closing hydrometric station Rãnusa is 76.2 km^2 and the basin mean altitude is 603 m.

In the Moneasa basin there are 8 hydrometric stations, whose sub-basins have areas between 1.15 and 49.4 km^2 (Fig. 1 and Table 1). Measurements at 7 of the 8 hydrometric stations was performed continuously starting in 1975.

The good data base for this basin allowed the study of several issues in the field of small basin hydrology, such as the dependency of the nature of flood waves on the rainfall characteristics and factors of the natural environment, and the dependency of

runoff coefficients and times of concentration of runoff on the rainfall characteristics and conditional factors (Mita and Bulgar, 1971; Mita, 1979). In the context of the results obtained the Moneasa representative basin was suggested and accepted in 1993 into the European Network of representative and experimental basins (ERB).

An important issue which has not been analyzed yet is the quantitative explanation of the anomalies of surface runoff for sub-basins where karst prevail.

Table 1: The values of discharges corresponding to the hydrometric stations and hydrographic areas uncontrolled hydrometrically in the frame of the Moneasa representative basin. * Hydrographic areas uncontrolled hydrometrically. (1) between h. s. Boroaia and confluence Ruja - Moneasa, (2) between confluence Ruja - Moneasa and confluence Meghes - Moneasa (right), (3) between confluence Ruja - Moneasa and h. s. Moneasa (left river Moneasa).

River	Hydrometric station	F (km^2)	$\bar{H}$ (m)	Of the relation $\bar{q} = f(\bar{H})$		Of recorded date		$\Delta\bar{Q}$ (l/s)	$\Delta\bar{Q}$ (%)
				$\bar{q}$ (l/s/km^2)	$\bar{Q}$ (l/s)	$\bar{q}$ (l/s/km^2)	$\bar{Q}$ (l/s)		
Moneasa	Boroaia	14.3	653	18.0	257	17.3	248	-9	-3.5
Ruja	Ruja	6.6	660	18.2	120	18.9	125	5	4.2
V. Lunga	Pastravarie	5.5	570	14.8	81.4	14.0	77.0	-4.4	-10.6
ΔF_1	(1) *	1.89	515	13.0	24.6	-	-	-	-
Meghes	Sonda	10.0	681	19.2	192	8.4	84.0	-108	-56.2
ΔF_2	(2) *	4.0	510	12.8	51.2	-	-	-	-
ΔF_3	(3) *	3.05	450	11.2	34.2	-	-	-	-
Valea Baii	Moneasa	1.15	520	13.1	15.0	181.7	209	193	1286.7
Pârâul Pietros	*up-stream river Moneasa	2.9	665	18.5	53.6	-	-	-	-
Moneasa	Moneasa	49.4	619	16.8	830	18.9	936	106	12.8
Fânuri	Ranusa	19.5	500	12.6	241	13.3	260	19	7.9
Moneasa	Ranusa	76.2	603	16.0	1220	16.4	1250	30	2.5

2 Brief presentation of the geology of the Moneasa representative basin

This brief presentation of the geology of the Moneasa representative basin aims to underline in general its role on the variation of the surface runoff in the basin.

Thus, under the conditions of the volcanic rocks and crystalline schists in the upper part of the basin (the Boroaia, Ruja and Valea Lungã sub-basins) and also in its lower part (the Fânuri sub-basin), Fig. 1 presents the normal variation of the surface runoff. The volcanic rocks and crystalline schists in these sub-basins mean that the groundwater component of streamflow is relatively small.

Unfortunately, there is a totally different situation in the Meghes sub-basin and the downstream area where the strongly karstified calcareous rocks are fissured, allowing significant amounts of underground flow. As a result, surface runoff is low and water is exported from the topographically-defined catchment to other hydrographic areas. Explanation of these changes of surface runoff is the main objective of this paper.

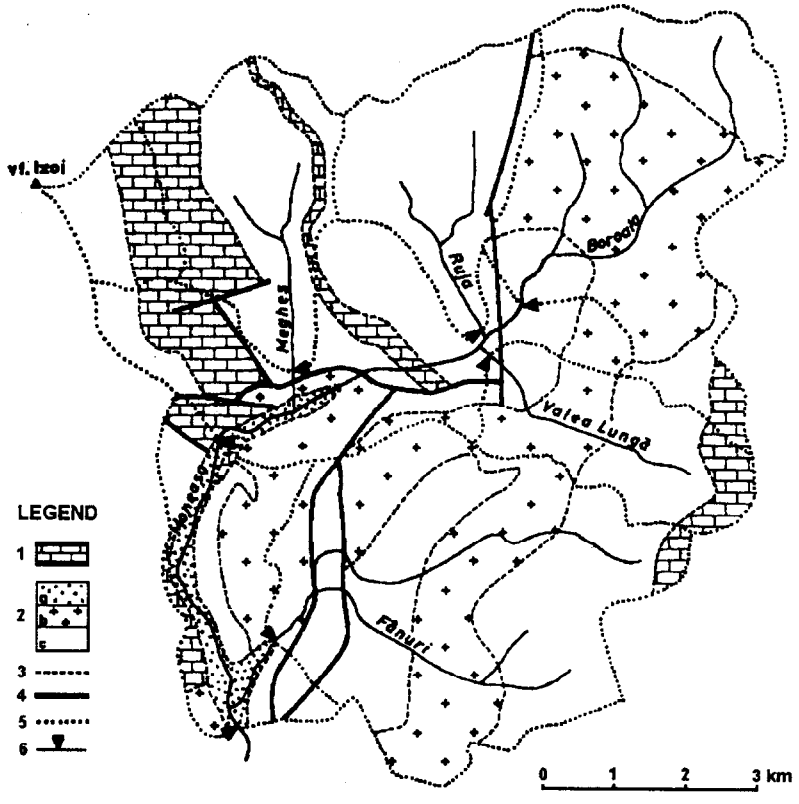

Figure 1: Geological map of the Moneasa zone (Bleahu, 1965). 1. Karstifiable rocks; 2. Unkarstifiable rocks: a) sands and gravels, b) igneous rocks, c) clays, mares, sandstones, calcareous spar; 3. Geological limit; 4. Fault; 5. Sub-basins limit; 6. Hydrometric section.

3 Means of determination of the quantitative influence of karst on surface runoff

In order to establish the quantitative influence of karst on the surface runoff, the relations between the specific multiannual mean discharge, $\bar{q}$ (l/s/km^2), and the basin mean altitude, $\bar{H}$ (m), were established; the relation $\bar{q} = f(\bar{H})$ was obtained on the basis of the data from the hydrometric stations uninfluenced by karst, and the labelling and measurement of discharge downstream the resurgences.

The analysis was concentrated on the medium area of the basin, between the Teia creek and the Moneasa hydrometric station. In that area, the Meghes sub-basin is situated (the Sonda hydrometric station) and part of the Moneasa sub-basin (the Moneasa hydrometric station) strongly affected by karst. As presented in Fig. 2, very diminished values of $\bar{q}$ (l/s/km^2) result for the Sonda hydrometric station (the Meghes sub-basin) as compared to the $\bar{q}$ values from the hydrometric stations uninfluenced by karst, while for the Moneasa hydrometric station (the Moneasa sub-basin) much larger values than the normal ones of the surface runoff result. The labellings in Fig. 3 confirm these anomalies of the surface runoff as a result of the underground water exchanges between various basins and sub-basins.

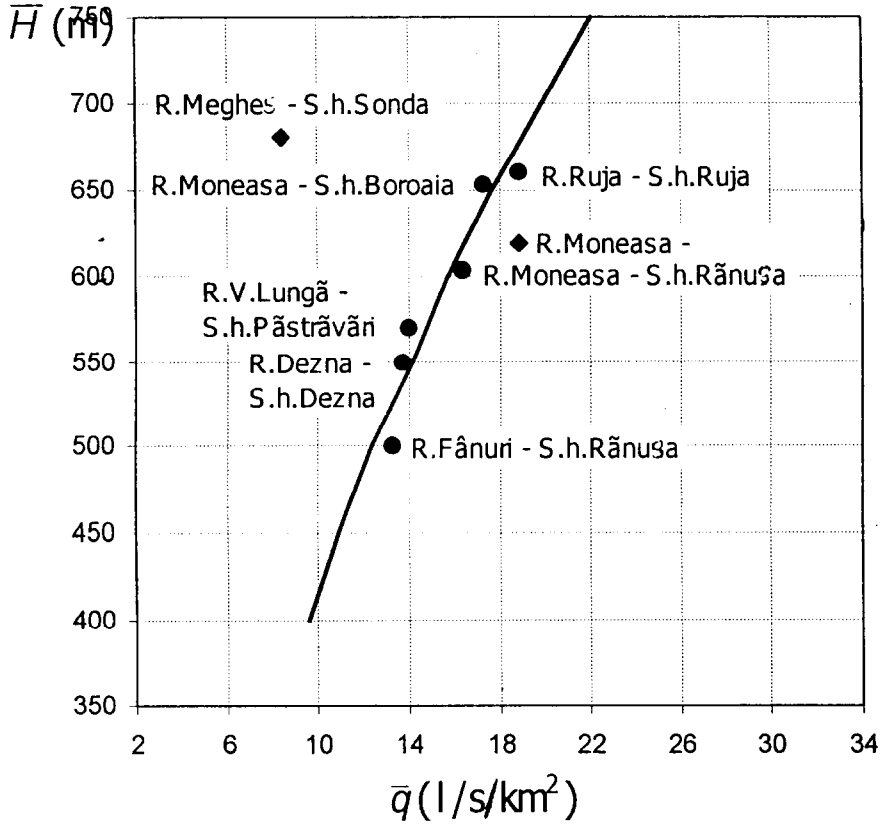

Figure 2: The relation $\bar{q} = f(\bar{H})$ for the Moneasa - Dezna hydrographic zone.

The cause is not represented by either the precipitation, which varies very little across the whole basin (1023 mm at the Moneasa hydrometric station and 1130 mm at the Izoi meteorological station), or the types of soil and vegetation which are also the same in the Moneasa basin.

The cause is the karst, as will explained briefly in the context of the water balance for each of the two basins.

4 The substantial diminishing of discharges for the Meghes sub-basin

Fig. 1 presents the limits of the Meghes sub-basin. The Sonda hydrometric station controls a basin area, $F = 10$ km^2, with a mean basin altitude $\bar{H} = 680$ m. The multiannual mean discharge computed for the period 1975–1997 is $\bar{Q} = 84$ l/s and thus, $\bar{q} = 8.4$ l/s/km^2. From the relation $\bar{q} = f(\bar{H})$ presented in Fig. 4, without the karst influence at the Sonda hydrometric station $\bar{q} = 19.2$ l/s/km^2 and therefore, $\bar{Q} = 192$ l/s. There is a loss 108 l/s.

It is appreciated that this loss is closely analyzed in Table 2 and Fig. 4. From Table 2 it results a total value of loss in the Meghes sub-basin, 104 l/s, which is close to the values of this loss, 108 l/s, which initially resulted from $\bar{q} = f(\bar{H})$ (Fig. 4).

This is almost the same as the 103 l/s value for the karstic area of 4.2 km^2 in the northwestern part of the Meghes basin. From Fig. 4 results that for this area with mean altitude, $\bar{Q} = 800$ m, $\bar{q} = 24,5$ l/s/km^2 and $\bar{Q} = 103$ l/s. This discharge is flooded over the basin (Oraseanu, 1987). A sketch of water balance is shows in Fig. 5.

The surface runoff decreases are justified by the underground flowlines presented on Fig. 3 and by measurement carried out at Grota Ursului Spring (Oraseanu, 1985a,b).

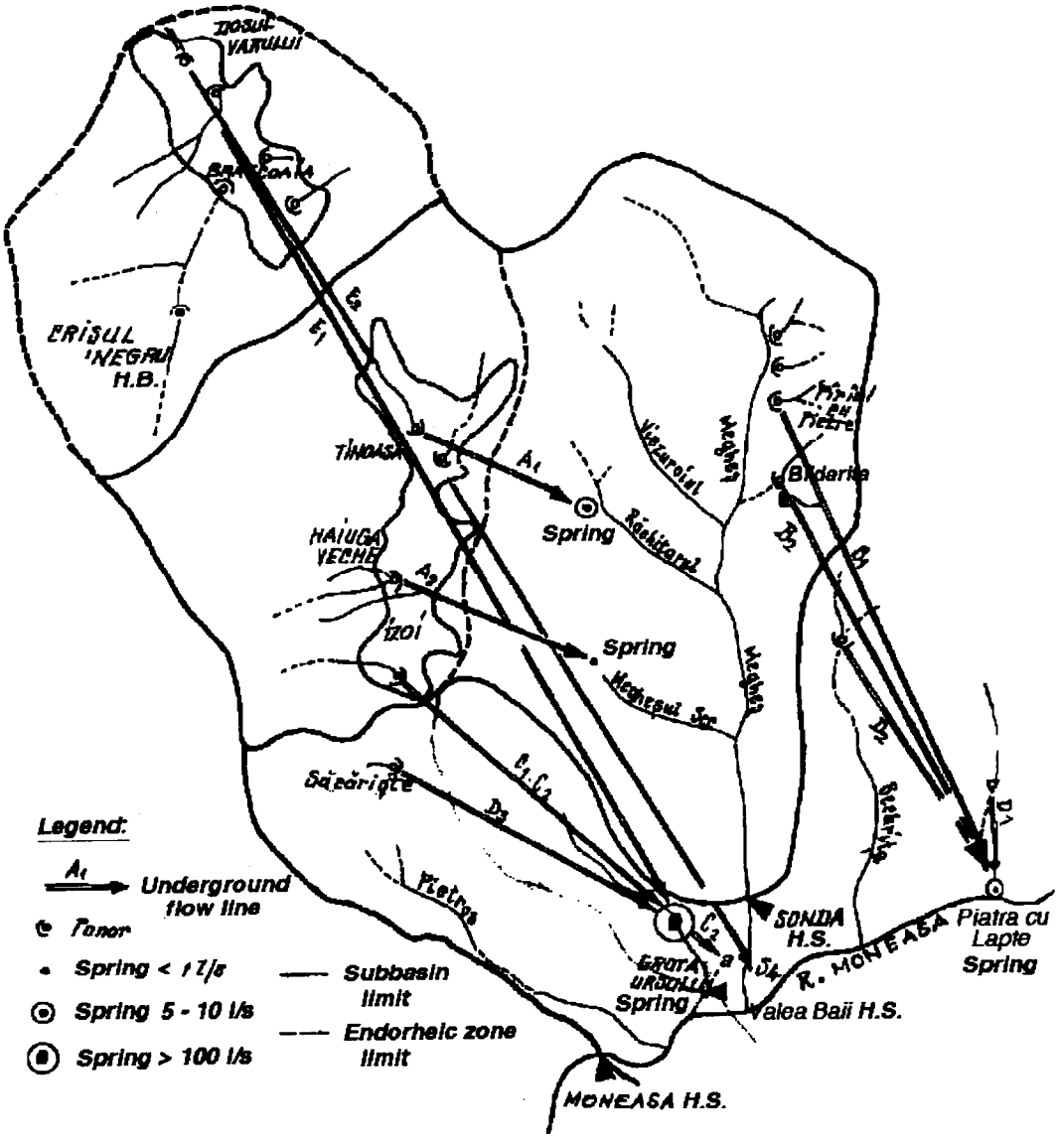

Figure 3: The underground flowlines in the hydrographic zone of Meghes-Moneasa (Crisul Alb River) - Bratcoaia (Crisul Negru River).

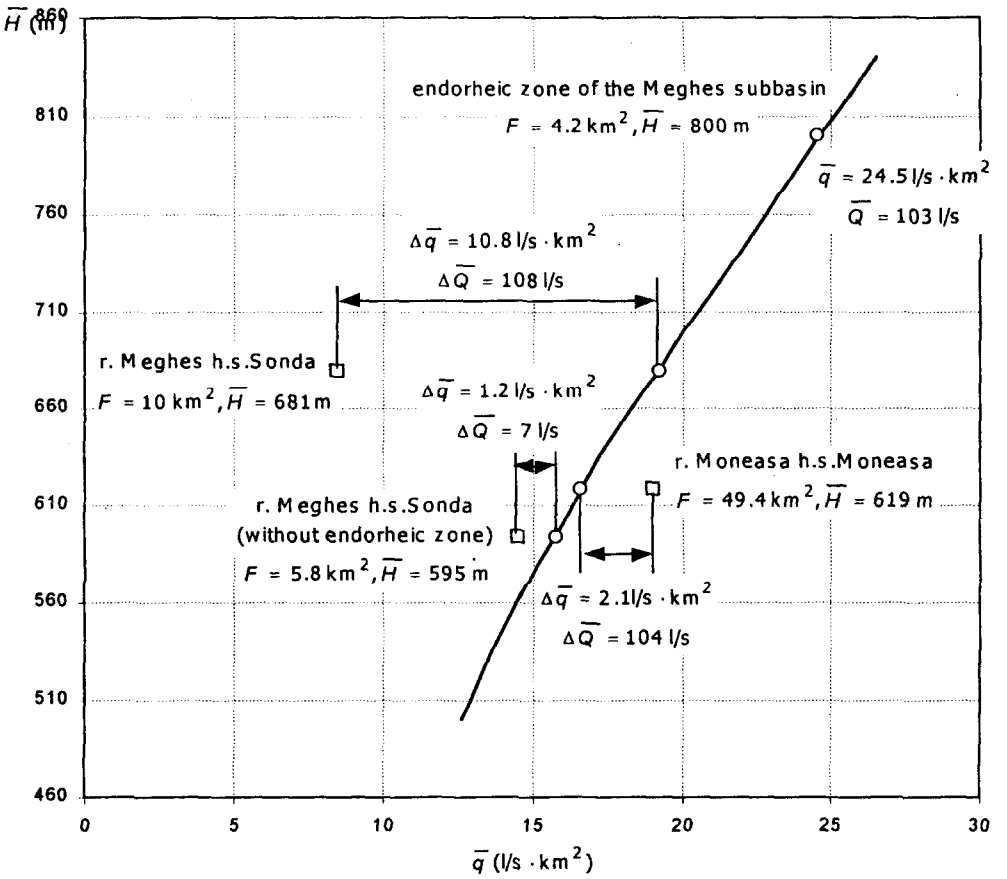

Figure 4: Water balance in the Moneasa representative basin using $\bar{q} = f(\bar{H})$.

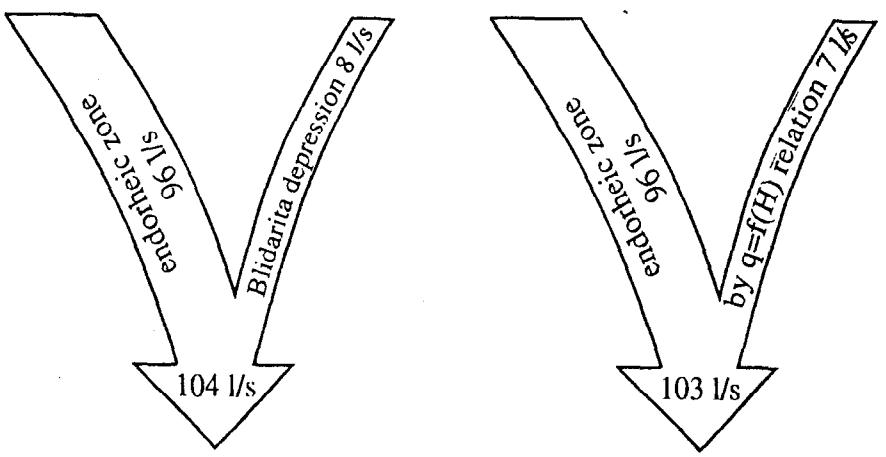

Figure 5: Water balance at the Meghes sub-basin.

5 The supplementary contribution of discharge at Moneasa hydrometric station (Moneasa river)

The Moneasa sub-basin at the Moneasa hydrometric station has area $F = 49.4$ km^2 and a mean basin altitude $\bar{H} = 619$ m. The Moneasa sub-basin includes another 4 small sub-basins hydrometrically controlled, 3 of them not being influenced by karst. The area in its sub-basin influenced by karst is situated closely upstream to the Moneasa hydrometric station and includes mainly the Meghes sub-basin (Fig. 1). Over the measurement period (1975–1997) the multiannual mean discharge at the Moneasa hydrometric station was $\bar{Q} = 936$ l/s. From the synthesis relation $\bar{q} = f(\bar{H})$ it is only 830 l/s.

Also, in this case (Meghes sub-basin) the difference between the results obtained through various methods are rather small, supporting the view that analysis presented is, in general, correct.

The difference, $\Delta\bar{Q} = 106$ l/s is attributed mainly to the discharge contribution in the Crisul Negru basin, in the Bratcoaia depression (Fig. 1). The underground flow lines presented in Fig. 3 indicate these transfers. This karstic depression has a surface area of $F = 3.72$ km^2 and a mean altitude $\bar{H} = 831$ m. Using the relation $\bar{q} = f(\bar{H})$ for this area results a value $\bar{q} = 26$ l/s/km^2 and $\bar{Q} = 96.7$ l/s.

Table 2: Water infiltration and resurgence of Meghes - Moncasa zone.

Infiltration zone	Total discharge of zone $\bar{Q}$ (l/s)	Infiltration points	Resurgence points				Underground flow lines (Fig. 1)
			Inside of Meghes sub-basin	Q (l/s)	Outside of Meghes sub-basin	Q (l/s)	
Izoi-Tinoasa endorheic zone ($F = 4.2$ km^2; $\bar{H} = 800$ m)	103 determinate of Relation $\bar{q} = f(\bar{H})$ $\bar{q} = 24.5$ l/s/km^2	Tinoasa Ponor	Rachitarul Spring	6	-	-	A_1
		Haiuga Veche Ponor	Meghesul Sec Spring	1	-	-	A_2
		Izoi-1 Ponor	-	-	Grota Ursului Spring	92	C_1
		Izoi-2 Ponor	-	-	Subtermal-1 Spring	4	C_2
					Total loss	96	-
Blidarita Depression		Pârâu; cu Pietre Ponor	-	-	Piatra cu Lapte Spring	4	B_1
		Blidarita Ponor	-	-	Piatra Lapte Spring	4	B_2
					Total loss	8	-
					Total loss in Meghes sub-basin	104	-

A check of magnitude of this discharge was done by analyzing the supplementary discharge from the Valea Baii hydrometric station situated closely upstream to the Moneasa hydrometric station, as presented in detail in Table 3. The multiannual mean discharge determined at this hydrometric station is $\bar{Q} = 209$ l/s. The largest contribution to this discharge is from the Grota Ursului Spring with $\bar{Q} = 194$ l/s. The value of discharge is determined by contributions of the Meghes sub-basin (endoreic zone), $\bar{Q} = 96$ l/s and of the Bratcoaia depression, $\bar{Q} = 94$ l/s. A sketch of water balance is shown in Fig. 6.

Table 3: Water balance at Valea Baii h. s. (= 209 l/s) of Moneasa sub-basin upstream Moneasa h. s.

Infiltration zone	Total discharge of zone $\bar{Q}$ (l/s)	Infiltration points	Resurgence points	Q (l/s)	Underground flow lines (Fig. 1)
A. Supplementary discharge contribution of Bratcoaia depression					
Bratcoaia depression (Crisul Negru hydrographic basin) $F = 3.72$ km^2; $\bar{H} = 831$ m	96.7 determinate by $\bar{q} = f(\bar{H})$ relation $\bar{q} = 26$ l/s/km^2	Dosul Varului Ponor	Grota Ursului Spring	90	E_1
		Dosul Varului Ponor	Foraj S_4	4	E_2
	Total supplementary contribution from Bratcoaia depression			94	-
B. Contribution from Moneasa sub-basin					
Izoi - Tinoasa endorheis zone	B1. - From karstic zone				
	103	Izoi-1 Ponor	Grota Ursului Spring	92	C_1
		Izoi-2 ponor	Subtermal-1 Spring	4	C_2
	Total supplementary contribution from endorheic zone			96	-
	B2. - From Valea Baii superficial basin ($F = 1.15$ km^2, $\bar{H} = 520$ m, $\bar{q} = 13.1$ l/s/km^2)			15	-
	Total contribution from Moneasa sub-basin			111	-
Total contribution from Bratcoaia depression and Moneasa sub-basin				205	

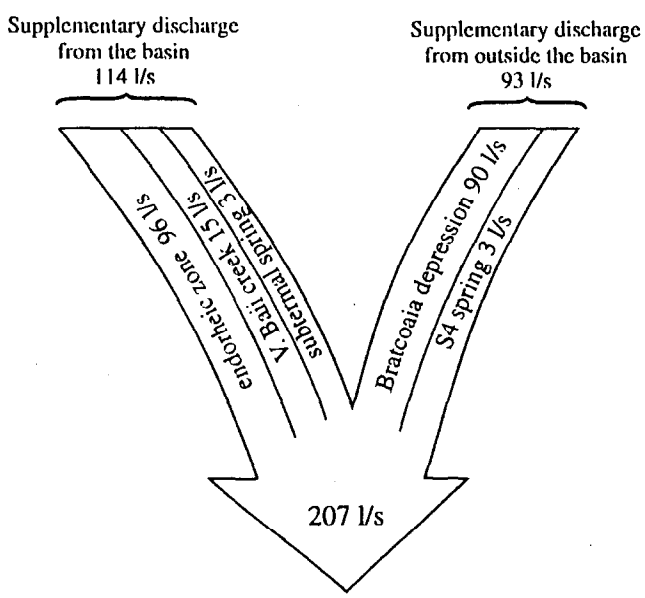

Figure 6: Water balance at the Valea Baii hydrometric station.

As mentioned before, this is the most important contribution which comes from outside the basin at the Moneasa hydrometric station, where it was estimated that the total contribution is 106 l/s.

6 Conclusions

The main results regarding the karst influence on the surface runoff were obtained as a result of three ways of analysis: hydrological synthesis, labelling and measurements of expeditionary-oriented discharges.

The difference between the results obtained by the different methods are small. This suggests that the analysis was generally correct.

Through this study, the degree of knowledge of the influence of the natural karst factors on the surface runoff in this representative basin was completed.

References

[1] Bleahu, M. (1965): Geological maps of Romania, Scale 1:100.000, sheet Moneasa. Geological Geophysical Institute Bucharest.

[2] Mita, P., Bulgar, A. (1971): Contributions to the study on water runoff on river influenced by karst in the hydrometric area between the Cerna and Gilort rivers. Hidrotehnica, vol. 16, no. 9, Bucharest.

[3] Mita, P. (1979): Specifications regarding the water exchange in the karstic area of the upper basin of the Dâmbovita river. Hidrotehnica, vol. 24, no. 10, Bucharest.

[4] Oraseanu, I. (1985a): Considerations on the hydrology of Vascău Plateau (Codru Moma Mountains). Theoretical and Applied Karstology. Institutul de Speologie "Emil Racovitä", Bucharest.

[5] Oraseanu, I. (1985b): Partial captures and difference surfaces. Examples from the northern Karst area of Pädurea Craiului Mountains. Theoretical and Applied Karstology. Institutul de Speologie "Emil Racovitä", Bucharest.

[6] Oraseanu, I. (1987): Hydrological study of Moneasa area (Codru Moma Mountains). Theoretical and Applied Karstology. Institutul de Speologie "Emil Racovitä", Bucharest.

Infiltration of water into soil with cracks

V. Novák[1] and J. Šimůnek[2]

[1]Institute of Hydrology, Slovak Academy of Sciences, Račianská 75, P. O. Box 94, SK 830 08 Bratislava, Slovak Republic. [2]U.S. Salinity Laboratory, USDA-ARS, West Big Springs Road, Riverside, CA, 92507-4617, U.S.A.

1 Introduction

Porous media often exhibit a variety of heterogeneities such as fractures, fissures, cracks, macropores of biotic origin, and inter-aggregate pores (Gerke and van Genuchten, 1993; Jarvis, 1998). These heterogeneities can significantly affect water and solute movement into soils by creating non-uniform velocity fields with spatially variable flow velocities. The resulting non-uniform flow process is often referred to as preferential flow. Preferential flow may be especially significant in fine-textured, shrinking/swelling soils containing drying cracks. Infiltration of precipitation and/or irrigation water into such low-permeable soils is normally very slow and frequently accompanied with surface runoff. The presence of drying cracks often decreases the amount of surface runoff by increasing the total infiltration rates and, concomitantly, the soil water content in deeper parts of the soil profile. At the same time crack infiltration is also associated with accelerated solute transport, with surface-applied solutes generally penetrating much deeper into the soil profile, thus posing risks for soil and groundwater pollution, including nutrients moving quickly below the root zone of agricultural crops.

Adequate descriptions of water infiltration into initially dry, cracked, fine-textured soils are missing in most soil-water-atmosphere-plant models. Ignoring the infiltration of water via soil cracks into the soil matrix usually leads to severely underestimated infiltration rates, too high predictions of water accumulating at or near the soil surface, overestimation of surface runoff and, consequently, to unrealistic descriptions of the soil water regime.

Flow in heterogeneous porous media is frequently also described using dual permeability models (Gerke and van Genuchten, 1993). Approaches of this type assume that the soil consists of two regions, one associated with macropores (the crack network), and the other with the less permeable matrix region. The difficulty in applying this approach to cracked soils is that flow in both regions is described using the Richards equation, an assumption which is likely not valid for flow in large drying cracks.

2 Conceptual model

A schematic of the conceptual model forming the basis of the FRACTURE submodel is shown in Figure 1. Precipitation or irrigation (the potential infiltration flux, $q_o(t)$) falls

on the soil surface and, as long as the soil surface is unsaturated, is equal to the actual infiltration rate $q(t)$. After the soil surface becomes saturated, excessive water is first used to form a surface layer, the maximum thickness of which is a function of surface roughness. We further assume that surface runoff or flow into cracks can start only after the surface water layer reaches a critical thickness, h_s. At that time water starts flowing into the cracks as long as the potential flux is higher than the actual surface infiltration flux. When the potential flux becomes smaller than the actual infiltration rate, the flow into cracks stops and water in the soil surface layer infiltrates directly into the soil until it is completely used. The infiltration process hence can be divided into several stages:

1. unsaturated infiltration when the soil surface is still unsaturated: $q(t) = q_o(t)$,
2. the formation (or disappearance) of a surface layer of water after the soil surface becomes saturated: $q(t) < q_o(t)$ $(q(t) > q_o(t))$,
3. flow into cracks when the soil surface is saturated and the surface water layer has reached a certain critical height, h_s: $q(t) < q_o(t)$,
4. horizontal infiltration from cracks into the soil matrix, and runoff when cracks are either full or not considered, $q(t) < q_o(t)$.

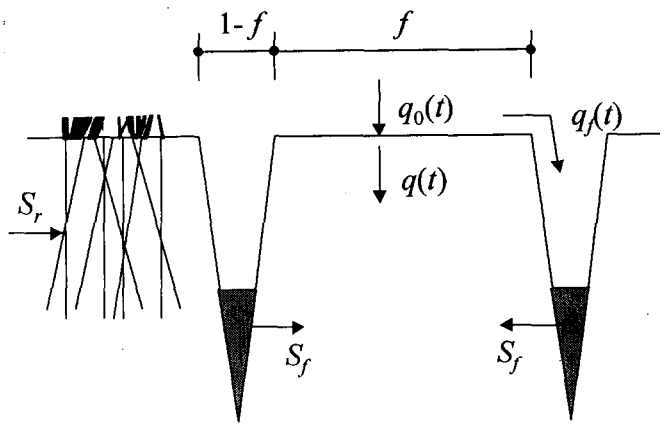

Figure 1: Schematic of the FRACTURE submodel. The potential infiltration rate, $q_o(t)$, is divided between the soil surface infiltration rate, $q(t)$, and flow into the cracks, $q_f(t)$. $S_f(z,t)$ represents the horizontal infiltration rate from the cracks into the soil matrix.

3 Mathematical model

The FRACTURE mathematical submodel is part of the HYDRUS-ET code (Šimůnek et al., 1997). The one-dimensional Richards equation is assumed to describe water flow in the soil matrix. Matrix and preferential flow are mutually linked using an extension of the Richards equation as follows (Feddes et al., 1988):

$$\frac{\partial \theta}{\partial t} = \frac{\partial}{\partial z}\left[k(h,z)\left(\frac{\partial h}{\partial z} + 1\right)\right] - S_r(z) + S_f(z) \qquad (1)$$

where h is the pressure head, θ is the volumetric water content, t is time, z is the vertical coordinate (positive upward), $k(h,z)$ is the unsaturated hydraulic conductivity, $S_r(z)$ is a sink term quantifying the volume of water extracted from soil by roots (the root extraction term), and $S_f(z)$ is the horizontal infiltration rate of water from cracks into the soil matrix.

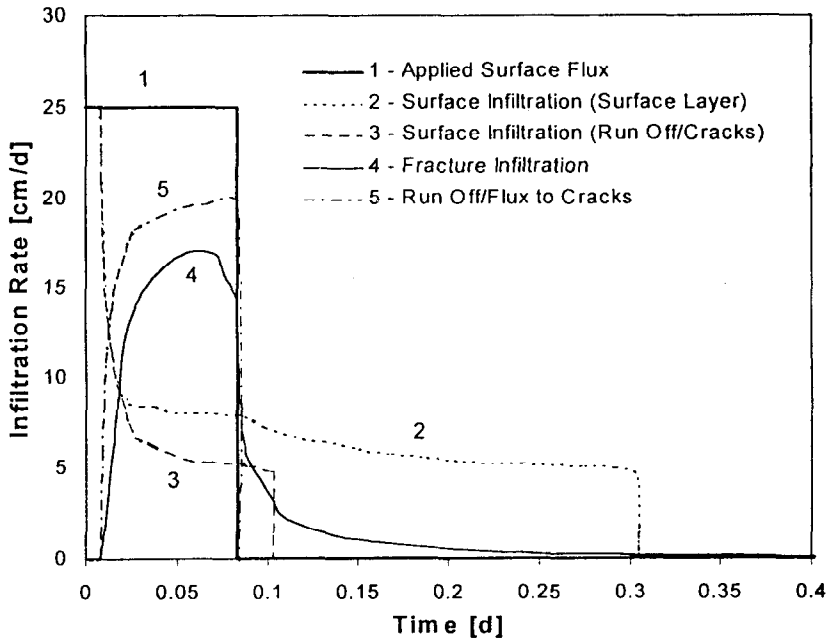

Figure 2: Infiltration rates versus time for the three scenarios considered in this study (q_o = 25 cm.d^{-1}, duration t = 2 hours, K_s = 5 cm.d^{-1}): (1) potential infiltration rate, $q_o(t)$, (2) infiltration, $q(t)$, into the soil without cracks with water accumulating on the soil surface, (3) infiltration, $q(t)$, through the soil surface into the soil with surface runoff (with or without cracks present), (4) infiltration, $q_f(t)$, from the cracks into the soil matrix, and (5) flow into cracks $(q_o(t) - q(t))$.

The source term $S_f(z)$, i.e., the lateral infiltration rate from the water-filled part of soil cracks into the soil matrix, is calculated using the Green-Ampt approach

$$S_f = \left(K_h(z) \frac{h_o - h_f}{l_f} \right) A_c \tag{2}$$

where K_h is the hydraulic conductivity of the crack-matrix interface, h_o is the positive pressure head at the point of infiltration, h_f is the pressure head (negative) at the leading edge of infiltration at a distance l_f from the infiltration surface, and A_c is the specific surface of the cracks [L^2 L^{-3}]. The distance l_f can be calculated according to the Green-Ampt approach as follows:

$$l_f = \sqrt{2 K_h \frac{h_o - h_f}{\theta_s - \theta_i} t_f} \tag{3}$$

where θ_i and θ_s are the initial and saturated volumetric water contents, respectively, and t_f is the time interval since the start of infiltration, generally different for each node.

We further assume that soil cracks during a certain precipitation event do not change their dimensions. This assumption is based on field observations that even for heavy rainfall soils generally swell so slowly that cracks do not shrink significantly during first several hours of a rainfall event. Since shrinking and swelling soils usually contain a high fraction of clay minerals, their permeability for water is low and thus the infiltrating water can only slowly penetrate into clay mineral layers. Visible narrowing of soil cracks takes usually several days. The physical processes of crack formation and swelling, and especially its quantification into mathematical models still need further investigation.

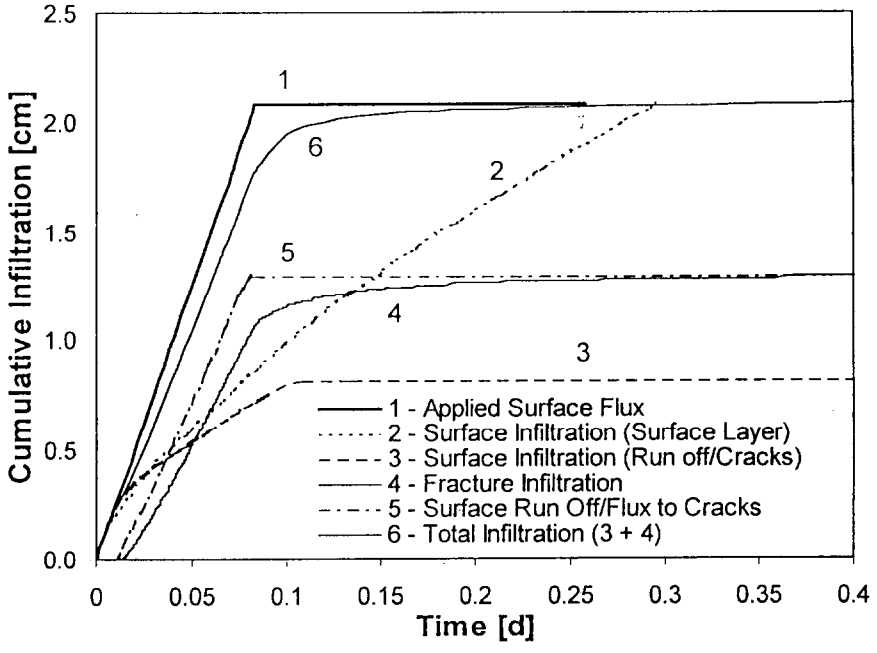

Figure 3: Cumulative infiltration versus time for the three scenarios considered in this study: (1) cumulative potential infiltration rate, (2) cumulative infiltration into the soil without cracks with water accumulating on the soil surface, (3) cumulative infiltration through the soil surface into the soil with surface runoff (with or without cracks present), (4) cumulative infiltration from the cracks into the soil matrix, (5) cumulative flow into cracks, and (6) the total cumulative infiltration into the soil matrix for the soil with the cracks.

4 Results of infiltration modeling

Figures 2 and 3 shows calculated infiltration rates and cumulative infiltration volumes, respectively, during infiltration into the soil for three scenarios, i.e., (a) a soil without cracks with water accumulating at the soil surface, (b) a soil without cracks, but with surface runoff, and (c) a soil with cracks. The model was applied to a fine-textured (clay) soil from the Trnava area of Southern Slovakia. Parameters characterising soil cracks were estimated both in the field (the specific length of the soil cracks, $l_c = 0.046$ m m^{-2}) and in the laboratory (the shrinkage curve, the relationship between crack porosity and the soil water content $P_c(w)$) (Novák, and Šimůnek, 1997, Novák, 1999). Infiltration curves (Fig. 2) estimated for different boundary conditions on the soil surface and for the same soil with and without cracks illustrate the difference between a traditional approach to infiltration (homogenous soil) and infiltration into the soil with cracks. Cumulative infiltration curves for the same soil and boundary conditions presented in Fig. 3 demonstrate even better the importance of cracks infiltration on cumulative infiltration and soil water regime of cracked soils. While at the end of a 2-hour precipitation event 86 % of the cumulative precipitation infiltrated into cracked soil, only less than 40 % infiltrated into soil without cracks. Depending on the slope of the soil surface and soil surface morphology, the excess water can either run off or can be accumulated on the soil surface. The contribution of soil cracks to infiltration and soil water regime formation depends on the soil hydraulic properties and actual soil water profiles. However, there is no doubt that for fine-textured soils it can significantly improve their typically poor infiltration properties.

5 Conclusions

Field observations of infiltration into fine-textured cracked soils, and the results of modeling presented in this paper, demonstrate the importance of crack infiltration for soil water dynamics.

Presented submodel requires only two additional input data: specific length of cracks per unit soil surface area, l_c, and relationship between the crack porosity P_c and the soil gravimetric water content w.

The example presented in this paper demonstrates the importance of soil cracks in determining rates of infiltration into a soil during heavy rain or irrigation. A comparison with the more traditional approach involving only surface infiltration indicates important differences in the soil water content distribution during a rainfall/irrigation event. An extension of the classical approach to include crack infiltration can significantly improve the identification and prediction of the soil water regime.

References

[1] Feddes, R. A., P. Kabat, J. van Bakel, J. J. B. Bronswijk, and J. Halbertsma. 1988. Modeling soil water dynamics in the unsaturated zone - state of art. J. Hydrology, 100, 69–111.

[2] Gerke, H. H., and M. Th. van Genuchten. 1993. A dual-porosity model for simulating the pereferential movement of water and solutes in structured porous media. Water Resources Research, 29(2), 305–319.

[3] Jarvis, N. J. 1998. Modeling the impact of preferential flow on nonpoint source pollution. In: Physical nonequilibrium in soils: modeling and application, Selim, J. M. and L. Ma, eds., Ann Arbor Press, Chelsea, Michigan, 195–221.

[4] Novák, V., and J. Šimůnek, 1997. Mathematical submodel of the infiltration of water into cracked soil. In: Majerčák, J. and T. Hurtalová (Eds.) Transport vody, chemikálii a energie v systéme pôda-rastlina-atmosféra. Inst. of Hydrology and Inst. of Geophysics, Slovak Acad. Sci., Bratislava, 82–84.

[5] Novák, V. 1999. Cracked soils in the NOPEX area: The influence of a soil cracks on the infiltration process. Agric. Forest Meteorol., (submitted for publication).

[6] Šimůnek, J., K. Huang., M. Šejna, M. Th. van Genuchten, J. Majerčák, V. Novák, and J. Šutor. 1997. The HYDRUS-ET software package for simulating the one - dimensional movement of water, heat and multiple solutes in variably - Saturated media. Version 1.1. Institute of Hydrology, Slovak Academy of Sciences, Bratislava.

Nutrient and sediment transport simulation

in the upper Torysa catchment during the catastrophic flood of July 1997

P. Pekárová, A. Koníček, P. Miklánek

Institute of Hydrology, Slovak Academy of Science, Račianská 75, P. O. Box 94, SK 830 08 Bratislava, Slovakia.

1 Introduction

Catastrophic floods occurred in some regions of central Europe in July 1997. One of the most severe events in Slovakia was in the upper Torysa basin. As the construction of the drinking water reservoir Tichý Potok was planned in this catchment, temporary observations were organised during 1996–1997 in four experimental microbasins of the area. Results of the short-term hydrological observations were used for calibration of the AGNPS model. This model was used for simulation of nutrient and sediment transport at flood events of July 9, 1997.

2 Basic characteristics of the Torysa river and the experimental microbasins

The Torysa river is situated in Eastern Slovakia. The area of the basin to the planned water reservoir is 88.2 km^2, the length of the stream is 18.3 km and the mean elevation is 910 m a. s. l. (between 600 and 1235 m a. s. l.). Geologically it is a flysch area with alternating layers of clay and sandstone. Mean annual precipitation is 781 mm and runoff depth is 250 mm. About 50 % of the area is forested, 31 % are meadows and 19 % is arable land. Four monitoring microbasins were selected in the area in 1996 (Fig. 1): No. 1 Jedlinka - arable land; No. 2 Repiská - grass; No. 3 Chmeľov - coniferous forest; No. 4 Dlhý jarok - coniferous forest.

Water quality in the streams is good. During snow melt and storm floods intensive washout of accumulated pollutants from the soil cover occurs. The groundwater quality in the area was also studied by Hyánková et al. (1995).

Table 1: Basic characteristics of the experimental microbasins in upper Torysa region.

Basin	Area km^2	Elevation max	m a. s. l min	Vegetation	Elevation of the raingauge
Jedlinka	0.95	930	807	arable land	843
Repiská	0.90	1105	832	grass	939
Chmeľov	0.66	1094	692	coniferous	

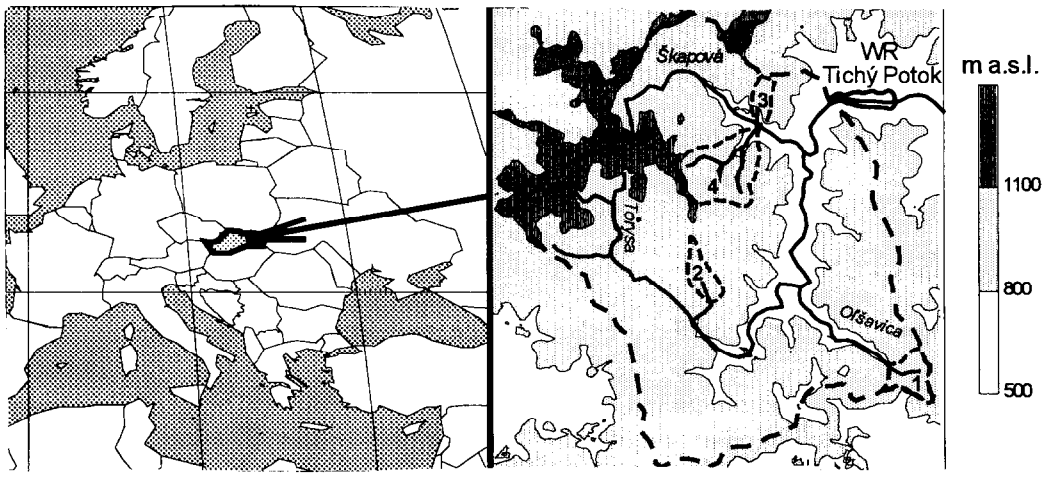

Figure 1: Scheme of the Torysa basin to the planned Water reservoir Tichý Potok. Experimental microbasins: 1. Jedlinka - arable, 2. Repiská - grass, 3. Chmeľov - forest, and 4. Dlhý Jarok - forest.

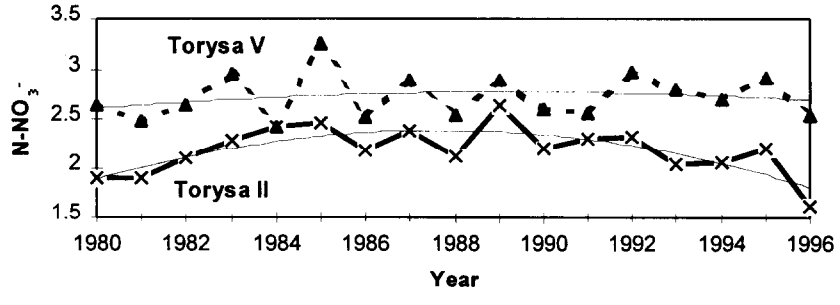

Figure 2: The temporal development of the mean annual nitrate-nitrogen concentrations (mg l^{-1}) in two sampling sites of the Torysa river main stream.

3 Results

3.1 Water quality in the Torysa river main stream

Selected water quality parameters were analysed in six sampling profiles in the upper part of Torysa. The main topics of the study were trend analysis for the period 1980–1996, the annual regime of water quality parameters at individual sites and their development along the main stream of Torysa. The water quality data from the SHMI databank were used for the trend analysis (Halmová, 1996). The monthly data series of nitrates, nitrites, phosphates, sulphates and chlorides for 1980-1996 were analysed. An example of the mean nitrate-nitrogen concentrations (mg l^{-1}) at two of the sampling sites is shown in Fig. 2.

Taking into account the situation at all sites and all the parameters we can conclude that the highest concentrations of pollutants were observed in late 1980s. After 1990 an improvement of water quality in Torysa river can be observed due to economic decline (lower fertiliser application). The water quality development along the Torysa river is demonstrated in Fig. 3.

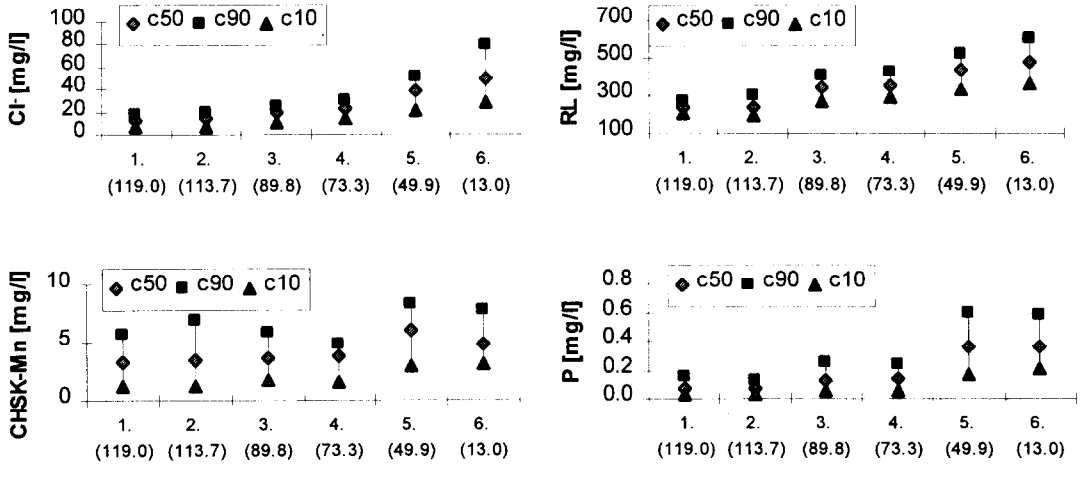

Figure 3: Development of the chlorides Cl^-, soluble matter (RL), total phosphorus (P) and COD (CHSK) along the Torysa, mean values and values with the probability of non-exceedance 90 % resp.10 % (c_{90} resp. c_{10}) for 1992–1996. On axis x there are the station numbers and river km.

3.2 Land use effect on the stream water quality in headwater microbasins

The land use effect on the washout of the pollutants was studied in three microbasins in the Torysa headwater. The microbasins were selected upstream of the reservoir under consideration. These microbasins were established and equipped for complex environmental monitoring of the reservoir Tichý Potok area at the beginning of 1996. The basic characteristics of the experimental microbasins are given in Table 1.

Environmental monitoring of the experimental basins included precipitation, runoff, water quality and spring yield. The measured specific discharges (yields) on the days of water quality sampling in individual basins are shown in Fig. 4. The chosen units allow comparison of the yield of areas with different land use. An important indicator of soil erosion is the content of insoluble matter (suspended load). It can be estimated that the total volume of transported suspended load from the monitored basins was between 2.5 and 4.4 tons per km^2 for the period 24th May to 18th December 1996.

Table 2: Mean values of basic monitored parameters in 1996.

Basin	q $l\ s^{-1}$"km^{-2}	pH	Conductivity $mS\ m^{-1}$	Soluble matters $mg\ l^{-1}$
Jedlinka	6.82	7.3–8.4	49.4	296–458
Repiská	7.75	7.5–8.4	29.7	156–280
Chmeľov	6.00	7.3–7.6	27.6	159–251

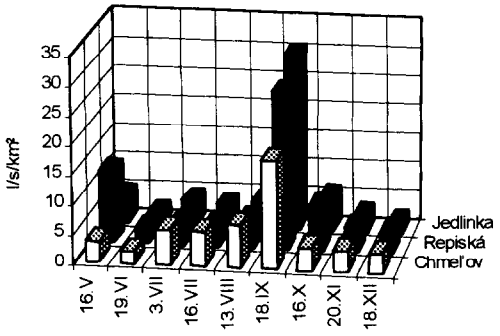

Figure 4: Yields of the microbasins.

Monitoring has confirmed that nitrate-nitrogen concentrations in the streams are highly influenced by the land use of the basins (Pekárová et al. 1995; Pekárová and Pekár 1996). The observed concentrations in the arable Jedlinka basin are 3 times higher than in the grassland Repiská basin. These values are 5.5 times higher if compared with the forested Chmeľov basin. The values of nitrate-nitrogen concentrations in arable Jedlinka basin were between 4.5–10.5 $mg\ l^{-1}$ (Fig. 5).

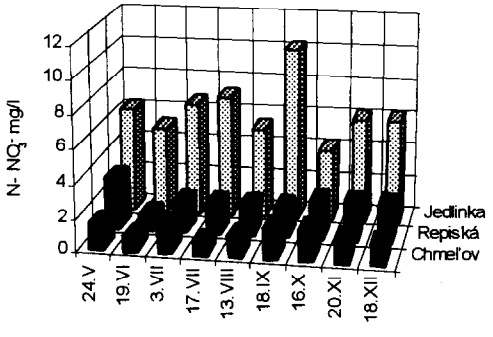

Figure 5: $N\text{-}NO_3^-$ concentrations in basins with different land use.

A pedological survey of the area has been undertaken (Stančík et al., 1997). The whole basin is in flysch area (alternating layers of sandstone and clays). The prevailing soil types in the area are the cambisoils. The parameters studied were soil structure, pH, humus, nutrients, contamination (heavy metals), phosphorus and magnesium, retention capacity,

capillary suction and other hydrophysical properties. Similar parameters were analysed in the stream sediments. The infiltration capacity of the soils was measured at three points in each basin using infiltration cones. The arable parts of the basin are subject to erosion due to the steep slopes.

3.3 Simulation results

The model AGNPS 5.0 was used for simulation of the runoff and nutrient transport in the stream. A detailed description of the model can be found in its manual (Young et al. 1989; 1996). AGNPS is a model with distributed parameters for simulation of runoff, soil erosion, sediment yield and nutrients during single rainfall-runoff events.

3.3.1 Input parameters

The area of the basin was divided into 90 cells (1 km x 1 km). About 20 input parameters are to be defined for each cell. Most of them can be derived from topographical and thematic maps (slopes, flow directions, land use, etc.). Fig. 6 shows the dominant flow directions in particular cells. Mean slopes and land use are shown in Figs. 7a and 7b. Flow directions and slopes were determined from the topographical maps. The runoff was modelled using SCS (U. S. Soil Conservation Service) curves (Young et al., 1996). It is possible to choose one of three curve numbers for each cell depending on the saturation conditions (the higher the saturation, the higher the curve number).

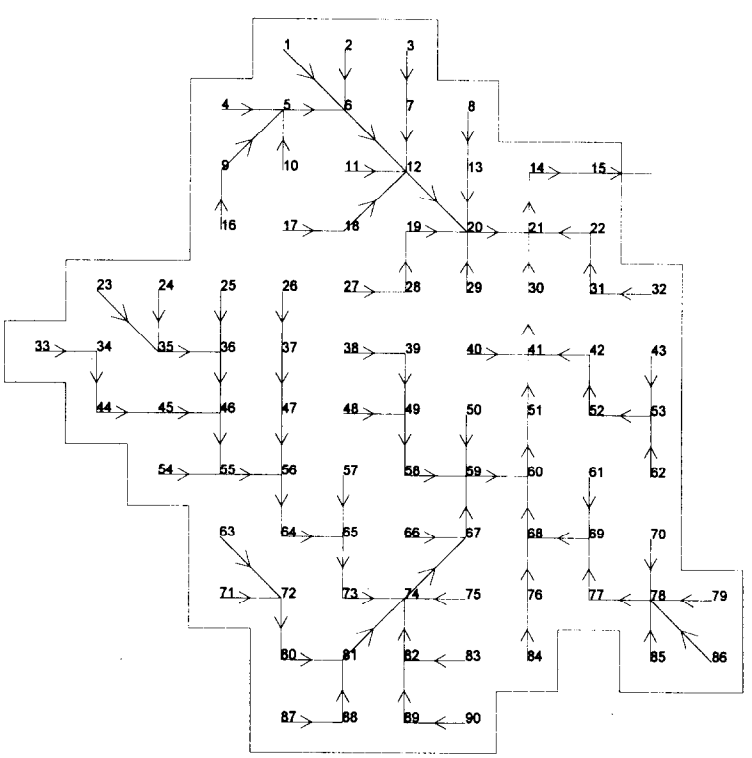

Figure 6: Scheme of the Torysa basin to the planned Tichý Potok reservoir, grid cells with their numbers and flow directions. (Input to the AGNPS model.)

The main parameters for the simulation are rainfall depth and duration. The model can be applied for simulating different events (dry and wet periods, different land use, initial concentrations, fertiliser applications, etc.).

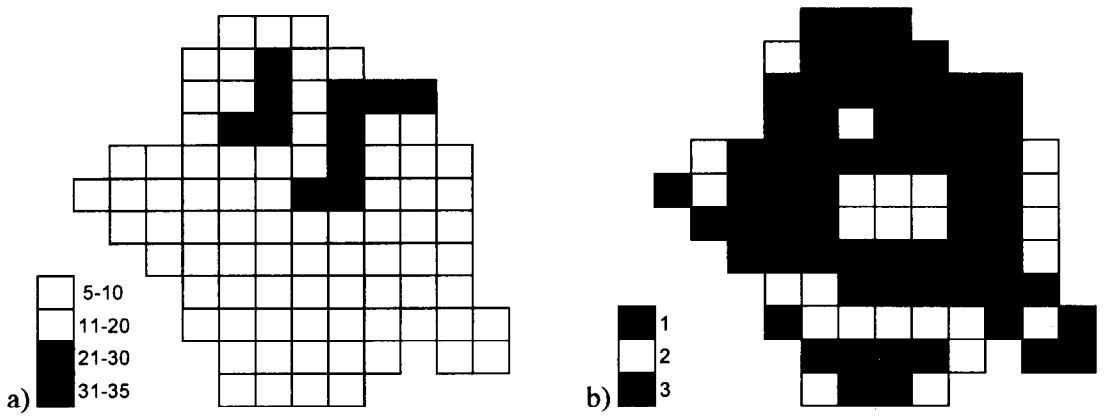

Figure 7: a) Mean slopes (in %) in individual cells. Upper Torysa basin. (Input to the AGNPS model.) b) Land use in the upper Torysa basin. 1 - forest, 2 - grass, 3 - arable land. (Input to the AGNPS model.)

3.3.2 Runoff simulation results

The model AGNPS 5.0 was used for simulation of the runoff and nutrient transport in the stream during a single rainfall-runoff event. The 50-year maximum daily precipitation is 90 to 100 mm in the area. Simulations were performed for 24-hour precipitation depths from 50 to 100 mm at increments of 10 mm. A special analysis was undertaken for a flood which occurred from the 5^{th} to the 9^{th} of July 1997. The precipitation over the five days was 177 mm at the nearest station. The areal precipitation in the basin was estimated on 180–190 mm. In the first 3 days 90 mm fell. The highest 24-hour precipitation of 55 mm (Faško et al., 1997) on the fourth day produced a significant part of the flood.

Comparison of the model results with the measured runoff is necessary to verify the simulation. Unfortunately, there is no gauging station on the stream and direct flood measurements are missing. We therefore used an indirect estimate of the peak flood flow at the planned dam profile (river km 110.2). According to Bučková and Hrošár (1997) the peak runoff rate at this point was 45 $m^3\ s^{-1}$ on July 9, 1997. Theoretical maximum flows, prepared as design data for the reservoir construction, are as follows (Schürger, 1998):

$$Q_1 = 17\ m^3\ s^{-1} \qquad Q_{100} = 170\ m^3\ s^{-1}$$
$$Q_5 = 56\ m^3\ s^{-1} \qquad Q_{1000} = 280\ m^3\ s^{-1}$$
$$Q_{10} = 77\ m^3\ s^{-1}$$

The graphical results presented in the paper are concerned with the case of 55 mm rainfall over 24-hours in highly saturated conditions. Basic results of all simulations are given in Table 3. The simulated runoff depths and peak runoff in individual cells are shown in Figs. 8a and 8b.

The reconstructed peak discharge of 45 $m^3\ s^{-1}$ corresponds to a return period of about four years. The simulated peak runoff was higher by 1.6 $m^3\ s^{-1}$, an overestimation of only 3.5 %. The simulated runoff depth was 29 mm and the runoff coefficient 0.52. In the case of the 50-year daily rainfall (90–100 mm) the peak runoff would be 104–120 $m^3\ s^{-1}$ according to model simulation.

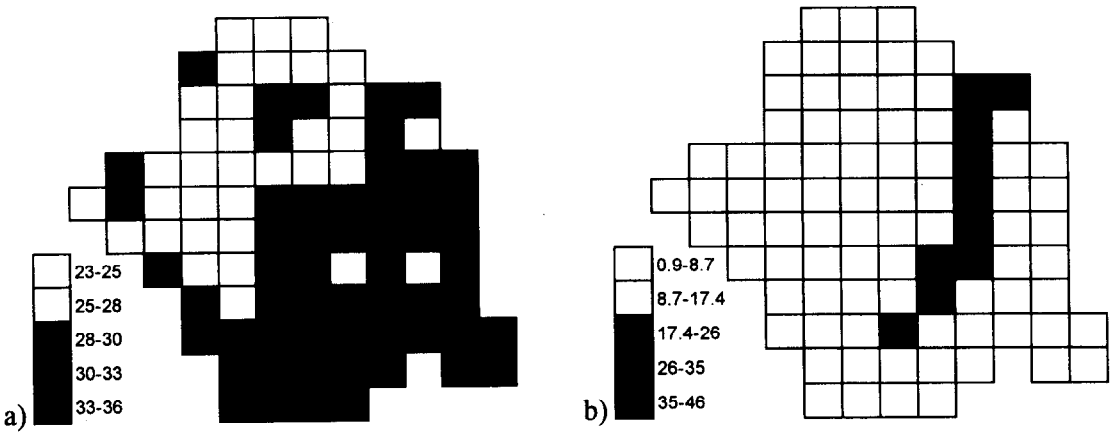

Figure 8: a) Simulated runoff depths in mm in the individual cells of the upper Torysa basin for the 24-hours 55 mm rainfall on July 9, 1997. (Output of the AGNPS model.) b) Simulated peak runoff rate in $m^3\ s^{-1}$ in the individual cells of the upper Torysa basin for the 24-hours 55 mm rainfall on July 9, 1997. (Output of the AGNPS model.)

3.3.3 Sediments and nutrients simulation

The model gives also estimation of sediment yield and nitrogen concentrations produced by the flood. No direct measurements or other indirect estimates are available for this ungauged flood. Therefore comparison or verification of the model results concerning the sediments and pollutants is not possible. Estimates of sediment loads are given in Table 3 and the possible spatial distribution of sediment yield and nutrient concentration is shown in Figs. 9a and 9b.

Table 3: Input precipitation and simulated runoff, peak runoff rate, total sediment yields and runoff coefficient for the situation on July 9, 1997.

Precipitation (mm)	Runoff depth (mm)	Peak runoff rate ($m^3\ s^{-1}$)	Total sediment yields (tons)	Runoff coeff.
40	17	23.1	386	0.43
50	24	38.1	697	0.49
55	29	46.6	908	0.52
60	33	55.4	1157	0.55
70	42	72.2	1766	0.59
80	50	87.7	2559	0.63
90	59	104	3597	0.66
100	69	120	4900	0.69

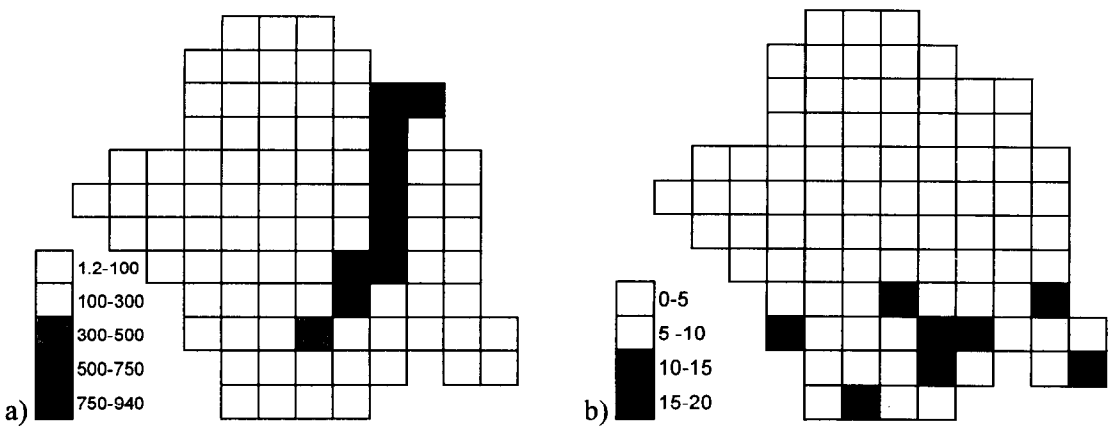

Figure 9: a) Sediments area yield in the individual cells of the upper Torysa basin in tons for the July 9, 1997 flood. b) Total nitrogen concentrations (mg l^{-1}) in the surface water in the individual cells of the upper Torysa basin for the July 9, 1997 flood. (AGNPS model output.)

4 Conclusions

Conclusions of the case study can be summarised as follows:

- Water quality in the Torysa upper stream is relatively good. The concentrations of the studied pollutants do not exceed national standards for the surface water quality.
- The water quality is on the mend after the early 1990s due to lower applications of fertiliser (Fig. 2, also Halmová, 1996).
- The arable land is being threatened due to steep slopes (erosion).
- Land use impact on the stream water quality is high.

In spite of certain drawbacks, the AGNPS model was found to be a suitable instrument for estimation and analysis of the rainfall-runoff process during the flood event on July 1997. The estimate of the peak runoff rate fits the independently reconstructed flood peak. There is no estimate of the sediment and nutrient transport in the basin during the flood wave other than the model simulation. This information should be used, therefore, only as an indication of possible conditions in the catchment.

A premature end to the project financing due to the economic situation meant that collection of the data needed for a more detailed and reliable analysis was not possible. Data sets used for calibration and verification of the model were short. It was not possible to obtain data from several floods with corresponding water quality sampling in short time intervals. The primary goal of the paper is therefore to demonstrate the application and suitability of the complex basic models for assessment of the environmental monitoring results. More detailed data would allow to use more dense grid division with elaboration of the input files by GIS (Liao and Tim, 1997).

References

[1] Bučková, G. and Hrošár, M. (1997) 'Assessment of the flood situation on the streams of Eastern Slovakia on July 1997'. (In Slovak.) Práce a štúdie 56, SHMÚ Bratislava, 41–45.

[2] Faško, P.; Nejedlík, P. and Šťastný, P. (1997) 'Atmospheric precipitation in Slovakia on July 1997.' (In Slovak.) Proc. Stoleté výročí extrémních atmosferických srážek, ČHMÚ Praha, 141–157.

[3] Halmová, 2.(1996) 'Pollution trends in the upper and middle parts of the Torysa stream.' (In Slovak) Proc. Transport vody, chemikálií a energie v systéme pôda-rastlina-atmosféra. ÚH SAV, Bratislava, 23–25.

[4] Hyánková, k.; Ženišová, Z.; Janský, L.; Fendeková, M. and Flaková, R. (1995) 'Influence of agricultural activity on the nitrate content in drinking water sources in Slovakia.' Hrvatske vode, 3, 12, 293–300.

[5] Liao, H. and Tim, U. S. (1997) 'An interactive modeling environment for non-point source pollution control.' J. Am. Wat. Resour. Assoc, Vol. 33, 1997, No. 3, 591–603.

[6] Pekárová, P.; Miklánek, P. and Rončák, P. (1995) 'Stream load and specific yield of nitrogen and phosphates from Slovakia.' J. Hydrol. Hydromech., 43, 4–5, 233–248.

[7] Pekárová, P. and Pekár, J. (1996) 'The impact of land use on stream water quality in Slovakia.' J. Hydrol., 180, 333–350.

[8] Schürger, J. (1998) 'Floods on Torysa river and their influence on the water sources of the waterworks.' (In Slovak.) Proc. Povodne a protipovodňová ochrana, SVP, B. Štiavnica, 97–98.

[9] Stančík, Š.; Koníček, A.; Miklánek, P. and Pekárová, P. (1997) 'Complex monitoring of the environment for the construction of Tichý Potok reservoir - Part Soils.' (In Slovak.) PIAPS, Žilina, 29 pp.

[10] Young, R. A.; Onstad, C. A. and Anderson, W. P. (1989) 'AGNPS: a non-point source pollution model for evaluating agricultural watersheds.' J. Soil and Wat. Conserv. 44, 168–173.

[11] Young, R. A.; Onstad, Ch. A.; Bosch, D. and Anderson, W., P. (1996) 'Agricultural non-point source pollution model, Version 4.03.' User's guide. Minnesota, MPCA.

A comparative assessment of two rainfall-runoff modelling approaches: GR4J and IHACRES

C. Perrin[1], I. G. Littlewood[2]

[1]Cemagref, Division Hydrologie, Parc de Tourvoie, BP 44, 92163 Antony CEDEX, France. [2]Institute of Hydrology, Crowmarsh Gifford, Wallingford, Oxon, OX10 8BB, United Kingdom.

Abstract

Personal computer (PC) versions of two catchment-scale rainfall-runoff modelling approaches, GR4J and IHACRES, are compared using qualitative and numerical criteria. The assessment of the modelling methodologies includes comments on the structures of the models, the parameter optimisation procedures and the use of both models as operational tools on PCs. Differences between the models occur in the level of non-linearity in their loss and transfer modules, the way effective rainfall is routed to the outlet, the identification of quick and slow components of streamflow, and their parameter optimisation procedures. GR4J and IHACRES performances were assessed numerically on eight catchments in the United Kingdom and on four catchments in the Orgeval experimental basin in France. On average, GR4J yielded a better Nash-Sutcliffe criterion in calibration and simulation modes whereas IHACRES provided less biased results. The parameters of the empirical GR4J model structure are automatically calibrated using a local search optimisation procedure by maximising the Nash-Sutcliffe criterion. In contrast, the model structure adopted by IHACRES uses unit hydrograph (UH) theory in the transfer module, and 'best' model parameters are selected semi-automatically on the basis of a trade-off between maximising the Nash-Sutcliffe criterion and minimising an indicative average error associated with the UH parameters (other diagnostic statistics can also be called upon).

1 Introduction

The present study assesses and contrasts two rainfall-runoff PC packages. The GR4J model and package was developed at Cemagref, France (Edijatno and Michel, 1989; Nascimento and Michel, 1992; Nascimento, 1995), and PC-IHACRES Version 1.0 was developed collaboratively by the Institute of Hydrology, United Kingdom and the Australian National University, Canberra (Jakeman et al., 1990; Littlewood et al., 1997). Both GR4J and IHACRES are spatially lumped conceptual models, each having loss and transfer modules, and require the same amount of input data. For full accounts of each of the models, the reader is directed to the corresponding literature cited above.

In this paper, the outline structures of both models will first be presented before contrasting their loss and transfer modules, following the procedures of Franchini and Pacciani (1991) and Zhang and Lindström (1996). Both modelling approaches were tested on 12 catchments at a daily time step. Comments are made on their performances according to selected numerical and graphical criteria, and their relative computing times and ease of use.

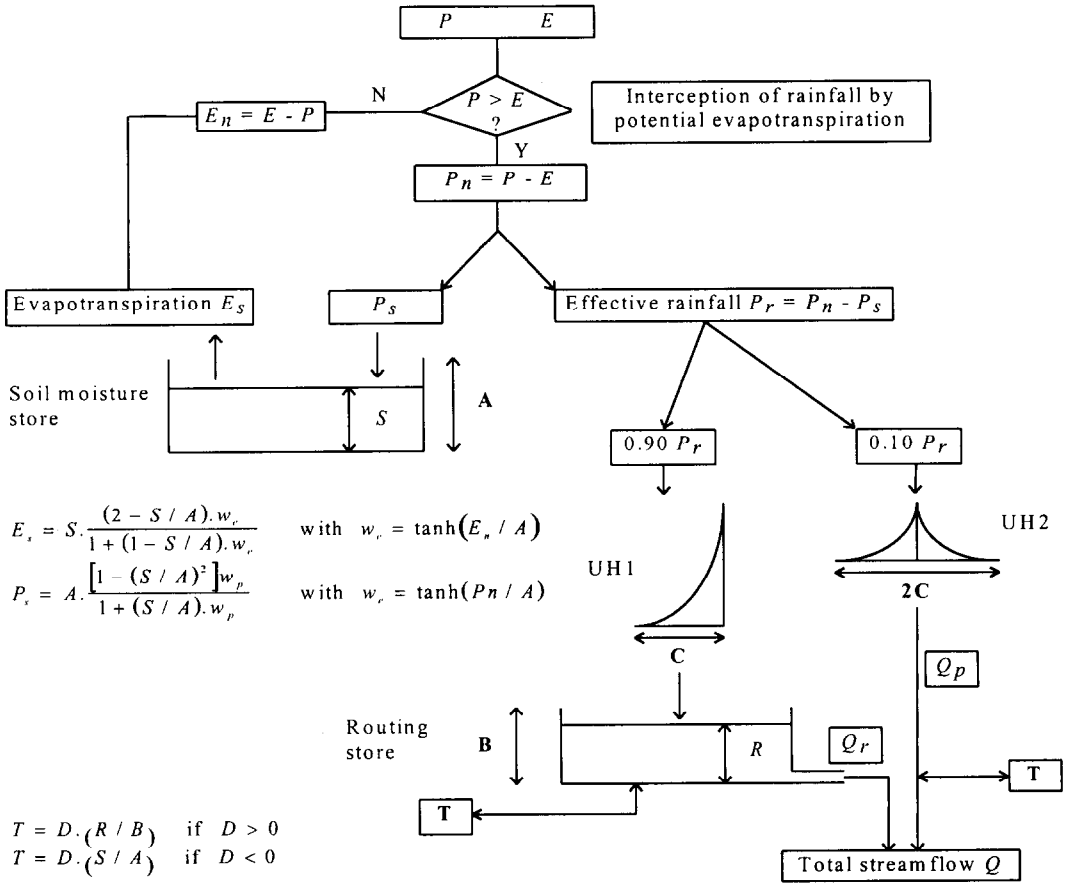

Figure 1: Structure of GR4J (adapted from Nascimento and Michel, 1992) in which P is rainfall, E is Penman potential evapotranspiration, A and B are maximum storage capacities of soil store S and routing store R, C defines the time-bases of functions UH1 and UH2 which distribute effective rainfall in time, T is a transfer term for groundwater exchanges, and Q is the streamflow.

2 General structure of IHACRES and GR4J

GR4J was originally developed for use at a daily time step (Edijatno, 1991; Nascimento and Michel, 1992; Nascimento, 1995). A very empirical approach was adopted to develop this model; its structure was chosen on the basis of an analysis of data from 121 catchments in France. Data requirements are rainfall and streamflow time-series and Penman potential evapotranspiration data. The general structure of GR4J is given in Fig. 1. A snowmelt module has been proposed by Makhlouf (1994) but was not used in the present study. GR4J has four parameters which are required to be optimised.

IHACRES is a six-parameter model which was first applied to two Welsh catchments and since then has been used on a wide range of catchments in Great Britain, Australia, the United States and elsewhere. The use of IHACRES is not restricted to a daily time step, as time intervals ranging from minutes to one month can be applied. In contrast with GR4J, the 'routing' module of IHACRES has a theoretical (linear systems/unit hydrograph) basis. The data requirements are essentially the same as for GR4J, but temperature instead of potential evaporation is usually used in the loss module to take account of the evaporative demand. A snowmelt module has been recently developed (Schreider et al., 1997), and a loss module which includes two additional parameters has been developed and applied for catchments in semi-arid climate zones (Hansen et al., 1996; Ye et al., 1997). The general structure of IHACRES is presented in Fig. 2.

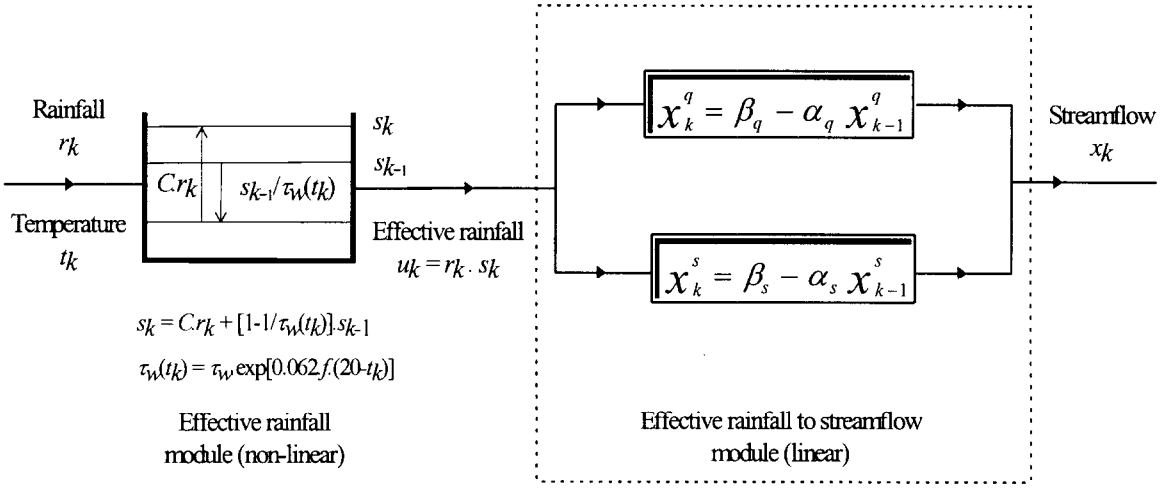

Figure 2: Structure of IHACRES (adapted from Post and Jakeman, 1996) in which C is a volume-forcing constant, τ_w is a catchment drying time-constant, f is a temperature modulation factor, t_k is the temperature, s_k is a soil moisture index, x_k^q and x_k^s are the quick and slow components of the flow, and x_k is total streamflow.

3 Comparison of loss modules

Without paying attention to the detail of the physical processes involved (a deliberate strategy in order to keep the number of model parameters small), both models have a simple loss module which accounts for losses from rainfall – to leave effective rainfall.

In GR4J, daily rainfall is first reduced by the amount of potential evapotranspiration (see Fig. 1). If evapotranspiration exceeds the amount of rainfall, the remaining evapotranspiration energy is used to evaporate water contained in a soil store, at an actual rate governed by a function of the store level. Alternatively, i.e. if evapotranspiration is less than rainfall, the remaining net rainfall is split into two parts. The first is the effective rainfall directed to the transfer module and the other component fills the soil store. The split rate is governed by a function of the level in the soil store. The evaporation from soil store S and the effective rainfall determination depend on the ratio $(S/A)^2$. The evaporation losses are complemented with an exchange term T characterised by parameter D which is applied to both components of the flow to simulate the net import or export of groundwater to or from the catchment (see Fig. 1). The loss module in GR4J is highly non linear.

In PC-IHACRES V1.0 (see Fig. 2), the effective rainfall u_k is determined at a given time step k using a catchment wetness index s_k, which is calculated from rainfall r_k and the value of the catchment wetness index at the previous time step s_{k-1}. Catchment wetness s_k decays (as a result of evapotranspiration) at a rate determined by temperature t_k. This scheme was developed using data from temperate humid region catchments and is best suited to topographically defined basins which do not have net imports or exports of groundwater. Modified loss modules for use with IHACRES, such as those described by Hansen et al. (1996) and Ye et al., (1997), have been devised for semi-arid catchments.

The loss process in GR4J depends on two parameters: the maximum capacity A of the soil store S; and parameter D of the groundwater transfer term (T). The loss module in PC-IHACRES V1.0 has three parameters: a temperature modulation factor f; a catchment drying time constant τ_w; and a volume-forcing constant C. Parameters f and τ_w are calibrated by a user-driven procedure (e.g. Littlewood et al., 1997) using the PC package, whereas C is simply calculated within PC-IHACRES such that the volumes of effective rainfall u_k and recorded streamflow over the model calibration period are equal (model calibration periods are, therefore, selected to start and finish at the end of long streamflow recessions).

4 Comparison of transfer modules

The two models differ in the way in which streamflow components are dealt with. In GR4J, the effective rainfall is always first split into two pre-set volumetric components: 90 % is routed through a non-linear routing store R characterised by its maximum capacity B, after being progressively delayed by the function UH1; and 10 % is routed straight to the outlet but subjected to function UH2. The two functions UH1 and UH2 are defined by the time-base parameter C (see Fig. 1). The whole transfer process in GR4J is non-linear and depends on two parameters (B and C).

The IHACRES transfer module invokes the theory of unit hydrographs first proposed by Sherman (1932). The originality of the IHACRES methodology is the identification of unit hydrographs for dominant quick *and* slow response components of streamflow (and therefore a unit hydrograph for *total* streamflow). Each unit hydrograph (UH) is characterised by two parameters (the α and β parameters shown in Fig. 2). Dynamic response characteristics (DRCs) for quick and slow flows, such as unit hydrograph decay response times and relative quick and slow flow volumetric throughputs (different for different catchments), can be determined from the values of the α and β parameters (Jakeman et al., 1990; Littlewood and Jakeman, 1993, 1994). The IHACRES routing module depends on four parameters but only three of them (any three of $\alpha_s, \beta_s, \alpha_q, \beta_q$) are required to be known as they are linked by a simple relationship.

5 Parameter optimisation procedures

The four parameters of GR4J (A, B, C and D) are optimised with a local direct search technique known as the 'step-by-step' method developed in Cemagref (Michel, 1989). The parameter search is conducted by optimising the Nash-Sutcliffe criterion. This simple method locates a reliable optimum of the model-fit criterion and has proved as efficient as global search techniques for GR4J, as suggested by Nascimento (1995). The calibration procedure is fully automatic in GR4J.

The IHACRES methodology includes a semi-automatic parameter optimisation. The UH parameters of the linear module are identified automatically using the 'simple refined instrumental variable' technique (Jakeman, 1979; Young, 1984). Parameters f and τ_w in

the loss module are determined by a trial-and-error search procedure, the user of the package making a trade-off between several statistics computed by the model [but principally the Nash-Sutcliffe criterion and an average measure of precision on the UH parameters – e.g. see Littlewood et al. (1997) for details].

6 Computing times and ease of use

Due to its fully automatic procedure and lower number of parameters to be optimised, the calibration of the GR4J model is easier and quicker than for IHACRES. However, the manual optimisation of the IHACRES loss module makes the user more aware of the role of the parameters in the model and it can be more flexible with respect to the specific interests of the user (e.g. hydrograph separation, low flow simulation). The efficiency of IHACRES in calibration mode depends partly on the experience of the user with the package. In simulation mode, computing times are about the same for both packages. GR4J is an MS-DOS application whereas PC-IHACRES is a Windows application. The use of both packages is facilitated by detailed user guides (see Cemagref, 1997 for GR4J; Littlewood et al., 1997 for IHACRES).

7 Numerical performances

The packages were tested on 12 catchments representing a wide range of characteristics as shown in Table 1 (four catchments in the Orgeval experimental basin in France and eight catchments in the United Kingdom).

Table 1: Catchment characteristics and locations.

River name	Gauging station name	Location	Area (km^2)	Mean daily streamflow (cumecs)	Mean annual rainfall (mm)
Derwent	Buttercrambe	UK (Yorkshire)	1586.0	16.46	779
Fal	Tregony	UK (Cornwall)	87.0	1.98	1229
Nidd	Hunsingore Weir	UK (Yorkshire)	484.3	8.13	973
Orgeval	Melarchez	France (Seine-et-Marne)	7.0	0.06	678
Orgeval	La Gouge	France (Seine-et-Marne)	24.7	0.22	683
Orgeval	Avenelles	France (Seine-et-Marne)	45.7	0.32	688
Orgeval	Theil	France (Seine-et-Marne)	104.0	0.70	684
Ouse	Skelton	UK (Yorkshire)	3315.0	48.82	906
Snaizeholme Beck	Low Houses	UK (Yorkshire)	10.2	0.57	1758
Swale	Crakehill	UK (Yorkshire)	1363.0	19.45	851
Teifi	Glan Teifi	UK (Wales)	893.6	28.30	1349
Ure	Westwick Lock	UK (Yorkshire)	914.6	20.68	1133

The numerical performances were assessed for each catchment on at least one calibration period and one simulation period according to the split-sample test recommended by Klemes (1986). Three main numerical criteria were used to evaluate the model-fit quality: the Nash-Sutcliffe criterion; the water-balance error; and the absolute deviation. However, these numerical criteria were often usefully complemented by graphical assessments, i.e. comparisons of observed and estimated (i) hydrographs, (ii) flow duration curves and (iii) cumulative water yields over the period of study. In total, GR4J and IHACRES were each tested on 27 calibration and 38 simulation periods.

In this short paper it is not possible to present the details of all the results obtained for the 12 catchments; further details are given by Perrin (1997). However, a few general comments can be made. Table 2 shows the percentage of runs when GR4J was ranked first. Figures 3 and 4 show the compared results of GR4J and IHACRES for the Nash-Sutcliffe criterion and the water balance error.

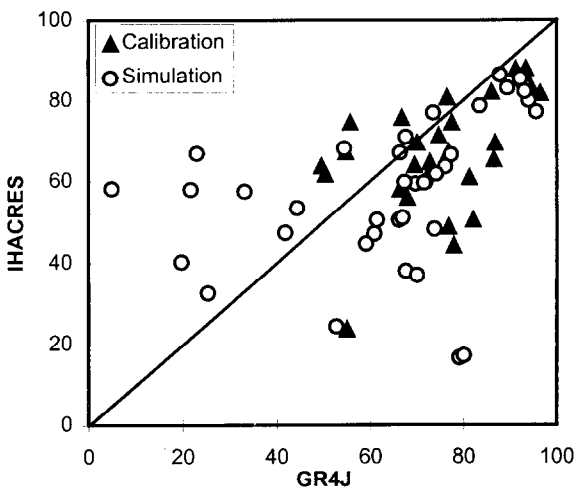

Figure 3: Scatter plots of GR4J and IHACRES Nash-Sutcliffe criteria (%).

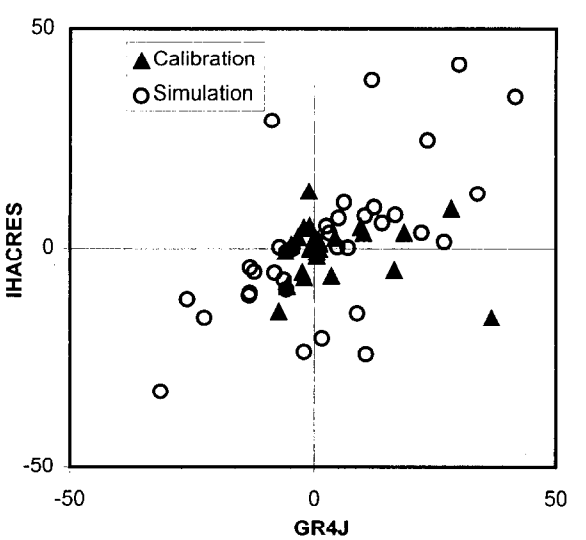

Figure 4: Scatter plot of GR4J and IHACRES water balance errors (%).

On average, GR4J performed better than IHACRES in terms of the Nash-Sutcliffe criterion and absolute deviation, both in calibration and simulation modes. GR4J showed better ability than IHACRES to explain streamflow variance but it is interesting to note in Fig. 3 that for several cases where GR4J performed poorly in simulation mode PC-IHACRES V1.0 performed tolerably well. For the water-balance error (bias) IHACRES, on

average, gave better results than GR4J (Table 2). These results may be partly related to the way the model parameters are optimised. GR4J parameter optimisation relies *only* on the Nash-Sutcliffe criterion, whereas IHACRES employs a trade-off between several statistics including (at least) the Nash-Sutcliffe criterion and an average precision on the unit hydrograph parameters. The volume-forcing through parameter C in IHACRES may be largely responsible for the less biased results.

Table 2: Summary of the statistical performances (percentage of runs when GR4J was ranked first).

	Calibration (%)	Simulation (%)	Total (%)
Nash-Sutcliffe criterion	72	61	65
Balance error	45	46	45
Absolute deviation	72	76	75

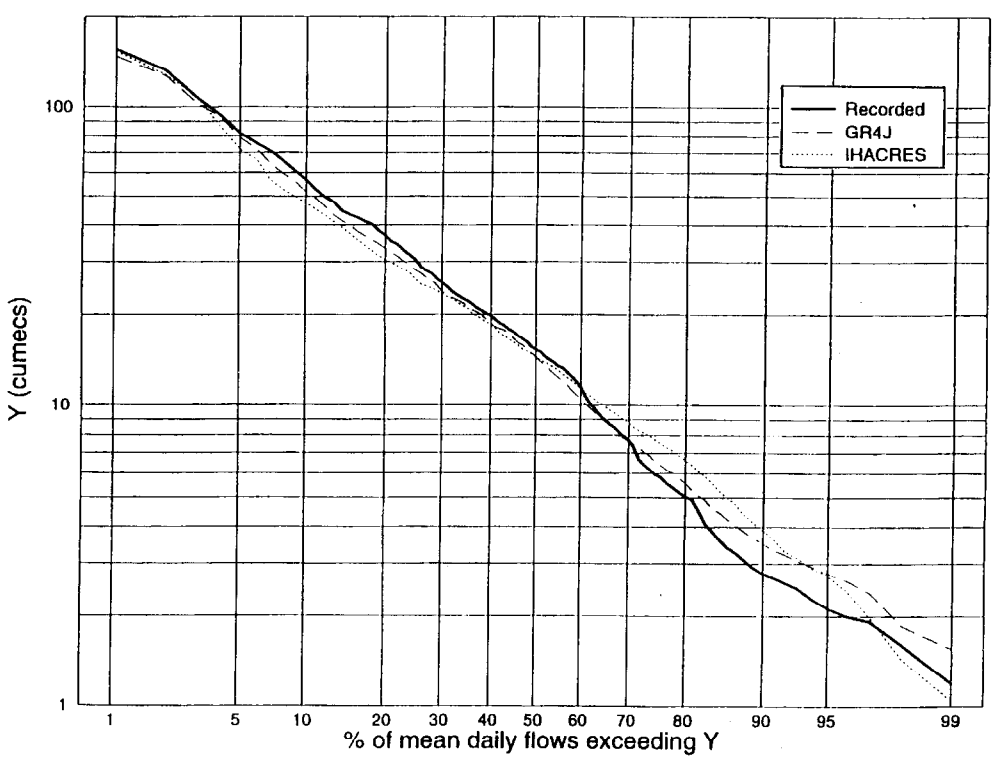

Figure 5: Flow duration curves for the Teifi at Glan Teifi (simulation period from 01/10/1972 to 31/08/1976).

Both models showed a better ability to yield satisfactory results with good rainfall data quality, i.e. when the areal rainfall was estimated from a sufficient number of rain-gauges spread over the catchment. They also gave better results for catchments where the streamflow regime is essentially natural, i.e. where streamflow is largely unaffected by engineering works or other anthropogenic factors. With good rainfall data and nat-

ural flow regimes, both models gave satisfactory results, e.g. for the Teifi at Glan Teifi the Nash-Sutcliffe criterion exceeded 85 % in simulation and there was good agreement between measured and estimated flow-duration curves for both models (see Fig. 5).

Problems of model 'warm-up' can occur with GR4J to a greater extent than with IHACRES, i.e. at the start of the modelled period the level of modelled flows gradually approaches that of observed flows. For calibration periods where some problems of water balance arise, the GR4J optimisation procedure tends to increase the model storage capacities (A and B) to get a better water balance, which lengthens the model warm-up time required to fill these storages. IHACRES can cope with such problems more easily due to the volume forcing constant (C) which forces the volume of effective rainfall over the model calibration period to be the same as that for observed flow. For GR4J, this problem of warm-up could, however, be minimised by choosing suitable initial values of the storage levels or by lengthening the warm-up period, as shown in Fig. 6 (the GR4J curve corresponds to a calibration run using a 18-month warm-up period and the GR4J(b) curve corresponds to a run with a 12-month warm-up period).

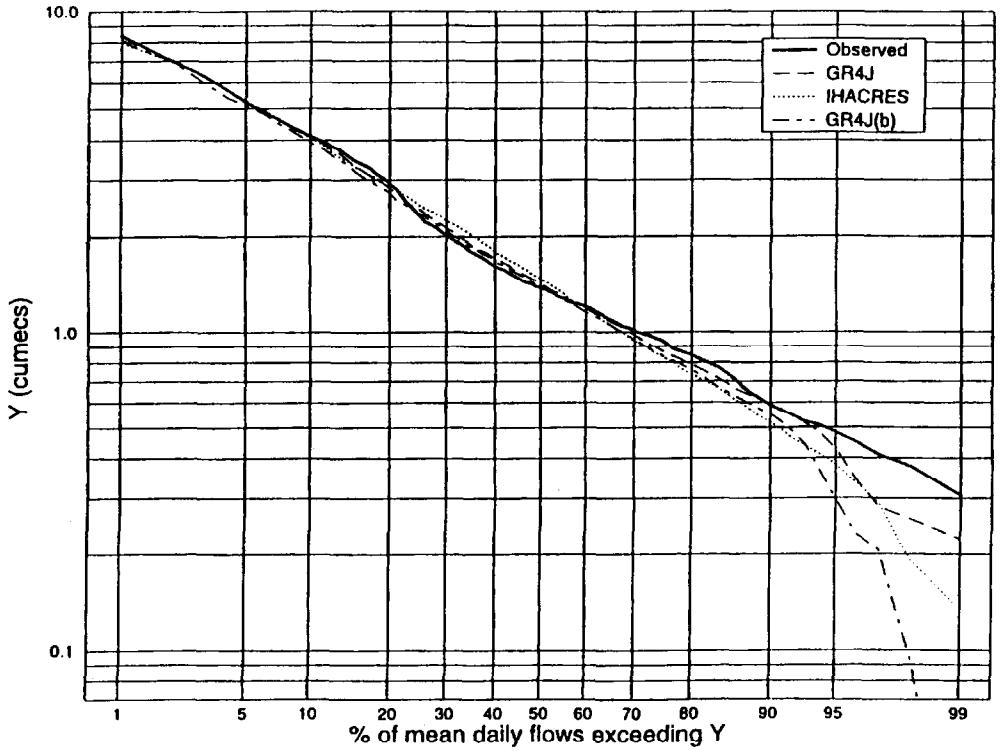

Figure 6: Flow duration curves for the Fal at Tregony (calibration period from 28/08/1984 to 28/08/1989).

Cases of non-satisfactory estimation of the areal rainfall occurred for some of the Yorkshire catchments (Table 1) where a motivation for application of the models was to try to extend streamflow time-series backwards in time using only a few long-term rainfall time-series (Perrin, 1997).

When compared on a limited number of datasets, as in this paper, each model exhibits strengths and weaknesses, and this perhaps reflects the different applications which the developers of the models originally had in mind. PC-IHACRES V1.0 does not appear to cope well for rain events during low summer flow conditions in the relatively dry Orgeval basin which exhibits a more highly non-linear relationship between rainfall and streamflow than the humid, temperate zone, Teifi at Glan Teifi. The use of alternative loss modules with IHACRES (e.g. Hansen et al. (1996); Ye et al., 1997) will help to solve this problem.

The identification of unit hydrographs for the dominant quick and slow flow components of streamflow by IHACRES is more appealing to the hydrologist interested in catchment dynamic behaviour than the constant 10 % volumetric contribution 'directly' to the outlet in GR4J (irrespective of catchment). For some flashy catchments (e.g. the Snaizeholme Beck at Low Houses), in which the quick flow component represents an important volumetric part of the streamflow, the prescribed 10 %/90 % volumetric split in GR4J may be inappropriate.

8 Conclusion

This short paper has presented a necessarily restricted comparative assessment of the PC versions of two rainfall-runoff packages, GR4J and PC-IHACRES V1.0, based on qualitative and quantitative criteria.

Although both GR4J and IHACRES are simple, spatially lumped, models with only a few parameters, there are major differences in the modelling methodologies. GR4J uses potential evapotranspiration whereas PC-IHACRES usually uses temperature to take account of the evaporative demand. GR4J seems more able than PC-IHACRES V1.0 to simulate highly non-linear rainfall - streamflow behaviour. The transfer of *effective* rainfall to the outlet is linear in IHACRES and non-linear in GR4J. However, the identification of dominant quick and slow streamflow components is more flexible in IHACRES than in GR4J.

Both models, tested on 12 catchments under temperate climate, performed well. GR4J yielded better efficiencies in calibration and simulation whereas IHACRES yielded less biased results. These results are partly related to the way model parameters are optimised and the choice of objective function(s), e.g. GR4J uses only one objective function but the IHACRES methodology employs a trade-off between a minimum of two functions. The use of a different objective function (or functions) with GR4J and IHACRES may well give a different comparative story, as suggested by Gan et al. (1997). However, neither of the models gave better results than the other for every catchment. Work is underway to investigate GR4J, IHACRES and other modelling approaches on a larger number of catchments than was possible here.

Acknowledgements

This paper is based on a program of work carried out at the Institute of Hydrology, Wallingford, United Kingdom, as part of the final year study of the first author (CP) at ENGEES (Engineering School for Water and Environment, Strasbourg, France). Thierry Leviandier of ENGEES, and Claude Michel and Vazken Andréassian of Cemagref, Antony, are gratefully acknowledged for their help and advice during this study and for providing data for the Orgeval catchments. Mike Law from the Environment Agency in York is thanked for providing long rainfall time-series for the Yorkshire catchments. Thanks are due also to Paul Wass for arranging a period of field work for CP in Yorkshire. The authors would like to also thank many colleagues at the Institute of Hydrology for their helpful advice.

References

[1] Cemagref (1997) 'Daily rainfall-runoff models - User guide' (In French). Hydrology Division, Cemagref (Antony), 30 p.

[2] Edijatno (1991) 'Elaboration of a simple daily rainfall-runoff model' (In French). Ph.D. dissertation, Louis Pasteur University (Strasbourg) / Cemagref (Antony), 625 p.

[3] Edijatno and C. Michel (1989) 'A three parameter daily rainfall-runoff model' (In French). La Houille Blanche, 2, 1989, p. 113–121.

[4] Franchini, F. and M. Pacciani (1991) 'Comparative analysis of several conceptual rainfall-runoff models'. J. of Hydrol., 122, 1991, p. 161–219.

[5] Gan, T. Y., E. M. Dlamini and G. F. Biftu (1997) 'Effects of model complexity and structure, data quality, and objective functions on hydrologic modeling'. J. of Hydrol., 192, p. 81–103.

[6] Hansen, D. P., W. Ye, A. J. Jakeman, R. Cooke and P. Sharma (1996) 'Analysis of the effect of rainfall and streamflow data quality and catchment dynamics on streamflow prediction using the rainfall-runoff model IHACRES'. Environmental Software, 11(1–3), p. 193–202.

[7] Klemes, V. (1986) 'Operational testing of hydrologic simulation models'. Hydrological Sciences Journal, 31(1), p. 13–24.

[8] Jakeman, A. J. (1979) 'Multivariable instrumental variable estimators: the choice between alternatives'. Proceedings of the 5th IFAC Symposium on Identification and System Parameter Estimation, Darmstadt, R. Isermann (Ed.), Vol. 2, Pergamon, Oxford, p. 1219–1225.

[9] Jakeman, A. J., I. G. Littlewood and P. G. Whitehead (1990) 'Computation of the instantaneous unit hydrograph and identifiable component flows with application to two small upland catchments'. J. of Hydrol., 117, p. 275–300.

[10] Littlewood, I. G., K. Down, J. R. Parker and D. A. Post (1997). The PC version of IHACRES for catchment-scale rainfall-streamflow modelling. Version 1.0. User Guide. Institute of Hydrology, 89 p.

[11] Littlewood, I. G. and A. J. Jakeman (1993) 'Characterisation of quick and slow streamflow components by unit hydrographs for single- and multi-basin studies'. In M. Robinson (Ed.), Proc. Fourth Conference of the European Network of Experimental and Representative Basins, Oxford, September 29–October 2, 1992, published as Institute of Hydrology Report 120.

[12] Littlewood, I. G. and A. J. Jakeman (1994) 'A new method of rainfall-runoff modelling and its applications in catchment hydrology'. In: P. Zannetti (Ed.) Environmental Modelling (Vol. II), Computational Mechanics Publications, Southampton, UK, p. 143–171.

[13] Makhlouf, Z. (1994) 'Further information about rainfall-runoff model GR4J and attempt of estimation of its parameters' (In French). Ph.D. dissertation. University of Paris XI Orsay / Cemagref (Antony), 228 p.

[14] Michel, C. (1989) 'Applied hydrology for small rural catchments' (In French). Cemagref (Antony), 528 p.

[15] Nascimento, N. O. (1995) 'Assessment with an empirical model of the impacts of human activities on catchment-scale rainfall-runoff processes' (In French). Ph.D. dissertation. CERGRENE / ENPC, 550 p.

[16] Nascimento, N. O. and C. Michel (1992) 'Some epistemological aspects of the development and use of hydrologic conceptual models'. Proceedings of the 4th Junior Scientist Course "Assessment of Modelling Uncertainties and Measurement Error in Hydrology", S^{t}-Etienne (France).

[17] Perrin, C. (1997). Comparative assessment of two rainfall-runoff modelling approaches: GR4J and IHACRES. Unpublished dissertation. Ecole Nationale du Génie de l'Eau et de l'Environnement de Strasbourg (France) / Institute of Hydrology, Wallingford (UK), 153 p.

[18] Post, D. A. and A. J. Jakeman (1996) 'Relationships between catchments attributes and hydrological response characteristics in small Australian mountain ash catchments'. Hydrological Processes, 18, p. 877–892.

[19] Sherman, L. K. (1932) 'Streamflow from rainfall by the unit hydrograph method'. Eng. News-Record, 108, p. 501–505.

[20] Schreider, S. Y., A. J. Jakeman, B. G. Dyer and R. I. Francis (1997) 'A combined deterministic and self-adaptative stochastic algorithm for streamflow forecasting with application to catchments of the Upper Murray basin, Australia'. Environmental Modelling and Software, 12(1), p. 93–104.

[21] Ye, W., B. C. Bates, N. R. Viney, M. Silvapan and A. J. Jakeman (1997) 'Performance of conceptual rainfall-runoff models in low-yielding ephemeral catchments'. Water Resour. Res., 33(1), p. 153–166.

[22] Young, P.C. (1984) 'Recursive estimation and time-series analysis - An introduction'. Springer-Verlag, Berlin, 300 p.

[23] Zhang, X. and G. Lindström (1996) 'A comparative study of a Swedish and a Chinese hydrological model'. Water Resour. Bull., 32, p. 985–994.

Experimental analysis of different runoff generation mechanisms

G. Peschke[1], C. Etzenberg[1], G. Müller[2]

[1]International Graduate School Zittau, Markt 23, D-2763 Zittau, Germany. [2]University of Technology, Institute of Hydrology and Meteorology, Mommsenstr. 13, D-01069 Dresden, Germany.

1 Introduction

The analysis of runoff generation in hydrological catchment areas is one of the key research problems to get an improved understanding of the physical generating mechanisms of flood producing runoff. The quick runoff components (Hortonian overland flow - infiltration excess and Dunne overland flow - saturation excess) represent the direct response to a storm event and determine the shape of a flood hydrograph and its main characteristics: the rising and the falling limbs of the hydrograph; the peak discharge; and the streamflow volume as decisive variables to different problems of design and management of flood constructions (e.g. dams). Additionally, outflowing 'old' water from the hill base due to infiltrating rain water into the hill-top regions can considerably contribute to the direct catchment response.

Various catchment features and the properties of the causing precipitation event influence the interrelation between these flood characteristics. However, there seems to be a significant difference. The terrain features dominate as influence factors on small floods, which are produced by convective heavy rains during dry catchment conditions, whereas large floods are greatly reflected by the rain hyetograph and the higher antecedent soil moisture (Merz and Plate, 1997; Grayson et al., 1997). The change-over between these two different runoff production mechanisms is related to the exceedance of certain thresholds. It is the main subject of this paper to investigate the different runoff generation mechanisms - based on experimental work in the experimental and research basin Wernersbach (Peschke et al., 1990; Etzenberg et al., 1997; Peschke et al., 1998; Peschke, 1997) - and to find the thresholds of the change-over between terrain dependency and event dependency.

2 Area of investigation

Attention is focused on the small representative research basin Wernersbach of 4.6 km^2 catchment area (Fig. 1). This allows to neglect the

- considerable degree of the spatial variability of the rain,
- time of concentration (period of time required of storm runoff to flow to the outlet from the point of a drainage basin having the longest travel time).

That means that the catchment response is primarily governed by hillslope response and not by the stream network response (Robinson et al, 1995).

We have obtained our experimental findings in the adjacent sub-basins Triebenbach (TB) and Upper Wernersbach (UWB) with sizes of 1.55 km^2 and 0.93 km^2, respectively (Fig. 1). There are some characteristic differences in the basin features. The UWB-basin has a significantly greater percentage of less permeable gleys than the TB-basin. The higher percentage of steeper slopes of the TB-basin is considerable.

In addition to these differences one remarkable feature of the UWB-basin is significant in order to understand the runoff generation mechanism: impermeable roads of 2.6 km in length altogether transform the rain into Hortonian overland flow.

Let us now consider the various responses of these adjacent basins.

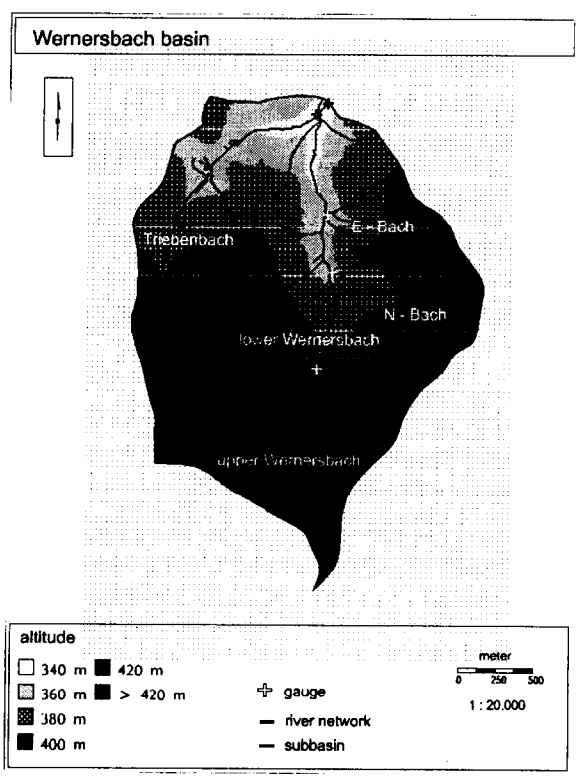

Figure 1: The Wernersbach basin with zones of altitude, the main stream network and the sub-basins.

3 Results and discussion

Fig. 2 (right) illustrates that the same high-intensive hourly rain of a convective storm event produces quite different hydrological responses in the adjacent sub-basins. Owing to the infiltration excess (Hortonian overland flow) on the roads the hydrograph of the UWB-basin steeply increases and reaches a higher maximum, whereas the attenuated temporal course of the TB-hydrograph is occasioned by the higher percentage of infiltrating and water storing areas. This difference in flood hydrographs diminishes during a larger rain which brings along a higher moisture level of the catchments' soils. This moister state activates the first saturation areas to produce overland flow as saturation excess thus thrusting the percentage of Hortonian overland flow into the background.

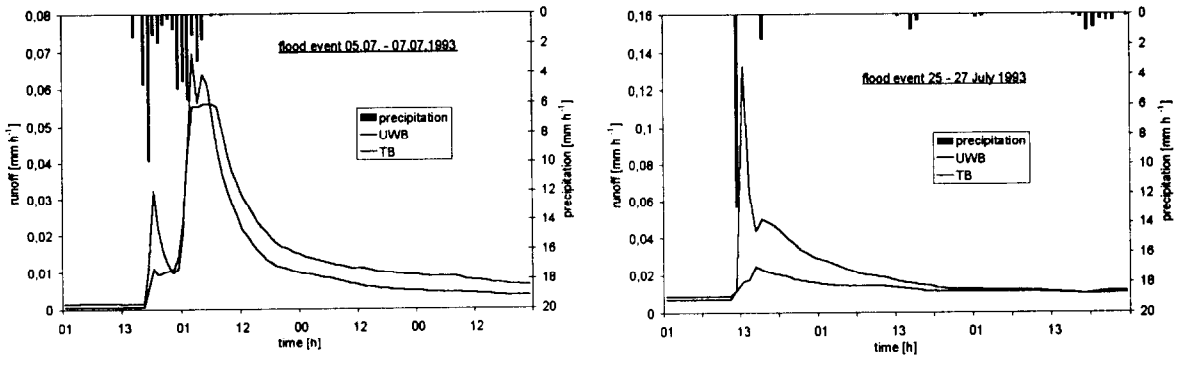

Figure 2: Different responses of the adjacent sub-basins Upper Wernersbach (UWB) and Triebenbach (TB) to the same rain input in a summer period with low antecedent soil moisture.

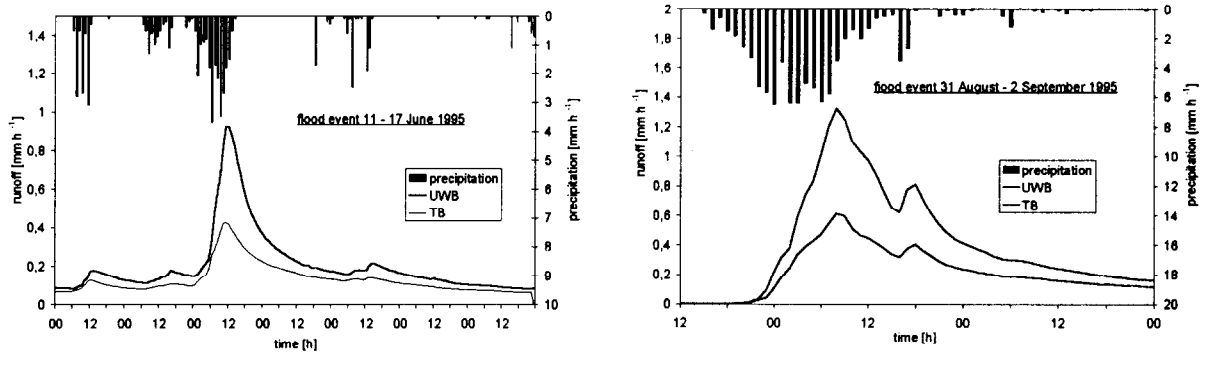

Figure 3: Under wetter conditions, either by a high degree of antecedent soil moisture (left) or by a large rain amount (right), the shapes of the runoff hydrographs become more similar.

If this moisturizing of the basin continues - either by a large antecedent soil moisture (Fig. 3, left) or by a large rain amount (Fig. 3, right) - the basin responses become more similar than those in Fig. 2. Now their shape is primarily governed by the rain parameters, whereas the differences in the runoff generation mechanisms as discussed with regards to Fig. 2 lose their significance. The ability of the two basins to extend the contributing saturation areas is now dominant. This ability is quite different. Owing to the steeper slopes of the TB-basin the saturated area quickly reaches its boundary and remains limited to the valley bottom. However, in the relatively flat and impermeable UWB-basin the contributing areas can expand further. Thus the latter generates more flood producing runoff - in spite of the smaller catchment area - than the TB-basin (Fig. 3).

These results may be confirmed and generalized by Fig. 4, which shows - for a variety of daily runoff values - the relation of the certain sub-basin outflow to the whole basin outflow in dependence on the increasing runoff (increasing moisture). Under dry conditions we see a great variance owing to great differences in the runoff production. This variance decreases with growing moisture and the share approaches a limiting value, which in the case of the TB-basin decreases in consequence of the limited saturation area.

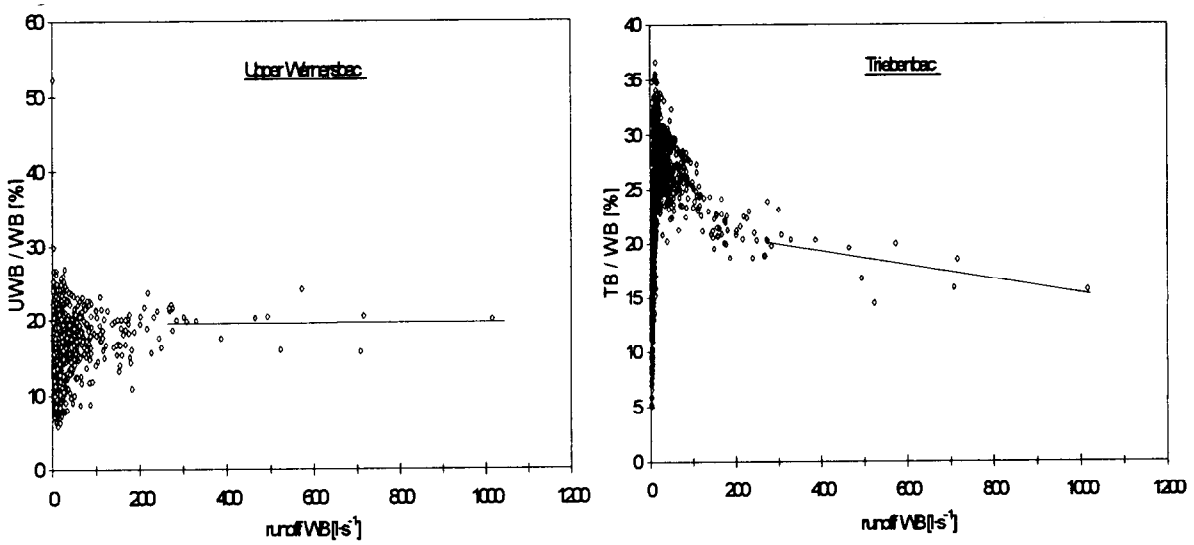

Figure 4: The share of the sub-basin runoff in the whole Wernersbach runoff versus the runoff level as measure of the moisture conditions.

The change-over in the runoff production process from the dominating terrain influence to the dominance of the rain event appears when thresholds or critical values are exceeded.

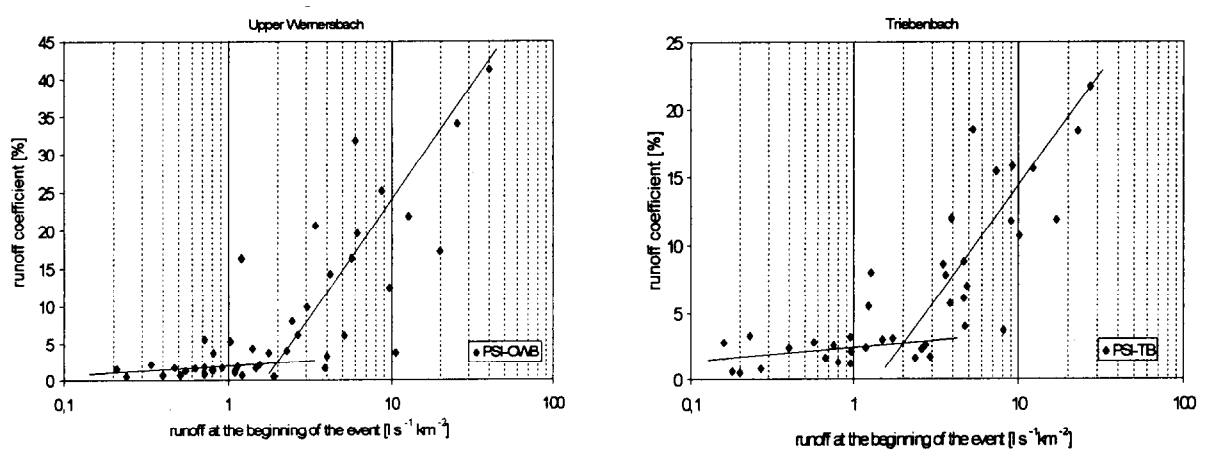

Figure 5: Runoff coefficient of all measured floods in dependence on the antecedent soil moisture, characterized by the runoff at the beginning of the event.

The switch between the two states seems to be associated with a dominance of lateral over vertical water fluxes. We have analysed the runoff coefficient of all measured floods in the two sub-basins in dependence of antecedent soil moisture (Fig. 5). The same value of 2 l $s^{-1}km^{-2}$ in both sub-basins separates two different types of runoff regimes: on the one hand small floods as in Fig. 2, on the other hand large floods as in Fig. 3.

References

[1] Etzenberg, C.; Müller, G. and G. Peschke (1997): Water balance study in a small representative mountainous forested basin. Strasbourg-Conf. "Ecohydrological processes in small basins" (1996), submitted to IAHS Publ.

[2] Grayson, R. B.; Western, A. W.; Chiew, H. S. and G. Blöschl (1997): Preferred states in spatial soil moisture patterns: local and nonlocal controls. Water Resour. Res. 33, 2897–2908.

[3] Merz, B. and E. J. Plate (1997): An analysis of the effects of spatial variability of soil and soil moisture on runoff. Water Resour. Res. 33, 2909–2922.

[4] Peschke, G. (1997): The spatial and temporal variability of hydrological processes in mountainous areas. In: Brilly, M. and A. Gustard (eds.): LDC proceed. 3rd Intern. Conf. FRIEND, Postojna 1997; Acta Hydrotechnica 15/18, 113–122.

[5] Peschke, G.; Etzenberg, C.; Müller G.; Töpfer, J. and S. Zimmermann (1998): Runoff generation regionalization - analysis and a possible approach to a solution. Braunschweig-Conf. "Regionalization in Hydrology" (1997), submitted to IAHS Publ.

[6] Peschke, G.; Miegel, K.; Etzenberg; C. and H. Hebentanz (1990): On the spatial variability of hydrological processes in a small mountainous basin. IAHS Publ. No. 1993, 61–69.

[7] Robinson , J. S.; Sivapalan, M. and J. D. Snell (1995): On the relative roles of hillslope processes, channel routing, and network geomorphology in the hydrologic response of natural catchments. Water Resour. Res. 31, 3089–3101.

Streamwater acidification in the Krušné hory, northern Bohemia, Czech Republic

N. E. Peters[1], J. Černý[2], M. Havel[2], V. Majer[2]

[1]U. S. Geological Survey, 3039 Amwiler Rd., Suite 130, Atlanta, Georgia 30360-2824, USA. [2]Czech Geological Survey, Klárov 3/131, CZ 118 21 Praha 1, Czech Republic.

1 Introduction

Acidic atmospheric deposition has affected aquatic ecosystems throughout the world. Since the mid-1970s, much has been learned about the effect of atmospheric pollutants on biogeochemical processes, particularly in sensitive areas where natural catchment alkalinity generation is insufficient to buffer acidic deposition. Emissions from fossil-fuel combustion have caused some of the highest loads of atmospheric pollutants globally to the "Black Triangle" region of northern Czech Republic and adjacent areas in Germany and Poland (Moldan and Schnoor, 1992).

The objective of this paper is to evaluate both temporal and spatial variations in precipitation and streamwater acidity with respect to controlling processes in an area affected by high pollutant deposition from fossil fuel combustion in the Krušné hory, Czech Republic.

2 Background

The Krušné hory (Ore Mountains or Erzgebirge) are in northwestern Bohemia along the German border. The mountains range from 400 to 1100 m above sea level. The underlying bedrock consists of Proterozoic metamorphic rocks and granites. The lithology of the adjacent basin at the southeastern base of the Krušné hory is composed of brown coal deposits and clay. Industrialization began in the valley in the 1800s, and coal from the basin became the main energy source for former Czechoslovakia. The former Czechoslovakia's entire brown coal mining occurs in the valley and 50 % of the mined coal is burned in the valley. After World War II, coal mining increased rapidly. Surface mining of brown coal increased from 13 to 72 Mt $year^{-1}$ from 1946 to 1986. The S-rich coal (1 to 15 % S) is combusted locally in several power plants (Moldan and Schnoor, 1992), which operated without any abatement technologies until 1994.

Forest dieback was first observed soon after the construction of the first brown coal power plants in the valley (Vins, 1965). The forest dieback began in the 1960s and 50 % of the coniferous vegetation, which dominated the high elevations (600–800 m), died from 1972 to 1989 (Ardö et al., 1997).

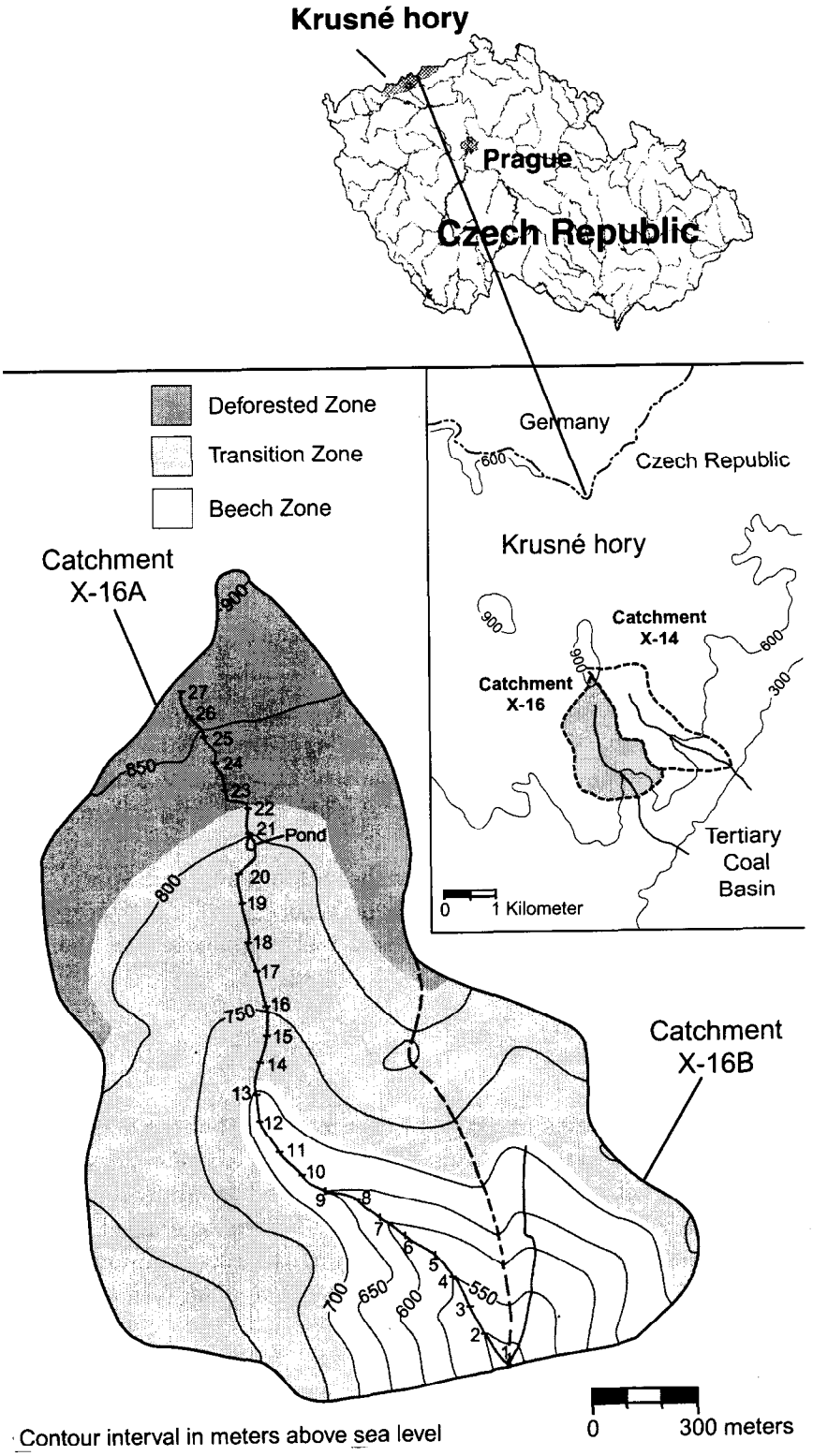

Figure 1: Map of the Jezeří catchments showing the vegetation zones associated with forest dieback and the longitudinal streamwater sampling sites of X-16A in the Krušné hory, northern Bohemia, Czech Republic.

The annual SO_2 emission in the area peaked at 1100 kt in the 1980s, declining to about 420 kt in 1996 (Czech Hydrometeorological Institute, written communication, 1997). Most emissions originate from four power plants, 10 to 18 km from the mountain plateau. For 1988–89, the annual deposition of S and N in the mountains was about 160 and 46 kg ha^{-1}, respectively (Ardö et al., 1997). Dry deposition can contribute 80 to 90 % of the total deposition in mature spruce stands (Černý, 1995). The leaf area index LAI is directly proportional to the accumulated dry deposition, and for mature spruce, the LAI decreases with increasing damage, ranging from 8 for healthy stands to 3 for severely damaged stands (Havel et al., 1996). Consequently, the forest dieback and the associated loss of canopy have reduced total atmospheric deposition (Havel et al., 1999).

Remediation included logging of the dead and dying trees, excavation of ditches for drainage, partial removal of the topsoil using bulldozers, liming, fertilizing, and reforestation (Kubelka et al., 1992). The remediation began as early as the late 1970s and the more intensive landscape alterations began in the mid 1980s.

Table 1: General characteristics of the Krušné hory and study sites.

DRAINAGE AREA: Krušné hory, 200,000 hectares; Jezeří X-16, 260 hectare; Jezeří X-16A, 210 hectare; and Jezeří X-14, 270 hectare.
ELEVATION: 400–1000 m a. s. l.
CLIMATE & HYDROLOGY: Moderately wet and cold; mean daily temperature is 4.5°C, annual precipitation averages 1000 mm at the top and 500 mm at the bottom, and annual water yield ranges from 30 to 40 %.
GEOLOGY: Proterozoic coarse grained orthogneiss and granite.
SOIL: 10-m thick on ridges, decreasing to 1 m on lower elevation slopes. At higher elevations - humid gley and peat, and podzolic and oligotrophic brown earth.
At lower elevations - sandy-loam oligotrophic brown earth and podzol.
VEGETATION ZONES (Jezeří X-16):
Beech Zone: elevation from 482 to 705 m a. s. l. and contains mature beech (*Fagus silvatica*, 100–140 years old).
Transition Zone: elevation from 705 to 815 m a. s. l., has been affected by spruce dieback and contains some remnant mature spruce (*Picea abies*, > 60 year old) and reforested mixture of young trees (< 25 year old) including birch (*Betula pubescens*, *Betula verrucosa*), mountain ash (*Sorbus aucuparia*), European larch (*Larix decidua*) and spruce (*Picea pungens*, *Picea abies*).
Deforested Zone: elevation from 815 to 915 m a. s. l, had the worst damage and contains some remnant mature spruce and a reforested mixture of very young (< 10 year old) trees and grassland.

3 Methods

3.1 Bulk precipitation

Bulk precipitation was monitored from November 1977 to April 1997 at Vysoká Pec, which is 2 km west of X-16 at 390-m elevation. Bulk precipitation samples were collected monthly. When the air temperature was above freezing, samples were collected in pairs

using a 122-cm^2 polyethylene funnel connected to a 1-litre linear polyethylene collection bottle for each sampler. In winter, snow was collected in a 380 cm^2 plastic bucket fitted with polyethylene sampling bag. The annual volume-weighted pH of bulk precipitation for each water year (WY) were calculated by dividing the annual bulk H^+ deposition by the annual precipitation volume and converting to pH (Table 2).

Table 2: Bulk precipitation amount and pH, converted from volume-weighted mean H^+ concentration, by water year at Vysoká Pec adjacent to the Jezeří catchments, Krušné hory.

Parameter	Water Year																		
	78	79	80	81	82	83	84	85	86	87	88	89	90	91	92	93	94	95	96
Water (mm)	772	888	1120	1040	728	893	754	577	915	987	802	906	768	668	976	763	975	1050	943
pH	4.31	4.25	4.26	4.21	4.13	4.27	4.42	4.27	4.24	4.35	4.32	4.25	4.33	4.28	4.29	4.23	4.22	4.21	4.32

3.2 Streamwater

Streamwater samples for the regional survey were collected during 1984–85 and during September 1997, and pH was determined the day of collection on an unfiltered aliquot. In 1984 and 1985, samples were collected from the 10 April to 10 November only during stable hydrologic conditions; that is, streamflow at the nearest gauging station was between 0.5 to 2 times the average discharge at the time of sampling (Veselý et al., 1986). The average sampling density was one site per 6.1 km^2. Samples were collected manually from the centroid of flow in a 500-ml polyethylene bottle after pre-rinsing the bottle with streamwater.

Streamwater samples were collected routinely from two small forest catchments. From 1977 to 1983, streamwater chemistry was monitored at the basin outlet (50°33'N, 13°29'E) of a 2.7 km^2 forest catchment, X-14 (Fig. 1; Pačes, 1985). The elevation of X-14 ranges from 335 to 925 m. From 1983 to present, streamwater chemistry was monitored at the basin of outlet (50°33'N, 13°30'E) of an adjacent 2.6 km^2 forest catchment, X-16 (Fig. 1). The elevation of X-16 ranges from 475–925 m. Samples were collected manually from the centroid of flow at each basin outlet in a 500-ml polyethylene bottle after pre-rinsing the bottle with streamwater. The sample collection frequency generally increased since monitoring began in 1977. From 1977 to 1991, samples were collected quarterly during the first part of the period and increased to monthly at the end. Since 1991, samples were collected biweekly and more frequently during high streamflow, particularly during the spring snowmelt period. In 1983 and during 1991–92, grab samples of streamwater were collected at X-14 and X-16 on the same day to assess the similarity between sites to justify combining the data for evaluating the longer-term hydrochemical variations and trends. A paired T-test of the streamwater solute concentrations at X-14 and X-16 for samples collected on the same day indicated no statistically significant differences between the sites.

Streamwater samples were collected approximately once each quarter for a two-year period at 100-m intervals (27 sites) along the main stem of the stream in X-16A (Fig. 1) resulting in seven collections during two water years (WY 1993, November 1992 through October 1993), WY 1993 and WY 1994. The sampling was conducted in November 1992, March 1993, May 1993, August 1993, January 1994, May 1994, and August 1994. Samples were collected manually from the centroid of flow in a 250-ml polyethylene bottle, which

was pre-rinsed with streamwater. For each sampling period, all sites were collected in one day starting at the outlet (site #1).

Streamflow (runoff) has been monitored at a V-notch weir on X-16 using a chart recorder having a float and pulley system, from 1982 to 1996 by applying a discharge and stage rating to daily estimates of stage. Since March 1996, discharge has been determined continuously by applying a discharge and stage rating to 15-minute electronic stage records.

3.3 Chemical analyses

All water samples were analyzed in the chemical laboratory of the Czech Geological Survey. Specific conductance, pH, and alkalinity (ALK) were measured within 24 hours of collection using a Radelkis OK-102/1 conductivity meter, Radiometer GK 2401C combination pH electrode, and automated Gran titration (TTT-85 with ABU-80 autoburette and SAC-80 autosampler; Gran, 1952) for parallel determination of pH and ALK, respectively. A filtered (0.45 μm) aliquot was analyzed for anions (Cl^-, NO_3^-, and SO_4^{2-}) using colourimetric techniques (Kobrová, 1983) prior to 1983 and a Shimadzu LC-6A ion chromatograph since then. Ammonium NH_4^+ was determined on a filtered aliquot using the indophenol blue method (Kobrová, 1983). An ion-sensitive electrode Crytur 09-27 was used to determine Fluoride (F^-). A filtered aliquot was acidified with Ultrex HNO_3^- and analyzed for cations (Ca^{2+}, Mg^{2+}, Na^+, K^+, and Al_{DIS}) using atomic absorption spectrophotometry through 1987 and a Perkin Elmer Plasma II inductively coupled plasma spectrometer since then. The quality assurance and quality control of analytical determinations were continuously assessed in the laboratory using standard laboratory procedures including blanks, sample splits, reference samples, and calibration standards; and in the field using a combination of blanks, replicate, split, and reference samples.

4 Results and Discussion

4.1 Bulk precipitation

The bulk precipitation pH at Jezeří is higher than that for the long-term average wet-only precipitation at sites in the eastern United States (Aulenbach et al., 1996) and average bulk precipitation at the Hubard Brook Experimental Forest (HBEF) prior to 1983 (Driscoll et al., 1989). The pH difference was unexpected given the much higher locally derived S emissions and atmospheric SO_2 concentrations at Jezeří than at these other sites. Bulk precipitation includes a variable amount of dry deposition, which typically contains neutralizing components from soil dust and aerosols (Vet et al., 1988). However, concentrations of the other solutes are several times higher at Jezeří, particularly the acid anions, than in the eastern U. S. and in other areas such as Wales (Reynolds, 1984; Robson and Neal, 1996) and Finland (Ukonmaanaho et al., 1998). The acid anions, SO_4^{2-} and NO_3^-, are 2 and 3 times higher at Jezeří than at these sites, respectively, but the negatively charged anions are balanced by an even higher relative concentration of positively charged cations. For example, Ca^{2+} concentration at Jezeří is 6 to 15 times higher than that at sites in the U. S. (Maryland, West Virginia, New Hampshire, New York) and Wales; Mg^{2+} is from 6 to 9 times higher; and NH_4^+ is from 5 to 7 times higher. The larger differences in base cations apparently are sufficient to buffer the acidifying effects of the acid anion enrichment. In contrast to the absence of a trend in bulk precipitation pH at Jezeří, pH at HBEF increases, and both Ca^{2+} and SO_4^{2-} concentrations decrease, which is attributed to larger rate of decrease in acid anions than base cations (Driscoll et al., 1989; Likens et al., 1996).

4.2 Streamwater

Regional streamwater sampling indicates that on average, pH was the same (median pH was 6.40 in 1985 and 6.46 in 1997) but less variable in 1997 than in 1985 (Fig. 2). The streamwater pH generally is neither as low as observed in many other sensitive areas in Europe, Scandinavia, and northeastern North America, nor as low as expected, given the high pollutant deposition.

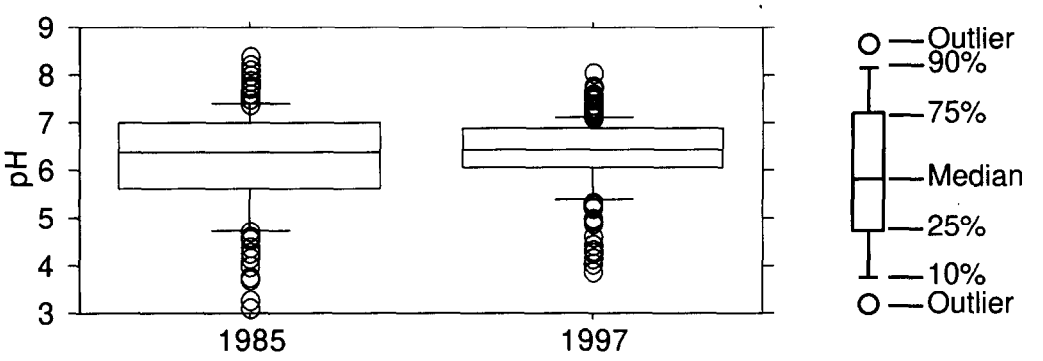

Figure 2: Streamwater pH in 1985 and in 1997 from synoptic sampling in the Krušné hory.

Watershed liming, which began prior to the onset of stream monitoring in the late 1970s, has undoubtedly contributed to neutralizing the acidic deposition (Peters et al., 1999). The largest increase in streamwater pH occurred in the headwater area of the Krušné hory north of the Jezeří catchment, where forest dieback and subsequent site remediation, including liming, was very intense. Also, atmospheric deposition decreased during the sampling period. In particular, dry acid-anion deposition to mature spruce stands was about 80 % of the total deposition (Černý, 1993). The forest dieback and removal, therefore, caused dry deposition to decrease, resulting in a decrease in streamwater acid-anion concentrations (Černý, 1995; Peters et al., 1999). However, the cause for the pH variability decrease from 1985 to 1997 cannot be readily attributed to a specific mechanism.

The largest long-term changes in streamwater chemistry at the outlets of the two adjacent Jezeří catchments (X-14 from WY 1978 to WY 1984 and X-16 from WY 1983 to WY 1997) occurred from WY 1978 to WY 1985 (Fig. 4). Annual median pH decreased from WY 1978 to a minimum of 4.65 in WY 1981 and then increased thereafter, consistent with the regional trend. Despite the dominance of SO_4 in streamwater, which comprises 86 % of the anion charge, NO_3 concentration is more highly correlated (negative) with pH (Havel et al., 1999; Peters et al., 1998). The lag between the pH minimum and NO_3 concentration maximum may be controlled by watershed liming, which has occurred repeated beginning in the late 1970's and ending in 1990 (Havel et al., 1999).

From the quarterly longitudinal sampling, streamwater in the X-16A catchment is relatively sensitive to acidification; 45 % of the samples had pH less than 5.6 and 90 % had alkalinity (ALK) less than 50 μeq l^{-1}. Furthermore, streamwater pH varies markedly not only spatially with elevation, but temporally (Fig. 5) with season and streamflow. The lowest streamwater pH correlates with the highest streamflows in winter and spring snowmelt. The highest pH variability occurs from the upper elevations of the Beech Zone through the highest elevations of the Deforested Zones. The increased pH variability is associated with the area where the most intensive landscape alteration, liming and reforestation occurred.

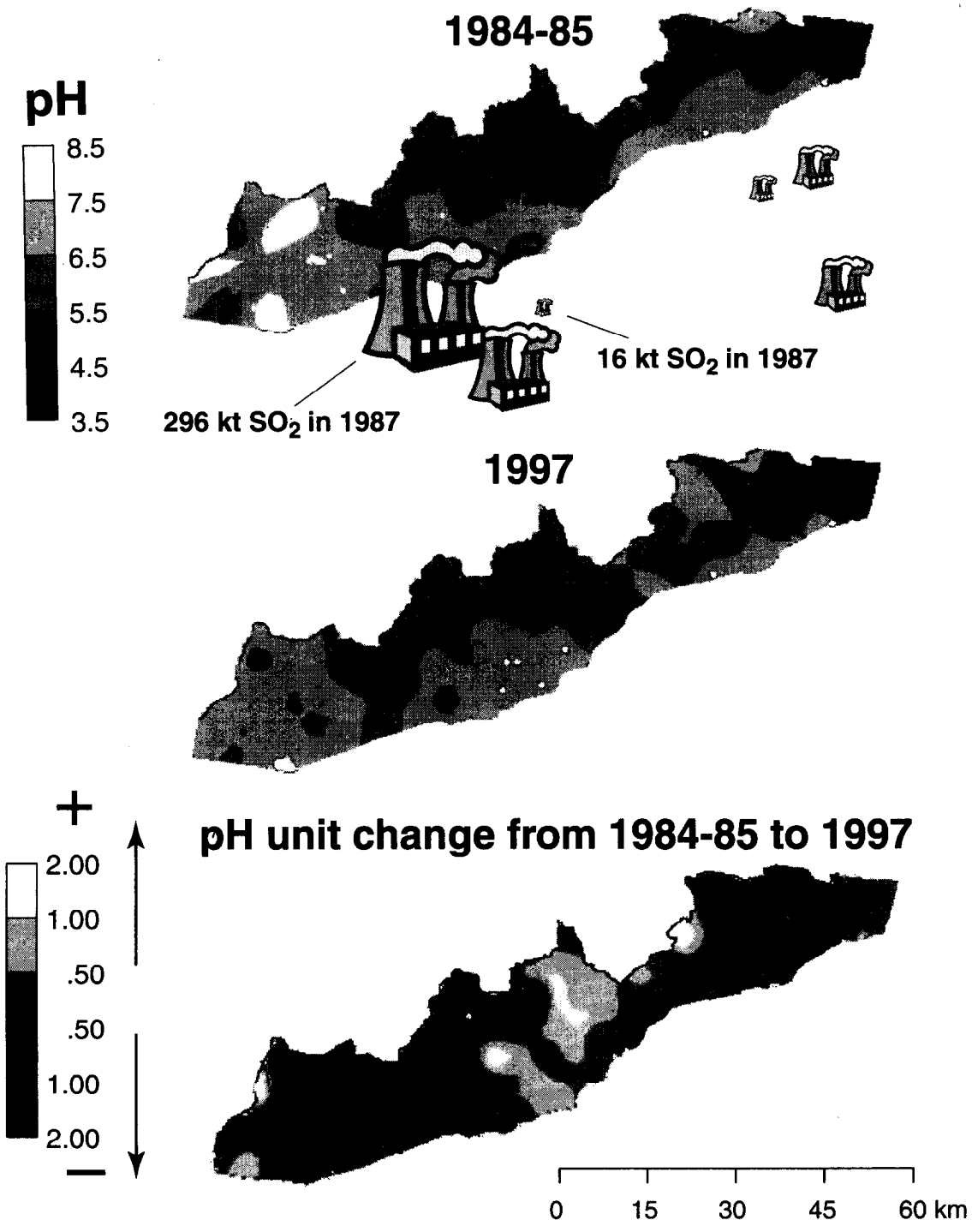

Figure 3: The spatial variation in streamwater pH during synoptic sampling in 1984–85 and in 1997, and the pH difference between these time periods, Krušné hory.

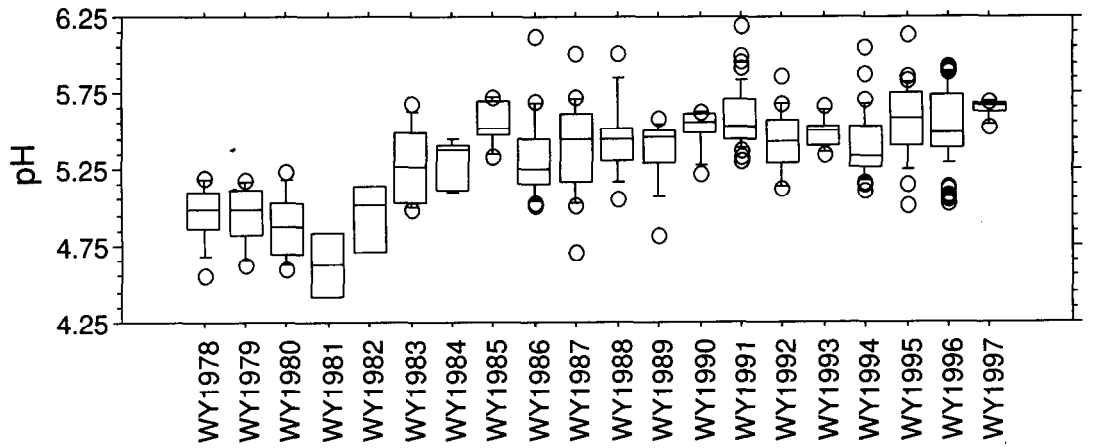

Figure 4: Long-term changes in streamwater pH at the outlet of the Jezeří catchments from WY 1978 to WY 1997. WY - Water Year, e. g. WY 1978 = November 1977 through October 1978.

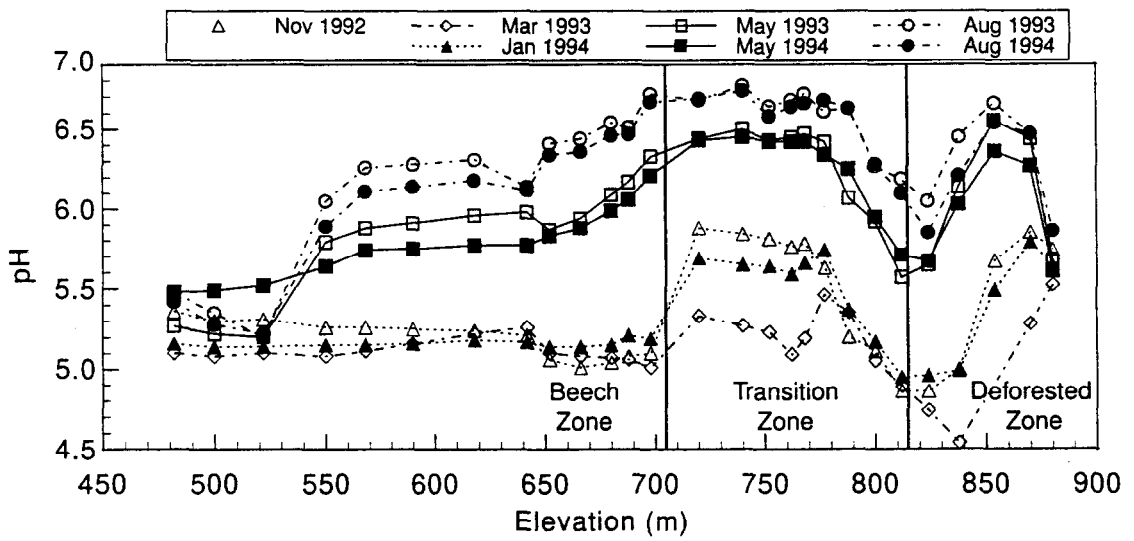

Figure 5: Variations in streamwater pH with elevation from quarterly sampling longitudinally along the main stem at the Jezeří catchment, X-16A.

Although pH and ALK are relatively high during low runoff periods in the Deforested and Transition Zones (Fig. 5), the lower pH and ALK during higher runoff and at lower elevations are in the range of controls by Al and associated organic complexes. Concentrations of H^+, F^-, ALK and Al_{DIS} correlate for all samples or if the samples were grouped by sampling period, sampling site or vegetation zone. For all data, the r^2 of a linear regression of H^+ on Al_{DIS} was 0.85 ($\alpha < 0.0001$) and the slope of regression was 0.5. Furthermore, the slope of linear regressions subset by vegetation zones were similar among zones. A linear regression for H^+ on F^- was more variable ($r^2 = 0.39$, $\alpha < 0.0001$) than that for H^+ on Al_{DIS} and had a slope of 0.5. However, a linear regression of H^+ on

F^- for individual sites were highly significant (median $r^2 = 0.90$ and $\alpha < 0.01$ for 25 of 27 sites), but the slopes varied among sites. The high correlation between H^+ and Al_{DIS} suggests that Al, as monomeric Al and organic complexes with Al and F, may be the dominant control on streamwater acidity at Jezeří.

Prior to the landscape manipulations and lime additions, which began at Jezeří in the late 1970s and more intensively during the early to the middle of the 1980s, the Ca^{2+} and Mg^{2+} were primarily supplied by the soil exchange complex (Pačes, 1985). The evidence is that the S deposition and transport greatly exceeds the base cation weathering supply rate (Pačes, 1985), and consequently, the soil cation-exchange sites were severely depleted (Kubelka et al., 1992). During the period of maximum forest dieback in about 1980, the surface 10–20 cm of the soil were so severely depleted in exchangeable base cations that soil pH ranged from 2–3.5 and base saturation was less than 10 % (Kubelka et al., 1992). The liming re-supplied Ca^{2+} and Mg^{2+}, the dominant cations, and was a major source of ALK to buffer against current inputs of acidic atmospheric deposition.

5 Conclusions

On average, the pH of bulk precipitation was similar throughout the period 1984–85 to 1997. On average, streamwater pH during summer low flow conditions in the Krušné hory has remained the same, but has become less variable, from 1984–85 to 1997, as determined from synoptic sampling of 182 sites. Streamwater pH, in general, also increased from 1981 to 1997 in two small, forested catchments on the southern slope of the mountains adjacent to the Tertiary coal basin where fossil fuel is mined and combusted. Factors contributing to the pH increase include forest dieback and removal, and catchment liming. The loss of canopy associated with the forest dieback caused dry atmospheric deposition and associated total atmospheric deposition to decrease. Furthermore, liming provided positively charged base cations (Ca^{2+} and Mg^{2+}) to balance the negatively charged acid anions (SO_4^{2-} and NO_3^-) in streamwater and provided alkalinity (ALK) to buffer acid inputs. The negative correlation between streamwater NO_3 concentration and pH suggests that N dynamics may be important in controlling streamwater acidification. In addition, high correlation among ALK, pH, F^-, and Al_{DIS} suggests that Al and organic complexes also may be important in controlling streamwater acidification.

Acknowledgments

This research was supported by the US-Czech Science and Technology Agreement between the Czech Geological Survey and the U. S. Geological Survey, Grant #94018 entitled Hydrogeochemical Analysis of Water Pathways and Geochemical Factors Affecting Forest Dieback in an Area of High Deposition of Atmospheric Pollutants. We are grateful to Radovan Krejčí, Jan Havrda, Pavel Walter, Pavel Sobotka and Světla Matoušková for field support and Hyacinta Vítková, Pavel Pokorný, Petr Foch and Ed Drake for laboratory support.

References

[1] Ardö, J., Lambert, N., Henzlik, V., and Rock, B. N. 1997, Satellite-based estimations of coniferous forest cover changes: Krusne Hory, Czech Republic 1972–1989. Ambio, 26(3), 158–166.

[2] Aulenbach, B. T., Hooper, R. P., and Bricker, O. P. 1996, Trends in precipitation and surface-water chemistry in a national network of small watersheds. Hydrological Processes, 10(2), 151–181.
[3] Černý, J. 1993, Atmospheric deposition in the Krušné hory Mts., preliminary results of throughfall measurements. Acta Universitatis Carolinae Geologica, 37, 28–44.
[4] Černý, J. 1995, Recovery of acidified catchments in the extremely polluted Krušné Hory Mountains, Czech Republic. Water, Air, and Soil Pollution, 85, 589–594.
[5] Driscoll, C. T., Likens, G. E., Hedin, L. O., Eaton, J. S. and Bormann, F. H. 1989. Changes in the chemistry of surface waters. Environmental Science and Technology, 23, 137–143.
[6] Gran, G. 1952, Determination of the equivalence point in potentiometric titrations – part II. The Analyst, 77, 661–671.
[7] Havel, M., Krejčí, R., and Černý, J. 1996. Decrease of Acid Atmospheric Deposition in the Krušné hory Mts. Project Report, Grant Agency of the Czech Republic, Project # 205/93/0675, (in Czech.)
[8] Havel, M., Peters, N.E., and Černý, J. 1999, Longitudinal patterns of stream chemistry in a catchment with forest dieback, Czech Republic. Environmental Pollution 104(1), 157–167.
[9] Kobrová M. (ed.) 1983. Methods of the chemical analysis of natural waters. Czech Geological Survey, Prague, 200 p. (in Czech).
[10] Kubelka, L., Karásek, A., Rybář, A., Badalík, V., and Slodičák, M. 1992, Restoration of the emission endangered forest in the northeast Krušné hory Mts., Ministry of Agriculture of the Czech Republic, Prague.
[11] Likens, G. E., Driscoll, C. T., and Buso, D. C. 1996. Long-term effects of acid rain: response and recovery of a forest ecosystem. Science, 272, 244–246.
[12] Moldan, B. and Schnoor, J.L. 1992, Czecho-slovakia examining a critically ill environment. Environmental Science and Technology, 26(1), 14–21.
[13] Pačes, T. 1985, Sources of acidification in Central Europe estimated from elemental budgets in small basins. Nature, 315, 31–36.
[14] Peters, N. E., Černý, J., and Havel, M. 1998, Factors controlling streamwater nitrate concentrations in a forested headwater catchment, Krušné hory Mountains, Czech Republic. In: M. J. Haigh, J. Křeček, G. S. Rajwar, and M. P. Kilmartin (eds.), Headwaters: Water Resources And Soil Conservation, New Delhi, India, A. A. Balkema, Rotterdam, The Netherlands, 147–157.
[15] Peters, N. E., Černý, J., Havel, M., and Krejčí, R. 1999, Temporal trends of bulk precipitation and streamwater chemistry (1977–97) in a small forested area, Krušné hory, northern Bohemia, Czech Republic. Hydrological Processes, 13(17).
[16] Reynolds B. 1984. An Assessment of the Spatial Variation in the Chemical Composition of Bulk Precipitation Within an Upland Catchment. Water Resources Research, 20(6), 733–735.
[17] Robson, A. J. and Neal, C. 1996. Water quality trends at an upland site in Wales, UK, 1983–1993. Hydrological Processes, 10, 183–203.
[18] Ukonmaanaho, L., Starr, M., and Ruoho-Airoha, T. 1998. Trends in sulfate, base cations and H^+ concentrations in bulk precipitation and throughfall at integrated monitoring sites in Finland 1989–1995. Water Air and Soil Pollution, 105, 353–363.
[19] Veselý, J., Majer V., and Ševčík K. 1986, Methodology of Regional Geochemical Survey of the Czech Freshwaters. Internal Report of CGS, Prague (in Czech).
[20] Vet, R. J., Sirois, A., Jeffries, D. S., Semkin, R. G., Foster, N. W., Hazlett, P., and Chan, C. H. 1988. Comparison of bulk, wet-only, and wet-plus-dry deposition measurements at the Turkey Lakes Watershed. Can. J. Fish. Aquat. Sci., 45, 26–37.
[21] Vins B. 1965. A method of smoke injury evaluation – determination of increment decrease. Communicationes Institui Foestalis Chechosloveniae, 235–245.

Observations of subsurface hillslope flow processes in the Jizera Mountains region, Czech Republic

M. Šanda, M. Císlerová

Department of Drainage, Irrigation and Landscape Engineering, Faculty of Civil Engineering, Czech Technical University, Prague, Thákurova 7, CZ 166 29 Praha 6, Czech Republic.

1 Description of the study area

The vegetation over large areas of the Jizera Mountains region has been badly affected, by deforestation for example, due to air pollution. Before this happened, the Czech Hydrometeorological Institute established a set of small experimental watersheds to evaluate the impact of deforestation on the hydrological cycle. Recently, data acquisition for monitoring hydrological and climatic processes has been extended in terms of complete digital automatisation. From the measurements and observations performed so far it has become evident that most of the flow from the hillslopes leaves in form of subsurface flow. Hydrological research has been undertaken, therefore, with special attention to the flow processes operating on sloping soil profiles in the watershed Uhlířská, Černá Nisa river in Jizera Mountains (Císlerová et al., 1997).

Uhlířská is the most examined site of all experimental watersheds in this region. Its area is 1.87 km^2, of which 50 % was deforested in early 1980s, the average altitude is 822 m a.s.l. Its length is 2.1 km, the average width is 0.89 km, the average slope is 2.3 % and the average length of the hillslopes is 450 m. The catchment is situated in a humid region where the annual precipitation exceeds 1300 mm/year. In the area of interest, the sloping soil profile is shallow and highly heterogeneous. The upper hillslopes typically consist of 80 cm of Dystric Cambisol formed on the decayed fractured granite bedrock. The topsoil (15 cm) is of a peaty character, covered by bush grass vegetation. The profile below the organic layer comprises 10 cm of grey-black clayey loam, 25 cm of brown sandy loam and 30 cm of light brown loam with a high content of the bedrock particles. At the bottom of the valley the soil profile prevailingly consists of a layer of peat topsoil (Histosol) with a vegetation cover. Its depth varies from 0 to 300 cm and it lies on silty gelifluction gley material. The total thickness could not be measured due to the limitation of the techniques applied. According to an areal survey (Císlerová et al., 1998) Cambisols cover approximately 90 % of the total watershed area while the rest is formed by Histosol, found mostly in the bottom of the valley.

2 Study of flow processes in the hillslope vadose zone

Focusing on subsurface flow processes, the aim of the hydrological research was to reveal the flow mechanisms and the water regime in variably saturated soil profiles in the hillslope environment. To describe the flow processes in a shallow soil profile, one typical hillslope, located at Tomšovka, has been outlined. The study area is a hillslope transect, defined as a vertical plane running in the direction of steepest descent. The main part of the research concentrated on an experimental area below the local divide where a measuring trench was constructed. Advanced automatic data collection devices were installed in the trench for monitoring the short-term inflow-outflow characteristics of hydrological events. (Šanda and Císlerová, 1998).

In the trench, the subsurface flow was gathered in 3 soil horizons of 2 sections (A and B) each 4 m long. The instrumented section corresponds to soil layer interfaces Ah horizon (app. 0–30 cm of depth), B horizon (app. 30–50) and B-C horizon (60–70 cm). Spatial variation of the depths of horizons are caused by non-uniformity of the soil surface and the related soil profile.

Table 1: Depth of collectors below the surface.

A1	A2	A3	B1	B2	B3
12 cm	42 cm	57 cm	30 cm	60 cm	75 cm

The flow from all sections was gravitationally channelled into 6 tipping-bucket flowmeters. The pulses were recorded on CR10X-1M and Newlog3 dataloggers. The data were processed to give outflow rates from each particular soil horizon.

Suction pressure heads within the soil profile were monitored by a set of 15 soil tensiometers, nested in 5 triplets located uphill of the trench. Two of the triplets were installed 1 m above the subsurface trench in the centre of each section. One triplet was installed between the sections at the same distance of 1 m. The remaining two triplets were installed in the central axis further upslope of the trench. In every nest, tensiometers were installed into one of the soil layers. (approx. 20, 40 and 60 cm below the soil surface). All tensiometers were fitted with the pressure transducers for continuous soil tension recordings. Data were recorded at 10 minute intervals on the CR10X-1M datalogger.

3 Complementary measurements

As a control link to the processes over the whole length of the hillslope additional manual measurements were performed over the vegetation season. The ground water table was monitored by 20 shallow piezometers, soil moisture was measured at 14 access tubes by the neutron probe method and a set of 60 manual tensiometers were used for additional measurements of soil suction (Šanda and Císlerová, 1999).

In addition, a set of 10 shallow drills, located at the hillslope transect were performed to stratify the upper soil and rock layer formations. Measurement by means of dipole electromagnetic profiling was chosen to identify the bedrock surface geometry and the geological fracture system of the flow region. The vertical electrical survey was performed to estimate the depth of the unweathered bedrock at the study location. On the area of the experimental hillslope, 100 ponded infiltration test were performed to estimate infiltration capacities of the topsoil. Laboratory measurements of retention curves and saturated hydraulic conductivities on the samples collected at the vicinity of the trench from all horizons were performed.

4 Hydrological events in the subsurface trench

The experimental trench lies in the territory of clear-cut forest. Preferential flow pathways functioning as local sources or drains, e.g. where there are decayed tree roots, boulders or weathered bedrock particles conducting water through the subsurface, could strongly influence the route of the subsurface flow and therefore increase or decrease the contributing area of flow to the measuring trench. Uncertainties remain with respect to the shape and boundaries of the microcatchment contributing to the experimental trench due to unknown depth of the impermeable bedrock. By the indirect method of vertical electrical survey, its depth was estimated to be 4–5 meters below the surface at the vicinity of the trench. The general geophysical survey found significant electrical discontinuities, which might be related to geological fractures and different degree of weathering of the granite bedrock. This is a potential cause for percolation of water deeper than the profile beyond the face of the experimental trench. However, hydraulic tests on the soil samples collected at the bottom of the trench showed that the hydraulic conductivity of the soil matrix of deeper weathered bedrock mass was lower than 10^{-7} m.s^{-1}. In comparison to higher layers (topsoil K_s=10^{-4} m.s^{-1}, horizons 20–60 cm K_s=10^{-5} m.s^{-1}) this supports the hypothesis, that although deep, the layer of 1–4 (5) m below the soil surface only partially contributes to the subsurface runoff and has practically no influence on subsurface storm outflow. Although the trench samples only a thin and shallow part of the soil profile, it is considered that most of the subsurface outflow is captured by the trench.

Table 2: Distribution of the subsurface outflow from the collection trench (May-November 1998).

	Subsurface outflow (l)				Percentage of subsurf. outflow		
	horiz. 1	horiz. 2	horiz. 3	total	horiz. 1	horiz. 2	horiz. 3
Section A	80	566	20811	21457	0.4 %	2.6 %	97.0 %
Section B	85	9	30855	30949	0.3 %	0.0 %	99.7 %

From Table 2 it is evident that within the face of the trench the major part of the outflow takes place at the bottom of the sampling trench. At a depth of 60–70 cm the soil profile changes its structure to weathered bedrock material with a sharp decrease of saturated hydraulic conductivity of the matrix. This change is accompanied by a decrease in biotic activity and therefore the occurrence of root pathways. All of these facts result in decrease of vertical flow and an increase of the lateral downslope component of flow. A contribution to the outflow seeping out at the bottom horizon of the trench also comes from the interruption of the flow lines by the construction of the trench as its drainage effect.

In the period May to November 1998 four significant hydrological periods were recorded consisting of 1–3 single events producing outflow to the subsurface trench. These events met the following criteria: each event was separated by at least 2 hours of no rain; and event rainfall was greater than 15 mm. Often, these significant events follow previous quantitatively high rainfall periods of shorter and less intensive precipitation. The events were classified according to statistics based on 24-hour rainfall totals for Uhlířská watershed over the period 1981–1997. The period of observation (16 years) is short in terms of the statistical significance, therefore the rainfall occurrence interval has only informative value. The details are shown in the Table 3.

Table 3: Rainfall event characteristics at Uhlířská watershed.

Day of the event	Rainfall duration (h)	Rainfall total (mm)	Average rainfall intensity (mm/h)	Rainfall occurrence interval (days)	Total antecedent precipitation (mm)	Period antecedent precipitation (days)
13.6.98	18	66.6	3.7	769	44.4	6
6-8.7.98	51	44.1	0.9	250	10.2	5
10.7.98	18	23.3	1.3	60	69.4	9
13-15.9.98	39	44.4	1.1	251	41.3	8
16.9.98	7	20.2	2.9	39	94.4	12
18.9.98	19	16.4	0.9	23	122.1	13
1.11.98	10	35.0	3.5	151	64.5	7

Table 4: Outflow event summary.

Period of the event	Rainfall total at Uhlířská (mm)	Period of outflow event (hours)	Cum. outflow, Černá Nisa (mil. m^3)	Outflow height of event (mm)	Outflow ratio	Cum. outflow at soil horizon A3 (m^3)	Cum. outflow at soil horizon B3 (m^3)	Micro-catchment area of A3 (m^2)	Micro-catchment area of B3 (m^2)
13.6.98	66.6	52	0.105	56.34	0.85	2.44	4.41	36.69	66.30
6.7.98	44.1	90	0.076	40.53	0.92	0.97	1.33	22.07	30.10
10.7.98	23.3	52	0.055	29.25	1.26	1.57	2.70	67.30	115.99
15-18.9.1998	56.9	96	0.164	87.47	1.54	6.44	7.57	113.20	133.07
1.11.98	35.0	58	0.092	49.05	1.40	2.55	3.76	72.80	107.54

Table 4 shows the results of the stormflow measurement at the experimental trench and the Uhlířská watershed for selected rainfall events. Cumulative outflow in the Černá Nisa river, at the Uhlířská gauging station, presented here, is total measured cumulative outflow with a constant specific baseflow of 0.048 $mm.h^{-1}$ (25 $l.s^{-1}$), typical for this watershed, subtracted. The specific flood outflow rate is 0.2–2 $mm.h^{-1}$ (approximately 100–1000 $l.s^{-1}$), therefore the baseflow contribution has negligible effect on the flood amount. The events can be divided into two sets according to the duration and amount of cumulative outflow: summer short stormflow; and longer autumn flow events. A noticeable fact is that the total specific stormflow from an intensive single rainfall event is very similar to the precipitation total. The relationship is shown in Table 4 as an outflow ratio. However, during longer periods of rain, the total specific flood height related to the rainfall event, is even higher, as a result of the contribution of the outflow from the previous episode.

To show the outflow amount from the trench, the measurements of two bottom horizons are presented. The responsive nature of flow to the experimental trench is caused by the small area and thin soil cover of their microcatchments. The thin, loosely structured organic soil with limited potential water storage and short travel time to the weathered zone results in a short response time of flow formation.

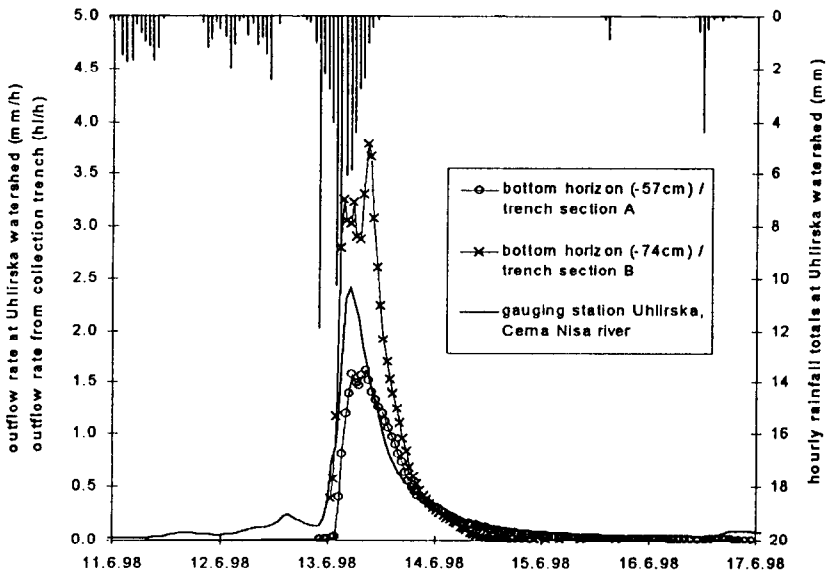

Figure 1: Outflow episode - June 1998.

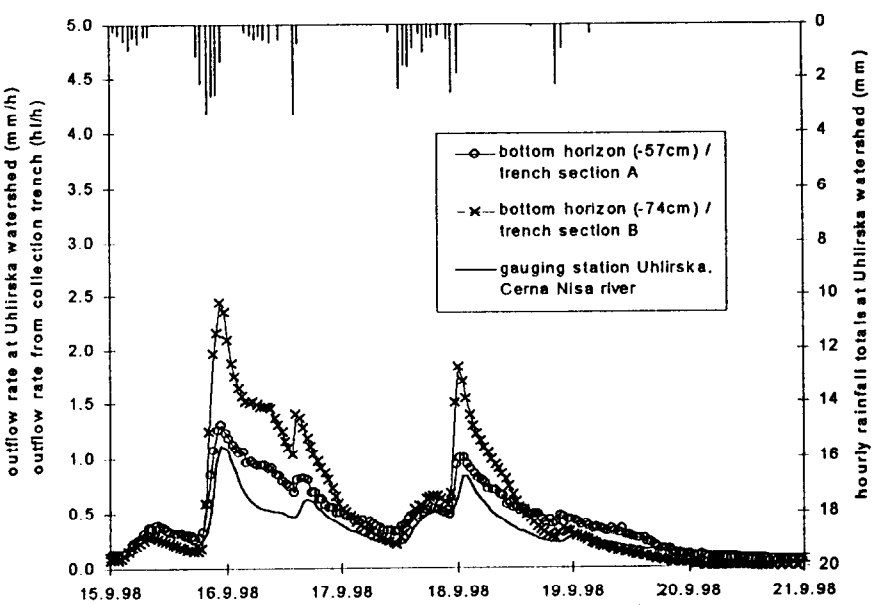

Figure 2: Outflow episode - September 1998.

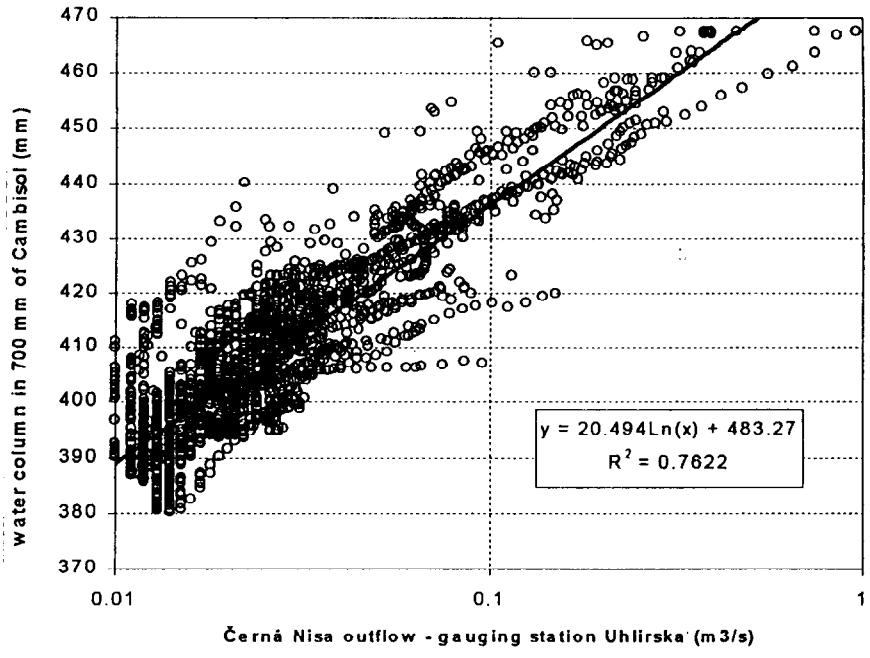

Figure 3: Relationship between soil water content and outflow from the watershed.

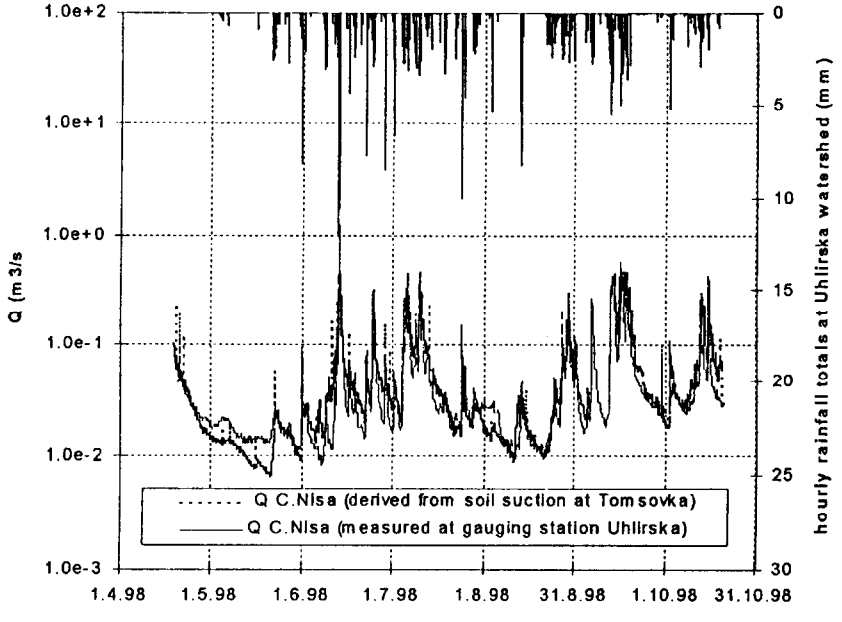

Figure 4: Derivation of the outflow from the watershed on the basis of soil suction measurements.

The mean corresponding contributing microcatchment areas are derived for each episode as a ratio of the total relevant outflow amount from the lowest trench sampling horizon and the total rainfall depth. The microcatchment areas are not constant, but vary according to the total rainfall amount, total antecedent precipitation and the duration of the episode. Outflow amounts from each trench section are significantly different in their total values. It may be caused by the extreme heterogeneity of the soil profile at the study site. Section A resembles behaviour of a soil profile with a small amount of visible preferential pathways. In section B, distinct flow pipes of diameter about 1 cm were found at the trench face after the heavy rainfall during the installation period. The ratio of the total outflow between sections changes from 1.83 for a heavy rainfall event with no direct antecedent precipitation to 1.17 for a sequence of short events. This is probably caused by the fact that during longer rain of lower intensity, the soil profile is gradually wetted and water is thus conducted also by smaller pores. In contrast, during short storms of higher intensity rainfall, water infiltrating into the drier soil profile is conducted by the larger macropores and pipes, which become the main contributor to the subsurface flow. The total amount of the outflow from the whole trench face area during the event period expressed as the outflow rate has the order of 10^{-4} m.s^{-1}. Although this value is relatively high, the actual velocities in the flow pathways could be 1–2 orders higher because the soil profile is drained in distinct spots, representing only small fraction of the total seepage area.

Figures 1 and 2 present the relation of the outflow from the bottom sections of the soil profile and the outflow from the whole watershed. It is clearly evident that the flow hydrographs have very similar shapes. Rising limbs are very steep and recession limbs last also for a short time, supporting the hypothesis that subsurface flow from the shallow soil horizons of the slopes in the watershed is the main forming part of the outflow from the whole watershed.

5 Relationship between soil water content and outflow

The soil moisture content of the soil profile was determined indirectly (Šanda, 1998). Retention curves measured in the laboratory on the soil samples collected in the vicinity of the trench were fitted by the van Genuchten formula and are used as transfer functions of soil suction into the soil moisture. From the point measurement at the tensiometer triplet, the soil water equivalent is obtained as the sum of the soil moistures of each horizon, measured by the tensiometers, multiplied by the width of each soil layer.

Figures 3 and 4 show the relationship of soil moisture and the outflow from the watershed. The top 70 cm of the soil profile, covered by tensiometer readings, is examined. It appears that corresponding values are best correlated by a logarithmic formula. The correlation coefficient is 0.87, which indicates a relatively strong relationship. The water regime of the subsurface, here represented by soil moisture, essentially affects the subsurface runoff formation that controls the channel surface flow. Figure 4 shows the course of the outflow rates derived using the optimised relationship in over the whole vegetation season. Again, it reveals a close relationship of the examined processes.

6 Results and conclusions

There is a relatively quick response to the rainfall apparent from the tensiometer readings. Almost simultaneous reaction in all three horizons implies a rapid vertical flow. The unsaturated regime within the soil profile is prevailing, nevertheless the soil moisture content is close to the saturation. No permanent water table has been observed on the

slope. Only a narrow range of soil moisture capacity was observed, and thus the change between saturated and unsaturated flow regime and vice versa is very fast and sudden. The heterogeneity of the subsurface flow is documented by comparison of very different amounts between 2 sections of bottom horizon outflow amounts. Local preferential flow paths are conducting water at significantly variable rates.

The results presented lead to some conclusions about the nature of storm flow generation in the watershed under study: A significant fraction of the rain falling on the hillslopes infiltrates vertically towards the practically impermeable weathered zone via preferential pathways. The remaining part slowly infiltrates into the soil matrix. A saturated layer is built up above this interface in the shallow part of the soil profile, where a rapid subsurface flow is formed. Water which seeps gradually into the deeper layer of gradually weathered bedrock contributes to groundwater storage and consequently to surface channel baseflow.

Acknowledgements

This research has been supported by CTU grant No. 3098K1432, from the Water Research Institute as a part of the research project No. VaV/510/3/96 "Ecological aspects of protection of water richness", and by CTU research project No. 3402143.

References

[1] Císlerová, M.; Šanda, M.; Blažková, Š.; Mazáč, O.; Grünwald, A.; Zeithammerová, J. and Tachecí, P. (1997) 'Monitorování procesů proudění vody v půdním profilu na experimetální ploše svahu v povodí Uhlířská, (The monitoring of the subsurface flow processes at the experimental hillslope at Uhlířská watershed)', (in Czech), project report VaV/510/3/96, DÚ 01, part 8,VÚV, ČVUT, Praha.

[2] Císlerová, M.; Šanda, M.; Vogel, T.; Tachecí, P.; Grünwald, A.; Zeithammerová, J.; Stodolovská, A., Votrubová, J.; Kundratová, J. and Picek, T. (1998) 'Výzkum transportních procesů v povodí dotčeném náhlými změnami odtokových poměrů - Jizerské hory (The research of the transport processes at the watershed affected by the rainfall-runoff relationship change)', (in Czech), project report VaV/510/3/96, DÚ 01, VÚV, ČVUT, Praha.

[3] Šanda, M. (1998) 'Flow of the water in the soil profile on the hillslope of the mountainous watershed'. PhD thesis minimum. (in Czech), ČVUT, Praha.

[4] Šanda, M., Císlerová, M. (1998) 'Monitoring of infiltration outflow process on variably saturated hillslope soil profile'. Workshop 98, ČVUT, Part III., 1003-1004, Praha.

[5] Šanda, M., Císlerová, M. (1999) 'Monitoring of inflow-outflow processes on variably saturated hillslope soil profile'. Workshop 99 (in Czech) ČVUT, Praha.

Nitrate leaching from a forest ecosystem with simulated increased N deposition

P. Schleppi[1], F. Hagedorn[1], H. Feyen[2], N. Muller[1], J. Mohn[3], J. B. Bucher[1], H. Flühler[2]

[1]Swiss Federal Institute for Forest, Snow and Landscape Research, CH-8903 Birmensdorf, Switzerland. [2]Institute of Terrestrial Ecology, ETH Zurich, CH-8952 Schlieren, Switzerland. [3]Institute of Plant Biology / Microbiology, University of Zurich, CH-8008 Zurich, Switzerland.

1 Introduction

Deposition of inorganic nitrogen N to natural or semi-natural ecosystems has increased over the past decades due to emissions by human activities. Inputs of ammonium NH_4^+ and nitrate NO_3^- can induce eutrophication of previously N-limited systems and finally cause their 'nitrogen saturation' (Ågren & Bosatta, 1988; Aber et al., 1989). This happens when the deposition rate is larger than the retention capacity of the soil and vegetation, in other words if the ecosystem's 'critical load' for nitrogen (Downing et al., 1993; Reynolds et al., 1998) is exceeded. Nitrate leaching is usually regarded as the main symptom of N saturation, at least in forests, where this form of N loss is more important than in non-forested natural or semi-natural ecosystems (van Breemen & van Dijk, 1988). Possible negative effects on the vegetation include nutritional imbalances, increased sensitivity to biotic and abiotic stresses, reduced root growth and altered competition between species (Ortloff & Schlaepfer, 1996).

As a non-point source, forests contribute to the eutrophication of streams, rivers and seas with N. Critical loads of N are exceeded in large tracts of Swiss forests (Kurz & Rihm, 1997). Nitrate leaching into surface and ground water is therefore a matter of concern. Leaching rates are obviously low compared to agricultural cropland, but forest areas are large enough to make them a considerable N source for Swiss water bodies (Braun et al., 1991).

Nitrogen deposition may have more impact on montane ecosystems because their N cycle is naturally tighter than in lower altitude ecosystems (McNulty & Aber, 1993). As part of the European research project NITREX (nitrogen saturation experiments: Wright & Rasmussen, 1998), we therefore studied the effects of an increased N deposition on a montane forest at Alptal, in the Swiss Prealps.

2 Material and methods

2.1 Site description

The Alptal valley is located in central Switzerland. The research site has an altitude of 1200 m and a cool, wet climate (6°C mean temperature and 2300 mm precipitation per year). It is moderately affected by atmospheric nitrate and ammonium deposition: 12 and 17 kg N ha^{-1} $year^{-1}$ in bulk and throughfall deposition, respectively (Schleppi et al., 1998b). Umbric Gleysols occur atop a Flysch substratum (calcareous sandstones with clay-rich shists). The mean slope is about 20 % with a west aspect. Dependent on the micro- topography, the soil bears different humus types: mor (raw humus) on the mounds and anmoor (muck humus) in the depressions, where the water table is high and reducing conditions frequent.

The trees are predominantly Norway spruce (*Picea abies*) with 15 % silver fir (*Abies alba*) and mainly grow on the mounds. The stand is naturally regenerated, with trees up to 250 years old. With a leaf area index of 3.8, the density of the canopy is low; the basal area is 41 m^2 ha^{-1} for 430 stems ha^{-1} (> 10 cm in diameter). The ground vegetation is well developed; different botanical associations form patches according to humus types and light conditions (Schleppi et al., 1999b).

2.2 Experimental catchments and N addition

Two forested catchments (approx. 1500 m^2 each) have been delimited by trenches (Schleppi et al., 1998b). Nitrogen (as NH_4NO_3) was added to rainwater during precipitation events and applied by sprinklers to one of the catchments. This simulated a deposition increase of 30 kg N ha^{-1} $year^{-1}$. The water used as a vector for the N addition corresponded to a supplementary precipitation of approximately 130 mm per year. During the winter, the automatic irrigation was replaced by the occasional application of a concentrated NH_4NO_3 solution on the snow with a backpack-sprayer. The effects of the treatment were compared with a control catchment receiving only unaltered rainwater and with one year of pre-treatment measurements on both catchments (Schleppi et al., 1998a).

2.3 Sampling and analyses

Water discharge was measured with V-notch weirs. Runoff proportional samples, bulk deposition and throughfall were collected weekly. Soil solution was collected from plots in a replicated design with the same treatments as the catchments. Suction plates were used to sample at 5 and 10 cm depth, suction cups for 30 cm (Gr horizon). Water analyses included ICP-AES or ICP-MS (cations + P), IC (anions) and FIAS (NH_4^+) (Schleppi et al., 1998b). Total dissolved N (TDN) was measured as nitrate after persulfate digestion: samples (10 ml) were autoclaved for 45 minutes at 130°C with 15 ml of potassium persulfate (20 g l^{-1}) and NaOH (6.67 g l^{-1}). Flasks (50 ml) were tightly closed for autoclavation, as this was found to reduce blank N values. Dissolved organic N (DON) was calculated as TDN-NO_3^--NH_4^+.

2.4 ^{15}N labelling

The added nitrogen was labelled with $^{15}NH_4{}^{15}NO_3$ during the first treatment year (Schleppi et al., 1999a). Quarterly-pooled water samples were concentrated over exchange resins. Anions and cations were eluted separately and nitrate was reduced to ammonium with Devarda's alloy. Ammonium was converted to ammonia and captured in fibreglass filters enclosed in teflon membranes (adapted from Downs et al., 1998). The filters were analysed

by mass spectrometry. Vegetation and soil pools were analysed during the treatment year following labelling.

3 Results and discussion

3.1 Water budget

Yearly water budgets (August to July) were calculated by estimating evapotranspiration according to Wendling (1975), but using the measured reflected radiation instead of a fixed albedo. Differences between inputs and outputs were within 7 % (Fig. 1). Water budgets were therefore considered closed and element budgets of these artificially delimited catchments could be calculated from precipitation and runoff samples.

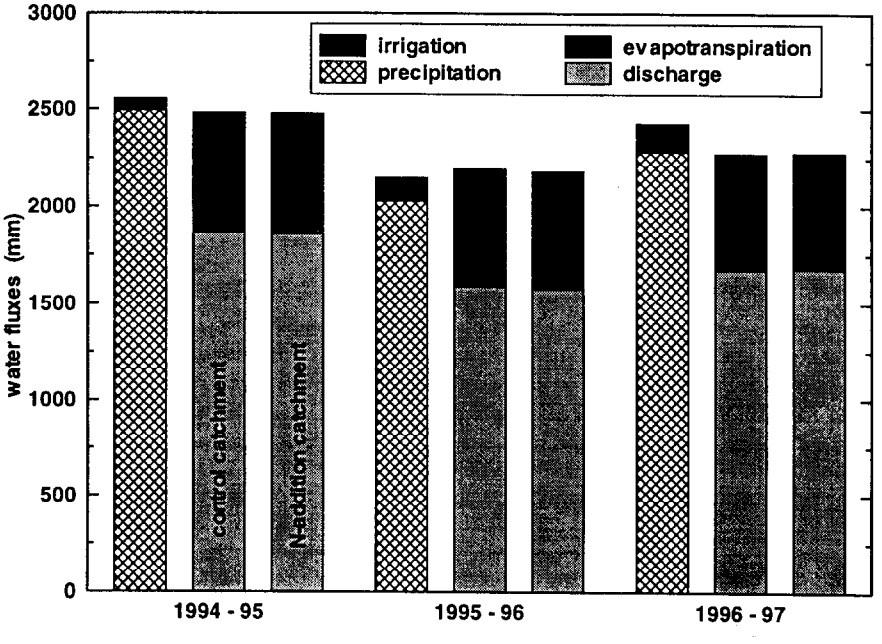

Figure 1: Water budget of the forested experimental catchments at Alptal.

3.2 Nitrate leaching

Both catchments were very similar during the pre-treatment calibration year (Schleppi et al., 1998b). Afterwards, the elevated N deposition caused a strong increase in nitrate concentrations in the runoff water and topsoil solution (Fig. 2). There was, however, no effect in the soil solution collected below 10 cm. The very low nitrate concentrations in the gleyic horizon at the 30 cm depth were due to reducing conditions, resulting in considerable losses via denitrification (Mohn, 1999). Comparison of the catchment runoff with the soil solution shows a close coupling between the topsoil solution and the runoff. Seasonal variations and absolute concentrations of nitrate at 5 cm depth corresponded to the catchment runoff. This was confirmed for other chemical compounds as well (Hagedorn et al., 1997). In contrast, the soil solution at 30 cm depth appeared to be completely uncoupled from runoff generation.

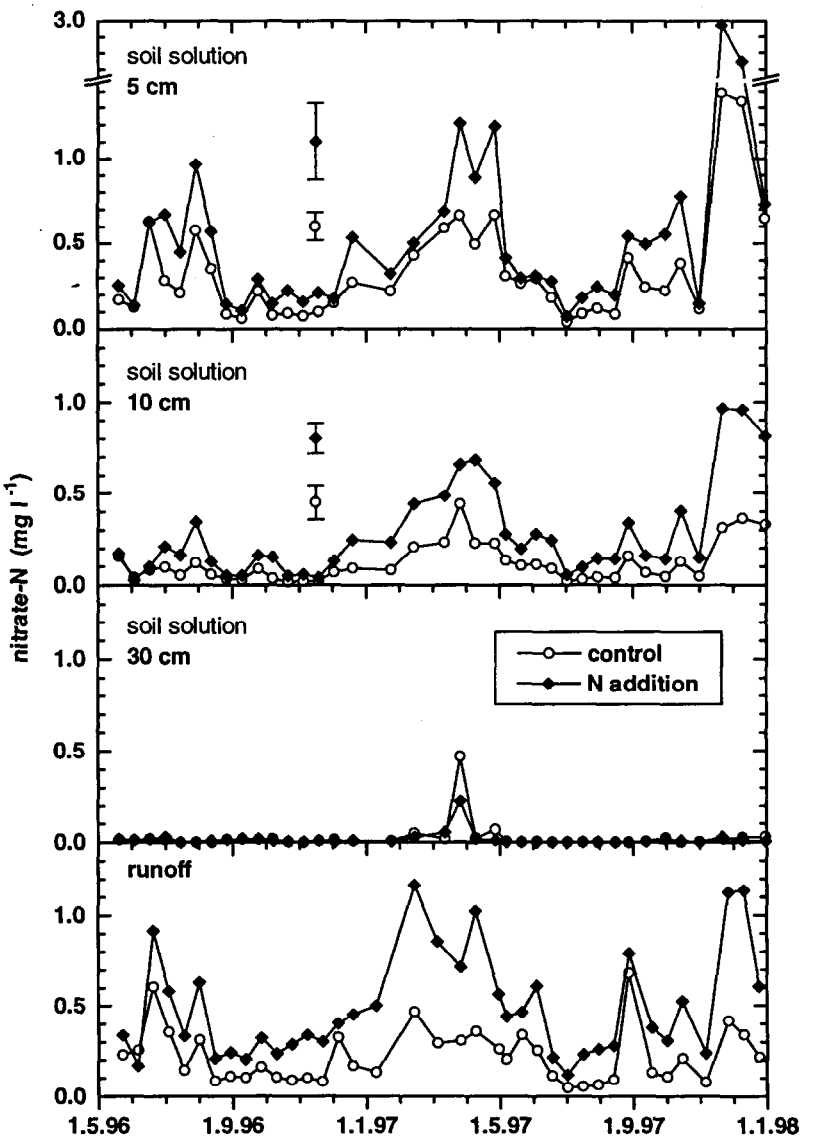

Figure 2: Nitrate concentration in the soil solution (mean ± standard error, n=5) and in the runoff.

The close linkage between soil water from the topsoil and the catchment runoff indicates the dominance of near-surface flow or preferential solute transport. This is supported by the fast response of surface and subsurface runoff to precipitation events (Feyen et al., 1996). As a consequence, water residence times and contact with the soil matrix are insufficient for a complete biological immobilisation of nitrate. Ammonium, on the contrary, is effectively retained by cation exchange. Net nitrification occurs only after a period of drying in small aerobic areas in the soil and enhances nitrate leaching during the next rainfall event (Hagedorn et al., 1999). Correspondingly, denitrification rates were increased on the treated plots only shortly after rain events with N addition (Mohn, 1999).

Higher nitrate concentrations were observed when the soil was dry and aerobic (June - July 1996, August - September 1997, November 1997), and during snowmelt events (February - April 1997), which led to considerable leaching. Nitrate leaching was about 4 kg N ha^{-1} $year^{-1}$ in the control catchment. It increased by 3.2 and 4.7 kg N in the first and second treatment years respectively, corresponding to 11 % and 16 % of the N addition (Fig. 3).

3.3 Nitrogen budget

Compared to other coniferous forests with manipulated N inputs (Bredemeier et al., 1998), Alptal has to be considered as a site with both moderate inputs and outputs of inorganic N (Table 1). The response of the ecosystem to the manipulation is also intermediate between unsaturated sites in Scandinavia and highly impacted sites in the Netherlands or Germany. In our case, however, it is not possible to relate the nitrate leaching to a nitrogen saturation of the ecosystem, because a large proportion of the soil is bypassed, which limits the biological immobilisation of nitrate. The micro-topography is a further heterogenic factor affecting water flow and N cycle. A lateral migration of nitrate (and other nutrients) from the mounds to the depressions probably explains the differences observed in the nutrient indicator values of the vegetation (Schleppi et al., 1998b). This also explains the apparent contradiction between nitrate leaching and the slight N deficiency in the trees.

Table 1: Nitrogen inputs and outputs of the forested experimental catchments at Alptal. [1]according to Fischer-Riedmann (1995); [2]according to Mohn (1999).

		control		N addition	
		(kg ha^{-1} $year^{-1}$)	(% of inputs)	(kg ha^{-1} $year^{-1}$)	(% of inputs)
bulk deposition:	NO_3^-	6.0	31	6.0	13
	NH_4^+	6.6	34	6.6	14
	DON	2.5	13	2.5	5
dry deposition[1]		4.6	23	4.6	10
N addition:	NO_3^-			13.9	29
	NH_4^+			13.9	29
total inputs		19.7	100	47.4	100
runoff:	NO_3^-	3.7	19	7.3	15
	NH_4^+	0.1	1	0.2	0
	DON	5.6	28	6.1	13
denitrification[2]		1.7	9	2.9	6
total outputs		11.1	57	16.5	35
apparent retention		8.6	43	30.9	65

Dissolved organic nitrogen (DON) is an important form of nitrogen loss from unpolluted forests (Hedin et al., 1995). This was also the case in our moderately impacted site since more DON was leached than nitrate (Table 1). So far, however, there has been no effect of the treatment on DON losses. After 7 years of N additions (up to 150 kg ha^{-1} $year^{-1}$) to both a deciduous and a coniferous forest, Currie et al. (1996) reported an increased production of DON in the forest floor. They, however, found no increase in the amount exported from the soil. This indicates that effects of an elevated N deposition can only be expected in the long term, as a consequence of a lowered C/N ratio in the soil organic matter (McDowell et al., 1998). DON also accounted for a considerable flux in the bulk deposition. The measured concentrations were in the range of the few data published so far (Qualls et al., 1991; Cornell et al., 1995; Michalzik et al., 1997).

Quantifying the N fluxes of the forest ecosystem showed that despite the increased nitrate leaching and denitrification due to the simulated increased deposition the system retained most of the added N. Isotope labelling allowed investigation of where this supplementary N was incorporated.

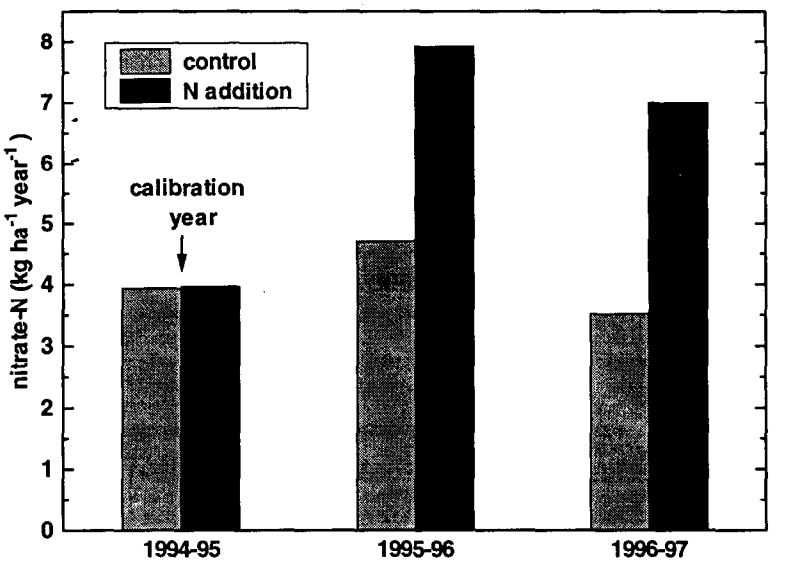

Figure 3: Nitrate leaching from the forested experimental catchments as affected by a deposition increase of 30 kg N ha^{-1} $year^{-1}$ (redrawn from Schleppi et al., 1998a).

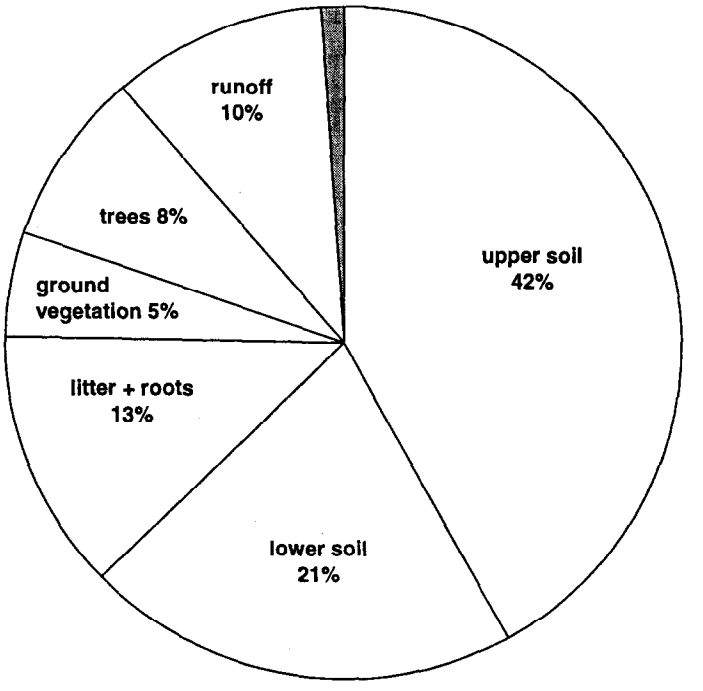

Figure 4: Partitioning of the added ^{15}N-labelled NH_4NO_3 into ecosystem pools and outputs (data from Schleppi et al., 1999a). Shaded segment: tracer not recoverd.

3.4 ^{15}N partitioning

Neither the ground vegetation, nor the needles, bark or wood of the trees showed any increase in their nitrogen content (Schleppi et al., 1999b). Analyses of ^{15}N confirmed that the vegetation contained only small amounts of labelled N in both the year of application and the following year (Schleppi et al., 1999a).

On average, only 4 % of the N in the ground vegetation was labelled with ^{15}N, corresponding to 5 % of the N added to the system (Fig. 4). Current-year needles contained 1.1 % N. Only 2 % of it was from labelled N the year following the label application. The ^{15}N content of older needles was about 1/3 less. These results show that the uptake from current deposition is very small compared to the redistribution of N within the mature trees. This redistribution also takes place in the sapwood of the trunks, where labelled N could be recovered from at least 14 annual tree rings. A total of 8 % of the labelled N was recovered in the above-ground parts of the trees. Compared to other whole-ecosystem applications of ^{15}N (Nadelhoffer et al., 1999), this value is among the lowest. The relative small N-uptake by the vegetation is probably due to other ecological factors limiting plant and root growth at Alptal, especially phosphorus, anaerobic soil conditions and a short vegetation period (Schleppi et al., 1999b).

Most ^{15}N was recovered in the soil: 13 % in litter and roots; 63 % in the fine earth (< 2 mm). The ^{15}N labelling decreased markedly with increasing horizon depth. This corresponds to the chemical analyses (Fig. 2) but is in contradiction with the downward migration of ^{15}N from $^{15}NH_4$ and especially from $^{15}NO_3$ found by Buchmann et al. (1996). This discrepancy can certainly be ascribed to the reducing conditions of the Alptal soil and to the hindered permeability of its gley horizon.

Nitrate leaching into runoff water accounted for 10 % of the added N, corresponding to 2.8 kg N ha^{-1} for the year of $^{15}NH_4{}^{15}NO_3$ application. This amount is close to the increase in nitrate leaching measured by chemical analyses during the same period (3.2 kg N ha^{-1}) and indicates that most of the leached nitrate came directly from the treatment, without interaction with the soil N pool.

4 Conclusions

The Alptal forest is subjected to moderate N deposition rates. Under ambient conditions, this montane ecosystem exhibits nitrate and DON leaching and so loses half the amount of deposited N into runoff water. NH_4NO_3, experimentally added to the throughfall, increased nitrate losses by leaching and by denitrification. These effects, however, were less than proportional to the simulated deposition increase. Analyses of runoff processes and soil solution chemistry as well as a ^{15}N tracer application showed that the leaching of nitrate was to a large extent hydrologically driven. In spite of the rapid water flow, the limited contact with the soil matrix was sufficient for ammonium to be removed by cation exchange, but not for a complete biological immobilisation of nitrate. Nitrate leaching is therefore better explained by precipitation or snowmelt water bypassing the soil rather than by a soil-internal N surplus.

Most of the deposited N is retained in the soil and relatively small amounts are taken up by the vegetation. For this reason, the risk of the N deposition affecting tree health or plant biodiversity is quite small in the short term. However, long-term effects can be expected due to a continuous build up of the N content in the soil and in the perennial species.

Acknowledgements

This study, as part of the European project NITREX, was partly financed by the Swiss Federal Office of Science and Education, Bern. Most of the chemical analyses were done at the central laboratory of the Swiss Federal Institute for Forest, Snow and Landscape Research, Birmensdorf (D. Pezzotta). Analyses of ^{15}N were conducted at the Paul Scherrer Institute, Villigen (Dr. R. Siegwolf, Dr. M. Saurer and Dr. I. Bucher-Wallin). Technical assistance and correction of the manuscript were obtained from D. Tarjan.

References

[1] Aber J. D., Nadelhoffer K. J., Steudler P. & Melillo J., (1989) 'Nitrogen saturation in northern forest ecosystems'. BioSci., 39: 378–386.

[2] Ågren G. I. & Bosatta E., (1988) 'Nitrogen saturation of terrestrial ecosystems'. Environ. Pollut., 54: 185–197.

[3] Braun M., Frey M., Hurni P. & Sieber U., (1991) 'Abschätzung der Phosphor- und Stickstoffverluste aus diffusen Quellen in die Gewässer im Rheineinzugsgebiet der Schweiz unterhalb der Seen (Stand 1986)'. FAC, Liebefeld & BUWAL, Bern. 87 pp.

[4] Bredemeier M., Blanck K., Xu Y.-J., Tietema A., Boxman A. W., Emmett B., Moldan F., Gundersen P., Schleppi P. & Wright R. F., (1998) 'Input-output budgets at the NITREX sites'. For. Ecol. Manage., 101: 57–64.

[5] Buchmann, N., Gebauer, G., Schulze, E. D., (1996) 'Partitioning of ^{15}N-labeled ammonium and nitrate among soil, litter, below- and above-ground biomass of trees and understory in a 15-year-old Picea abies plantation'. Biogeochem., 33, 1–23.

[6] Cornell S., Rendell A & Jickells T., (1995) 'Atmospheric inputs of dissolved organic nitrogen to the oceans', Nature, 376: 243–246.

[7] Currie W. S., Aber J. D., McDowell W. H., Boone R. D. & Magill A. H., (1996) 'Vertical transport of dissolved organic C and N under long- term N amendments in pine and hardwood forests'. Biogeochem., 35: 471–505.

[8] Downing R. J., Hettelingh J.-P. & de Smet P. A. M., (1993) 'Calculation and mapping of critical loads in Europe: status report 1993'. UN-ECE & RIVM Bilthoven, NL. 163 pp.

[9] Downs, M. R., Michener R. H., Fry B., Nadelhoffer K. J., (1998) 'Routine measurement of dissolved inorganic ^{15}N in streamwater'. Environ. Monit. Assess., in press.

[10] Feyen H., Leuenberger J., Papritz A., Gysi M., Flühler H. & Schleppi P., (1996) 'Runoff processes in catchments with a small scale topography'. Phys. Chem. Earth, 21: 177–181.

[11] Fischer-Riedmann A., 1995: 'Atmosphärische Konzentration und Deposition von N-haltigen Komponenten im Wald des hydrologischen Einzugsgebietes Erlenbach im Alptal'. Diss. ETH Zürich 11035.

[12] Hagedorn F., Schleppi P. & Bucher J. B., (1997) 'N-Umsetzung in einem Gley eines subalpinen Fichtenwaldes in der Schweiz - Auswirkungen von künstlich erhöhter N-Depositionen'. Mitt. Dtsch. Bodenkundl. Ges., 85: 241–244.

[13] Hagedorn F., Mohn J., Schleppi P. & Flühler H., (1999) 'The role of rapid flow paths for nitrogen transformation in a forest soil - a field study with micro suction cups'. Soil Sci. Soc. Am. J., accepted.

[14] Hedin L. O., Armesto J. J. & Johnson A. H., (1995) 'Patterns of nutrient loss from unpolluted, old-growth temperate forests: evaluation of biochemical theory'. Ecology, 76: 493–509.

[15] Kurz D. & Rihm B., (1997) 'Modellierung von Säure- und Stickstoffeinträgen: werden kritische Werte überschritten?' In: WSL (Hrsg.): Säure und Stickstoffbelastungen - ein Risiko für den schweizer Wald? Forum für Wissen 1997. p. 23–36.

[16] McDowell W. H., Currie W. S., Aber J. D. & Yano Y., (1998) 'Effects of chronic nitrogen amendments on production of dissolved organic carbon and nitrogen in forest soils'. Water Air Soil Pollut., 105: 175–182
[17] McNulty S. G. & Aber J. D., (1993) 'Effects of chronic nitrogen additions on nitrogen cycling in a high-elevation spruce-fir stand'. Can. J. For. Res., 23: 1252–1263.
[18] Michalzik B., Dorsch T. & Matzner E., (1997) 'Stability of dissolved organic nitrogen (DON) and mineral nitrogen in precipitation and throughfall'. Z. Pflanzenernähr. Bodenk., 160: 433–434.
[19] Mohn J. G., 1999: 'Field measurement of denitrification within the scope of the nitrogen saturation experiments in Alptal (CH)'. Thesis, Univ. of Zurich.
[20] Nadelhoffer K. J., Emmett B. A., Gundersen P., Kjønaas O.J., Koopmans C. J., Schleppi P., Tietema A. & Wright R. F., 1999: 'Nitrogen deposition makes a minor contribution to carbon sequestration in temperate forests'. Nature, 398: 145–148.
[21] Ortloff W. & Schlaepfer R., (1996) 'Stickstoff und Waldschäden: eine Literaturübersicht'. Allg. Forst- Jagdztg., 167: 184–201.
[22] Qualls R. G., Haines B. L. & Swank W. I., (1991) 'Fluxes of dissolved organic nutrients and humic substances in a deciduous forest'. Ecology, 72: 254–266
[23] Reynolds B., Wilson E. J. & Emmett B. A., (1998) 'Evaluating critical loads of nutrient nitrogen and acidity for terrestrial systems using ecosystem-scale experiments (NITREX)'. For. Ecol. Manage., 101: 81–94.
[24] Schleppi P., Muller N. & Bucher J. B., (1998a) 'Dépôts atmosphériques d'azote et charges critiques: résultats d'une expérience d'addition dans la vallée d'Alptal (SZ)'. J. For. Suisse, 149: 1–15.
[25] Schleppi P., Muller N., Feyen H., Papritz A., Bucher J. B. & Flühler H., (1998b) 'Nitrogen budgets of two small experimental forested catchments at Alptal, Switzerland'. For. Ecol. Manage., 101: 177– 185.
[26] Schleppi P., Bucher-Wallin I., Siegwolf R., Saurer M., Muller N. & Bucher J. B., (1999a) 'Simulation of increased nitrogen deposition to a montane forest ecosystem: partitioning of the added ^{15}N'. Water Air Soil Pollut., in press.
[27] Schleppi P., Muller N., Edwards P. J. & Bucher J. B., (1999b) 'Three years of increased nitrogen deposition do not affect the vegetation of a montane forest ecosystem'. Phyton, in press. van Breemen N. & van Dijk H. F. G., (1988) 'Ecosystem effects of atmospheric deposition of nitrogen in the Netherlands. Environ. Pollut., 54: 249–274.
[28] Wendling U., (1975) 'Zur Messung und Schätzung der potentiellen Verdunstung'. Z. Meteor., 25: 103–111.
[29] Wright R. F. & Rasmussen L., (1998) 'Introduction to the NITREX and EXMAN projects'. For. Ecol. Manage., 101: 1–7.

Direct and indirect evapotranspiration measurements and data processing

V. A. Shutov

Valday Branch of State Hydrological Institute, 175400, Valday, Pobeda St. 2, Russia.

Abstract

Long-term 10-day average evapotranspiration measurements using weighing lysimeters are presented. It was found that agricultural plants influence the seasonal variation of evapotranspiration as their biogeophysical features change. An empirical relationship was found between relative evapotranspiration and available soil moisture. It is non-linear, particularly for dry conditions, and corresponds to the moisture dependence of soil hydraulic conductivity. Indirect measurements of evapotranspiration were performed based on Penman's approach and profile method. The automatic equipment, its principles and measurement accuracy are described. As a result, the daily evaporation for the summer season is calculated. Climatic indices of wetness have been proposed for applications. Finally, some problems of experimental research and development are discussed.

1 Introduction

The purpose of evapotranspiration measurements from the land surface is to estimate and to predict the dynamics of soil moisture, water resources and crop water sufficiency in a changing climate. Manifold methods to solve this problem are based on simulation models of the soil-plant-atmosphere system. This variety of models proceeds from the wish of investigators to include diverse aspects of the evapotranspiration phenomenon. Some methods pay regard to the plant physiology, while others describe turbulent transfer within surface boundary layer or develop water transport through root system and soil. All models simulate the various climatic influences, including their rare combinations. To estimate evaporation and crop water sufficiency in real-time, simple empirical models are used such as the heat-water balance HWB method proposed by M. I. Budyko (1971). They have been improved for practical usage (Georgievsky et al., 1993, Shutov, 1986, 1998).

This method considers potential evaporation and, in addition, the soil moisture dependence of evaporation and the plant features that control transpiration activity. Such simplified schemes cannot be compared with detailed simulation models. Indeed, the latter type have been reduced to simple HWB-schemes by parameterisation for climatic studies (Budagovsky and Busarova, 1991, Dickinson, 1987, Lindstrom et al., 1994).

Experimental investigations and modelling studies are closely interrelated. In recent years field experiments have become more purposeful. They certainly aid the estimation of model parameters and their verification using measured data (Jogan and Lozinskaya, 1993, Ol'chev and Stavisky, 1990). Establishing field investigations we have to choose the type of experimental approach: either heat balance, or eddy correlation, either turbulent diffusion (profile) method, or weighing soil lysimeters which are traditional for hydrology (Fedorov, 1978, Ward, 1971). We undertook this summary of accessible observation data to modify the HWB-method and, in addition, to develop the indirect measurements of evapotranspiration described in earlier works (Shutov, 1986, 1993, 1998).

The investigations described are necessary to achieve fundamental results relevant to the problem of food production, which is complicated today by global climate change. There is an urgent need to evaluate changes in the hydrological cycle and possible re-distribution of plant communities related to them. How might evapotranspiration and productivity of natural plant communities change in the future? What plant species will be assumed as the most advantageous for agriculture? Problems of soil moisture deficit and crop productivity are also very important. The influences of a wide range of factors on soil moisture dynamics and crop water consumption needs to ascertained. On this basis recommendations can be made concerning optimal irrigation and drainage measures. Such data analysis assists with planning agriculture during droughts.

2 Results of direct observation

Measurements of evapotranspiration at Valday were taken over about 30 years with use of experimental weighing soil lysimeters 0.3 m^2 in area and 0.6 m depth. Evaporimeters, and soil moisture and meteorology information are also used to analyse the data.

Comparative studies of the 10-day evapotranspiration obtained by 0.3 m^2 lysimeters and by the unique big hydraulic (floating) evaporimeter of 5 m^2 area and 2.5 m height showed that the differences are normally distributed. Therefore, we consider that there are not any significant systematic errors inherent to measurements using standard soil lysimeters of 500 cm^2 area.

Monthly evapotranspiration amounts are quoted in Table 1. They are accurate to about 10 %. It has been shown (Shutov, 1986) that in most cases the 10-day coefficient of variation C_v ranges between 0.3 and 0.4 (Table 2). Hence, the observation period of 22 years is enough to evaluate 10-day means and the results described here can be used confidently for local climate research. The seasonal variations of evapotranspiration (Fig. 1) are individual for various plant species. These are affected by biophysical factors which change over the vegetation cycle, primarily the so-called leaf area index LAI (Slatyer, 1967). Maximum rates are observed during the flowering time for all the plant species, then they decrease under the influence of biological factors (stomatal conductivity, cell turgor, etc.) and by dry weather conditions of the late summer.

The average ratios β of evapotranspiration from plants E_c and evaporation from bare soil E_s were examined (Shutov, 1986), which is possible only by observation data. The seasonal change of this ratio (Table 3) may be specified as the crop water consumption curve.

Table 1: Monthly evapotranspiration (mm) from different crops at Valday.

Month	Fallow	Grass	Rye	Oats	Clover I	Clover II	Flax	Potatoes
May	54	79	97		88	91		
June	62	96	104	112	104	92	98	76
July	69	76	73	96	84	75	94	102
August	50	64		56	68	67	77	64
September	41	35			38	39		43
Growth season	276	350	274	264	382	364	269	285

Table 2: In-time variation coefficient of 10-days evapotranspiration rates.

Month	Fallow	Grass	Rye	Oats	Clover I	Flax	Potatoes
May	0.21	0.31	0.31	0.46	0.25		
June	0.20	0.24	0.31	0.28	0.37	0.19	0.36
July	0.24	0.32	0.45	0.33	0.43	0.20	0.29
August	0.28	0.30	0.36	0.23	0.36	0.28	0.34
September	0.31	0.33			0.40		0.32

Table 3: Water consumtion coefficient as the ratio of evapotranspiration from crops and evaporation from fallow surface (practically bare soil).

Month	Decade	Fallow	Grass	Rye	Oats	Clover I	Flax	Potatoes
May	1	1.00	1.31	1.56		1.56		
	2	1.00	1.53	1.82	0.94	1.59	0.82	
	3	1.00	1.52	1.95	1.14	1.71	1.05	0.86
June	1	1.00	1.89	2.16	1.68	2.05	1.37	1.00
	2	1.00	1.43	1.57	1.90	1.57	1.62	1.19
	3	1.00	1.36	1.36	1.82	1.45	1.73	1.45
July	1	1.00	1.00	1.13	1.48	1.22	1.48	1.48
	2	1.00	1.14	1.14	1.45	1.32	1.41	1.55
	3	1.00	1.17	0.92	1.25	1.13	1.21	1.42
August	1	1.00	1.33	1.22	1.28	1.50	1.28	1.39
	2	1.00	1.31		1.13	1.44	1.13	1.25
	3	1.00	1.19		0.94	1.13		1.19
September	1	1.00	0.88			0.94		0.81
	2	1.00	0.86			0.93		0.86
	3	1.00	0.82			0.91		

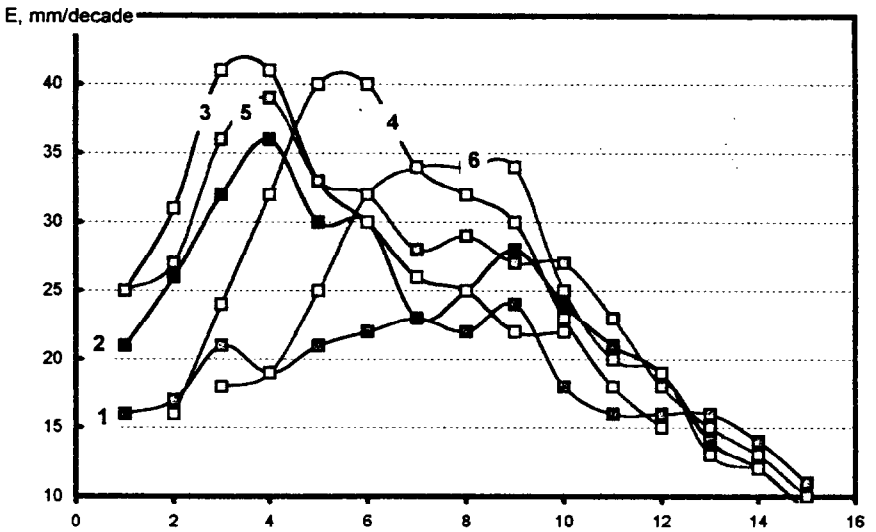

Figure 1: Crops' water consumption and evaporation from bare soil by long/term observation. Numbers of decade since the outset of growth season are given on the x-axis. 1 - bare soil (fallow), 2 - meadow, 3 - winter rye, 4 - oats, 5 - clover, 6 - potatoes.

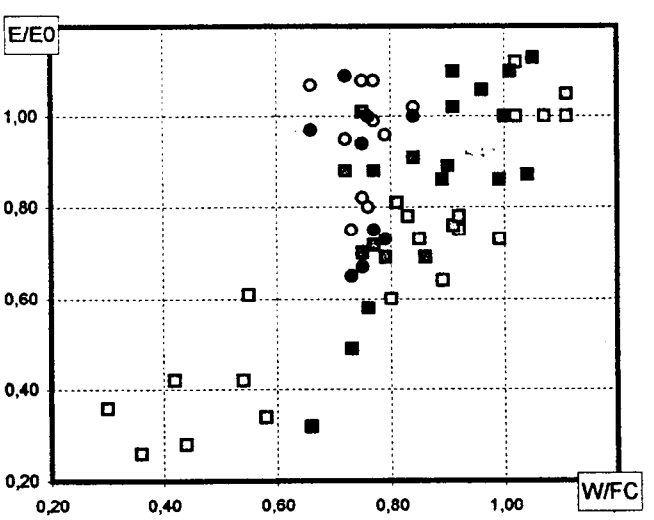

Figure 2: Relative evapotranspiration E/E_o and relative soil moisture W/FC at Valday.

3 Evaporation and soil moisture

The relationship between evapotranspiration and soil moisture has been described by many empirical methods (e.g. Budyko, 1971, Hansen and Jensen, 1986). These relationships (Fig. 2) were developed on the basis of observation data on evapotranspiration from meadow grass E_s, evaporation from water E_w and relative soil water content W^*. The latter is described as

$$W^* = (W - WP)/(FC - WP), \tag{1}$$

where W is actual soil moisture, FC - field capacity of the soil and WP - wilting point of the plant. These ratios were acquired for summer seasons with various precipitation and other climatic conditions.

In spite of considerable dispersion of the data we may affirm that: (1) the evapotranspiration reaches a maximum when the soil moisture is close to FC; (2) the moisture dependence discovered is somewhat non-linear particularly during droughts. In the range of W^*-values from 0.20 to 0.95 the moisture dependence is described as follows:

$$f(W) = W^*\{1 - [1 - (W^*)^{1/m}]^m\}^2 \tag{2}$$

The non-linearity of this dependence was discovered by Denmead and Shaw (1964). We reckon that it follows from the non-linear shape of the soil water conductivity $K(W)$ which affects the water flux out of soil column. As can be found, Eq. (2) corresponds to the model of soil water conductivity (Shutov and Kaljuzny, 1994). Although the exponent m is 0.88, for this case it certainly differs from the value adopted $K(W)$-function. Models similar to Eq. (2) were found earlier proceeding from the structure of soil porous media (van Genuchten, 1980), where the m-value conforms to soil textural type.

The linear moisture dependence adopted in the HWB-method (Budyko, 1971, Kharchenko, 1975) is true only for high moisture and by the 'intermediate' point by $FC > W_c^* > WP$. The dispersion can be proceeded from the instability of this crucial point W_c^* (Novák, 1989), from variability of soil moisture and also from inevitable instrumental errors. The exponential law assumed to be suitable for droughts (Hansen and Jensen, 1986) has to be re-adjusted. However, it may allow the linear $f(W)$-curve for computation of evapotranspiration in humid areas. Since the drought conditions have to be examined particularly, the non-linear $f(W)$-function can be appraised as valuable improvements of HWB-scheme.

4 Principles of indirect measurements

The heat balance and profile methods do not have any defects peculiar to lysimeters and particularly to empirical methods adjusted locally. They are more adaptable for automatic devices and computer-based data processing techniques, and mainly they render a short-time resolution of evapotranspiration and the main factors which control it.

Estimation of climatic humidity or wetness with use of quantitative criteria, such as the ratio of heat- and water resources, is the most effective way to control the natural ecosystems. The parameters subjected to control are the radiative index offered by M. I. Budyko (Budyko, 1971) and also the ratio of actual and potential evapotranspiration. We confirmed this for the summer season using data acquired from the Automated System for Data Sampling and Assimilation (ASDSA) which was built up as computer-base, which describes the daily variation of solar radiation and other meteorological variables. Although the computer technique we used is now out-of-date, we suggest that this approach confirms the indirect measurement of evapotranspiration as the basis of energy and water cycling in the soil-plant-atmosphere system.

The potential evaporation E_o has been defined by the well known Penman approach, which serves for the real-time estimation (Brutsaert, 1982, Oke, 1978). We use it as follows:

$$E_o = -\delta(1/L)(R - B)/(\delta + \gamma) + \gamma D(e_s^* - e)/(\delta + \gamma) \quad (3)$$

where L is the latent heat rate (2.51 MJ/kg), δ is derivation of vapour pressure by air temperature, γ is psychrometric constant, R is net radiation flux, B is the heat flux into the soils, D is so-called bulk transfer coefficient (the Dalton ratio), e_s^* and e are saturation vapour pressure by surface temperature and actual atmospheric vapour pressure.

The bulk transfer coefficient D was calculated using wind velocity, and the aerodynamic roughness parameter z_o estimated through logarithmic transformation of wind profiles. Net radiation was defined as the balance between the shortwave and longwave radiative fluxes. The heat exchange within soil was not measured but assumed approximately to be $0.1R$ (Brutsaert, 1982).

The actual evaporation rate may be evaluated more reasonably by the profile method, because the heat balance approach gives considerable errors for small values of near-surface fluxes. Therefore, we suggest that the more simple version of the profile method should be adopted, which does not require more detailed information on the wind profile. Thus, the actual rates were determined as (Shutov, 1993, 1998):

$$E = 0.622\, r_a\, K_p\, u_1\, f(Ri)\, \Delta e / P_a \quad (4)$$

where r_a is air density, K_p is transfer coefficient for equilibrium conditions, u_1 is wind speed at 1 m above the land surface, $f(Ri)$ is non- linear function of the Richardson ratio which tests the stability conditions of the atmospheric surface layer (Oke, 1978), Δe is gradient of water vapour pressure among two levels 0.5 and 2.0 m, P_a is air pressure.

It was found that about 94 % of whole data are confined to a range for Ri from -0.04 to 0.1. All tested expressions of the function $f(Ri)$ for this Ri-range gave similar results. The results deviate by only about 10 %. Therefore, we may use the following expressions:

$$f(Ri) = \begin{cases} (1 - 3\,Ri)^2 & \text{if} \quad Ri < 0 \\ (1 - 5\,Ri)^2 & \text{if} \quad 0 < Ri < 0.4 \\ 0 & \text{if} \quad Ri > 0.4 \end{cases} \quad (5)$$

which were confirmed by experiments (Bush, 1976, Thom, 1975). It must be noticed that these expressions were successively used and approved by evaluating the heat exchange over the snow surface during the snow melt season (Shutov, 1993), using the same approach.

5 Techniques and results

The Automatic System for Data Sampling and Assimilation (ASDSA) was made in the Institute for Water Automatic located in Bishkek (now the capital of Kirghiz Republic), commissioned by the State Hydrological Institute. It was operated at Valday during only three summer seasons (1988–90). The ASDSA-sensors (Fig. 3) were installed on stakes above a meadow grass surface on a slight hillslope of north-east exposure. The four-level profile measurements of air temperature, air humidity and wind speed were repeated half-hourly with use of automatic equipment and controlled by a computer system. Global solar flux, long-wave and net radiation were integrated in-time. The daily evaporation rates from land and water surfaces were measured using a weighing and hydraulic (floating) lysimeter and basin respectively. Standard meteorological and actinometric recorder data were also applied.

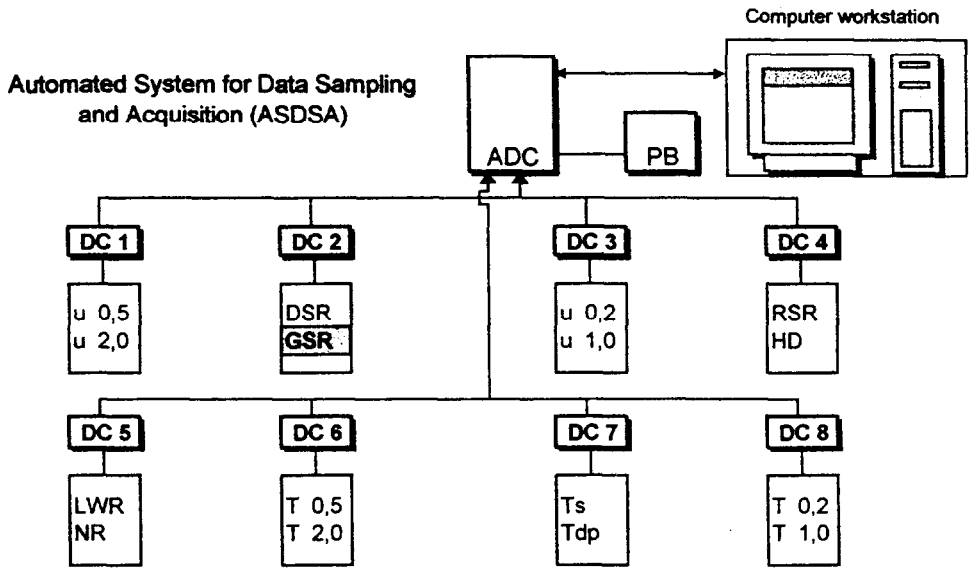

Figure 3: Automated system for data sampling and assimilation ASDA. DC - data controller, ADC - analog/digital convertor, PB - power block, T - air temperature (at four levels), Ts - surface temperature, Tdw - dew point temperature, u - wind speed (at four levels), HD - air humidity detector (LiCl humistor), DSR - direct solar radiation, GSR - global solar radiation, RSR - reflect solar radiation, LWR - long wave radiation, NR - net radiation (radiation budget).

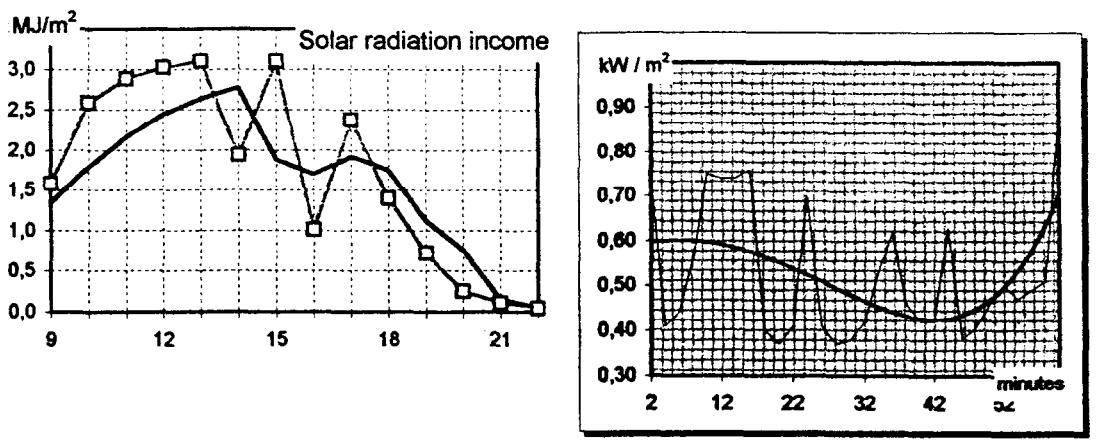

Figure 4: Solar radiation income fluctuated over day-time (left) and over an hour (right) as recorded by ASDSA sensors. It suggests the urgency of time averaging these data.

Research has been carried out since the summer 1987 to control the accuracy and to evaluate the errors. In particular, attention was paid to estimation of the errors related to in-time discretization of continual meteorological variables and partly determined by inertia of the transducers. For this purpose model devices were used which replaced the electrical output of the sensors. Prior to testing, the re-evaluation coefficients for each couple sensor-transducer were determined.

It was clearly justified that the most important source of errors proceeds from the variability of the solar radiation income by changing cloudiness (Fig. 4). The errors of individual data can be about 30 %. Hence, the measurements of radiative fluxes have to be integrated in-time before they may be used for evapotranspiration.

Using only ASDSA the short-term and coupled variations of atmospheric parameters were observed. Daily variation in actual evapotranspiration reflects that the meteorological variables are oscillating and differ from a smoothed curve (Fig. 5). Decreases in net radiation and potential evapotranspiration in the afternoon are due to *cumulus* clouds which form at this time. At the same time the actual evapotranspiration decreases slowly. During rain showers the intensity of potential and actual evapotranspiration fall to zero, but after the rainfall they increase again in spite of the late evening time.

Peculiarities of diurnal evapotranspiration are certainly smoothed by in-time average for a number of days and they express the classical smooth curves (Fig. 6). The standard deviations $\sigma(E_o)$ and $\sigma(E)$ reflect variable weather conditions. The variations change with time of day: in the evening they will be more than in the morning, being influenced by summer rainstorms from *cumulonimbus* clouds. Variations of potential evapotranspiration are such that $\sigma(E)/E > \sigma(E_o)/E_o$.

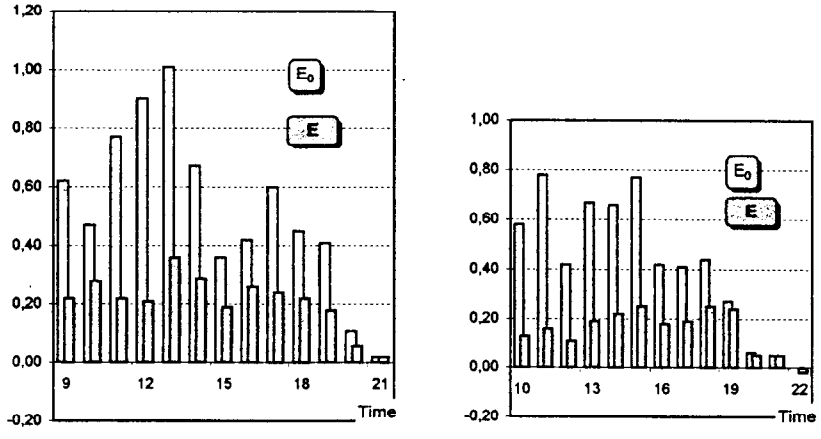

Figure 5: Two examples of individual daily course of potential E_o and actual E evaporation (mm/h) as recorded by ASDSA using Penman's approach and the profile method.

The structure of the heat budget is usually described through the radiative Budyko's index LE/R and the Bowen ratio $Bo = P/LE$. The condition of $LE/R > 1$ conforms to mainly advective influences on the evapotranspiration. Small values of the LE/R-indices are coupled with large Bo-ratios. These are peculiar to morning and midday, when the intensive turbulent heat flux takes place. By the evening time and stable conditions both the sensible heat flux P and the Bowen ratio become negative.

During the summer season the daily evapotranspiration rates change from 0.9 to 5.0 mm, while the potential evaporation rates change from 2.5 to 12.0 mm. The cli-

matic wetness index expressed as $(E_o - E)$ reaches 4 mm/day and the index determined as the ratio of E/E_o oscillates over the range 0.25 to 0.85 around an average of 0.48. The correlations between these diverse climatic indices are of special interest for evaluation of the local climate peculiarities.

It was also discovered as a result of comparative analysis of the data samples obtained using the automatic equipment (ASDSA) and weighing soil lysimeter, that their daily rates are poorly correlated. As was found, the correlation between daily evaporation from open water surface and the evaporation rates obtained by Penman's approach is really absent. This signifies that the profile method (or its adapted version) and the lysimeter data are incompatible for short time intervals.

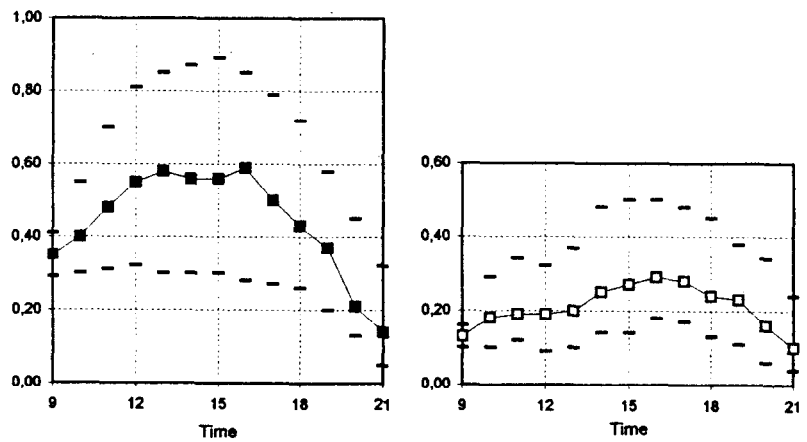

Figure 6: Time-average daily courses of potential (on the left) and actual evaporation by ASDSA measurements. Possible deviations from average are shown as dashes.

6 Summary and perspectives

There are two independent approaches for experimental research of evapotranspiration: (1) the method of evaporimeters, which delivers satisfactory results only for large time intervals greater than about one month; (2) the profile (turbulent) method involving indirect measurements, which is suitable for the short-time variability of evaporation including its daily variation. Some problems remain.

1. The choice is to estimate potential evapotranspiration either by Penman's approach or by using water evaporimeter data. The latter is preferable as a direct evaluation method, although the data from standard pan evaporimeters are spatially non-homogenous (Kokoreva, 1989) due to heat flux from the surrounding soil. Water evaporation may be obtained as the continual spatial field using the thermo-isolated pan evaporimeters which were proposed for observation.
2. There is a choice between two versions of gradient (profile) method: either detailed profile measurements, or its bulk-scheme, which assumes there are meteorological data available only at a single height and at the surface. Empirical dispersion is conditioned by inevitable measurement errors, and by micro-scale atmospheric phenomena. Hence, it proceeds that the higher level is preferred for sensor installation on a stake mast, since the effect of sensor-born biases on the measurement accuracy will be less.

3. It is necessary to estimate the boundary conditions (surface temperature and air humidity) of the vegetation cover. It very important to obtain the moisture of the utmost upper soil layer to assign the near-surface humidity (Monsi et al., 1990). In this case probably the remote sensing of the infrared emissivity of the surface (Kalma and Jupp, 1990) and micro-wave detection will be preferable.
4. Of importance also are the biometrical features of plants, which define the solar radiation income, the turbulent exchange under and within a plant canopy and also the stomatal control of transpiration. The choice appears again either to assume all the properties in detail, or to estimate the vegetation index (VI) corresponding to the biophysical features of the plant community. These estimations are carried out upon satellite-based imagery of high resolution in different spectral bands (Kondratjev, 1992).
5. Precise knowledge is required of the relationships between evapotranspiration and soil water content. It needs to ascertained which soil layers participate in the water flux. This problem ensues from traditional objectives of experimental hydrology. It also affects the spatial variability of evapotranspiration and it affirms the non-linear moisture dependence (Shutov, 1998). The in-situ soil moisture measurements with neutron scattering method (Kapotov and Shutov, 1993) and based on profiles of soil water pressure (Shutov and Kaljuzny, 1994) are convenient for this purpose.

These experiments are usually realised within the soil columns (monoliths of lysimeters), thereafter the study concept proposed for the investigation of the within-soil water flux. It may be defined as the concept of an undisturbed soil column with native soil cover. This concept presents the alternative: either direct measurements of the soil water fluxes in disturbed conditions of lysimeter; or an indirect method involving evaluation of the moisture gradient and the water conductivity within the soil in its natural state.

Concerning evapotranspiration into the atmosphere, a similar concept may be proposed. Indirect measurement such as the bulk-scheme profile method involving remotely sensed surface conditions can certainly be assumed as far more suitable for operational estimation of evapotranspiration and climate wetness indices. When we call for direct measurements using the eddy correlation method, we must consider that the complications of this method are excessive for the problems examined.

References

[1] Brutsaert, W. (1982) Evaporation into the atmosphere. - D. Reidel Publ. Comp., Dordrecht.

[2] Bush, N. (1976) The surface boundary layer. - Boundary-Layer Meteorol., vol. 4, No 1–4, 213–240.

[3] Budagovsky, A. I., Busarova, O. E. (1990) Principles of the method for estimating soil water resources and river runoff from various scenarios of climatic change. - Water Resour., No 2, 5–16 (in Russian).

[4] Budyko M. I. (1971) The climate and the life. - L., Gidrometeoizdat (in Russian).

[5] Denmead, O. T., Shaw, R. H. (1964) Availability of soil water to plants as affected by soil moisture content and meteorological conditions. - Agron. J., vol. 54, No. 4, 385–390.

[6] Dickinson, R. (1987) Evapotranspiration in global climate models. - Advanced Space Research, vol. 7, No 1, 17–26.

[7] Fedorov, S.F. (1978) Investigation of water balance components in the forest zone of European part of USSR. - L., Gidrometeoizdat. (in Russian).

[8] Hansen, S., Jensen, H. (1986) Spatial variability of soil water and evapotranspiration. - Nord. Hydrol., vol. 17, No 4/5, 261–268.
[9] Genuchten R. van (1980) Calculating the unsaturated hydraulic conductivity with a new closed-form analytical model. - Soil Sci. Soc. Amer. J., vol. 44, No. 5, 892–898.
[10] Georgievsky, V. Yu., Shalygin, A. L., Doganovskaja, T. M. (1993) Modern and future dynamics of crop demand for irrigation in relates with climate. - Meteorol. and Hydrol., No. 12, 81–87 (in Russian).
[11] Jogan, L. Ya., Lozinskaja, E. A. (1993) A procedure for averaging the relative leaf area in the mesoscale evaluation of the heat and moisture exchange. - Water Resour., No. 6, 693–700 (in Russian).
[12] Kalma, J., Jupp, D. (1990) Estimating evapotranspiration from pasture using infrared thermometry. - Agr. and Forest Meteorol., vol. 51, No 3–4, 223–246.
[13] Kapotov A. A., Shutov V. A. (1993) Method and results of investigation of soil water content on an experimental catchment with use of neutron probe. - Meteorol. and Hydrol., No. 12, 88–93 (in Russian).
[14] Kharchenko, S. I. (1975) Hydrology of irrigated lands. - L., Gidrometeoizdat (in Russian).
[15] Kokoreva, K. M. (1989) Estimating up-to-date state of the water evaporimeter network. - Meteorol. and Hydrol., No. 1, 85–93 (in Russian).
[16] Kondratyev, K. Ya. (1992) The global climate. - St. Petersburg, Nauka Publ. House. (in Russian).
[17] Lindstrom, G., Gardelin, M., Persson, M. (1994) Conceptual modelling of evapotranspiration for simulations of climate change effects. - Swedish Meteorol. and Hydrol. Inst., Repts. Hydrol., No. 10.
[18] Monsi, N., Hamotani, K. and Omoto, Y. (1990) Dynamic behavior of the moisture near the soil-atmosphere boundary. - Bull. of Univ. Osaka, vol. 42, 4–69.
[19] Novák, V. (1989) Evaluation of critical soil moisture by evapotranspiration. - Water Resour., No 2, 137–141 (in Russian).
[20] Oke, T. R. (1978) Boundary layer climates. - London, Methuen & Co Ltd.
[21] Ol'chev, A. V., Stavisky, D. B. (1990) Two-layered parametrization of evapotranspiration to use in meso-meteorological models. - Water Resources, No 6, 16–27 (in Russian).
[22] Shutov, V. A. (1986) Use of land surface evaporation observed data for the characteristics of water consumption of crops - Proc. of the SHI, No 311, 24–42 (in Russian).
[23] Shutov, V. A. (1993) Estimation of the water sufficiency using automated system of data sampling and assimilation. - Meteorol. and Hydrol., No. 10, 114–118 (in Russian).
[24] Shutov, V. A. (1998) Experience and problems of experimental studies of evaporation from land surface. - Meteorology and Hydrology, No 1, 82–93 (in Russian).
[25] Shutov, V. A.,Kaljuzny, I. L. (1994) Analysis of soil hydro-physical parameters on an experimental watershed. - Meteorol. and Hydrol., No 7, 103–109 (in Russian).
[26] Slatyer, R. O. (1967) Plant-water relationships. - Academic Press, London and New York, 1967.
[27] Thom, A. (1975) Momentum, mass and heat exchange of vegetation.- In: Vegetation and Atmosphere. - London: Academic Press, 57–109.
[28] Ward, R. C. (1971) Measuring evapotranspiration: a review. - J. Hydrol., vol. 13, 1–21.

In-situ measurement of oscillation phenomena in gravity-driven drainage

M. Šír[1], M. Tesař[1], Ľ. Lichner[2], O. Syrovátka[3]

[1]Institute of Hydrodynamics, Academy of Sciences of the Czech Republic, Experimental Basis Nový Dvůr 31, CZ 384 73 Stachy, Czech Republic. [2]Institute of Hydrology, Slovak Academy of Sciences, Račianská 75, P. O. Box 94, SK 830 08 Bratislava 38, Slovakia. [3]Institute of Entomology, Academy of Sciences of the Czech Republic, Branišovská 31, CZ 370 05 České Budějovice, Czech Republic.

1 Introduction

Within the scope of a hydrological program launched in 1983, the soil water regime was measured by water tensiometers and analysed with respect to corresponding rainfall and evapotranspiration data. In certain periods, the soil water regime could be explained only by assuming an irregularly oscillating outflow of soil water into lower horizons. In some situations, the water supplied by rain caused a pronounced decrease in the soil water content. Situations of this type were observed several times during a vegetative season (Pražák et al., 1992). In these situations a large volume of water flows through the soil; therefore, on the hydrological scale, this phenomenon forms a great part of the outflow from a watershed. From the qualitative point of view, the outflow oscillation is formed by water held in the soil matrix for some weeks. It means that the outflow from the soil cover is a mixture of old and new water.

The main purpose of our experiments was to reproduce the phenomena observed in situ under controlled conditions: to hold water sprayed over the soil surface in the soil profile; to release the water held, to generate outflow oscillations.

2 Experimental site

The Department of Hydrology and Ecology of the Institute of Hydrodynamics established an experimental study site in the Šumava Mts. in 1964. The Šumava Mts. are a mountain range forming the boundary between south-west Bohemia, Germany and Austria. This area was selected due to its well-preserved, little influenced natural character representing a typical hydrological system of Central Europe. Our research is concentrated on the Spůlka-river drainage basin. In this catchment, the experimental runoff area Zábrod is situated. Its soil cover is formed by acid brown soil developed on paragneiss. The soil profile has a 30 cm A horizon covered with permanent grass. The mean elevation is 790 m a. s. l., the average annual air temperature is 6.1°C and the average annual precipitation is 840.6 mm. The soil water regime has been measured since 1983 (Tesař, 1996).

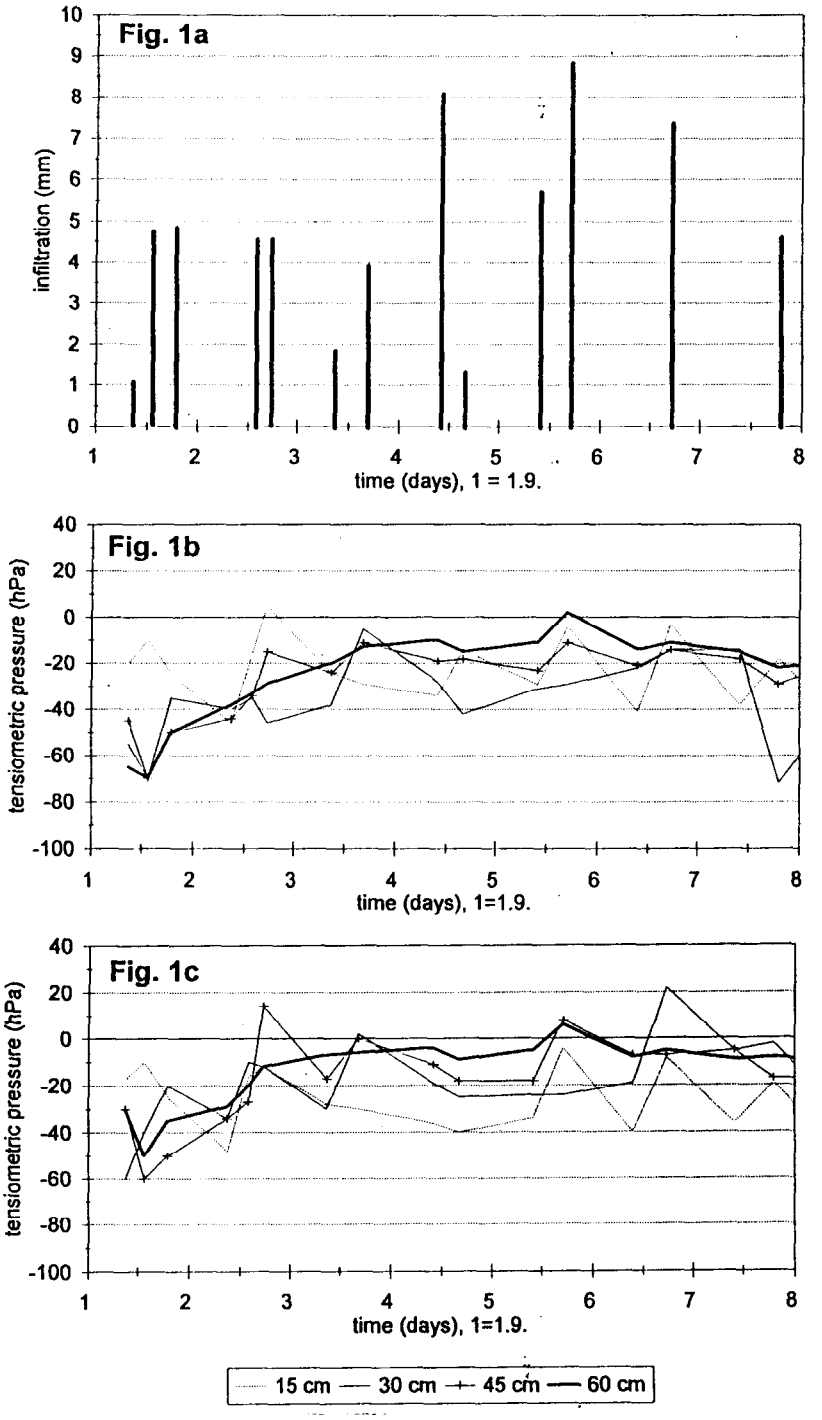

Figure 1: (a) Rain and added water, plot 2, 1.9.–7.9. (b) Tensiometric pressure at depths of 15, 30, 45 and 60 cm, plot 2, site A, 1.9.–7.9. (c) Tensiometric pressure at depths of 15, 30, 45 and 60 cm, plot 2, site B, 1.9.–7.9.

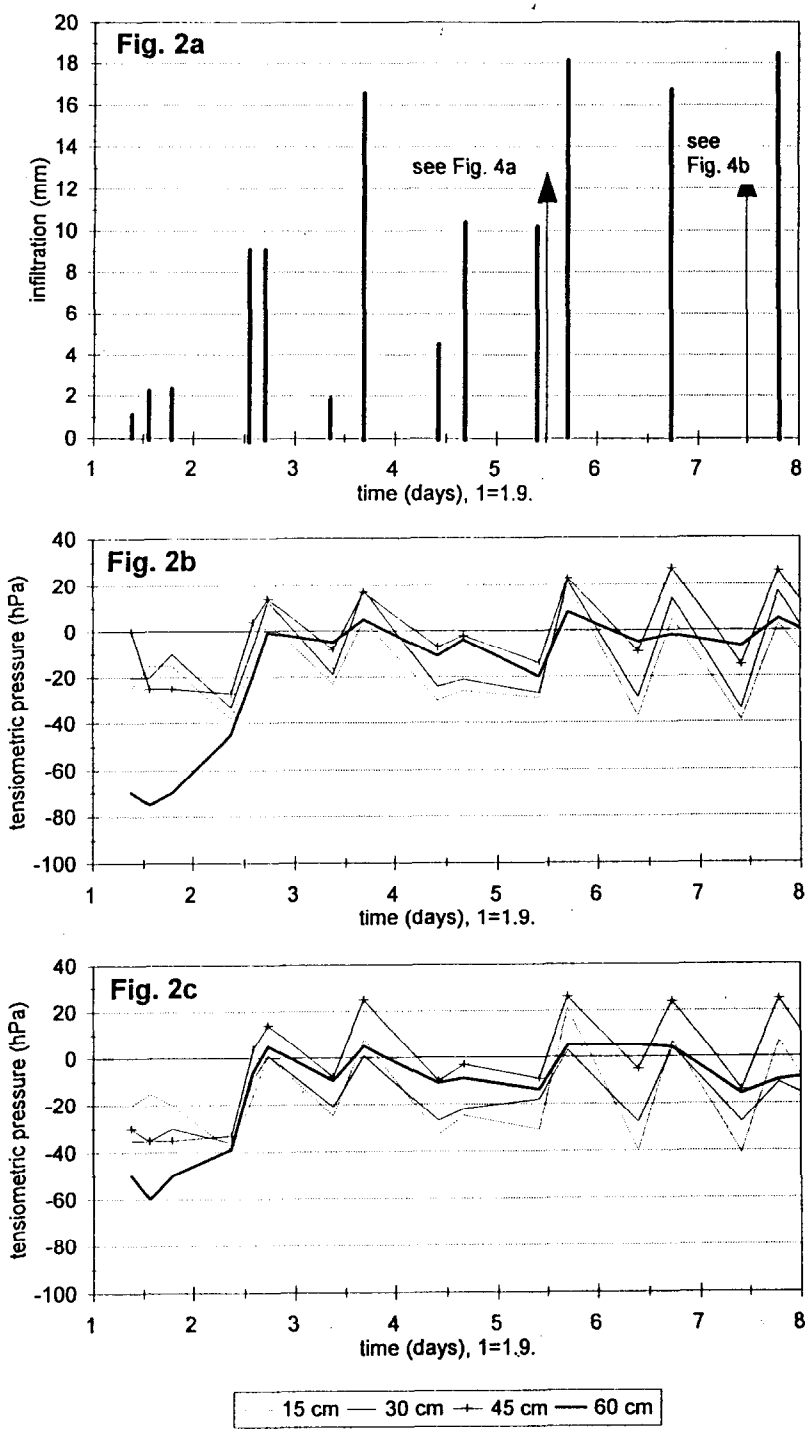

Figure 2: (a) Rain and added water, plot 3, 1.9.–7.9. (b) Tensiometric pressure at depths of 15, 30, 45 and 60 cm, plot 3, site A, 1.9.–7.9. (c) Tensiometric pressure at depths of 15, 30, 45 and 60 cm, plot 3, site B, 1.9.–7.9.

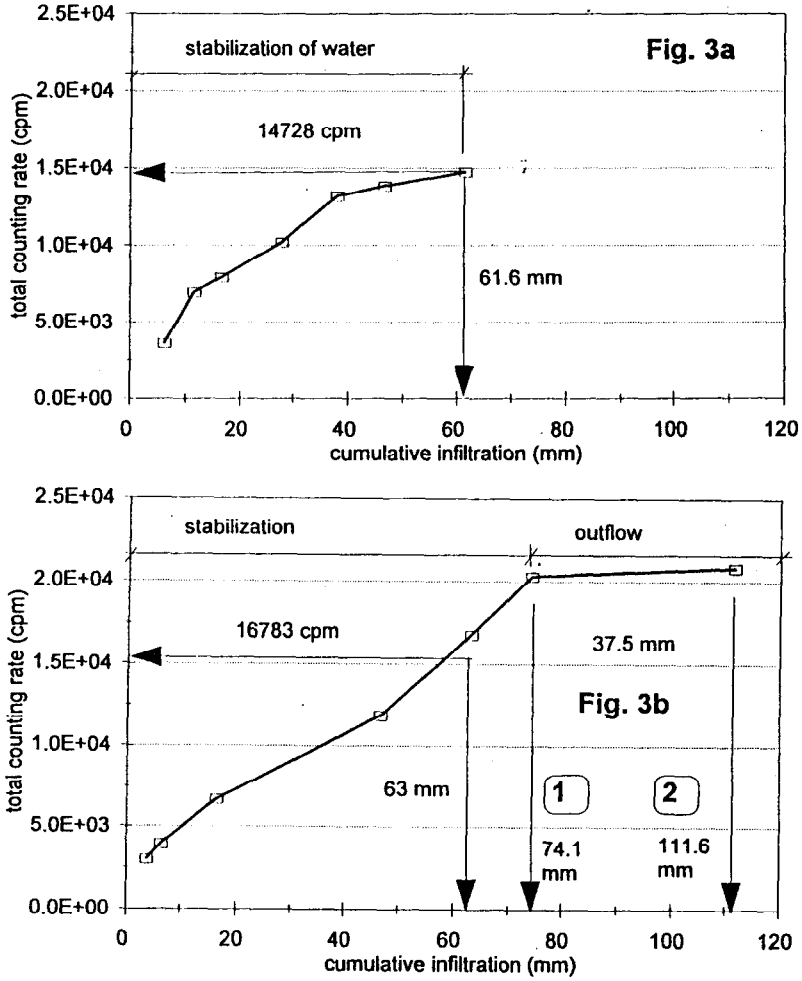

Figure 3: (a) Tracer mass, plot 2, soil layer 20–80 cm. (b) Tracer mass, plot 3, soil layer 20–80 cm, 1 = 5.9., 11–12 hours, see Fig. 4a, 2 = 7.9., 10–12 hours, see Fig. 4b.

The Institute of Entomology operates three experimental localities in the spring area Senotín (610–690 m a. s. l.). This area lies in the Novobystřická Mts. near the boundary between South Bohemia and Austria. Natural and soil conditions are very similar to the runoff area Zábrod.

3 Field measurements

In the experimental runoff area Zábrod, nine plots 5 x 5 m were equipped with water tensiometers at depths 15, 30, 45 and 60 cm.

Two parallel plots (marked 2 and 3) were chosen for nuclear tracer experiments. In each of these plots five vertical access tubes allowing the measurement of radioactivity in the soil layer of 0–100 cm were installed. Radioactivity was measured with a Geiger - Müller detector 21 mm in length and 6.3 mm in diameter. Radioactivity is detected in a diameter of about 20 cm, and the averaging volume of the detector remains constant (Moltayner, 1989). Radioactivity measured as a counting rate can be considered proportional to the tracer concentration (IAEA, 1975). The reproducibility of the detection is about 20 counts per minute (cpm). The natural radioactivity of soil in the given plots is less then 10 cpm.

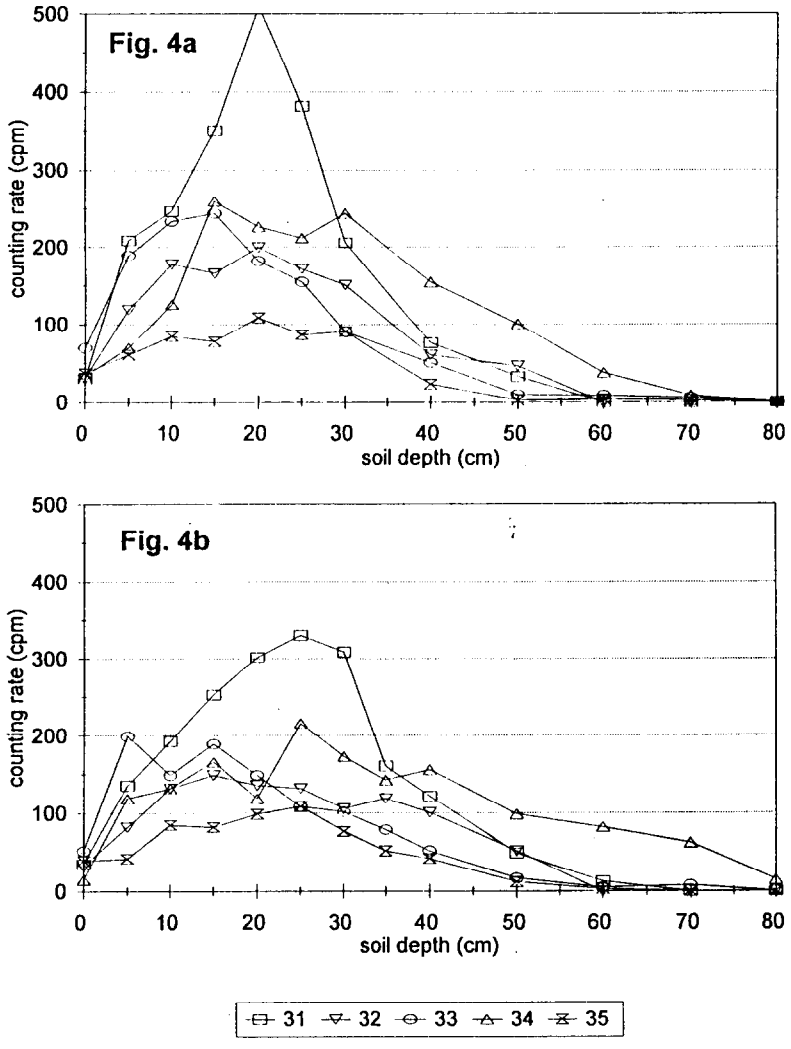

Figure 4: Radioactivity vs. soil depth, access tubes 31, 32, 33, 34, 35, (a) plot 3, 5.9., 11–12 hours, (b) plot 3, 7.9., 10–12 hours.

The measurement positions in every access tube were at depths 0, 5, 10, 15, 20, 25, 30, 40, 50, 60, 70, 80, 90 and 100 cm below the soil surface. The counting rate was measured at every position of the detector for one minute. The measured counting rate was normalized to the starting time with the help of the appropriate half-time of radioactive decay. A water solution of $Na^{131}I$ was used as a tracer. This tracer is negligibly sorbed into the soil complex. To minimize the incorporation of active iodine into soil bacteria, non active iodine was used as a carrier (Lichner et al., 1999).

Around each of the five access tubes inserted into the soil to a depth of 100 cm, the narrow pulse of the tracer was trickled with a syringe into an annulus 10 cm in diameter, and the initial counting rates at the soil surface were measured in all tubes.

After this initial measurement rainfall of very low intensity was simulated, without causing soil surface ponding. Then detectors were installed into the access tubes and counting rates were measured as a function of soil depth. There was no tracer added in the rain water. This scenario was repeated several times using different simulated rainfall amounts and intervals between two successive events. Tensiometric pressure, simulated rainfall amount, air temperature, global radiation and evaporation from a free water surface were simultaneously recorded.

4 Experimental results

Some interesting results are introduced in the following Figures. Figs. 1a and 2a show rain totals and added water amounts (simulated rain) for plots 2 and 3. Figs. 1b-1c and 2b-2c indicate measured tensiometric pressures for plots 2 and 3 in two sites marked A and B. Negative pressure is the so called suction pressure, i.e. the soil is not saturated by water. Positive pressure means hydrostatic pressure. Figs. 4a and 4b give the depth profile of the counting rate (i.e. concentration of tracer proportional to the soil moisture) in two successive situations in plot 3. The profiles in Fig. 4b were measured 48 hours later than those in Fig. 4a. The rain total between these two measurement is 37.5 mm. Figs. 3a and 3b show the total activity (proportional to the soil water storage) in the soil layer 20–100 cm plotted against cumulative infiltrated water in the soil profile in plots 2 and 3.

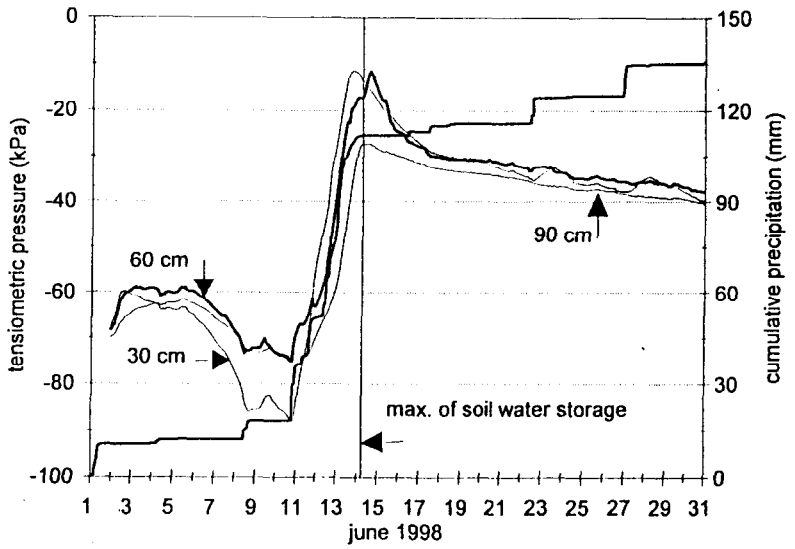

Figure 5: Tensiometric pressure and cumulative precipitation measured in the area Senotín.

5 Discussion and conclusions

The first goal of our experimental work, i.e. the storage of rain water in the soil profile, was fulfilled. In plot 2, 61.6 mm were held, and in plot 3 at least 74.1 mm of rain water in 7 days. At the beginning the soil profile was highly saturated. The tracer was detected at a depth of 50 cm in plot 2 and at 60–80 cm in plot 3 after 7 days of infiltration and redistribution of rain pulses. In plot 3, the outflow oscillation was generated. These results are in full conformity with our previuous laboratory and field measurements (Pražák et al., 1988, 1992, Šír et al., 1996).

One episode of soil water storage and successive outflow of soil water is given in Figs. 5 and 6 (spring area Senotín). Fig. 5 shows profiles of tensiometric pressure measured in depths of 30, 60 and 90 cm in comparison with cumulative precipitation. Fig. 6 gives a water discharge measured in a small brook and drainage outlet corresponding to the precipitation and soil conditions shown in Fig. 5. This episode can be fully explained with the help of our tracer measurement of soil water dynamics.

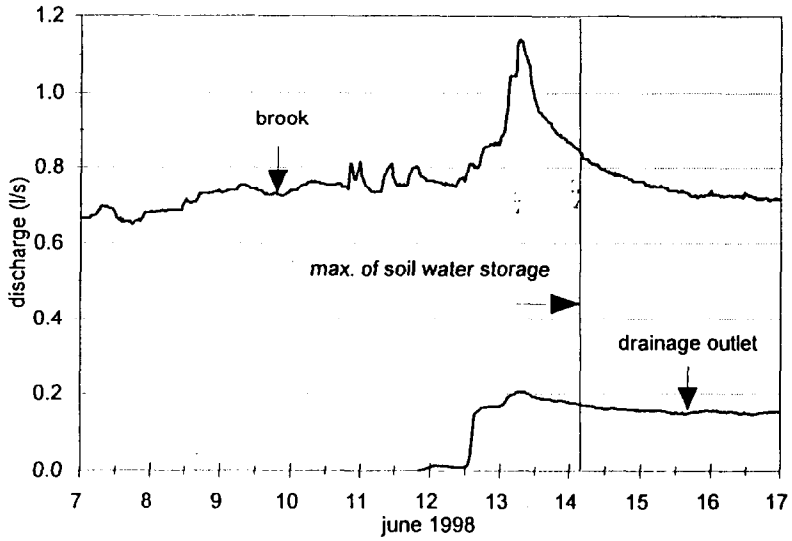

Figure 6: Water discharge in brook and drainage outlet measured in the area Senotín.

Acknowledgements

Grant Agency of the Academy of Sciences of the Czech Republic (Project No A306071) and Grand Agency of the Czech Republic (Project No 526/98/0805) supported this work.

References

[1] IAEA: Laboratory manual on the use of radiotracer techniques in industry and environmental pollution. Technical Reports Series No. 161. International Atomic Energy Agency, Vienna, 1975, 120 pp.

[2] Lichner, Ľ., Meszároš, I., Germann, P., Mdaghri Alaoui, A., Šír, M., Faško, P.: Impact of land-use change on nutrient fluxes in a structured clay-loam soil. In: Heathwaite, L. (ed.): Proc. Int. Symp. Impact of land-use change on nutrient loads from diffuse sources, Birmingham 1999. IAHS Publ. No. 257, Wallingford 1999, 171–177.

[3] Moltayner, G. L.: Mixing-cup and through-the-wall measurements in field-scale tracer tests and their related scale of averaging. J. Hydrol., 89, 1989, 3/4, 281–302.

[4] Pražák, J., Šír, M., Kubík, F., Tywoniak, J., Zarcone, C.: Oscillation phenomena in gravity-driven drainage in a coarse porous media. Water Resources Research, Vol. 27, No. 7, 1992, 1849–1855.

[5] Pražák, J., Šír, M., Kuráž, V., Zarcone, C.: Microscopic aspects of the infiltration of rainwater into light-textured soil (In Czech). Meliorace, 24, Vol. 2, 1988, 127–138.

[6] Šír, M., Kubík, F., Tesař, M., Pražák, J.: Liquid transport in porous media - discontinuous phenomena. Part I: Theory. J. Hydrol. Hydromech., 44, Vol. 2–3, 1996, 81–90.

[7] Šír, M., Kubík, F., Tesař, M., Pražák, J.: Liquid transport in porous media - discontinuous phenomena. Part II: Examples. J. Hydrol. Hydromech., 44, Vol. 4, 1996, 235–251.

[8] Tesař, M.: Experimental basis and catchments in the Šumava Mts. (the Czech Republic). ERB Newsletter. No. 11, 1996, 6–11.

Factors affecting base-flow recessions in a granite mountaineous catchment

J. Stehlík

Department of Experimental Hydrology, Czech Hydrometeorological Institute, Na Šabatce 17, CZ 143 06 Praha 4, Czech Republic.

1 Introduction

A recession curve (hydrograph falling limb) represents the depletion of subsurface storage within the basin. The paper deals with a recession curve analysis aimed at examining factors causing its time variability.

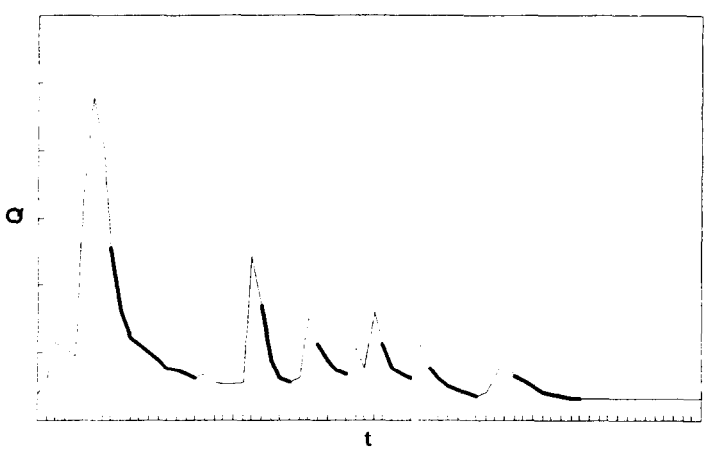

Figure 1: Observed recession curves.

The recession curve is applied in surface water hydrology for forecasting low flows and relevant water stages. In groundwater hydrology the recession curve provides information on parameters of the saturated zone and its water storage capacity. Analysis of recession curve parameters can be applied for estimating the linearity or non-linearity of the depletion process and for assessing the behaviour of the aquifer. The integration of the recession curve in time produces runoff volume, which can be used for water balance analyses. For these analyses a variety of models have been developed. Parameters of these models are often derived from a master recession curve of the basin. Reviews of recession curve analysis include those by Toebes and Strang (1964), Hall (1968), Singh and Stall (1971) and Tallaksen (1995).

2 The pilot basin

The experimental basin (area 4.75 km^2, mean altitude 889 m a. s. l.) is located in the Jizera Mountains in the northern part of the Czech Republic (Fig. 2). The basin is underlain by granite rock and has shallow podzolic, gley and peaty soils. About 75 % of the catchment is covered by young forest (up to 10 years age).

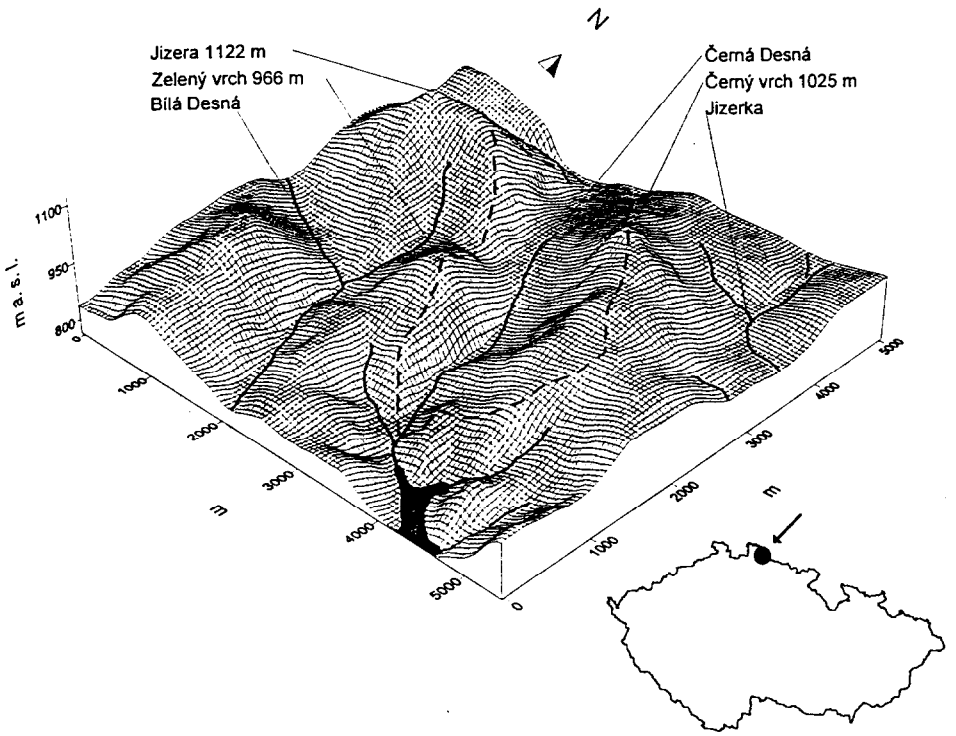

Figure 2: The pilot basin.

3 Methods

The variability of recession curves was studied using the decay time parameter of an exponential function, which was fitted by the least-squares method to the measured curves. The method was modified by applying weights giving preferences to the base flow in affecting the shape of the fitted curve. The exponential function:

$$Q_t = Q_o e^{(-Kt)} \tag{1}$$

simulates the basin response by the outflow $Q = KS$ from a linear reservoir, where S is the water storage, K is the recession parameter and t is time. The recession parameter K controls the shape of the recession curve: the higher the value of K, the steeper the curve. The advantage of this function is that the recession parameter is independent on the initial discharge Q_o of the recession curve. Variability of the recession parameter has been investigated by several authors, recently by Tallaksen (1989).

Recession curves were selected from daily runoff series using the following criteria: (a) the inititial discharge of the recession curve Q_o was selected as the flow one day after the discharge maximum, (b) decreasing discharge values only, c) convex shape of the

recession curve, d) minimum duration - 4 members of the time series = 3 days, (e) the selected curves must belong to the summer half-year (May to October) in order to exclude the influence of snowmelt.

The causes of recession curve variability are described by the dependence of the recession parameter K on a set of 14 variables. These variables are:

(a) variables representing the conditions during the recession period: average air temperature AVG-T, precipitation AVG-P, air humidity AVG-H, discharge AVG-Q;
(b) variables representing antecedent conditions prior to the recession period, which are expressed by means of the index of antecendent conditions AXI for $n = 10$ and 30 days respectively, where X is notation for daily air temperature T, daily precipitation amount P, daily mean air humidity H, daily mean discharge Q:

$$\mathrm{AXI} = \sum_{t=1}^{n} \bar{X}_t C^t \tag{2}$$

where C is a constant less then zero (by this definition the following variables were obtained: indices of antecendent precipitation API-10, API-30, temperature ATI-10, ATI-30, air humidity AHI-10, AHI-30, discharges AQI-10, AQI-30);
(c) initial discharge of the recession curve Q_o and the length of the recession curve L.

The construction of a master recession curve considering only non influenced periods could be another way to detect the influence of factors affecting the shape of the curve. Such a master recession curve, which is not influenced by external factors, should represent the response of the subsurface water storage only. However, besides the problem of defining the difference between an influenced and non influenced recession curve (every curve is more or less influenced), it would be difficult to find enough really non influenced periods for the master recession curve construction. Therefore the above described method was used.

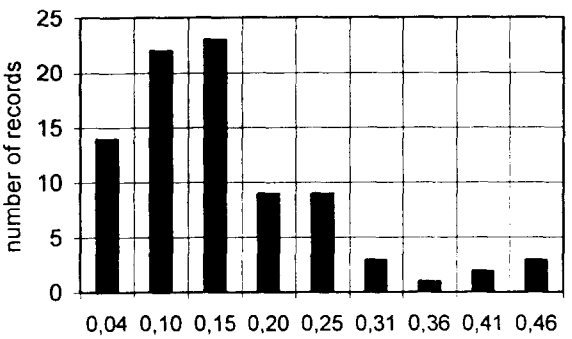

Figure 3: Frequency analysis of the recession parameter K.

4 Results and discussion

The main statistical characteristics concerning the recession parameter K are summarized in Table 1 and Fig. 3.

Based on the time of occurence, every recession curve belongs to the appropriate month. Seasonal variability of the recession parameter K is shown in Fig. 4.

The seasonal course of the recession parameter for the period May–October (black bars) shows a significant effect of the evapotranspiration cycle: high air temperature is reflected in an accelerated depletion of water from the basin and thus a steeper recession curve. Another way to present this result is to consider the master recession curves for each month (Fig. 5). The steepest curves were obtained for August and July. The flattest curves are curves of October and May. (The curves were modelled for the duration of 20 days and Q_o is the long term average discharge.)

Table 1: Statistics of the recession parameter K.

No. of rec.	Average	Median	Max.	Min.	STD	C_v
86	0.185	0.166	0.516	0.043	0.100	0.540

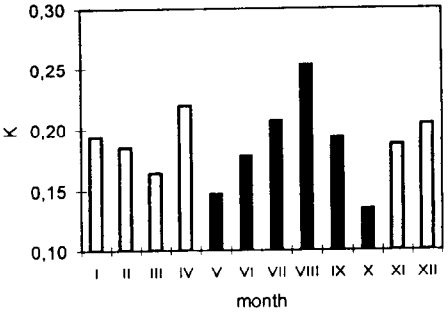

Figure 4: Seasonal variability of the recession parameter.

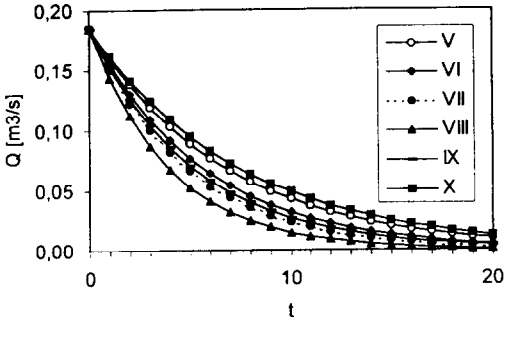

Figure 5: Master recession curves.

In Fig. 4 the average recession parameters for the period November–April are also presented (white bars). Despite the negligible evapotranspiration rate in winter compared to summer, the recession parameters are relatively high. This fact is probably caused by snowmelting.

The influence of the evapotranspiration cycle is confirmed in the correlation matrix in Table 2 (significant correlation coefficient between the recession parameter and temperature during the recession). The variability of the recession parameter is always influenced by the saturation of the basin (API) and antecendent temperatures.

Table 2: Dependence of recession parameter on independent variables (monthly values). * 0.1 *** 0.01 1 - tailed significant.

	AVG-T	AVG-P	AVG-H	AVG-Q	API-10	API-30	ATI-10
K	0.779*	0.047	-0.319	-0.064	0.743*	0.799*	0.953***
	ATI-30	AHI-10	AHI-30	AQI-10	AQI-30	Q_o	L
K	0.957***	-0.449	-0.558	-0.106	-0.436	0.634	-0.712

Table 3: Dependence of recession parameter on independent variables (monthly values). ** 0.05 *** 0.01 1 - tailed significant.

	AVG-T	AVG-P	AVG-H	AVG-Q	API-10	API-30	ATI-10
K	0.006	0.126	0.133	0.353***	0.410****	0.420****	0.062
	ATI-30	AHI-10	AHI-30	AQI-10	AQI-30	Q_o	L
K	0.141***	0.074	0.025	0.245**	0.060	0.431***	-0.359***

Results of the correlation analysis for all 86 individual (not master) recession curves are given in Table 3. Unlike monthly master recession curves, the dependence of the recession parameter on Q_o and L has appeared. It is probably not caused by the inaccuracy of the exponential model but by the methodological assumptions: the modelled curves were fitted under the condition that the observed and fitted values should be identical at the point of minimal discharge. This was done to increase the influence of base flow values on the recession parameter. The suitability of the model is proved by the significant correlation of all measured and modelled discharge values (with a great reserve at the level p = 0.001). The dependence on temperature variables has disappeared. The significant influence of the basin saturation was confirmed.

In order to use information from all independent variables for the explanation of the recession parameter variability, multiple regression could have been used. However, conclusions could be then affected by correlation between some of selected variables. Therefore, multivariate statistical methods, namely principal components analysis and factor analysis, were applied in further research. Using these methods, new variables - components or factors - are obtained by means of linear combinations of original variables. Components (factors) are independent of each other. By means of component or factor analysis, the number of variables is reduced and the structure in the relationships between variables is detected. The difference between these two methods is that in principal components analysis we assume that all variability of a variable should be used in the analysis, while in factor analysis we only use the variability in a variable which it has in common with the other variables.

Table 4 contains the percentage of total variability (variability of all variables) and recession parameter variability accounted for by seven and five extracted components (factors). More than 80 % of the total variability is explained in all analyses. In the explanation of the recession parameter variability there are differences between principal components analysis and factor analysis due to the different methodological assumptions. From the results of the factor analysis it follows that in the case of seven extracted factors 52 % of the recession parameter variability is explained, whereas in the case of five

extracted factors less than 30 % is explained. The variability of the recession parameter is therefore probably caused also by additional influences than the set of 14 variables investigated here.

Table 4: Percentage of total variability and recession parameter K variability explained by seven and five extracted components (factors). * Principal components analysis, ** Factor analysis.

Method	PCA*		FA**	
Number of components (factors)	7	5	7	5
Percentage of total variability (%)	93	86	89	82
Percentage of K variability (%)	89	64	52	27

Table 5: Component (factor) loadings of the recession parameter. * Principal components analysis, ** Factor analysis.

Method	PCA		FA	
Component (factor)	7	5	7	5
API and discharge (Q_o,AVG-Q, AQI)	-	**0.46**	-	-
API and discharge (Q_o, AQI-10)	**0.49**	-	**0.45**	**0.39**
Supplementary discharge (AVG-Q, AQI-30)	-0.03	-	0.05	0.18
Length of the recession curve L	**0.78**	**0.59**	**0.56**	-
Temperature (AVG-T, ATI)	-	0.18	-	0.19
ATI	0.04	-	0.07	-
AVG-T	0.10	-	0.04	-
Moisture (AVG-H, AHI)	0.08	-0.19	0.02	**-0.21**
AVG-P	-0.06	-0.13	-0.02	0.01

Component factor loadings of the recession parameter (equal to the correlation between components (factors) and the recession parameter) are shown in Table 5. In three from four analyses, the dominating components (factors) are those representing the saturation of the basin (antecendent precipitation index API), discharge variables and the duration of the recession (the two highest loadings are printed in bold font). The analysis for five extracted factors is difficult to interpret due to the low explanation of the recession parameter (27 %). The influence of the evapotranspiration on the recession parameter variability could be detected (but very weakly) only for the variant of five extracted components.

5 Conclusions

For the examination of possible causing factors of the recession curve time variability, 14 variables representing antecedent climate and runoff conditions, as well as conditions during the recession period, were selected. In addition to the variables relevant to the recession period, analyses were also performed using monthly values of the variables with the intention of detecting the potential influence of the evapotranspiration cycle.

The following are the main conclusions resulting from the correlation analysis:

- A significant effect of the evapotranspiration cycle can be substantiated for the master recession curves (recession curves averaged for a time step of one month). The intensity of basin depletion and average air temperature during the recession period are closely correlated in the summer season, when high air temperature is reflected in an accelerated depletion of water from the basin and thus a steep slope for the recession curve. The basin saturation represented by the index of antecendent conditions has a similar influence.
- For individual recession curves, the effect of the evapotranspiration cycle seems to be not significant, while a more important variable is the saturation of the basin.

However, the above conclusions could be affected by correlation between some of the selected variables. Therefore, multivariate statistical methods, namely principal components analysis and factor analysis, were applied in further research. From this research, the following was concluded:

- The analyses showed that the dominating factor is probably the saturation of the basin represented by the antecendent precipitation index.
- The depletion of water from the basin could also be affected by factors not included in the selected 14 variables.

Some results of the recession curve analysis concern also the environment of the experimental basin. Especially the behaviour of the weathering mantle in the winter season was confirmed by means of the recession curve analysis. The mantle gets frozen, disables infiltration and therefore the subsurface water storage is not replenished. Most discharge events in the winter season result from snowmelt. For the most part they are formed by the surface runoff. This is proved by the shape of the modelled monthly master recession curves in winter. They have high values of the recession constant which results in the steep shape of the curves. So these curves are not less steep than those in the summer which are influenced by evapotranspiration only.

The shallow position of the groundwater level in the basin was proved by the analyses. Only under this condition the monthly master recession curves could be affected by the evapotranspiration cycle because its influence could not be detected in the case of deeper groundwater level. Only a shallow groundwater level can contribute to the evaporation and plant transpiration.

The results of the recession curves analysis in the Černá Desná basin evoke also some general ideas concerning runoff and associated processes under different natural conditions. Reliability of possible generalisation of the conclusions made in the Černá Desná basin is of course relevant mainly to the representativeness of its physical and geographical characteristics. However, the following can be concluded from the analyses and the theoretical considerations made during the study:

- The research substantiated the fact that moisture conditions (expressed as antecendent precipitation index) affect significantly the intensity of depletion process. The dynamics of the depletion is therefore influenced by the type of the soil layer and the geological structure of the bedrock. In areas with deep groundwater circulation (e.g. in deep aquifers formed by Cretaceous sandstones), the depletion coefficient will probably be lower and less dependent on actual climate conditions. This coefficient is related to the mean detention time of water in the aquifer and it decreases with an increase in the detention time.
- The depletion coefficient increases probably also with an increase in the slope conditions in the basin as a result of more rapid depletion of the water storage in layers that are close to the land surface.

References

[1] Hall, F. R.: Base flow recessions - a review. Water Resour. Res., 4(5), 1968, 973–983.

[2] Singh, K. P. and Stall, J. B.: Derivation of base flow recession curves and parameters. Water Resour. Res., 7(2), 1971, 292–303.

[3] Tallaksen, L. M.: Analysis of time variability in recessions. IAHS Publ., 187, 1989, 85–96.

[4] Tallaksen, L. M.: A review of baseflow recession analysis. J. Hydrol., 165, 1995, 349–370.

[5] Toebes, C. and Strang, D. D.: On recession curves, 1 - Recession equations. J. Hydrol. NZ, 3(2), 1964, 2–14.

Ponded infiltration experiments in the Uhlířská catchment

P. Tachecí[1], M. Šanda[2]

[1]Dept. of Hydraulics and Hydrology, [2]Dept. of Drainage, Irrigation and Landscape Engineering, Faculty of Civil Engineering, Thákurova 7, CZ 16612 Praha 6, Czech Republic.

1 Introduction

In early 1980s, the Czech Hydrometeorological Institute (CHMI) established a network of experimental catchments in the Jizera mountains to assess the effect of massive deforestation due to air pollution. The most intensively investigated catchment is Uhlířská (Černá Nisa river). The total area of the catchment is 1.87 km^2 and its average altitude is 822 m a. s. l. Average annual precipitation is about 1230 mm (1961–1997), average discharge is 58 l/s (1982–1997) and average air temperature is 4.7°C (1961–1997). The climate is mild, mixed continental - oceanic, central European, with temperatures below 0°C and snow cover in winter months (November to March).

Subsurface flow clearly dominates the runoff forming process in this catchment (e.g. Šanda and Tachecí, 1997). A network of piezometers, neutron probe access tubes and nests of tensiometers at three sites (deforested and forested hillslopes, and valley bottom), was installed for subsurface flow observation (Císlerová et al., 1997; 1998; Šanda et al., 1997; Tachecí et al., 1998). The measurements presented here were performed as a part of research focused on the evaluation of soil hydraulic characteristics and description of the subsurface flow dynamics in the catchment.

2 Soil mapping

The Jizera mountains are part of the Krkonoše - Jizera mountains crystalline complex. The area of interest is situated in the middle of Variscan Krkonoše - Jizera mountains granite massif, which comprises granites and granodiorites (Chaloupský et al., 1989). The Uhlířská catchment is the source area of the Černá Nisa river. The valley is open to the south and has gentle convex - concave slopes. Typical length of the slopes is 450 m, the slope angle varies between 5 and 20 %. Van den Akker and van Haselen (1995) described this catchment as a typical gelifluction valley. A detailed soil survey of the catchment was conducted in 1997 and 1998, focusing on the valley bottom. The survey comprised 196 manually drilled soil profiles in 17 transects. Fig. 1 shows the map of the transects. Approximately 190 other drills were spread over the catchment.

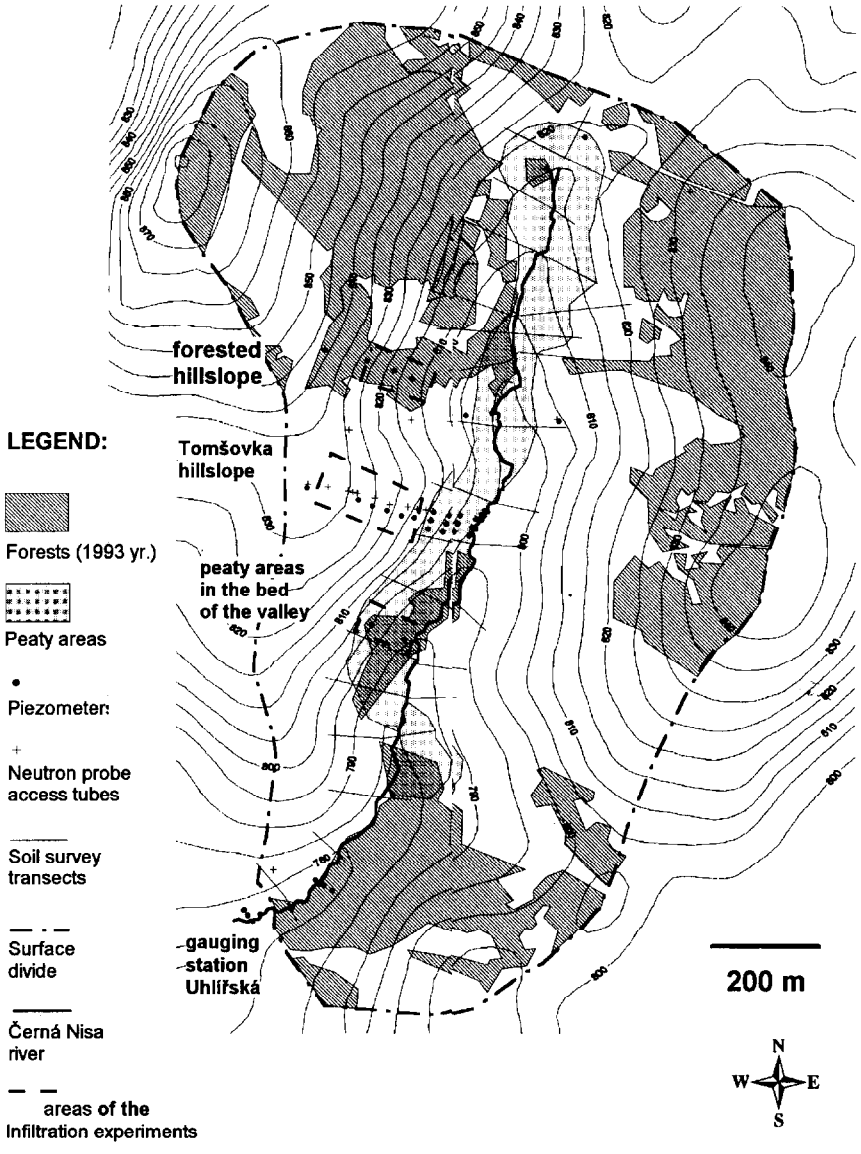

Figure 1: The map of the activities related to the observation of the subsurface flow at Uhlířská catchment.

Three main soil types were found in the catchment. The first, which covers slopes of the valley, is of average depth approximately between 60 and 90 cm, and is classified as a Dystric Cambisol with peaty topsoil (sandy loam). It consists of 5 cm of a humus (grass cover, *Calamagrostis villosa* prevails), a black - brown Ah horizon 20–25 cm thick, then 20–25 cm of brown Bv horizon and 20–50 cm of light brown (to greyish or yellowish) C horizon with increasing amount of solid particles. The bedrock consists of weathered and fractured granites. In the forest (*Picea abies* Karst. L.), 10–15 cm of litter can be found on the soil surface. A transition layer formed by a grey-black clayey loam up to 10 cm thick appears occasionally between the Ah and Bv horizons. A gleyed horizon was found at the forested hillslope. The thickness of the brown Bv horizon increases from 10 cm at the divide to 40 cm in the bed of the valley. Generally, a great amount of roots, old branches and other remains of trees occurs in the soil profiles (the consequences of clear-cutting). Also a high amount of boulders, bedrock particles and stones was detected in the profile. Decayed roots were found even in deep layers of the soil profile.

The second significant type of soil profile occupies mainly the valley bottom and is classified as Histosol. The topsoil is of a wet peaty character with humus (grass) or litter (forest) cover. The upper layer consists of 20–350 cm of dark (brown to black) recent peat, and the lower layer comprises grey or blue - grey clayey gravel. Gravel layers with low clay content or sandy layers often occur under this layer, but the granite bedrock was not reached. Van den Akker and van Haselen (1995) describe the alternation of sandy, gravelly and clayey layers in the valley bottom to the depth of 6 m. The peaty character of the soil profile can be found also on the slopes, especially in the confluent surroundings and local depressions. They are of local importance only. The peaty profile in the valley bottom covers approximately 10 % of the catchment area, its volume is estimated at about 240000 m^3. Fig. 1 shows its areal distribution.

The third type of soil profile has only a minor areal importance. It occurs near the river channel and consists of recent loamy sand and gravel depositions covered by grass. This profile type was found mainly in the lower part of the catchment, close to the Uhlířská stream gauging station. A set of 9 shallow drills in the vicinity of the Uhlířská gauging station was bored to investigate the stratification of the upper soil and rock layer formations. High resistance of deeper layers did not allow penetration of the boreholes to the bedrock. The surface of the impermeable bedrock has been estimated to be 5–20 m below the layer of very weathered and fractured granite. This depth was estimated on the basis of information provided by a combination of direct and geophysical measurements collected during the geological survey of the Bedřichov dam, situated 3 km to the south. The depth of the gradual transition zone between the weathered and non-weathered zone is highly variable (Geoindustria, 1989).

Table 1: The soil moisture conditions during the ponded infiltration experiments.

Site	Type of the soil profile	The 5-days antecedent precipitation index API_5 (mm)	The average soil moisture of top 50 cm soil layer ($cm^3.cm^{-3}$)
Deforested hillslope	Dystric Cambisol	0 - 4.9; 9.9 in one case	0.56
Forested hillslope	Dystric Cambisol	0–4.8	0.58
Valley bottom	Histosol	0–5.5	0.83

3 The ponded infiltration experiments

A set of ponded infiltration experiments was conducted to assess surface infiltration rates, one of the features controlling input of the water to the subsurface system. A single-ring method was used. The steel ring with diameter 37 cm was driven into the ground to a depth of 15 cm. One hour duration or 50 l of infiltrated water were used, in general, as a stopping rule for the experiment. The average of the last three values of steady state infiltration rate was used as the estimate of the soil saturated hydraulic conductivity of the topsoil. The experiments were performed during August to September of 1997 and 1998 under similar climatic and soil moisture conditions (after several rainless days) with the exception of three rainy days in August 1997. The soil moisture of the profile was measured during the field campaign in the nearest neutron probe access tubes (Fig. 1). The ponded infiltration experiments were conducted at three sites - at the forested and deforested hillslopes, and in the valley bottom (see Table 1).

The locations of these three sites are bounded by a dashed line in Fig. 1. The high occurrence of boulders, roots and remains of trees in soil profile does not allow location of ponded infiltration experiments on a regular grid. Therefore the locations of the infiltration experiments were nested into irregularly scattered groups, each containing about 13 experiments. Six groups of experiments were situated at the deforested hillslope, and two groups in the valley bottom. An additional two groups were located in the lower concave part and middle part of the forested hillslope.

4 Analysis of the results

The infiltration rates obtained formed three data sets, one for each experimental site. The data sets were statistically analysed. Table 2 presents a summary of the results. Mean values of the steady state infiltration rate were 1.7 10^{-4} m.s^{-1} for the deforested hillslope Tomšovka, 5.0 10^{-5} m.s^{-1} for the forested hillslope and 4.3 10^{-7} m.s^{-1} for the valley bottom. The coefficient of variation C_v is 126 % and 92 % at the hillslopes, and 66 % in the valley bottom.

Table 2: Measured steady state infiltration rates of ponded infiltration experiments (m.s^{-1}). H = Histosol, C = Cambisol.

Location of the experiment	Average	Standard deviation	Median	Coeff. of variation	No. of exper.
	The average values in the particular nests				
Valley bottom, central part, H	3.7 10^{-7}	2.1 10^{-7}	3.5 10^{-7}	0.56	15
Valley bottom, close to the river, H	4.8 10^{-7}	3.4 10^{-7}	3.3 10^{-7}	0.70	16
Forested hillslope, lower part, C	5.3 10^{-5}	5.5 10^{-5}	4.1 10^{-5}	1.05	15
Forested hillslope, middle part, C	4.7 10^{-5}	3.6 10^{-5}	3.2 10^{-5}	0.78	16
Deforested hillslope, upper part, C	1.4 10^{-4}	1.7 10^{-4}	8.0 10^{-5}	1.23	35
Deforested hillslope, middle part, C	1.6 10^{-4}	1.6 10^{-4}	9.4 10^{-5}	1.04	24
Deforested hillslope, lower part, C	2.5 10^{-4}	3.1 10^{-4}	1.3 10^{-4}	1.24	22
	Average values at three sites				
Bed of the valley, Histosol	**4.3 10^{-7}**	2.8 10^{-7}	3.3 10^{-7}	0.66	31
Forested hillslope, Cambisol	**5.0 10^{-5}**	4.6 10^{-5}	3.5 10^{-5}	0.92	31
Deforested hillslope, Cambisol	**1.7 10^{-4}**	2.1 10^{-4}	8.8 10^{-5}	1.26	81

To check the probability distribution of the steady state infiltration rates data set, the fractile diagram was plotted (Fig. 2). The shape of the diagram obtained is close to the straight line and indicates log-normal distribution for each of the three data sets. The logarithms of the steady state infiltration rates were tested for the goodness of fit to the normal distribution at 95 % significance level by the Kolmogorov-Smirnov test with the conclusion that the log-normal distribution fits well.

The data sets measured on both hillslopes were compared using hypothesis testing (two sample t-test). The mean values of the infiltration rate at the forested and deforested hillslopes differ at 95 % level of statistical significance. Nevertheless the difference is small from the point of view of subsurface flow processes. In contrast, the difference between the infiltration rates at the hillslopes and the valley bottom (more than two orders of magnitude) is significant.

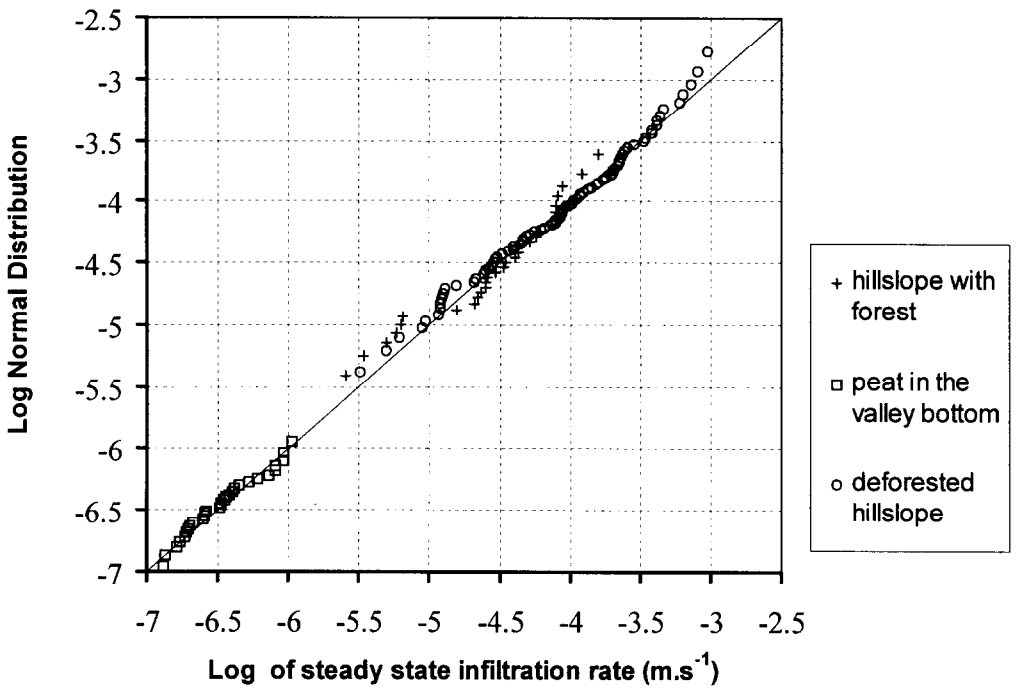

Figure 2: Fractile diagram of the steady state ponded infiltration rates. The logarithms of the measured steady state infiltration rates are plotted against the values of the log-normal distribution keeping the same exceedance probability.

Bubeníčková (1990) measured infiltration rates by the same method under comparable conditions at Černá Desná catchment, approximately 13 km from the Uhlířská catchment. Steady state infiltration rates of 36 experiments were analysed in three data sets, each containing 13 experiments. The average values of the steady state infiltration rate were $7.7\ 10^{-5}$ m.s^{-1} with C_v 133 % (new clearing), $9.9\ 10^{-5}$ m.s^{-1} with C_v 108 % (old clearing) and $6.7\ 10^{-5}$ m.s^{-1} with C_v 47 % (forest) respectively. The 5-day antecedent precipitation index (API_5 varied between 1.6 and 6.9 mm with one exception - the experiments situated in the forest were affected by higher daily precipitation total (26 mm). The soil moisture, determined from the undisturbed soil core samples, was about 0.53 cm^3.cm^{-3}. Both values at the clearings are slightly lower than our results, but the coefficient of variation shows a similar high value. The average steady state infiltration rates in the forest are slightly higher than those obtained in the Uhlířská catchment, but the coefficient of variance is only half of our value. The lower variance in this case may be explained by higher initial saturation of the soil profile.

The two data sets, originating from the experiments at forested and deforested hillslopes in the Uhlířská catchment, were further analysed. Firstly, the relationships of the steady infiltration rate to the type of the microrelief (hillock, plate, slope, pit), to the depth of the soil profile and its sub-type (colour, stains, appearance of weathered particles) were investigated by means of multiple linear regression. No significant relationship was found for any of the tested factors. The mean values of the steady state infiltration rate of individual nests were correlated with the distance from the divide. This relationship was statistically significant (at the 95 % level of significance). However the differences between particular mean infiltration rates were small. Considering the coefficient of variation within each group, the change of the mean infiltration rates downslope is insignificant.

Geostatistical methods were used to investigate the spatial variability of the steady state infiltration rates. The three data sets were established from infiltration rates measured at forested and deforested hillslopes (Table 3). The semivariograms and the autocorrelograms were calculated for the data sets listed in Table 3. No spatial dependence was found (Fig. 3).

Table 3: Summary of the steady state infiltration rates used for the geostatistical analysis.

The location of ponded infiltration experiments	The number of the experiments included	The covered area
central part of the deforested hillslope	21	25x35 m
central part of the deforested hillslope	47	45x35 m
central and lower part of the forested hillslope	30	70x100 m

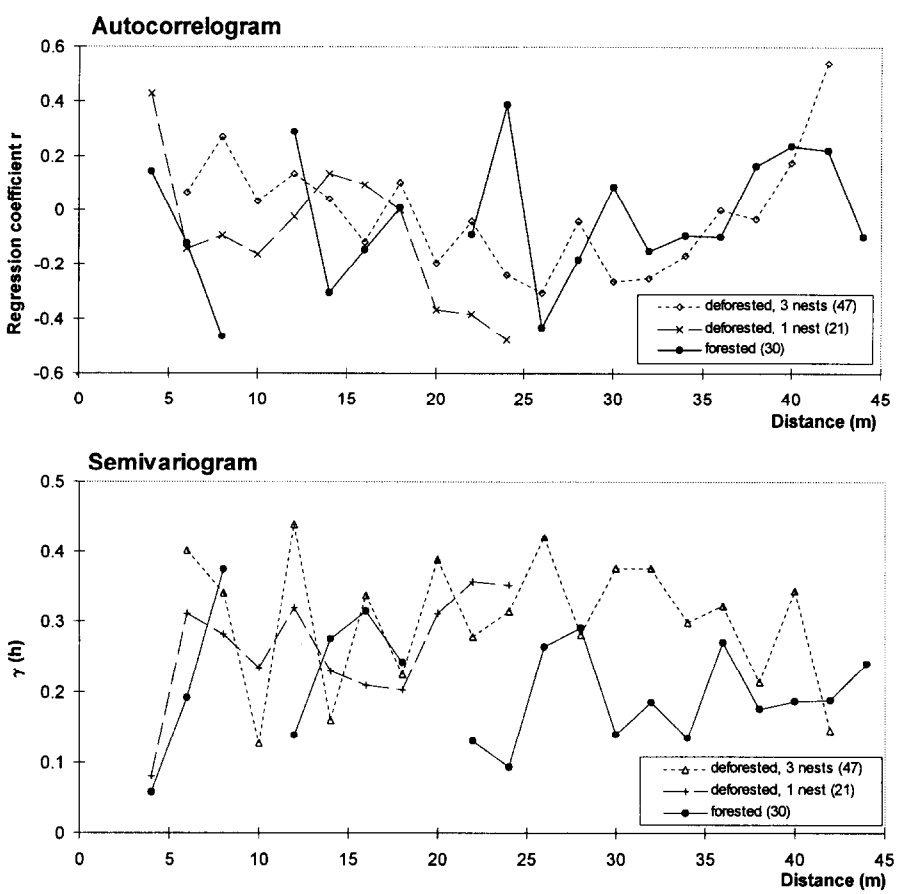

Figure 3: Autocorrelogram and semivariogram of logarithms of steady state infiltration rates. The ponded infiltration experiments, Uhlířská catchment, deforested hillslope (Tomšovka) and forested hillslope. The number in brackets indicates the number of experiments included.

5 Conclusions

The hillslopes and the valley bottom areas can be distinguished as two parts of the catchment area with different soil types and hydraulic properties of the top layer of soil (steady state infiltration rate). While values of the infiltration rate about $1x10^{-4}$ $m.s^{-1}$ (hillslope, cambisol) indicate that there is no barrier for rainfall infiltration in the top 30 cm of sloping profiles, in case of peaty areas (steady state infiltration rate $4x10^{-7}$ $m.s^{-1}$) in the valley bottom only a very small amount of water can infiltrate. In comparison with the highest observed rainfall intensity (1996–1998) 13.1 $mm.h^{-1}$, the value of the infiltration rate at the hillslopes is one order of magnitude higher (360 $mm.h^{-1}$), while in the peaty areas it is one order of magnitude lower (1.4 $mm.h^{-1}$). This fact explains the differences in the flow type observed: (1) at the hillslopes, surface overland flow rarely occurs and the wet areas are evenly connected with the poorly weathered bedrock bassets or with the topographic concavities covered by the thin soil layer. The infiltration capacity of the surface soil layer is not exceeded in the most of cases; (2) the peaty areas in the valley bottom (10 % of catchment area) act as practically impermeable areas with the minimal infiltration capacity, producing quick surface runoff, mostly concentrated in the old ditches. In the wet areas frequent surface ponding appears in the peaty areas situated close to the foot of slopes. It is evident, that the Hortonian flow concept, the basic assumption of the great number of the lumped models, is inappropriate in the case of hillslopes. Saturated subsurface runoff or vertical percolation to the deeper layers, with probable preferential flow contribution, can be expected because of the hydraulic properties of the Bv and C horizons. In the case of peaty soil profiles, decrease of the ponding infiltration velocity during the infiltration experiment was very sudden, just after the depression storage filled. With the exception of low rainfall intensities, peaty areas can be considered as impermeable from the very beginning of the rainfall.

The difference in the infiltration rates between the forested and the deforested hillslopes is small. This result does not support the widespread assumption of a decrease in infiltration capacity after clear cutting.

Generally, a high variability of steady state infiltration rate was found at the three sites across the Uhlířská catchment. The high values of the coefficient of variation of the steady state infiltration rates at the deforested and forested hillslopes are probably the result of preferential flow in the soil profiles. Higher values for deforested hillslopes may be the result of the clear - cutting practices (irregular compaction and/or disturbance of the soil cover). No spatial dependency between the measured values was found.

This analysis adds information about surface characteristics to the measured characteristics of the deeper soil layers (Císlerová et al., 1997;1998) and the observed subsurface flow dynamics (Císlerová et al., 1997; 1998; Šanda et al., 1997; Tachecí et al.,1998).

Acknowledgements

This research has been supported by CTU grants No. 3098K1432 and 3098K1412 and CTU FCE grants No. 3097K1412 and No. 2028K1430. This study was also supported by Water Research Institute as a part of the research project No. VaV/510/3/96 "Ecological aspects of protection of water richness". Dr. M. Císlerová and Dr. Š. Blažková are kindly acknowledged for their overall help.

References

[1] Bubeníčková, L. (1990) 'Infiltrační pokusy na Černé Desné, dílčí zpráva úkolu Sledování antropogenních vlivů na odtokový režim, DÚ 02 (Infiltration experiments at Černá Desná catchment)' (in Czech), project report ČHMÚ Praha

[2] Císlerová, M.; Šanda, M.; Blažková, Š.; Mazáč, O.; Grünwald, A.; Zeithammerová, J. and Tachecí, P. (1997) 'Monitorování procesů proudění vody v půdním profilu na experimetální ploše svahu v povodí Uhlířská, (The monitoring of the subsurface flow processes at the experimental hillslope at Uhlířská catchment)', (in Czech), project report VaV/510/3/96, DÚ 01, part 8,VÚV, ČVUT, Praha

[3] Císlerová, M.; Šanda, M.; Vogel, T.; Tachecí, P.; Grünwald, A.; Zeithammerová, J.; Stodolovská, A., Votrubová, J.; Kundratová, J. and Picek, T. (1998) 'Výzkum transportních procesů v povodí dotčeném náhlými změnami odtokových poměrů - Jizerské hory (The research of the transport processes at the catchment affected by the rainfall-runoff relationship change)', (in Czech), project report VaV/510/3/96, DÚ 01, VÚV, ČVUT, Praha

[4] Chaloupský, J. (1989) 'Geologie Krkonoš a Jizerských Hor (Geology of the Krokonoše and Jizera mountains)' (in Czech), ÚÚG Praha

[5] Geoindustria (1989) 'Inženýrsko-geologický průzkum VD Bedřichov (The geological survey of the Bedřichov dam)', (in Czech), project report, Geoindustria Praha

[6] Šanda, M.; Kulasová, A.; Hancvencl, R.; Bubeníčková, L.; Císlerová, M.; Tachecí, P. and Blažková, Š. (1997) 'Měření půdní vlhkosti neutronovou metodou a experimentální pozorování nasycených ploch v povodí Uhlířská (The soil moisture measurement by means of neutron moisture probe at Uhlířská catchment)' (in Czech), project report VaV/510/3/96, DÚ 01, part 2, VÚV, ČVUT, Praha

[7] Šanda, M. and Tachecí, P. (1997) 'Měření půdních vlhkostí a infiltračních rychlostí v povodí Uhlířská (The soil moisture measurement and ponded infiltration experiments at Uhlířská catchment)', (in Czech), proc. of workshop The hydrologic balance and the possibilities of retention increase in small catchments, ČZU Praha, 1997

[8] Tachecí, P.; Kulasová, A.; Šanda, M. and Hancvencl, R. (1998) 'Měření půdních vlhkostí neutronovou sondou v povodí Uhlířská (The soil moisture measurement by means of neutron moisture probe at Uhlířská catchment)' (in Czech), project report VaV/510/3/96, DÚ 01, VÚV, ČVUT, ČHMÚ Praha

[9] van den Akker, M. F. A. and van Haselen, C. O. G. (1995) 'Hydrogeological reconnaissance of the Jizera Mountains', project report WAU Wageningen, and ČHMÚ Praha

Simulation and verification of evapotranspiration and rainfall - runoff processes

in the Liz (Czech Republic) and Gallina (Italy) experimental basins

M. Tesař[1], J. Buchtele[1], M. Šír[1], F. Di Nunzio[2]

[1]Institute of Hydrodynamics, Academy of Sciences of the Czech Republic, Experimental Basis Nový Dvůr 31, CZ 384 73 Stachy, Czech Republic. [2]National Research Council of Italy, CNR - IRPI, Strada delle Cacce, 73 - 10135 Torino, Italy.

Abstract

The article describes the instrumented experimental basins Liz in the Šumava Mts. (Czech Republic) and Gallina (Italian Alps). Its objectives are: (1) to present the examples of rainfall-runoff monitoring; (2) to estimate the amount of evapotranspiration during the vegetation season using: (i) an energy balance method, (ii) a hydropedological method and (iii) the BROOK90 model; and (3) to simulate the rainfall-runoff process with the use of two models (Sacramento Soil Moisture Accounting model and BROOK90).

1 Introduction

Much of our basic knowledge on hydrological processes has come from studies in research basins. These well-instrumented basins have also produced much very suitable data for hydrological investigations on water resources management studies. The two research basins presented here were set up as representative basins for investigation of the hydrological cycle, with the general aim of extrapolating the results in time and space. The relationship between the environmental model and an instrumented basin is characterized by the process of simplification, an important factor for successful extrapolation of the simulation results to other areas.

2 Study catchments

Two catchments were selected for detailed study: the Liz watershed in SW Bohemia (Czech Republic) and the Gallina watershed in NW Alps (Italy). Both catchments have

hydrological and hydrometeorological data, including rainfall and flows, dating back to the mid-1970s (Liz) and to the early-1980s (Gallina).

The Liz catchment is situated in central part of the Šumava Mts. (Pražák et al., 1994). This mountainous basin lies near the borders of the Czech Republic, Germany and Austria. The vegetation cover is mixed forest with an average age of about 84 years. The main species is spruce (88 %) with additional fir, larch, beech, pine, etc. In the early 1980s about 6 % of the drainage area was harvested but this influence is negligible now.

Table 1: Characteristics of the Gallina (Italy) and Liz (Czech Republic) basins.

Characteristic of the basin	Units	Gallina			Liz		
Drainage area	(km^2)	1.083			0.989		
Mean discharge	($m^3.s^{-1}$)	0.02 (1982–1997)			0.01 (1976–1997)		
Runoff coefficient	(-)	0.60 (1982–1997)			0.38 (1976–1997)		
Mean annual air temperature	(°C)	11.0 (1982–1997)			6.30 (1976–1997)		
Lithology		Rhyolites			Paragneiss		
Vegetation cover	(%)	77			100		
Average slope	(%)	49			17		
Basin length	(km)	1.35			1.45		
Channels length	(km)	1.57			1.43		
		Min.	Mean	Max.	Min.	Mean	Max.
Precipitation total	($mm.y^{-1}$)	938.8	1258.0	1717.0	664.7	850.7	1142.0
		1990	1982–97	1984	1985	1976–97	1995
Runoff depth	($mm.y^{-1}$)	519.0	768.0	1128.0	238.9	324.2	483.7
		1990	1982–97	1996	1984	1976–97	1996
Elevation	(m a. s. l.)	330.0	417.0	522.0	828.0	941.5	1074.0

The Gallina watershed is located in the north-western region of Italian Alps, in a piedmont environment connecting the mountains to the high Po plain (Caroni et al., 1986). The geology of the catchment is rhyolite rocks, and the vegetation is trees and shrubs forming a dense cover with some bare areas along the divides. The prevailing species is chestnut (*castanea nativa*) with an average age of about 100 years. Human influence is practically absent. Summary characteristics of the two catchments are given in Table 1.

3 Methodology

Data sets from the two well instrumented experimental basins were used to monitor and analyse the rainfall-runoff process in as much detail as possible.

The percolation of soil water to strata underlying the root zone, water storage of the individual soil layers and the uptake of water from the soil to the atmosphere (actual evapotranspiration) were estimated with the aid of the hydropedological balance method from time series of tensiometric measurements made at 2-day intervals and from precipitation totals per day. Retention curves were used in the recalculation of tensiometric data as data on soil moisture, and thus also on the volume of soil water. The retention curves of individual genetic soil horizons were obtained by the inverse solution of Richards' equation (Šír et al., 1988). The structure of the soil profile and the depth of the root zone were established with the aid of profile pits. By balancing and the volumes of water present in the root zone of the soil profile at 2-days intervals, the withdrawal of water from the root

zone, designated 'loss' L, was obtained. The analysis of tensiometric and precipitation data revealed that during the balance period several episodes occurred in which precipitation in combination with the actual soil moisture caused the outflow of soil water to the strata underlying the root zone (Šír et al., 1996). The volume of water thus drained away is termed 'output' O. The amount of water taken up for transpiration was obtained using Eq. (1) assuming that in the given experimental areas no surface runoff occurred.

$$T = L - O \tag{1}$$

where T - transpiration, L - withdrawal of water from the root zone, O - outflow of soil water to the strata underlying the root zone.

The estimation of potential evapotranspiration PET from the vegetation cover during the growing season was evaluated as the water requirement for cooling (Pražák et al., 1994; 1996). The calculation uses hourly values of air temperature and of global radiation totals. Properties of the vegetation cover are expressed in terms of two phenomenological constants, i.e. the effective absorptivity and the effective thickness of leaves (or needles). Both above-mentioned constants were obtained by calibration.

Table 2: Results of the evapotranspiration calculations using the hydropedological and energy balance methods and BROOK model for the Liz basin. Notes: O - output of water below the root zone, T - transpiration calculated as a withdrawal of water by roots, PET - transpiration calculated as a need of water for cooling the plants, ET - total evapotranspiration (transpiration, evaporation and interception) and Tr - transpiration.

Year	Observat. Period of the time	Rainfall total (mm)	Hydropedol. method O (mm)	Hydropedol. method T (mm)	Energy b. PET (mm)	BROOK ET (mm)	BROOK Tr (mm)
1985	16.5.–30.9.	375.0	178.0	236.0	229.0	338.7	230.5
1986	16.5.–30.9.	351.0	173.0	222.0	227.0	313.5	213.3
1987	16.5.–30.9.	377.0	285.0	197.0	176.0	323.9	198.4
1988	1.6.–30.9.	326.0	164.0	184.0	195.0	282.7	189.9
1989	16.6.–30.9.	400.0	243.0	148.0	148.0		

Long-term data were used for simulations of the rainfall-runoff process. Two deterministic models were used: the physically based BROOK model (Federer, 1993); and the conceptual model SACRAMENTO Soil Moisture Accounting (SAC-SMA) model (Burnash et al., 1973; Buchtele, 1993). Attempts were made to prepare the appraisals of evapotranspiration and transpiration using both BROOK (ET and Tr) and SAC-SMA models, and to compare these outputs with values ascertained by methods mentioned above.

4 Results and discussion

Analyses presented here are based on discharge observations at 5 minute intervals for the Gallina and at 10 minute intervals for the Liz (Fig. 1 and Fig. 2). From these observations it can be seen that daily cycles in the natural flows appear during drought periods. Several reasons could be considered for that: evapotranspiration, global radiation, air temperature, air pressure, etc., if the thermal dependence of the runoff sensor can be neglected.

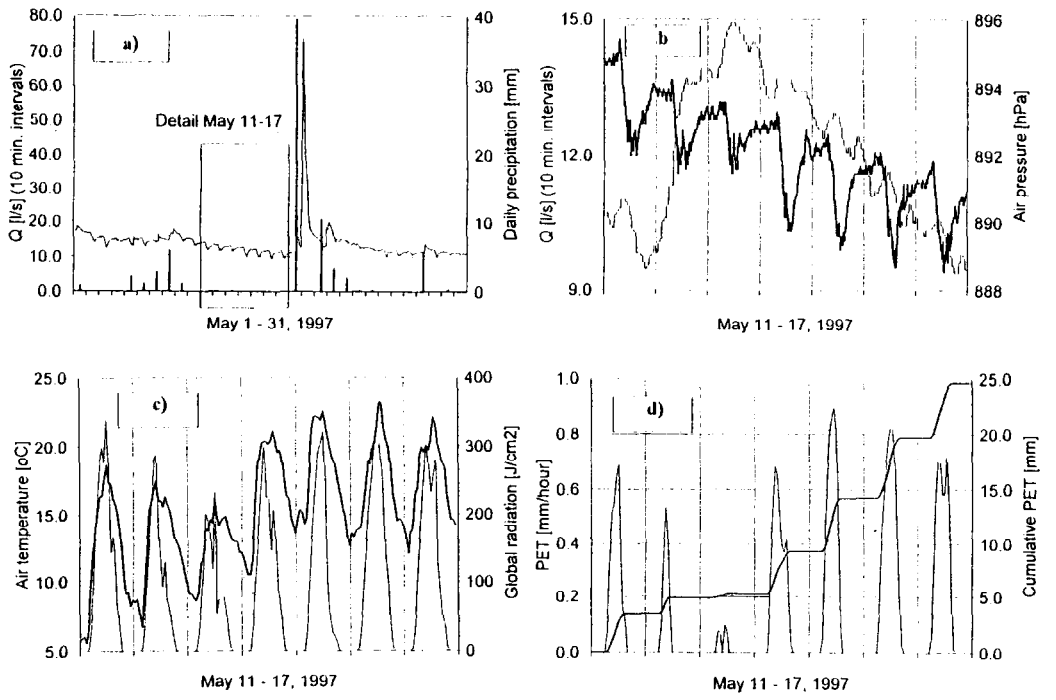

Figure 1: Variation of hydrological and hydrometeorological data in the Liz basin - May 1997; (a) 10 min. variation of observed discharges in relation with causual precipitation; (b) 10 min. variation of observed discharges in relation with air pressure; (c) variation of the hourly means of the air temperature and hourly sums of the global radiation totals; (d) PET calculated as a need of water for cooling plants.

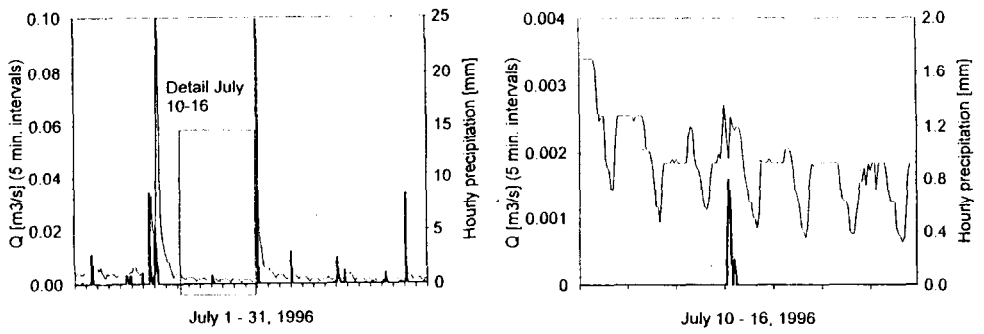

Figure 2: Five-minute interval variation of observed discharges in relation with causual precipitation in the Gallina basin - July 1996.

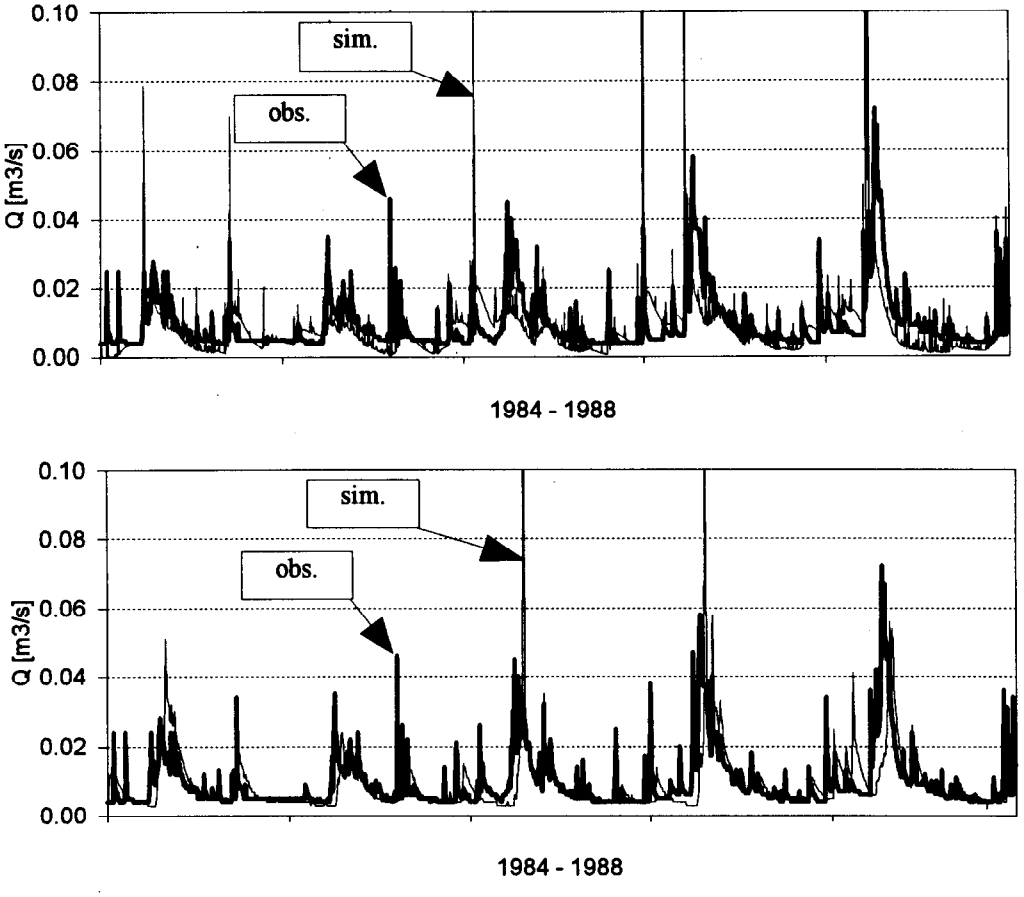

Figure 3: Daily observed discharges compared with simulations by the BROOK model (upper part) and the SAC-SMA model (bottom part) in the Liz basin in the course of 1984–1988.

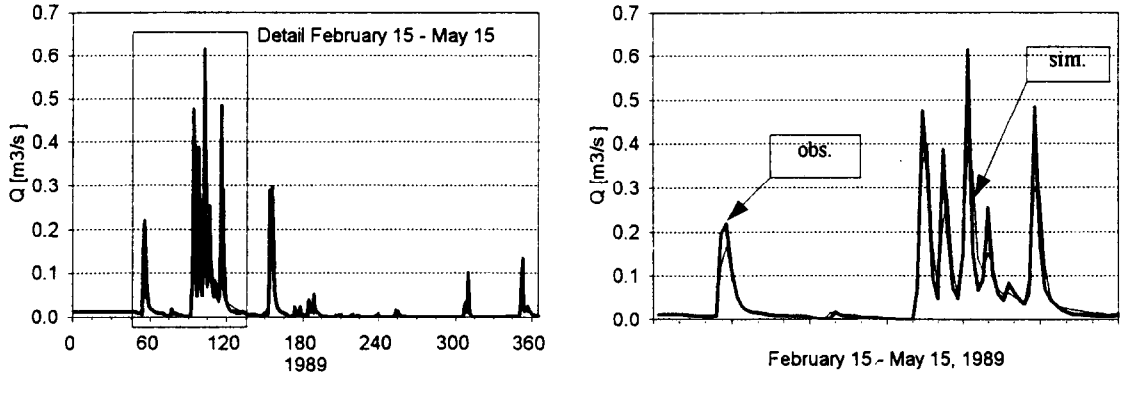

Figure 4: Daily observed discharges compared with simulations by the SAC-SMA model in the Gallina basin in the course of 1989 and detailed depiction for the spring season (right side).

A hydropedological method based on the water tensiometers measurements (Kutílek and Nielsen, 1994) and an energy balance method (Pražák et al., 1994, 1996) were used to estimated the evapotranspiration during the growing season. The results for summer periods are compared with the amounts obtained by the BROOK model in Table 2.

The results of simulations using the Sacramento SAC-SMA and BROOK models for the Liz basin are shown in Fig. 3. Results from the SAC-SMA model for the Gallina basin are shown in Fig. 4. These simulations fit quite well the natural outflows measured in both experimental watersheds.

5 Conclusions

The following conclusion can be drawn:

- detailed observations and measurement of the natural flow during drought periods indicates the sensitivity of runoff to evapotranspiration;
- the hydropedological-balance method and the energy-balance method were applied for the forested catchment Liz over the period 1985–1989 with good results - differences between ET and T do not exceed 5 % of the seasonal precipitation totals;
- the physically based BROOK model was used to estimate the daily values of the total evapotranspiration and transpiration for the Liz basin from 1985–1988 - the results are in a good harmony compared to the above mentioned methods;
- in order to simulate natural flows the Sacramento SAC-SMA and BROOK models both for Gallina and Liz basins were used - the simulations fit quite well the observations of the natural flow, and both models can be used as an effective tools enabling us to study the physical rules of outflow from natural watersheds.

Acknowledgements

The authors acknowledge the support of Grant Agency of the Czech Republic (Grant N° 526/98/0805) and Grant Agency of the Academy of Sciences (Grant N° A3060701). Research was also partly carried out in the framework of the Agreement for scientific cooperation between the National Research Council of Italy and Academy of Sciences of the Czech Republic.

References

[1] Buchtele, J.: Runoff changes simulated using a rainfall-runoff model. Wat. Resour. Manage. 7(8), 1993, 273–287.

[2] Burnash, R. J. C.: The NWS River Forecast System - Catchment modeling. In: Singh, V. P. (ed.) Computer Models of Watershed Hydrology. Water Resources Publications, ISBN N° 0-918334-91-8, 1995.

[3] Caroni, E., Rosso, R., Siccardi, F.: Nonlinearity and time-variance of the hydrologic response of a small mountain creek. V. K. Gupta et al. (eds.), Scale Problem in Hydrology, D. Reidel Publishing Company, 1986, 19–37.

[4] Federer, C. A.: BROOK 90 - A Simulation Model for Evapotranspiration. Soil Water and Streamflow. USDA Forest Service, Durham, New Hampshire, USA, 1993.

[5] Kutílek, M., Nielsen, D.: Soil hydrology. Catena Verlag, Cremlingen, 1994.

[6] Pražák, J., Šír, M., Tesař, M.: Estimation of plant transpiration from meteorological data under conditions of sufficient soil moisture. J. of Hydrol., 162, 1994, 409–427.

[7] Pražák, J., Šír, M., Tesař, M.: Parameters determining plant transpiration under conditions of sufficient soil moisture. J. of Hydrol., 183, 1996, 425–431.

[8] Šír, M., Kubík, F., Tesař, M., Pražák, J.: Liquid transport in porous media - discontinuous phenomena. Part I: Theory. J. Hydrol. Hydromech., 44, 1996, 81–90.
[9] Šír, M., Kubík, F., Tesař, M., Pražák, J.: Liquid transport in porous media - discontinuous phenomena. Part II: Examples. J. Hydrol. and Hydromech., 44, 1996, 235–251.
[10] Šír, M., Kutílek, M., Kuráž, V., Krejča, M., Kubík, F.: Field estimation of the soil hydraulic characteristics. Soil Technol., 1, 1988, 63–75.

Long-term cloud and fog water deposition monitoring in southern Czech Republic

M. Tesař[1], M. Šír[1], D. Fottová[2]

[1]Institute of Hydrodynamics, Academy of Sciences of the Czech Republic, Experimental Basis Nový Dvůr 31, CZ 384 73 Stachy, Czech Republic. [2]Czech Geological Survey, Klárov 3/131, CZ 118 21 Praha 1, Czech Republic.

Abstract

The objectives of this article are to: (1) present the results of statistical analysis of the occurrence and duration of individual types of occult precipitation (the so-called climatological normals are presented); (2) estimate the amount of fog and cloud water deposition; (3) characterize the chemical composition of fog and cloud water on the basis of long-term monitoring (1989–1997) in the Šumava Mts.; and (4) determine if site-to-site differences exist. Forests of the mountainous regions of the Czech Republic can be subject to relatively significant deposition of water and chemicals via cloud droplet impaction. This deposition has been estimated using a micrometeorological mathematical resistance model. Water inputs from fogs and clouds are about 8 percent of the total precipitation (mean for the compared time periods), and chemical inputs range from 25 to 130 percent of the amounts in bulk precipitation measured above the canopy in open areas. A wide range of concentrations were encountered, exceeding concentrations occurring in rain by a factor ranging from 3 to 18 (comparing median values of the fog and cloud water and weighted means of the bulk precipitation). Estimated wet deposition for NH_4^+, NO_3^- and SO_4^{2-} via fog and cloud droplets impaction and sedimentation represents 870, 1767 and 2109 kg km^{-2} year^{-1}, respectively (i.e. 129, 77 and 79 % with respect to weighted means of amounts in precipitation).

1 Introduction

It has been shown that occult precipitation can be an important delivery mechanism for water and pollutants in high elevation ecosystems. According to Brechtel (1990) and Eliáš et al. (1995), occult precipitation can be divided into deposited (dew, hoar frost) and collected (fog, cloud-water, rime) precipitation. Deposited occult precipitation condenses or sublimates directly onto plant surfaces and other acceptors. Collected occult precipitation is condensed in the atmosphere in liquid or solid form and transported by

air movement to surfaces. The deposition of water and chemicals to vegetation from wind-driven clouds and fogs has long been recognized as an important hydrological input not only in many mountainous and coastal environments (Lovett et al., 1982) but also in urban areas (Brewer et al., 1983). Since the concentration of chemical species is several times higher in cloud water than in precipitation, the chemical deposition associated with cloud and fog droplet interception by vegetation can be significant, or even predominant, with respect to deposition due to precipitation (Vong et al., 1991).

2 Sites description

The chemical and hydrological significance of occult precipitation has been studied in the higher elevation zones of the Šumava Mts. (Southern Bohemia, Czech Republic). These zones, especially above an elevation of 1000 m above sea level, are characterized by high wind speeds, lengthy periods of cloud and fog immersion, and coniferous vegetation, all of which contribute to high potential rates of cloud droplet capture. According to our statistical analysis and literature references (Strnad et al., 1988) the forest canopy in this region can be in low cloud or fog for 15 % of time. The sampling site for monitoring occult precipitation is located at an elevation of 1123 m a. s. l. on the hilltop Churáňov (13°36'56"E, 49°04'08"N) while the experimental site for the sampling of bulk precipitation was at an elevation of 837 m a. s. l. in the Liz experimental watershed (13°40'56"E, 49°04'14"N). These localities have been described in detail by Pražák et al. (1994). In order to determine if there are site-to-site differences in the chemical composition of fog water samples (Ogren and Rodhe, 1986) two further localities were chosen and equipped with instruments. The first locality (Šumava Mts.) represents the cleanest part of the Czech Republic while the second one (Krušné hory Mts.) is in a heavily polluted region. The third measuring site was in Prague (the capital of the Czech Republic) in order to estimate the influence of the occult precipitation on the water balance and chemistry in cities. The sampling site and precipitation network in the Krušné hory Mts. is located in the vicinity of Rudolice at an elevation of about 900 m a. s. l. The experimental location in Prague was the Libuš meteorological station at an elevation of about 300 m a. s. l.

3 Methodology

Statistical analysis of the individual types of the occult precipitation was undertaken and so-called climatological normals were obtained for the 1961–1990 time period.

A resistance model of the deposition of cloud droplets to a spruce forest canopy (Lovett, 1984) was tested. This model has two submodels, the first simulating a turbulent diffusion of cloud droplets into the forest and their deposition onto foliar and branch surfaces, and the second simulating the evaporation/condensation process under cloud-immersion conditions in the forest. Both the cloud deposition model and the evaporation/condensation model have been described (Lovett et al., 1982; Lovett, 1984; Lovett, 1988). Although these models depend on the estimation of a number of parameters whose accurate measurement is difficult (the leaf-area index, the droplet-size distribution and the cloud-liquid-water content), it represents a very instructive tool enabling us to estimate both gross and net deposition (total cloud-water deposition minus total evaporation) and examine their reactions to changes in meteorological and canopy-structure parameters. For calculating the ion deposition via cloud water a direct estimate of gross water input is needed, and that is why we have applied the above-mentioned model. Some canopy structure parameters are described in the literature (Thorne et al., 1982; Lovett and Reiners, 1986).

In order to estimate the cloud-liquid-water content LWC and to gain cloud water samples, a sample-taking device was constructed. The so-called active CWP collectors as described in literature (Daube et al., 1987) were installed in the Šumava Mts. on the hilltop Churáňov, in the Krušné hory Mts. in the vicinity of Rudolice village and in Prague at Libuš station. For this design, a propeller-type automobile cooling fan was chosen as a means of facilitating collection. Collectors of this type have been used during relatively extensive fog research in the U. S. A. (Weathers et al., 1988). The CWP active cloud-water collectors are constructed of chemically inert materials; the inlet is located on the bottom of the collector to avoid the collection of rain-water. The fan draws fog into a ventral inlet and through a bank of nylon strands. A strand diameter of 0.78 mm was selected. Satisfactory velocity through the strands, which is required for efficient collection, was achieved by reducing the internal cross-sectional area of the collector with a venturi. The distribution of the velocity of air through the cartridge was measured under laboratory conditions. The collector was operated manually, i.e. the instrument was switched on at the start of a fog event and switched off after its end. The air-flow rate of the fan through the strand area lasted from a few hours to a few days depending on the duration of the fog events. The collected volume of sampled water was from a few centilitres to approximately two litres - depending on the duration of the fog events and their cloud liquid water content LWC.

Samples collected were stored in 500 or 1000 ml polyethylene bottles at 4°C in the dark. Prior to use, storage bottles were washed with 6N HCl, followed by several distilled water rinses. The following chemical analytical methods were used: pH of the samples was measured with a Radiometer CG-2401C electrode; fluoride was determined by ion selective electrode; chloride, nitrate and sulphate by non-suppressed single column ion chromatography; ammonia spectrophotometrically; and metals by flame AAS.

Table 1: Climatological normals of the occurrence and duration of the individual types of occults precipitation in the Šumava Mts. (1961–1990). Intensity 0: small (for fog: visibility 500–1000 m), intensity 1: moderate (for fog: visibility 200–500 m), intensity 2: heavy (for fog: visibility 50–200 m), intensity 3: very heavy (for fog: visibility less than 50 m).

Type of occult precipitation	Number of days with the individual event	Duration of individual phenomenon (hour)				
		Intensity 0	Intensity 1	Intensity 2	Intensity 3	Total
Fogs and low clouds	147	122	223	585	314	1245
Rime	32	309	142	89	0	539
Dew and frozen dew	104	273	356	125	0	755
Hoar frost	44	180	122	45	0	348

4 Results and discussion

The results of model predictions of gross cloud droplet deposition, net cloud droplet deposition (gross cloud droplet deposition minus evaporation during the fog event) and simulated cloud water deposition velocity (gross flux divided by the liquid water content) are 0.505 10^{-3} g m^{-2} min^{-1}, 0.175 10^{-1} cm $hour^{-1}$ and 20.9 cm s^{-1}, respectively. Because of evaporation and condensation in the forest canopy the amount of water that

drips to the ground is frequently different than the actual cloud water deposition. For this reason the above-defined net cloud droplet deposition represents only a part of gross cloud droplet deposition (58 % in our case). Model predictions were made for canopy structure parameters and for annual mean meteorological conditions during cloud and fog events typical for the Šumava Mts. region, with wind speed 3.2 m sec^{-1}, relative humidity 96 %, cloud-water content 0.4 g m^{-3}, mean droplet diameter 10 μm, net radiation 0.071 cal cm^{-2} min^{-2} and air temperature -0.2°C. Data sets describing the occurrence and duration of the individual kinds of the horizontal events (i.e. fog, rime, hoar frost, dew and frozen dew) were analyzed in full detail and so-called climatological normals for the time period 1961–1990 were obtained (Table 1).

Table 2: Fog water chemistry (Churáňov station 1989–1997) and bulk precipitation chemistry (Liz station 1994–1997) in the Šumava Mts.

Ion	Units	Fog and low cloud water chemistry (samples collected at Churáňov station 1989–1997)				Bulk precipitation chemistry in the open air area (Liz station hydrological years 1994–1997)			
		Num. of samples	Min. value	Max. value	Median value	Num. of samples	Min. value	max. value	Weight. mean
pH	(-)	123	2.94	7.10	3.98	47	3.60	6.65	4.57
H^+	(μg/l)	123	0.00	115.80	104.71	47	0.22	251.19	38.60
Cond.	(mS/cm)	122	3.48	854.0	0178.00	47	6.30	209.00	25.74
Na^+	(mg/l)	120	0.01	5.17	0.49	47	0.04	0.65	0.17
K^+	(mg/l)	120	0.00	7.91	0.52	47	0.01	1.04	0.17
NH_4^+	(mg/l)	121	0.00	50.80	10.74	47	0.01	9.10	0.70
Mg^{2+}	(mg/l)	120	0.00	2.86	0.23	47	0.01	0.34	0.06
Ca^{2+}	(mg/l)	120	0.01	33.35	1.67	47	0.01	2.35	0.29
Mn^{2+}	(μg/l)	104	0.20	1270.00	36.45	47	2.00	57.00	8.80
Zn^{2+}	(μg/l)	62	35.00	30000.0	253.00	47	5.00	81.00	20.33
Fe^{2+}	(mg/l)	62	0.04	1.78	0.25	47	0.00	0.26	0.03
Al^{3+}	(mg/l)	62	0.04	1.41	0.31	37	0.00	0.18	0.04
F^-	(mg/l)	106	0.00	0.70	0.13	47	0.01	0.20	0.02
Cl^-	(mg/l)	119	0.00	10.30	1.84	47	0.07	1.30	0.30
NO_3^-	(mg/l)	122	0.32	134.00	21.82	47	0.15	26.10	2.39
SO_4^{2-}	(mg/l)	122	0.31	132.00	26.04	47	0.54	27.73	2.76
Pb	(μg/l)	42	12.40	525.00	56.45	24	0.20	19.50	3.43
Cd	(μg/l)	42	0.05	68.00	1.48	24	0.02	12.80	0.63
Ni	(μg/l)	42	1.00	230.00	7.00	24	0.25	3.00	0.68

If we take into account this information and assume that the spruce forests in the Šumava Mts. are immersed in clouds and fogs for 314 hours $year^{-1}$ on average (only very heavy intensity), and that for 89 hours $year^{-1}$ rime-ice accretion reduces the deposition rate by 50 % according to Lovett et al. (1982), then our estimated annual gross deposition of cloud-water is 81 mm $year^{-1}$ (8 %"of the annual vertical precipitation total), while the net deposition is 47 mm $year^{-1}$. The data presented above represent the average data describing the foggy time period under the examination. These estimates are admittedly crude, but they are the best estimates available. On the basis of these calculations the estimates of cloud water deposition in the Krušné hory Mts. and in Prague were made

taking into account the climatological studies for these regions. In the case of Prague this estimate is probably overestimated due to its low altitude.

During the period from 1989 to 1997 123 samples of fog water were collected at Churáňov station. Analytical results are summarized in Table 2 together with data on bulk precipitation chemistry (hydrological years 1994–1997). These concentrations have not been weighted for sample volume. A direct comparison of medians with precipitation-weighted means for rain given in the Table 2 has no exact quantitative significance. Nevertheless, it is of interest to note high concentrations of the major ions in cloud and fog water. Table 3 shows a comparison between calculated deposition due to fog and measured deposition via precipitation, on an annual basis in the Šumava Mts.

Table 3: Estimated deposition due to fog and low clouds and measured mean weighted bulk precipitation deposition in the Šumava Mts. Notice: F - estimated yearly fog deposition (kg km^{-2} $year^{-1}$), P - weighted precipitation yearly deposition (kg km^{-2} $year^{-1}$), F/P - ratio (%), Water - mean annual water deposition (mm).

Ion	H^+	Na^+	K^+	NH_4^+	Mg^{2+}	Ca^{2+}	Mn^{2+}	Zn^{2+}	Fe^{2+}
F	8.48	39.70	42.10	869.90	18.60	135.30	2.95	20.49	20.20
P	37.11	168.20	165.80	673.90	53.10	275.60	8.46	19.54	32.10
F/P	23	24	25	129	35	49	35	105	63
Ion	Al^{3+}	F^-	Cl^-	NO_3^-	SO_4^{2-}	Pb	Cd	Ni	Water
F	25.10	10.50	149.00	1767.00	2109.00	4.57	0.12	0.57	81.0
P	38.50	22.40	288.30	2299.00	2653.00	3.30	0.61	0.65	961.5
F/P	65	47	52	77	79	138	20	88	8

There was an insufficient number of chemical analyses of cloud water collected at Rudolice station in the Krušné hory Mts. and at Libuš station in Prague to allow any deeper evaluation. Therefore, these preliminary results will be only mentioned briefly in the conclusions.

5 Conclusions

Without wishing to generalize the above reported findings, the results clearly show that in the areas investigated (Šumava Mts., Krušné hory Mts. and Prague) the combined effect of high fog frequency and high ionic concentration of the solution droplets result in wet deposition rates for chemical substances which can be important to the environment. From the above-mentioned results the following conclusions can be drawn:

- The climatological normals presented here can be use for the quick and comprehensive evaluation of the importance of the phenomenon examined (occult precipitation in our case).
- Cloud and fog water deposition are important delivery mechanisms for pollutants both in the relatively clean part of the Czech Republic (the Šumava Mts.) and in a heavy polluted region (the Krušné hory Mts.). The influence of occult precipitation should also be taken into account in the capital of the Czech Republic (Prague).
- The gross water input via cloud and fog water represents about 8 % of the total annual vertical precipitation in the examined mountainous areas.

- Concentrations of major ions in cloud and fog water are approximately 10 times higher (the enrichment factor ranges from 3 to 18) in the Šumava Mts., 40 times greater (from 7 to 74) in the Krušné hory Mts. and about 35 times greater in Prague (from 9 to 50).
- In the Šumava Mts. cloud water droplets deposition can increase wet deposition of SO_4^{2-}, NO_3^- and NH_4^+ by 79, 77 and 129 %, respectively. This transport represents 2109, 1767 and 870 kg km^{-2} year^{-1}, respectively.
- In the Krušné hory Mts. cloud water droplet deposition can increase wet deposition of SO_4^{2-}, NO_3^- and NH_4^+ by 97, 160 and 186 %, respectively. This transport represents 4174, 4495 and 1446 kg km^{-2} year-1, respectively.
- In the capital of the Czech Republic (Prague) cloud water droplets deposition can increase wet deposition of SO_4^{2-}, NO_3^- and NH_4^+ by 215, 110 and 117 %, respectively. This transport represents 3212, 1773 and 593 kg km^{-2} year^{-1}, respectively.

Acknowledgements

We would like to express special thanks to Dr. G. M. Lovett for kindly supplying us with the computer programme of cloud water deposition. We are indebted to Dr. Šantroch from the Czech Hydrometeorological Institute in Prague for making available the chemical analyses of precipitation in Krušné hory Mts. for us. Funding for the project came in the framework of the Project COST 615.10 and 715.40. Grant Agency of the Academy of Sciences of the Czech Republic supported this work (Project A3060701).

References

[1] Brechtel, H. M.: Precipitation deposition situation in the Signatory States. United Nations Conference on Trade and Development, Geneva 10 (Chapter 2, ECE Interim Report on Cause-Effect Relationship), Hann, Munden, Germany, 1990.

[2] Brewer R. L., Gordon R. J., Shepard L. S., Ellis E. C. : Chemistry of mist and fog from the Los Angeles urban area. Atmospheric Environment, 17 (11), 1983, 2267–2270.

[3] Daube B., Kimball K. D., Lamar P. A., Weathers K. C. : Two new ground-level cloud water sampler designs which reduce rain contamination. Atmospheric environment, 4, 1987, 893–900.

[4] Eliáš, V., Tesař, M. and Buchtele, J.: Occult precipitation: sampling, chemical analysis and process modelling in the Šumava Mts. (Czech Republic) and in the Taunus Mts. (Germany). J. of Hydrol., 166, 1995, 409–420.

[5] Lovett G. M., Reiners W. A., Olson R. K.: Cloud droplet deposition in subalpine balsam fir forest: Hydrological and chemical inputs. Science, 218, 1982, 1303–1304.

[6] Lovett G. M.: Rates and mechanisms of cloud water deposition to a subalpine balsam fir forest. Atmospheric Environment, 18 (2), 1984, 361–371.

[7] Lovett G. M., Reiners W.A.: Canopy structure and cloud water deposition in subalpine coniferous forests. Tellus, 38B (5), 1986, 319–327.

[8] Lovett G. M.: A comparison of methods for estimating cloud water deposition to a New Hampshire (U. S. A.) subalpine forest. M. H. Unsworth and D. Fowler (eds.), Acid Deposition at High Elevation Sites, Kluwer, Norwell, 1988, 309–320.

[9] Ogren J. and Rodhe H.: Measurements of the chemical composition of cloudwater at a clean air site in central Scandinavia. Tellus, 38B, 1986, 190–196.

[10] Pražák, J., Šír, M., Tesař, M.: Estimation of plant transpiration from meteorological data under conditions of sufficient soil moisture. J. of Hydrol., 162, 1994, 409–427.

[11] Strnad, E., Tesař, M., Šír, M. and Kubík, F.: Basic characteristics of fog variation at Churáňov in 1976 1987 (in Czech). Meteorol. Bull., 1988, 41(4), 109–119.
[12] Thorne P. G., Lovett G. M., Reiners W. A.: Experimental determination of droplet impaction on canopy components of balsam fir. Journal of Applied Meteorology, 21(10), 1982, 1413–1416.
[13] Vong R. J., Sigmon J. T., Mueller S. F.: Cloud water deposition to Appalachian forests. Environ. Sci. Technol. 25(6), 1991, 1014–1021.
[14] Weathers K. C., Likens G. E., Bormann F. H., Bicknell S. H., Bormann B. T., Daube B. C., Eaton J. S., Galloway J. N., Keene W. C., Kimball K. D., McDowell W. H., Siccama T. G., Smiley D. and Tarrant R. A.: Cloud water chemistry from ten sites in North America. Environ. Sci. Technol. 22, 1988, 1018–1026.

Distributed runoff modelling in small catchments

I. Zlate

National Institute of Meteorology and Hydrology, Sos. Bucuresti-Ploiesti 97, Bucuresti 71552, Romania.

Abstract

In distributed runoff modelling, the output hydrograph is estimated by integrating space and time variables of the water balance components over the catchment area. The water balance in vertical and lateral directions is performed at raster scale, using physically-based models of component hydrological processes and a catchment digital terrain model DTM for process integration. The approach is applicable for information transfer in the upscaling and downscaling directions, as well as for modelling water erosion processes or surface pollutant dynamics. Being highly connected to descriptions of catchment land cover and topography at raster scale, the distributed model may also simulate the runoff behaviour corresponding to environment change scenarios. Key words: digital terrain modelling, distributed model, area variability.

1 Introduction

Runoff behaviour is highly dependent on the environmental structure in small catchments. The runoff hydrograph accuracy may be improved by using information on the topographic structure of the catchment. The water balance in vertical and lateral directions is performed at raster scale using physically-based models of component hydrological processes and a catchment digital terrain model DTM for process integration. Land cover, pedology, flow lines and local slopes are derived from the DTM. The distributed runoff model represents a synthesis of the process information observed in experimental basins, linking component models from the patch scale and a generalized kinematic wave model to produce a catchment scale model.

The approach is applicable for information transfer in upscaling and downscaling directions, as well as for modelling water erosion processes and surface pollutant dynamics. Being highly connected to the catchment land cover and topography at raster scale, the distributed model may also evaluate the runoff behaviour to different scenarios for environment changes.

2 Digital terrain modelling

Information available in a topographic map is organized by digital terrain modelling in specific info-layers of topography, vegetal cover, land use, infrastructure elements and soil which may be easily connected to the model water balance components. The raster resolution is usually chosen as a compromise for an acceptable DTM accuracy at a reasonable computing time of the output hydrograph.

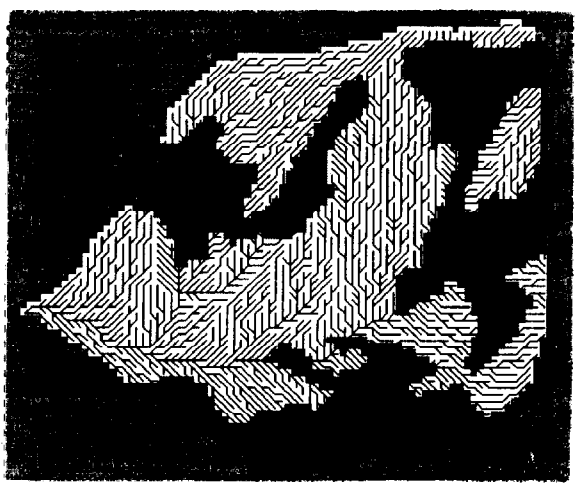

Figure 1: The drainage network and vegetal cover models for the Voinesti experimental basin.

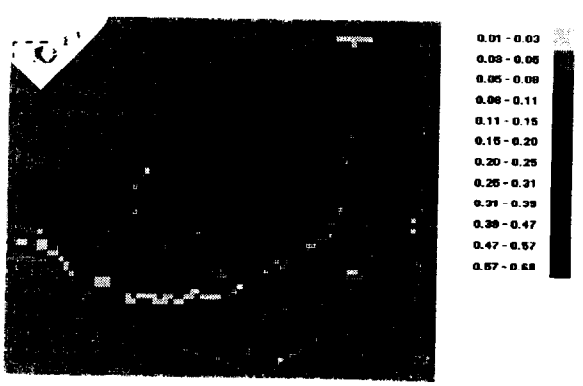

Figure 2: Local slopes in the catchment at raster scale.

The topographic info-layers are obtained with the use of an interpolation method based on cubic spline functions in case of two interpolating axes in the raster grid. The former estimates in grid nodes are transformed in pixel values as an elevation model, and the final version of this is obtained after filtering for a connected drainage network for the catchment in question. The drainage network is derived according to the lowest elevation in the current pixel surroundings, extracting flow lines from source pixels to the catchment outlet, as well as models of their local slopes and aspects.

The vertical profiles along the draining lines are corrected for pseudo-depression elimination and a further smoothing by moving average in a 3 pixel window. Such filtering highly affect the former worse elevation estimates and has no effect on the correct ones.

In distributed runoff modelling, the models of land cover, aspects and slopes are mainly concerned. Fig. 1 shows the estimates of the drainage network and vegetal cover for the Voinesti experimental basin, at a raster resolution of 15 m over an area of 78.4 ha.

The forested areas in the catchment are taken into account for local estimates of the interception component and the water balance in the lateral direction is managed by a transition function has been developed according to the catchment drainage network.

The runoff velocity is locally estimated in terms of the pixel slope values. The DTM derived slope model is presented in Fig. 2.

The raster resolution chosen for digital terrain modelling may be considered as being comparable to the scale of the runoff plots and the individual models of the water balance components. The runoff hydrograph estimating will be a result of numerical integration over the catchment area.

3 Vertical water balance modelling

The vertical water balance at the raster scale is usually performed at a 10 minute time step. The input rainfall is distributed between interception, depression storage, effective rainfall and infiltration. Infiltration is further separated into inputs for surface and subsurface runoff components.

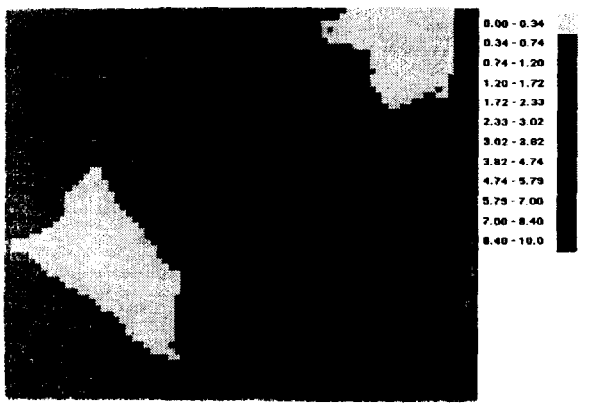

Figure 3: Kriging estimates of area rainfall intensities.

The rain intensities are usually accepted as being spatially uniform over small catchments, except for the case where there is a dense raingauge network and kriging point by point estimates may be derived, i.e. Fig. 3.

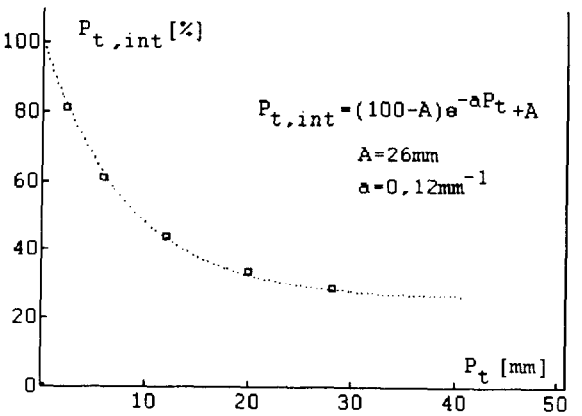

Figure 4: Experimental relationship for estimating the interception rates.

The interception model is based on a non-linear relationship between the retained water and rainfall amount, as in Fig. 4. The interception intensities are linearly dependent on vegetation type using a scale factor.

The vegetal cover in the DTM land cover info-layer are used to derive areal estimates of the interception rates at each time interval. The depression storage is considered as a reservoir of a certain capacity affecting the infiltration rates by means of a delayed rainfall distribution according to the S curve method. The infiltration model is developed according to the Horton equation. The parameters of the infiltration intensity at the initial moment or at large values of time are linearly dependent on the rain intensities, also including their low time variability during the rain event.

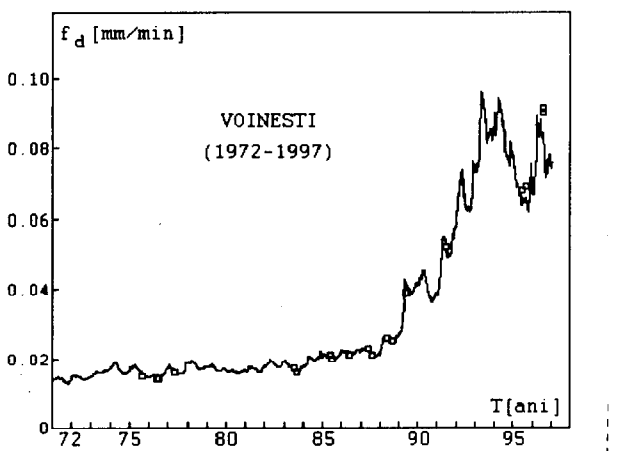

Figure 5: Estimated long term variability of the gravitational infiltration in connection with the daily rainfalls' occurrence.

The initial state of the system, as well as its updating during a 10 minute rainfall sequence is considered in units of time, a linear time variability of the soil moisture being assumed. The steady infiltration parameter includes a gravitational component of water flowing through the soil macropores. The soil dynamics under the atmosphere impact are estimated in terms of a time variable related to the occurrence of wet and dry periods. Such an estimate of its long term variability looks like the graph in Fig. 5.

The distribution of the infiltrated waters over the intermediate and saturated zones is also defined according Horton theory, taking into account specific delays for different depths. Exfiltration occurs over a certain storage capacity in the intermediate zone downstream of the slopes. The rates of exfiltration and base flow are low compared to surface runoff; their effect on the hydrograph shape is not significant. For the reason of the computing time economy they have been included in the surface runoff integration.

4 Area integration of the runoff depth

The lateral water balance is performed as local estimates of input-output-system state variable in the integration process related to the DTM drainage network and pixel slopes, with pixel runoff depth as the state variable.

The runoff modelling is developed as a generalized kinematic model. The former two-dimensional runoff process is reduced to one-dimensional case by means of a transition function managing the downstream mass transfer along the draining lines, from the source pixels to the catchment outlet at each computing time step.

The values of pixel runoff depths have a very high variability on the catchment area, which have to be integrated for a constant space step and time interval. In order to assure the integration numerical stability for an optimal computing time step, local corrections of

the state variable and output discharge decrease the approximation errors of the involved Lax-Wendroff scheme.

The correction factor is defined in terms of the kinematic wave parameters and computing time step, as a current estimate of the pixel celerity deviation from its area mean value, which corresponds to the ratio of space step versus the optimum time interval. A low perturbation of the local balance being introduced by the correction factor, with different values of the water discharge on the increasing and decreasing limb of the pixel hydrograph, the former approach as kinematic wave is transformed into a quasi-dynamic one.

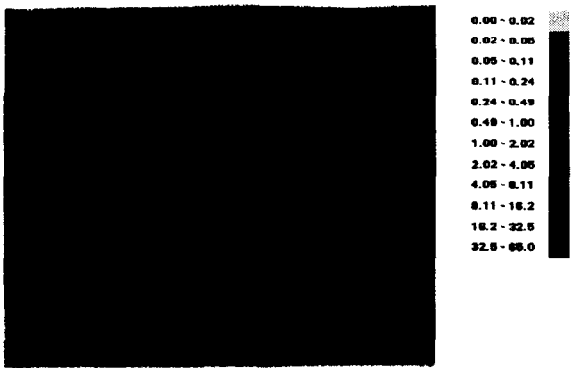

Figure 6: Class values of area runoff depth 30 min after the rain started, for the simulated event in Fig. 7.

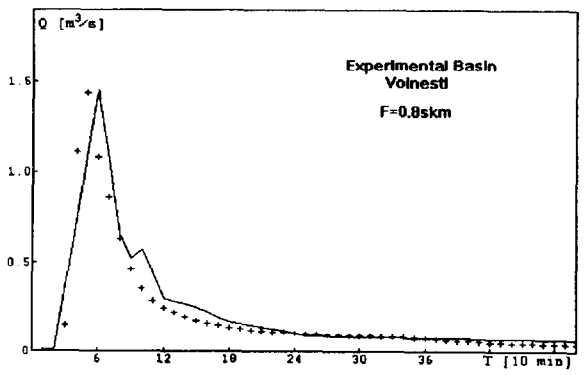

Figure 7: Estimated hydrograph by means of the runoff distributed model in case of the Voinesti experimental basin.

The optimum computing time step is a complex function of the rainfall characteristics, kinematic parameters and the maximum draining line in the catchment network, which was analyzed by means of regression analysis in terms of proper estimates for water balance of the input-output-state variables for the catchment area. Thus, at each analyzed rainfall-runoff event in a catchment, the optimum computing time interval Δt, also depends on the kinematic parameters. Although its estimated value by means of the performed regression relationships may assure an accuracy of about 2 %, the final hydrograph estimate is usually obtained after several trials updating the Δt values.

The model running continuously performs area estimates of the state variable. From their graphical representation on screen by means of class values and associated colours,

as in Fig. 6, one may notice the runoff depth evolution over the catchment area for each 10 minute time interval. The estimated hydrograph at the catchment outlet is presented in Fig. 7.

The area estimates of the water depth may be easily transformed in runoff discharges in any pixel in the catchment at an acceptable error. The distributed model was applied at recorded rainfall-runoff events over a long period in experimental basins for a larger investigation of its basic parameters at the catchment scale.

Under the circumstances, for proper estimates of the system initial state, the model may perform acceptable hydrograph predictions only in terms of the particular geomorphologic conditions in the catchments, a high model portability being concerned.

5 Application of the runoff distributed model for erosion processes

The distributed runoff model may be easily connected at raster scale to the water erosion processes related to occurring events in the catchment. The sediment source is a result of the impact rain energy, in a linear relation with 10 min rain intensities at a certain scale parameter, which has a low exponential time evolution. This two parameter model may estimate a potential material mass for the sediment transport process, highly dependent on the local water discharges in a parabolic function of two parameters.

In the sediment balance of pixel input-output values, the transport capacity may be higher than the reserve, when the slope surface is eroded, or lower, when deposition occurs. The area mass values for the sediment transport define the state variable in case of the erosion system.

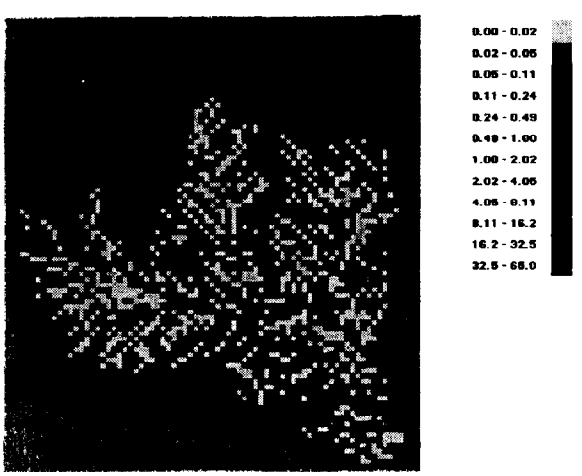

Figure 8: Area class values of sediments being remained in Aldeni experimental basin from the local created storage at the rainfall impact.

The end values of the state variable, as in Fig. 8, refer to the pixel quantities being remained on the surface from an initial storage over the catchment area, in case of the event recorded in the Aldeni experimental basin (64 ha). The simulated hydrographs are presented in Fig. 9 for water runoff, and Fig. 10 shows the sediment rates.

One may notice in Fig. 8 high changes in the local sediment storage only downstream of the slopes, as well as some small deposit areas in the river zone. The low concentration of the water runoff upstream of the slopes refers to some local movement of the sediments and the remained quantities are at least of one order higher than in the lower zones along the main flow lines.

From the analysis of successive events the scale factor of the sediment production may be correlated with the initial state of the hydrologic system. Long term estimates may be performed by means of continuous simulations at the event scale. Area sediment balance on long periods for plausible scenarios of rainfall occurrence may be transformed in changes of the catchment landscape.

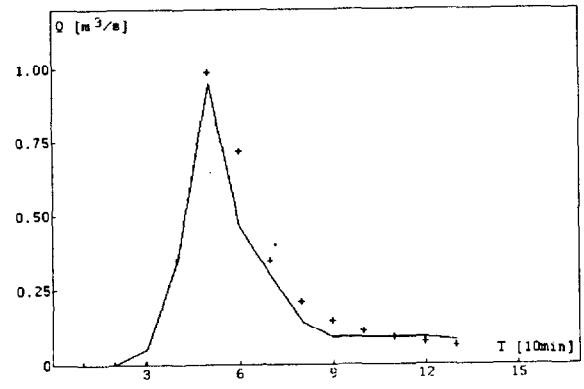

Figure 9: The simulated water runoff hydrograph.

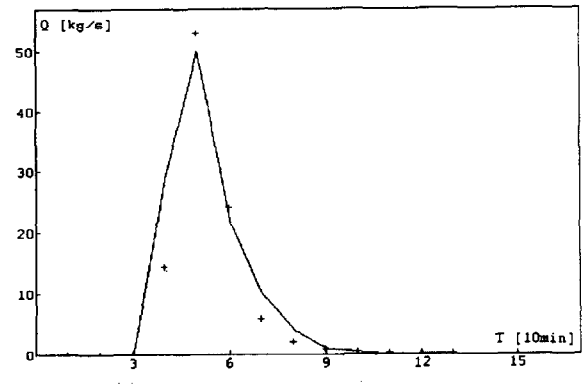

Figure 10: Simulated hydrograph of sediment rates.

Remarks

In case of distributed modelling, one may consider a complex hydrological process by means of physically based models of its components being applied at raster scale, which are numerically integrated over the catchment area in the particular environmental conditions in the analyzed territory.

Except for more accurate estimates of the runoff process, the area variability being also involved, the distributed modelling may offer a useful analyzing tool for environment surveying.

The water dynamics in a certain area may be predicted by means of three main factors, as being the catchment topography and land cover structure, long term soil-atmosphere interaction and the input rainfall characteristics.

The environment vulnerability may be analyzed in terms of water resources and erosion processes for different scenarios of the rainfall time variability in combination with land cover changes, in order to define non-structural measures for its protection or rehabilitation.

Landscape desertification by extensive agricultural use is usually related to high water erosion rates, systematically acting for a steeper topography on long periods. Deforestation in hilly areas leads to similar effects, in connection with more degradable soils, or favorable conditions for land sliding, also related to waters.

Analyzing the behaviour of small catchments in the framework of a larger area may be mapped for the actual hydrological risk or one may predict the territory vulnerability at future changes of land cover - land use, as useful actions for the environment integrated management.

References

[1] Beven, K. J. (1985) Distributed models, Hydrological Forecasting, Chapter 13, ed. by M. G. Anderson and T. P. Burt, John Wiley & Sons Ltd.

[2] Yoshino, F. (1995) Second draft on areal modelling and hydrological forecasting, WMO - 10th Commission for Hydrology.

[3] Kirkby, M. J. (1979) Hillslope Hydrology, John Wiley & Sons, Chichester, New York, Brisbane, Toronto.

[4] Zlate, I. (1991) Error of areal precipitation estimates for small dense networks and time intervals, Atmospheric Research, 27, Amsterdam.

[5] Zlate, I. (1997) Distributed runoff modelling emphasizing the process space and time variability in rural catchments, FRIEND '97 Regional Hydrology: Concepts and Models for Sustainable Wat. Res. Management, Postojna, Slovenia.